

AD-A102 358

MISSISSIPPI STATE UNIV MISSISSIPPI STATE ENGINEERING--ETC F/G 17/1
INVESTIGATION OF CEPSTRUM ANALYSIS FOR SEISMIC/ACOUSTIC SIGNAL --ETC(U)
JAN 81 F M INGELS, G KOLEYNI AFOSR-80-0086

UNCLASSIFIED

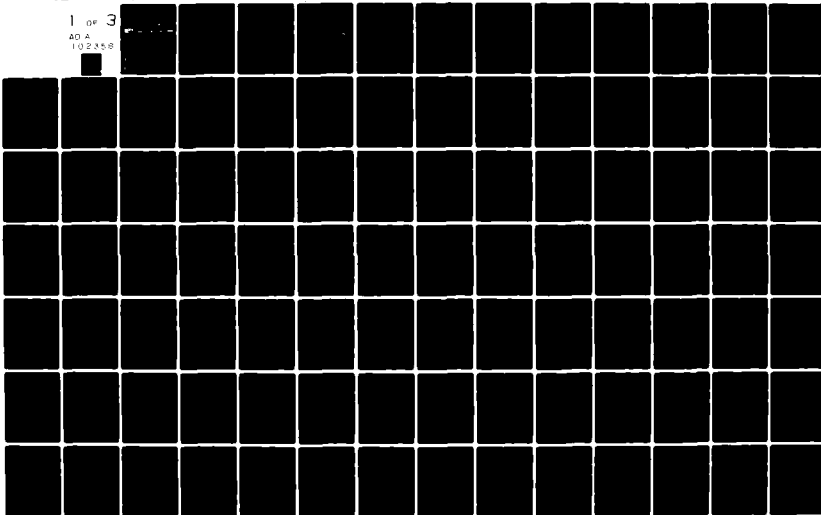
MSSU-EIRS-EE-81-2

AFOSR-TR-81-0603

NL

1 of 3

AD A
102358



AFOSR-TR-81-0603

INVESTIGATION OF CEPSTRUM ANALYSIS

FOR

4

SEISMIC/ACOUSTIC SIGNAL SENSOR

RANGE DETERMINATION

LEVEL III

eirs

ENGINEERING & INDUSTRIAL RESEARCH STATION

Electrical Engineering

FINAL REPORT

Submitted

by

FRANK M. INGELS
GHASSEM KOLEYNI

DTIC
AUG 3 1981

Prepared for

AFOSR

Approved for public release
distribution unlimited.

Mississippi State University
Mississippi State, MS 39762

MSSU-EIRS-EE-81-2

03 086

DTIC FILE COPY
AD A102358

COLLEGE OF ENGINEERING ADMINISTRATION

WILLIE L. MCDANIEL, PH.D.
DEAN, COLLEGE OF ENGINEERING

WALTER R. CARNES, PH.D.
ASSOCIATE DEAN

JOHN I. PAULK, PH.D.
ASSOCIATE DEAN

LAWRENCE J. HILL, M.S.
DIRECTOR, ENGINEERING SERVICES

CHARLES B. CLIETT, M.S.
AEROSPACE ENGINEERING

WILLIAM R. FOX, PH.D.
AGRICULTURAL & BIOLOGICAL ENGINEERING

JOHN L. WEEKS, JR., PH.D.
CHEMICAL ENGINEERING

ROBERT M. SCHOLTES, PH.D.
CIVIL ENGINEERING

B. J. BALL, PH.D.
ELECTRICAL ENGINEERING

W. H. EUBANKS, M.ED.
ENGINEERING GRAPHICS

FRANK E. COTTON, JR., PH.D.
INDUSTRIAL ENGINEERING

C. T. CARLEY, PH.D.
MECHANICAL & NUCLEAR ENGINEERING

ELDRED W. HOUGH, PH.D.
PETROLEUM ENGINEERING

For additional copies or information
address correspondence to

ENGINEERING AND INDUSTRIAL RESEARCH STATION
DRAWER DE
MISSISSIPPI STATE UNIVERSITY
MISSISSIPPI STATE, MISSISSIPPI 39762

TELEPHONE (601) 325-2266



Mississippi State University does not discriminate on the basis of race, color, religion, national origin, sex, age, or handicap.

In conformity with Title IX of the Education Amendments of 1972 and Section 504 of the Rehabilitation Act of 1973, Dr. T. K. Martin, Vice President, 610 Allen Hall, P. O. Drawer J, Mississippi State, Mississippi 39762, office telephone number 325-3221, has been designated as the responsible employee to coordinate efforts to carry out responsibilities and make investigation of complaints relating to nondiscrimination.



17 REPORT DOCUMENTATION PAGE		READ INSTRUCTIONS BEFORE COMPLETING FORM	
1. REPORT NUMBER AFOSR-TR-81-0603	2. GOVT ACCESSION NO. AD-A102	3. RECIPIENT'S CATALOG NUMBER 358	
4. TITLE (and Subtitle) INVESTIGATION OF CEPSTRUM ANALYSIS FOR SEISMIC/ ACOUSTIC SIGNAL SENSOR RANGE DETERMINATION		5. TYPE OF REPORT & PERIOD COVERED FINAL REPORT-January 1, 1980 December 31, 1980	
6. AUTHOR(s) Frank M. Ingels and Ghassem Koleyni		7. CONTRACT OR GRANT NUMBER(s) AFOSR-80-0086	
8. PERFORMING ORGANIZATION NAME AND ADDRESS Mississippi State University Drawer EE Mississippi State, MS 39762		9. PROGRAM ELEMENT, PROJECT, TASK AREA & WORK UNIT NUMBERS 2304/D9 6110P	
10. CONTROLLING OFFICE NAME AND ADDRESS Air Force Office of Scientific Research/NM Bolling AFB DC 20332		11. REPORT DATE January 1981	
12. MONITORING AGENCY NAME & ADDRESS (if different from Controlling Office) Final Report AFOSR-81-0603		13. NUMBER OF PAGES 218	
14. DISTRIBUTION STATEMENT (of this Report) Approved for public release; distribution unlimited.		15. SECURITY CLASS. (of this report) Unclassified	
16. DISTRIBUTION STATEMENT (of the abstract entered in Block 20, if different from Report)		15a. DECLASSIFICATION/DOWNGRADING SCHEDULE	
18. SUPPLEMENTARY NOTES The views and conclusions contained in this document are those of the authors and should not be interpreted as necessarily representing the official policies or endorsements, either expressed or implied, of the Air Force Office of Scientific Research or the U.S. Government.			
19. KEY WORDS (Continue on reverse side if necessary and identify by block number) Cepstrum, Echo Analysis			
20. ABSTRACT (Continue on reverse side if necessary and identify by block number) Cepstrum analysis is performed for damped sinusoids with arbitrary starting times within a discrete time window. Computer simulations are presented to verify the mathematical analysis.			

394 412

4

INVESTIGATION OF CEPSTRUM ANALYSIS
FOR
SEISMIC/ACOUSTIC SIGNAL SENSOR RANGE DETERMINATION

FINAL REPORT
Covering the Period
January 1, 1980 - December 31, 1980

Submitted
by

FRANK M. INGELS
GHASSEM KOLEYNI

Mississippi State University
Electrical Engineering
Mississippi State, MS 39762

Prepared for

AFOSR
under
Grant No. AFOSR-80-0086

DISTRIBUTION STATEMENT A
Approved for public release;
Distribution Unlimited

January, 1981
AIR FORCE OFFICE OF SCIENTIFIC RESEARCH (AFSC)
NOTICE OF TRANSMITTAL TO DDC
This technical report has been reviewed and is
approved for public release IAW AFR 190-12 (7b).
Distribution is unlimited.
A. L. BLASE
Technical Information Officer

Unclassified

SECURITY CLASSIFICATION OF THIS PAGE (When Data Entered)

REPORT DOCUMENTATION PAGE		READ INSTRUCTIONS BEFORE COMPLETING FORM
1. REPORT NUMBER AFOSR-TR- 81 - 0603	2. GOVT ACCESSION NO. AD-A102 358	3. RECIPIENT'S CATALOG NUMBER
4. TITLE (and Subtitle) INVESTIGATION OF CEPSTRUM ANALYSIS FOR SEISMIC/ ACOUSTIC SIGNAL SENSOR RANGE DETERMINATION		5. TYPE OF REPORT & PERIOD COVERED FINAL REPORT-January 1, 1980 December 31, 1980
7. AUTHOR(s) Frank M. Ingels and Ghassem Koleyni		6. PERFORMING ORG. REPORT NUMBER
9. PERFORMING ORGANIZATION NAME AND ADDRESS Mississippi State University Drawer EE Mississippi State, MS 39762		8. CONTRACT OR GRANT NUMBER(s) AFOSR-80-0086
11. CONTROLLING OFFICE NAME AND ADDRESS Directorate of Mathematical and Information Sciences Dr. Joseph Bram, AFSC Bolling Air Force Base, DC 20332		10. PROGRAM ELEMENT, PROJECT, TASK AREA & WORK UNIT NUMBERS 2304/D9 61102F
14. MONITORING AGENCY NAME & ADDRESS (if different from Controlling Office)		12. REPORT DATE January 1981
		13. NUMBER OF PAGES 218
		15. SECURITY CLASS. (of this report) Unclassified
16. DISTRIBUTION STATEMENT (of this Report)		15a. DECLASSIFICATION/DOWNGRADING SCHEDULE
<div style="border: 1px solid black; padding: 5px; display: inline-block;"> DISTRIBUTION STATEMENT X Approved for public release; Distribution Unlimited </div>		
17. DISTRIBUTION STATEMENT (of the abstract entered in Block 20, if different from Report)		
18. SUPPLEMENTARY NOTES The views and conclusions contained in this document are those of the authors and should not be interpreted as necessarily representing the official policies or endorsements, either expressed or implied, of the Air Force Office of Scientific Research or the U.S. Government.		
19. KEY WORDS (Continue on reverse side if necessary and identify by block number) Cepstrum, Echo Analysis		
20. ABSTRACT (Continue on reverse side if necessary and identify by block number) Cepstrum analysis is performed for damped sinusoids with arbitrary starting times within a discrete time window. Computer simulations are presented to verify the mathematical analysis.		

DD FORM 1 JAN 73 1473

EDITION OF 1 NOV 69 IS OBSOLETE
S/N 0102-014-6601

Unclassified
SECURITY CLASSIFICATION OF THIS PAGE (When Data Entered)

TABLE OF CONTENTS

<u>Chapter</u>	<u>Page</u>
LIST OF FIGURES	ii
LIST OF TABLES	iv
I. INTRODUCTION	1
II. THE CEPSTRUM	4
III. THE SHORT TIME AVERAGE CEPSTRUM	14
IV. EXPERIMENTAL RESULTS	27
V. CONCLUSIONS AND RECOMMENDATIONS	66
APPENDICES	72
APPENDIX A. Definition of the Terms Used in the Report	73
APPENDIX B. Cepstrum Derivation for Multiple Echoes	76
APPENDIX C. Cepstrum Derivation for Cosine Type Signals	80
APPENDIX D. Cepstrum Derivation for Cosine Type Waveforms When There is a Window Within a Window	90
APPENDIX E. Cepstrum Derivation for Damped Exponential Type Signals	96
APPENDIX F. A Listing of Computer Programs	105
APPENDIX G. Figures	133
APPENDIX H. Bibliography	190
1. Literature Survey	191
2. A Compiled Bibliography on the Cepstrum and Related Topics	203

Accession For	<input type="checkbox"/>
NTIS GRA&I	<input type="checkbox"/>
DTIC TAB	<input type="checkbox"/>
Unannounced	
Justification	
RV	
Distribution/	
Availability Codes	
Dist	
Ann and/or	
Special	

A

LIST OF FIGURES

<u>Figure</u>	<u>Title</u>	<u>Page</u>
2-1	Block diagram of cepstrum analysis	6
3-1	Cosine signal time plot.	16
3-2	Cosine cepstrum with simple echo	18
3-3	Cosine signal shifted time frame plot	19
3-4	Cosine cepstrum, shifted time frame plot	20
3-5	Damped exponential with echo time plot	21
3-6	Damped exponential with echo cepstrum	22
3-7	Damped cosine with echo time plot	25
3-8	Damped cosine with echo cepstrum	26
4-1a	Single echo cosine cepstrum	41
4-1b	Single echo damped exponential cepstrum	42
4-1c	Single echo damped cosine cepstrum	43
4-2a	Single echo cosine cepstrum	44
4-2b	Single echo damped exponential cepstrum	45
4-2c	Single echo damped cosine cepstrum	46
4-3a	Two echo cosine cepstrum	47
4-3b	Two echo damped exponential cepstrum	48
4-3c	Two echo damped cosine cepstrum	49
4-4a	Three echo cosine cepstrum	50
4-4b	Three echo exponential cepstrum	51
4-4c	Three echo damped cosine cepstrum	52
4-5a	Noise plus signal time plots	62

LIST OF FIGURES (CONTINUED)

<u>Figure</u>	<u>Title</u>	<u>Page</u>
4-5b	Noise plus signal cosine cepstrum	63
4-6a	Noise plus signal time plots	64
4-6b	Noise plus signal cosine cepstrum	65

LIST OF TABLES

<u>Table</u>	<u>Title</u>	<u>Page</u>
4-1a	Effects of windowing/smoothing	29
4-1b	Effects of windowing/smoothing	30
4-2	Effects of windowing/smoothing	30
4-3a	Power cepstrum magnitude variation	31
4-3b	Normalized form of Table 4-3a	32
4-4a	Power cepstrum magnitude variation	33
4-4b	Normalized form of table 4-4a	34
4-5a	Power cepstrum for damped exponential with windowing/smoothing	36
4-5b	Power cepstrum for damped exponential time differences	36
4-5c	Power cepstrum for damped exponential time differences	37
4-6a	Power cepstrum for damped cosine waveform	38
4-6b	Power cepstrum for damped cosine waveform	39
4-6c	Power cepstrum for damped cosine waveform	39
4-7a	Power cepstrum variation for one echo	53
4-7b	Power cepstrum variation for one echo (normalized)	54
4-8a	Power cepstrum variation for two echos, cosine	55
4-8b	Power cepstrum variation for two echos, cosine	56
4-9a	Power cepstrum variation for two echos, damped exponential	57
4-9b	Power cepstrum variation for two echos, damped exponential	58
4-10a	Power cepstrum variation for two echos, damped cosine	59
4-10b	Power cepstrum variation for two echos, damped cosine	60

LIST OF TABLES (Continued)

<u>Table</u>		<u>Page</u>
5-1	Single Echo	69
5-2	Multiple Echoes	70
5-3	Noise Case	71

CHAPTER I

INTRODUCTION

In seismology or in many other situations signals or waveforms are encountered that may be represented as the convolution of a few components. The signal might be distorted by transmission through a linear system. For example, the effect of multipath and reverberation may be modeled in terms of a signal that is passed through a linear system whose impulse response is an impulse train. One may wish to recover the undistorted signal, or in the case of receiving convolved signals one might want to determine these components so as to characterize the waveform or physical process from which it originated.

The process of separating components of a convolution is termed deconvolution. In this process one must determine an appropriate transformation of the waveform into the desired component waveforms, [3], [16]*.

In seismology arrivals of various waves or phases can be considered as the delayed arrival of more or less distorted echoes. The existence and timing of these echoes are not sufficiently apparent on the original seismograph traces for analysis. The main interest in this research is location and identification of target signal sources, or determining range from a target signal source to a sensor.

* Reference numbers refer to those entries in Appendix H, section 2, page .

Identification is accomplished mainly by using feature analysis usually in the frequency domain; location consists of two aspects, one is determination of the angle to the target, the other is range to the target. At the present time ranging is accomplished through use of doppler techniques or by using multiple sensors and performing cross correlation to determine the difference in time of arrival of components of the signals which travel at different velocities [12]. In this research it is desired to use only one sensor to detect both seismic and acoustic waveforms generated by the target signal source and to determine the range by acquiring the difference between arrival times of the two signals through use of the deconvolution technique - the cepstrum.

One deconvolution technique is based on the wiener theory of linear filtering. This technique has been extensively applied in processing seismic waveforms in detection of echoes.

Cepstrum analysis^{*}, which is a subclass of the homomorphic deconvolution techniques, is a method that can effectively separate the signals or determine the difference in time arrival of two signals. In this research an investigation is conducted using the cepstrum analysis technique for data sources which are not strictly coherent and periodic. The study has been divided into five parts:

1. The cepstrum is first defined and calculated in general.
2. The cepstrum is then calculated for noiseless cosine waveforms.

* For definition of terms see appendix A.

3. The cepstrum is then calculated for noiseless damped cosine waveforms.
4. The cepstrum is then calculated for noiseless exponential waveforms.
5. Finally, the cepstrum is calculated for noisy cosine waveforms.

Cosine waveforms for the noisy case are chosen because of several small spikes that usually exist in the cepstrum plot of these type signals, making them more prone to discrimination from the noise.

The period of observation is .5 seconds and the delay or epoch times are .01, .05, .07, and .12 seconds for the single echo case and .07, .09, and .15 seconds for double echo case. The sampling rate is 1/2048 seconds and there are 1024 samples in each observation interval.

The emphasis is on a single echo case since for more than one echo the study becomes very complicated and calculations if not impossible are very cumbersome. Furthermore the computer run time becomes prohibitive for multiple echoes.

The effect of the amplitude and epoch time of a single echo is observed and in the noisy case the study is done for several signal to noise ratios (SNR). In calculating the cepstrum for different cases the lengthy calculations are left for the appendix and the results are presented in the main text for the convenience of the reader.

CHAPTER II

THE CEPSTRUM

Definition of the Problem

In a listening post within listening range of a target, it is possible to have one single source with multipath propagation or multiple targets or multiple targets and multi-path. In either case, the received signal is a composite of the individual signals or of the multipath signals. One receives the signal in a majority of cases in a form which is the convolution of those generated signals. The task may be to decompose the signal into the original signals. This process of decomposing the convolved signal into the original is called deconvolution.

A deconvolution as commonly performed by means of inverse filtering or optimum zero-lag Wiener filtering suffers from the limitation that either the shape of the waveform to be removed must be known or the assumption that the wavelet is minimum-phase must be made [32].

In the field a problem of prime interest is one of determining only the range from a target to the sensor. Typically, this is accomplished by using two co-located sensors and performing an analysis such as cross correlation to determine the difference in arrival times between two signals of different propagation times such as acoustic/seismic, EM/acoustic, etc. [73]. These techniques require two sensors and, for various reasons, it is desirable to devise some technique that utilizes only one sensor. The problems

are numerous in that all signals and echoes have similar properties and a technique which may answer one problem might not be of any help in the other situation.

History

In 1959 when Bogert noticed banding in the spectrograms of seismic signals, he realized that this banding was caused by periodic ripples in the spectra and this was characteristic of the spectra of any signal consisting of itself plus an echo. The frequency of these ripples equals the reciprocal of the difference in time arrivals of the two waves. Tukey suggested that this frequency difference might be obtained by first taking the logarithm of the spectrum, thereby making the ripples nearly cosinusoidal. In 1960, Bogert programmed Tukey's suggestion on a computer (see Figure 2-1) and proceeded to analyze numerous earthquakes and explosions. Tukey, noticing similarities between time series and log-spectrum series analysis, introduced a new set of paraphrased terms. The spectrum of the log spectrum was called "cepstrum" [11].

The first paper on cepstrum was published in 1963 by Bogert, Tukey and Healy [3]. In this paper the main study concerned seismic waves, but later on, the idea of cepstrum analysis was used in speech signal analysis by A.M. Noll [4], in visual evoked response (VER) by R. C. Kemerait [31], in oceanography by J. C. Hassab [41], and even in analysis of full-term and premature infant's cries [46].

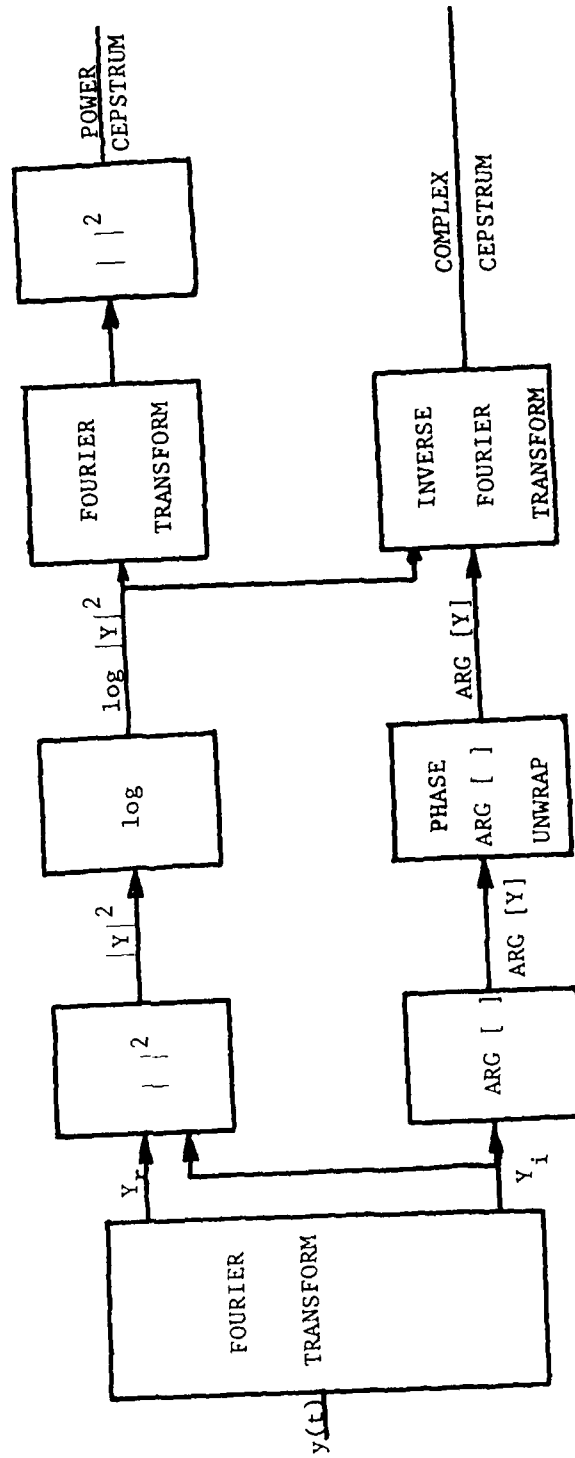


Figure 2-1. Block Diagram of Cepstrum Analysis.

Analytical Discussion

So far we are familiar with the word "cepstrum" but not with the mathematical means to obtain it. As was mentioned earlier when there is a composite signal one might be interested in decomposing the signal and obtaining the original signals or simply be interested in epoch or delay times. These two different ideas would lead us in pursuing two different methods each suitable to our desires. After introduction of the word cepstrum by Bogert et al, R. W. Schafer [16] introduced another name obtained from a former one called complex cepstrum. After this new invention the previous word cepstrum, which was solely used to show the method of detecting the echo delay time, was called power cepstrum.

Complex Cepstrum

The complex cepstrum technique was first described in a doctoral dissertation by R. W. Schafer [16] in November 1968. As previously mentioned the cepstrum is related to homomorphic deconvolution. The basic difference is that a Fourier transform (magnitude and phase) is employed, rather than the power or energy spectrum. This is done because of the concern over recovery of the actual signals rather than simply the different time of arrivals.

Power Cepstrum

As mentioned before in contrast to the complex cepstrum one is not concerned with the recovery of the actual signals by decomposing them, one is interested in detecting the echoes, and it is because of this difference that there are two different

cepstrum techniques. From this point on only the power cepstrum will be utilized.

Single Echo

In the simplest echo, values of time series $y(t)$ are multiplied by a constant α , delayed by a time difference τ and added to the original series to give a new series

$$z(t) = y(t) + \alpha y(t-\tau) \quad (2-1)$$

taking the Fourier transform from both sides of (2-1) one has

$$\begin{aligned} F[z(t)] &= F[y(t) + \alpha y(t-\tau)] \\ &= F[y(t)] + \alpha F[y(t-\tau)] \end{aligned} \quad (2-2)$$

considering the time shifting property of the Fourier transform one has

$$\begin{aligned} \text{if } g(t) &\longleftrightarrow G(\omega) \\ \text{then } g(t-\tau) &\longleftrightarrow G(\omega) e^{-j\omega\tau} \end{aligned} \quad (2-3)$$

and then calling the Fourier transform of $z(t)$ and $y(t)$, $Z(\omega)$ and $Y(\omega)$ respectively one has

$$Z(\omega) = Y(\omega)(1 + \alpha e^{-j\omega\tau}) \quad (2-4)$$

squaring the absolute values of both sides in (2-4) would give

$$|Z(\omega)|^2 = |Y(\omega)|^2 |1 + \alpha e^{-j\omega\tau}|^2 \quad (2-5)$$

taking the logarithm of both sides in (2-5) would result

$$2 \log |Z(\omega)| = 2 \log |Y(\omega)| + \log |1 + \alpha e^{-j\omega\tau}|^2 \quad (2-6)$$

Parameter α is the strength of the echo signal with respect to the original signal and it is usually less than one. If the series expansion of $\log_e (1+X)$ is examined we observe

$$\log_e (1+X) = X - \frac{X^2}{2} + \frac{X^3}{3} - \frac{X^4}{4} + \dots = \sum_{n=1}^{\infty} \frac{(-1)^{n+1}}{n} X^n \quad - \quad 1 < X < 1 \quad (2-7)$$

The relation between logarithms in two different bases is

$$\log_b A = \frac{\log_c A}{\log_c b} \quad (2-8)$$

In our case $b = 10$ and $c = e$ (natural log)

$$\log_{10} A = \frac{\log_e A}{\log_e 10} = .434295 \log_e A \quad (2-9)$$

Let us define the notation

$$\log X = \log_{10} X \quad \text{and} \quad \ln X = \log_e X \quad (2-10)$$

then one can write

$$\log |1 + \alpha e^{-j\omega\tau}| = .434295 \sum_{n=1}^{\infty} \frac{(-1)^n}{n} (\alpha e^{-j\omega\tau})^n \quad (2-11)$$

$$|\alpha e^{-j\omega\tau}| \leq 1$$

the complete term is then

$$2 \log |Z(\omega)| = 2 \log |Y(\omega)| + .868590 \sum_{n=1}^{\infty} \frac{(-1)^n}{n} \alpha^n e^{-j\omega\tau} \quad (2-12)$$

Taking the Fourier transform again from both sides of (2-12) one has

$$\begin{aligned} \text{Cepstrum} = C_p(z(t)) &= F[2 \log |z(\omega)|] = F[2 \log |Y(\omega)|] \\ &+ F[.868590 \sum_{n=1}^{\infty} \frac{(-1)^n}{n} \alpha^n e^{-jn\omega\tau}] \end{aligned} \quad (2-13)$$

or

$$\begin{aligned} C_p(z(t)) &= F[2 \log |Y(\omega)|] \\ &+ .868590 \int_{-\infty}^{\infty} \sum_{n=1}^{\infty} (-1)^n \alpha^n e^{-jn\omega\tau} e^{-j\omega t} d\omega \end{aligned} \quad (2-14)$$

notice that here ω is the variable of a function whose Fourier transform is desired. Interchanging \sum with \int gives

$$\begin{aligned} C_p(z(t)) &= \left| F[2 \log |Y(\omega)|] \right| \\ &+ |.868590 \sum_{n=1}^{\infty} \frac{(-1)^{n+1}}{n} \alpha^n \delta(t-n\tau)| \end{aligned} \quad (2-15)$$

from (2-15) disregarding shape of the original signal $y(t)$, one observes a set of ripples. It is clear that the "frequency" of the ripple is just τ , whose units are ripples per cycle per second or (necessarily) seconds [3].

The log power spectrum can be considered as a "frequency series", if estimated digitally, it will in fact be a discrete frequency series. In such a series Bogert et al [3], describe a (nearly) cosinusoidal ripple by its quefrequency, its gamnitude, and its saphe at some (frequency) origin.

When approximating the function $\ln(1+X)$ the condition was stipulated that

$$|\alpha e^{-j\omega\tau}| \leq 1 \quad (2-16)$$

if $\alpha > 1$, one can perform some mathematical manipulations as:

$$\begin{aligned} |1 + \alpha e^{-j\omega\tau}|^2 &= 1 + \alpha^2 + 2\alpha \cos \omega\tau \\ &= \alpha^2 (1 + 1/\alpha^2 + 2/\alpha \cos \omega\tau) \end{aligned} \quad (2-17)$$

Having $\alpha > 1$ one can say the term $1/\alpha^2 + 2/\alpha \cos \omega\tau$ for some τ and ω is less than one and because $\ln(AB) = \ln(A) + \ln(B)$, one can filter out the term $\ln \alpha^2$ and still have the ripples τ seconds apart.

As may be observed the cepstrum is a function of frequency and is determined over a range extending from zero up to a maximum frequency that is necessarily equal to the longest lag in the autocovariance used in the original power-spectrum calculations. The cepstrum is effective in detecting simple echoes even when autocovariance fails completely [3].

In speech analysis the cepstrum of a speech signal has a peak corresponding to the fundamental period for voiced speech but no peak for unvoiced speech [4]. Cepstral pitch detection has the important advantages that it is insensitive to phase distortion, and is also resistant to additive noise and amplitude distortion of the speech signal. The cepstrum, when calculated for a series of short time segments of a speech signal, has been shown to perform very efficiently as a pitch determinator particularly for vocoder applications [18].

In radar applications with low look angles, and similarly in sonar, measurement of echo delay helps reduce interference due to reflection by a neighboring boundary. In the processing of bioelectronic data, such as electroencephalograms and visually evoked responses, the cepstrum helps identify the origin of observed electrical activity [26], [59].

The non linear terms ignored in power series expansion of $\ln(1+X)$ deserve some attention. The first time that we took the Fourier transform in (2-4) we had a term $(1+\alpha e^{-j\omega\tau})$. The absolute value of this term when squared is

$$1 + 2\alpha \cos \omega\tau + \alpha^2 \quad (2-18)$$

and the natural logarithm of it is

$$\begin{aligned} \ln(1 + 2\alpha \cos \omega\tau + \alpha^2) &= (2\alpha \cos \omega\tau + \alpha^2) - \frac{1}{2} (2\alpha \cos \omega\tau + \alpha^2)^2 + \dots \\ &= \alpha^2 + 2\alpha \cos \omega\tau - 2\alpha^2 \cos^2 \omega\tau \end{aligned} \quad (2-19)$$

Using trig identities one has

$$\begin{aligned} 2\alpha^2 \cos^2 \omega\tau &= 2\alpha^2 \left(\frac{1}{2} + \frac{1}{2} \cos 2\omega\tau \right) \\ &= \alpha^2 (1 + \cos 2\omega\tau) \end{aligned} \quad (2-20)$$

substituting (2-20) in (2-19) gives

$$\begin{aligned} \ln(1 + 2\alpha \cos \omega\tau + \alpha^2) &= \alpha^2 + 2\alpha \cos \omega\tau - \alpha^2 - \alpha^2 \cos 2\omega\tau \\ &= 2\alpha \cos \omega\tau - \alpha^2 \cos 2\omega\tau \end{aligned} \quad (2-21)$$

The second harmonic represented by the term $\alpha^2 \cos 2\omega\tau$ contributes an amount to the variance of the ripple [3]. This is to be compared with the contribution of the fundamental. The ratio is $\alpha^4/4$ so that harmonics, although to be expected, should be rather small.

Another source of complexity, would be provided by multiple echoes, such as the case of two echoes with parameters α_1, τ_1 and α_2, τ_2 . These would multiply the original Fourier transform by

$$1 + \alpha_1 e^{-j\omega\tau_1} + \alpha_2 e^{-j\omega\tau_2} \quad (2-22)$$

and the power spectrum by

$$1 + 2\alpha_1 \cos \omega\tau_1 + 2\alpha_2 \cos \omega\tau_2 + 2\alpha_1\alpha_2 \cos \omega(\tau_1 - \tau_2) + \alpha_1^2 + \alpha_2^2 \quad (2-23)$$

so that the amount added to the log spectrum is

$$2\alpha_1 \cos \omega\tau_1 + 2\alpha_2 \cos \omega\tau_2 - \alpha_1^2 \cos 2\omega\tau_1 - \alpha_2^2 \cos 2\omega\tau_2 - 2\alpha_1\alpha_2 \cos \omega(\tau_1 + \tau_2) \quad (2-24)$$

to quadrature accuracy. Thus in addition to ripples at τ_1 and τ_2 , one expects a ripple at frequency $(\tau_1 + \tau_2)$ with magnitude of order twice that of the harmonic at frequencies $2\tau_1$ and $2\tau_2$.

In (2-24) if higher order approximation is used, the difference ripple would show up. Appendix B shows complete work for multiple echo case.

CHAPTER III

THE SHORT TIME AVERAGE CEPSTRUM

The terminology 'short time average cepstrum' might be confusing or in some cases misleading, but if the reader bears with us for a short time the ambiguities will be clarified. In the previous chapter the cepstrum was discussed in general, and the period of integration for the Fourier transform was from $-\infty$ to $+\infty$. Most of the realizable experiments are causal, that is, they cannot exist for the time period $-\infty$ to 0. The use of the digital computer for analysis adds another restriction, limiting the length of the experiment even if it is performed in real time.

In most applications one is interested in observing an event in a limited time, or in the other words, observing the event through a window. If the cepstrum is to be evaluated for a composite signal in the aforementioned circumstances; the limits of integration must be changed, and it is because of these limitations that the result is called the short time averaged cepstrum.

To derive some analytical expressions for short time average cepstrums we choose some functions of interest and find their cepstrum. As mentioned in the introduction three types of signals have been chosen:

1. cosine signal
2. damped cosine signal
3. damped exponential signal.

The cepstrum expression is derived for the cosine and the damped

exponential signals only when we have single echoes. The case of damped cosine is a special form of 1. or 3. depending on the damping coefficient.

Cosine Signal

The choice of signal has been

$$g(t) = \cos \omega_0 (t - \tau_1) u(t - \tau_2) + \alpha \cos \omega_0 (t - \tau_3) u(t - \tau_4) \quad (3-1)$$

which is shown in Figure 3-1. As one observes from the figure the signals are not in phase and they begin at two different times. The complete calculation is left for Appendix C, but some of the results are mentioned here.

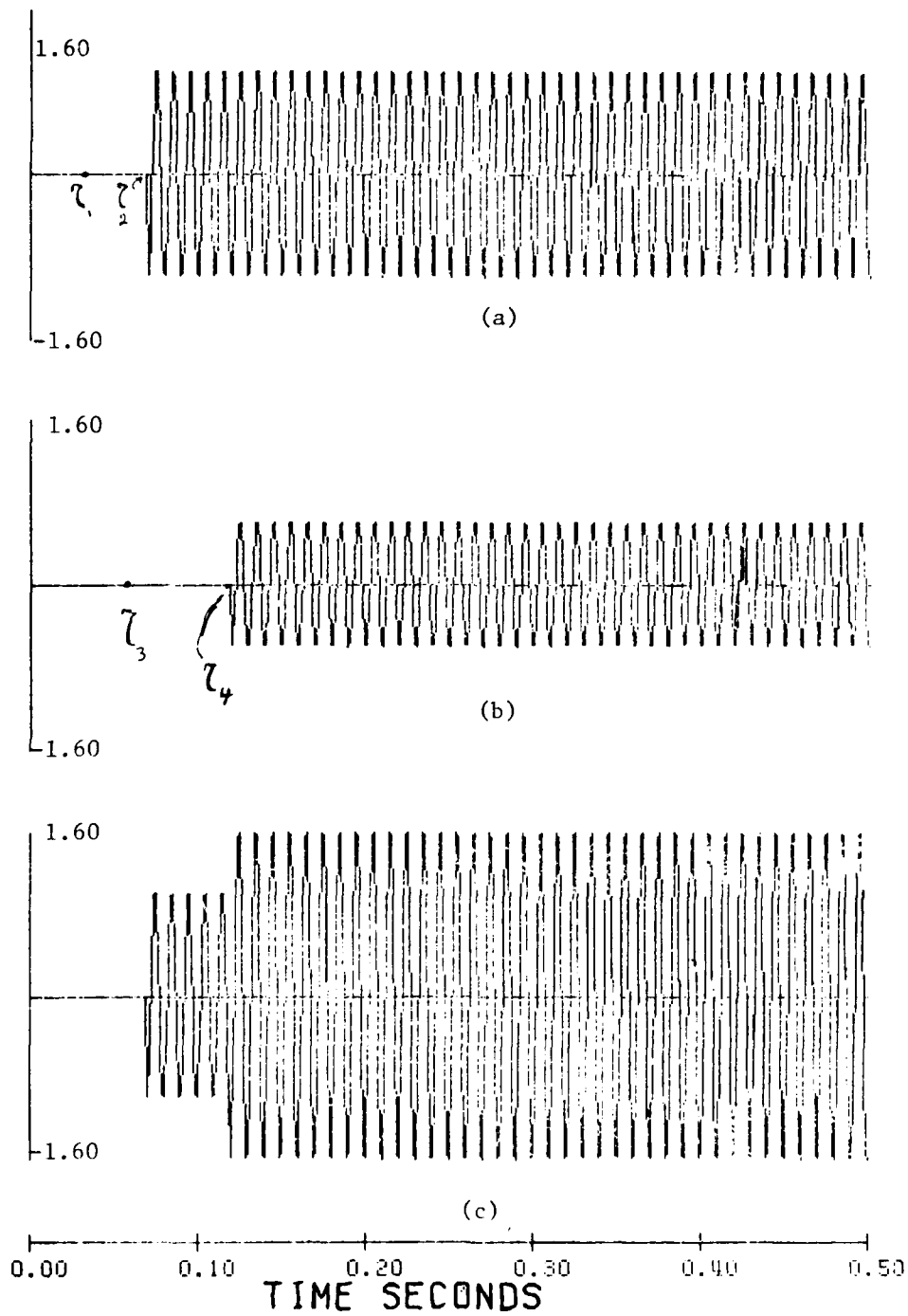
Taking the Fourier transform from both sides of (3-1) gives

$$\begin{aligned} F[g(t)] &= F[\cos \omega_0 (t - \tau_1) u(t - \tau_2) + \alpha \cos \omega_0 (t - \tau_3) u(t - \tau_4)] \\ &= \int_{\tau_2}^{\tau} \cos \omega_0 (t - \tau_1) e^{-j\omega t} dt + \int_{\tau_4}^{\tau} \cos \omega_0 (t - \tau_3) e^{-j\omega t} dt \end{aligned} \quad (3-2)$$

taking logarithm of the spectrum found from this Fourier transformation and after some mathematical manipulations one encounters terms with the following forms

$$\cos \omega (\tau - \tau_2) \quad \text{and} \quad \cos \omega (\tau - \tau_4).$$

Terms containing cosine, would have impulses in their Fourier transforms, so in our case presence of ripples at $\tau - \tau_2$ and $\tau - \tau_4$ is obvious. Because of the symmetrical property of the Fourier transform one should also obtain ripples at τ_2 and τ_4 , and



$$\cos(200\pi \cdot (t - \tau_{U1})) + 0.5 \cos(200\pi \cdot (t - \tau_{U2})) + 0.5 \cos(200\pi \cdot (t - \tau_{U2}))$$

Figure 3-1. a) Cosine waveform, b) the echo signal, c) composite signal

at $\tau - \tau_2$ and $\tau - \tau_4$. In Figure 3-2* we show such ripples and also existing ripples of the harmonics of τ_2 and τ_4 .

Throughout the calculation the window or time frame was from $t = 0$ through $t = \tau$ seconds, and the peaks are at τ_2 and τ_4 . Now if the time frame is $T2 - T1$ seconds where $\tau_1 < \tau_2 < T1$ and $\tau_4 < T2 < \tau$ as shown in Figure 3-3, we show by analysis in Appendix D and observe in Figure 3-4 that the only peak is at $\tau = T2 - T1$ or its multiples.

Damped Exponential Signal

For the damped exponential case the following function is used.

$$g(t) = (t - \tau_1) e^{-c(t - \tau_1)} u(t - \tau_1) + \alpha(t - \tau_2) e^{-c(t - \tau_2)} u(t - \tau_2) \quad (3-3)$$

which is shown in Figure 3-5. Taking Fourier transform of both sides of (3-3) gives

$$F[g(t)] = \int_{\tau_1}^{\tau} (t - \tau_1) e^{-c(t - \tau_1)} e^{-j\omega t} dt + \int_{\tau_2}^{\tau} (t - \tau_2) e^{-c(t - \tau_2)} e^{-j\omega t} dt \quad (3-4)$$

when, after some mathematical manipulations, the Fourier transform

*Keys for the figures are

- I WNDW = 1 windowing is performed
- I WNDW = 0 no windowing is performed
- I WNDF = 1 smoothing is performed
- I WNDF = 0 no smoothing is performed
- N = Total number of sample points in the original composite signal

$255(200 \times \pi \times (T - TRU1) \times U(T - TRU1) + B \times \cos(250 \times \pi \times (T - TRU2)) \times U(T - TRU2))$

Cepstrum Plot for Single Echo Cosine Waveform

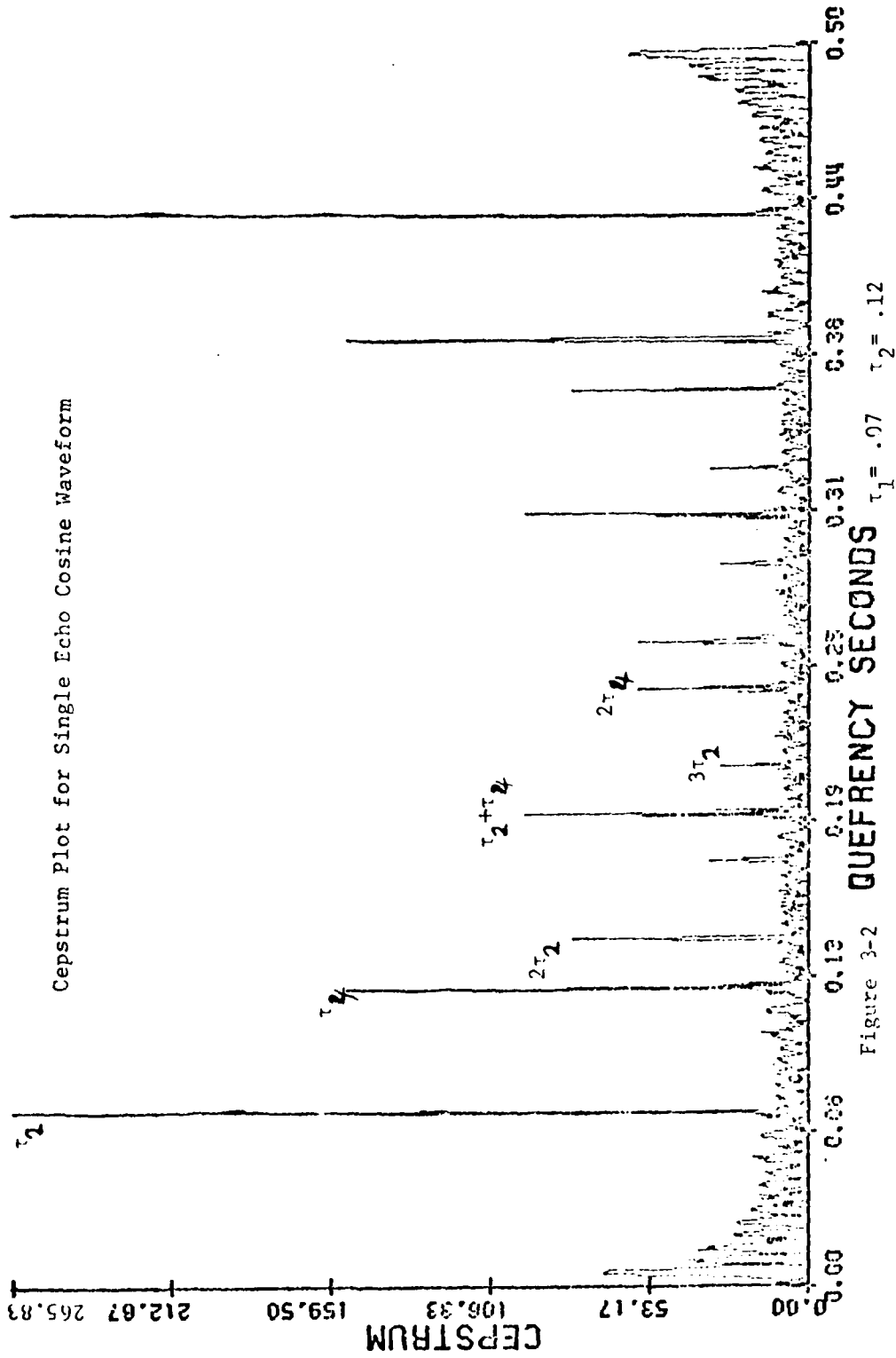


Figure 3-2 $\tau_1 = .07$ $\tau_2 = .12$

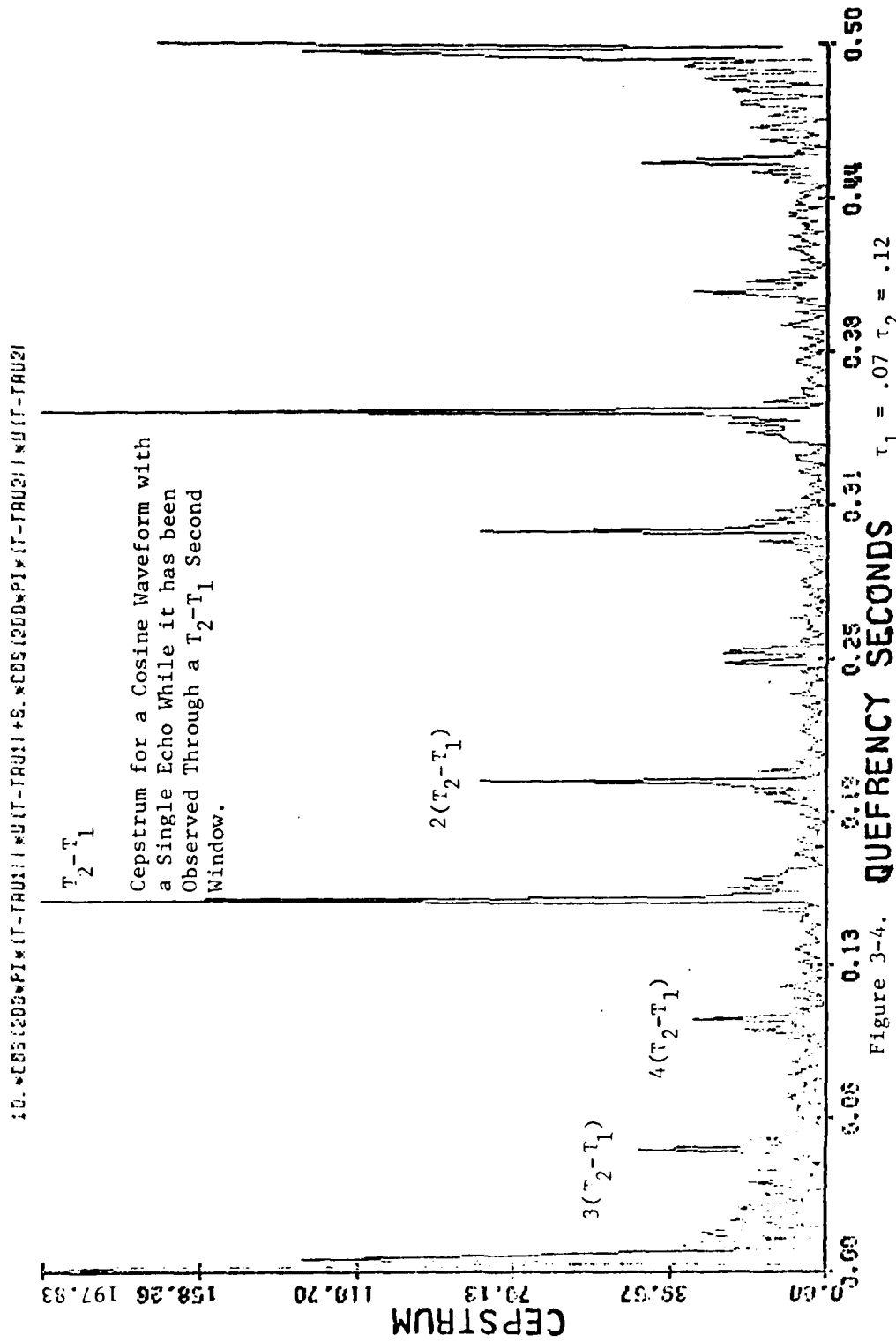


Figure 3-4.

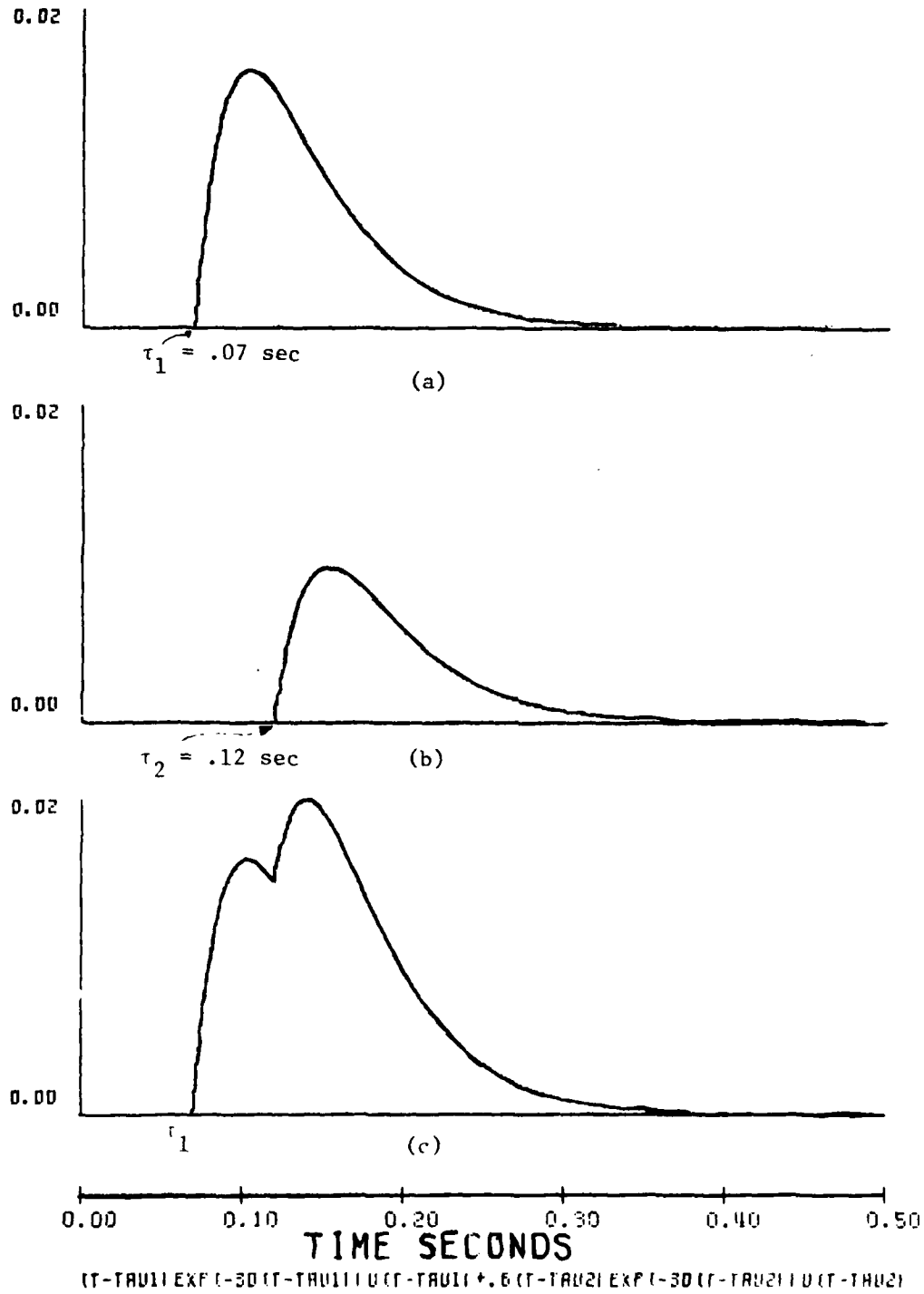


Figure 3-5. a) A damped exponential waveform,
b) its echo, c) the composite signal

has been calculated and the magnitude of the power spectrum is found one encounters terms such as

$$A \cos \omega (\tau - \tau_1) , \quad B \sin \omega (\tau - \tau_1) , \quad C \cos \omega (\tau - \tau_2) , \\ D \sin \omega (\tau - \tau_2) , \quad E \cos \omega (\tau_2 - \tau_1), \text{ and } F \sin \omega (\tau_2 - \tau_1)$$

Taking again the Fourier transform of the log spectrum of (3-4), one has to take Fourier transform of a few terms containing cosine and sine waveforms of τ_1, τ_2 and $\tau_2 - \tau_1$, which would result peaks at τ_1, τ_2 and $\tau_2 - \tau_1$. But as is shown in Appendix E, the magnitude of the ripples at τ_1 and τ_2 is very small and in the cepstrum plot of Figure 3-6 it is shown that it is not recognizable (it is safe to say that with the choice of c and α one might have different degree of distinguishability at τ_1 and τ_2). In fact we show in Appendix E for choice of $c = 30.$, $\tau = .5$, $\tau_1 = .07$ and $\tau_2 = .12$ seconds and $\alpha = .6$ this relative ratio is of the order 10^{-3} .

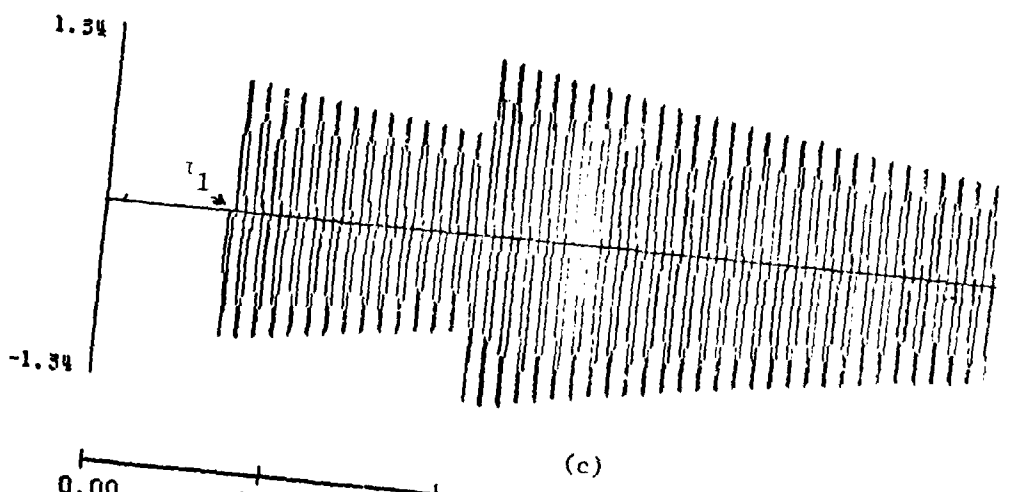
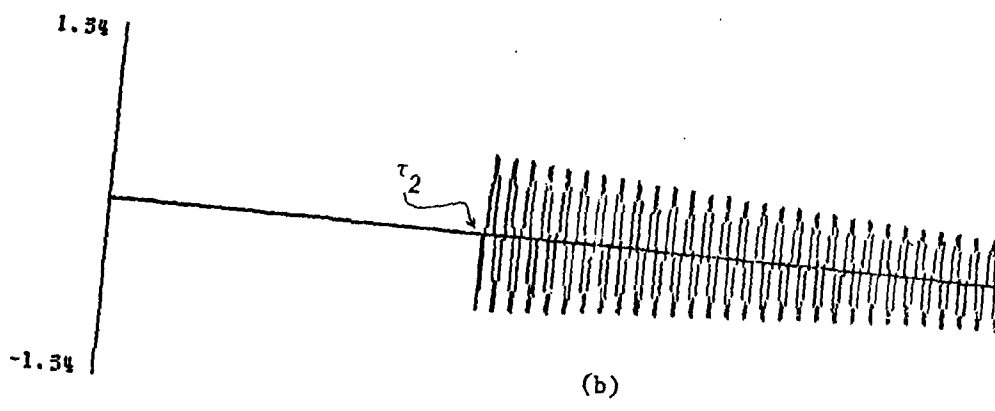
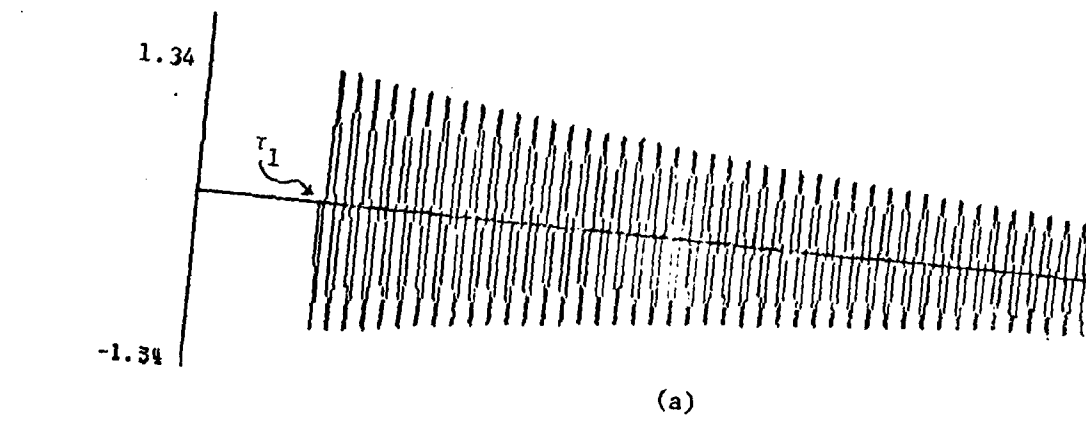
Damped Cosine Signal

In the damped cosine case the equation to be used is

$$g(t) = (t - \tau_1) \cos \omega_0 (t - \tau_1) e^{-c(t - \tau_1)} + (t - \tau_2) \cos \omega_0 (t - \tau_2) e^{-c(t - \tau_2)} \quad (3-5)$$

which is shown in Figure 3-7. Analytical calculation of the cepstrum for this case is extremely difficult, but experimental results have shown the cepstrum behaves like the cosine or damped exponential case, depending on values of c, α, τ_1 and τ_2 . In the next chapter the experimental results are discussed.

In all three cases if one takes into account the higher order terms in $\ln(1 + X)$ expansion, ripples are observed at $\tau_1 + \tau_2$ and its harmonics. Appendix C shows the existence of such ripples, at the points $\tau_2 - \tau_1$ and $\tau_2 + \tau_1$. Figures 3-7 and 3-8 show damped cosine waveform and its cepstrum respectively.



0.00 0.10 0.20 0.30 0.40 0.50
TIME SECONDS
DAMPED COSINE

Figure 3-7. a) A damped cosine waveform b) its echo, c) the composite signal

Cepstrum for a DAMPED COSINE Waveform With
A
Single Echo

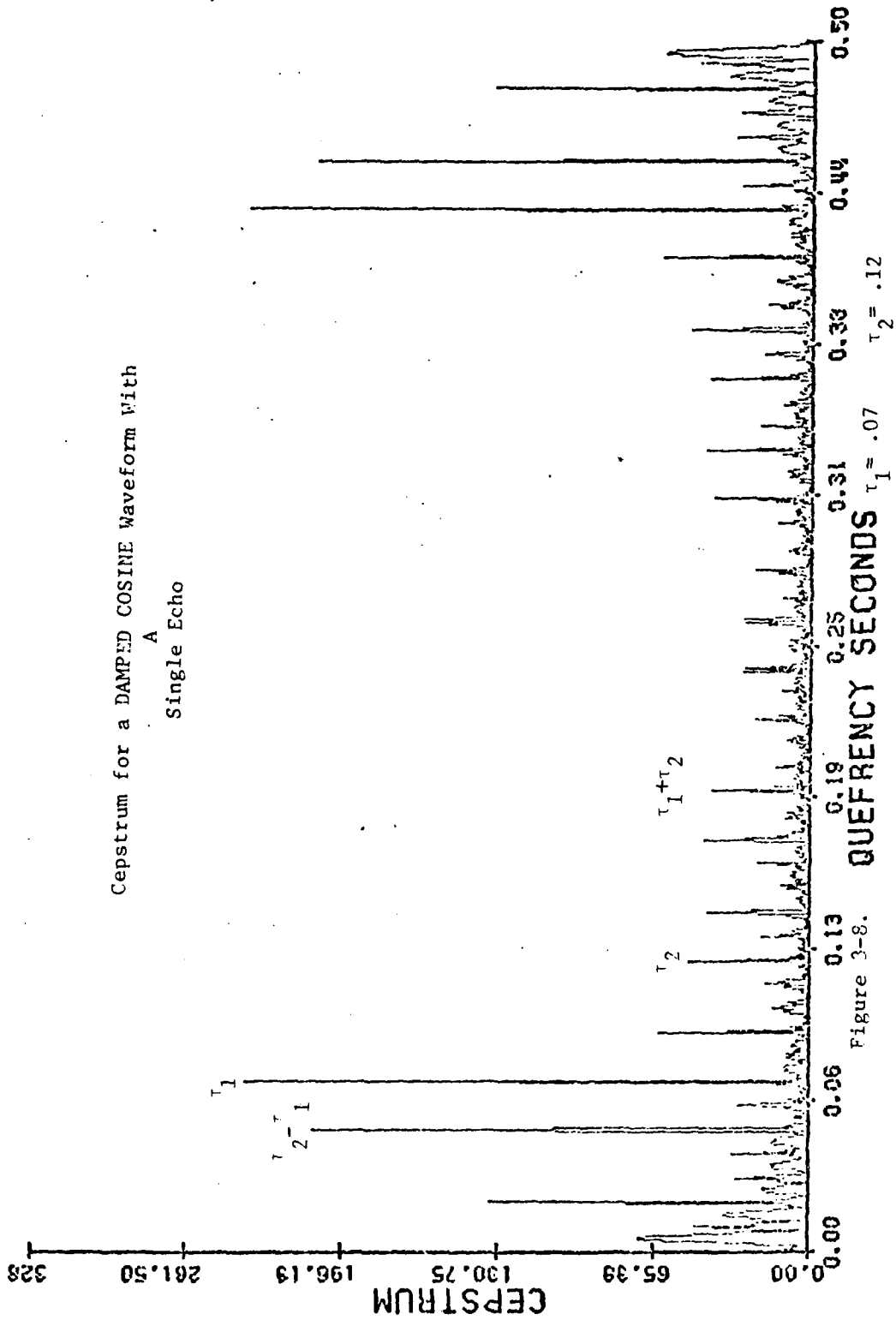


Figure 3-8.

CHAPTER IV

EXPERIMENTAL RESULTS

As previously stated the objective is to investigate the feasibility of applying cepstral analysis to echo or epoch detection. The study is conducted for two cases of noiseless and noisy conditions, with single or multiple echoes. The computer study is performed using Univac 1108 computer at Mississippi State University Computing Center.

Noiseless Case (Single Echo)

For the study of single echo, three types of signals; cosine, damped exponential, and damped cosine waveforms were chosen. The choice for cosine waveform is

$$\cos(200\pi(t - \tau_1))u(t - \tau_1) + .6 \cos(200\pi(t - \tau_2))u(t - \tau_2) \quad (4-1)$$

The above equation is comprised of two parts, the first part being the original signal and the second part the echo. If τ_1 is not zero one has the case of epoch detection for the original signal and echo or epoch detection for the second signal.

The total length of the time window is .5 seconds. The signals are sampled at 2048 samples per second and the delay times are $\tau_1 = 0.0$, $\tau_2 = .01$, and $.05$ seconds. Also the cases of $\tau_1 = .07$, $\tau_2 = .12$, and $\tau_2 = .21$ seconds are discussed. For each case of τ_1 and τ_2 the study is conducted in four different manners:

1. with no windowing or smoothing (NW,NS)
2. with no windowing but smoothing (NW,S)

3. with windowing but not smoothing (W,NS)

4. with windowing and smoothing (W,S)

In case 1, when no windowing or smoothing is used the signal is sampled, its Fourier transform and consequently its power spectrum is found and then the Fourier transform of logarithm of this power spectrum is calculated to give the new power spectrum or the cepstrum. In case 2, the windowing is performed in the time domain, before the first Fourier transform is calculated. The windowing process is based on Kaiser-Bessel equations with $\beta = 8$. In case 3, the smoothing process only is used. The smoothing process is based on the Hanning method. The smoothing is performed after finding the log spectrum and when ready to start the Fourier transform operation again. In case 4, both windowing and smoothing are done.

The results are illustrated in Appendix G showing that neither windowing nor smoothing was of any help in detecting the echo, or epoch delay time. Tables 4-1a and 4-1b show what effects the use of windowing and/or smoothing create. In other parts of the study τ_2 was chosen to be a multiple of τ_1 so $\tau_2 - \tau_1$ again is one of the harmonics of τ_1 . The result is obvious, as one sees a higher peak is at $\tau_2 - \tau_1$ only, with no significant difference in the value of the cepstrum at other points. These results are shown at Table 4-2 and can be compared with the values at Table 4-1b. The reason for this increase in value of the cepstrum is that instead of having only the amount of cepstrum at this point, harmonics of the cepstrum at point τ_1 add to the original cepstrum.

Included in the study was variation of the cepstrum as α or τ_2 or both were changed. Tables 4-3a and 4-3b show variation of cepstrum for a fixed τ_2 and variable α . As may be seen the value of the cepstrum remains almost the same in the range of $\alpha = .2$ to $\alpha = 1.6$. Table 4-3b shows the normalized values of cepstrum in Table 4-3a. In table 4-4a the value of the cepstrum at some important points is presented and as may be seen, changing α changes the value of the cepstrum (notice here τ_1 is no more zero). These results comply with what was found in Appendix C. Table 4-4b is the normalized form of Table 4-4a*.

TABLE 4-1a

POWER CEPSTRUM AT/FOR	NW,NS	NW,S	W,NS	W,S
$\tau_2 = .01$	381.339	339.922	54.4870	6.3023
$\tau_2 = .05$	415.792	290.384	47.9950	4.9561

Effect of using windowing and/or smoothing on the power cepstrum of cosine waveform, see Figures in Appendix G -1a, 2a for time waveform and Figures in Appendix G-1b, 2b for cepstrum plots. τ_2 shows the location of the highest peak value as well as being the epoch or delay time for the echo signal. $\tau_1 = 0$ for both cases.

* Key to the tables

NW: means no windowing is performed
 W: means windowing is performed
 NS: means no smoothing is performed
 S: means smoothing is performed

TABLE 4-1b

POWER CEPSTRUM AT/FOR	NW,NS	NW,S	W,NS	W,S
τ_1	265.834	38.6806	6.3689	.5999
τ_2	154.062	31.1605	5.2801	.3493
$\tau_2 - \tau_1$	14.4831	130.409	24.409	2.61198
$\tau_2 + \tau_1$	94.4225	37.1550	5.5992	.1950

Value of the power cepstrum at the epoch times as well as at the difference and sum of the epoch times for $\tau_1 = .07$ and $\tau_2 = 0.12$ seconds for a cosine type waveform (see Figure G-3), also of notice is the effect of windowing and/or smoothing.

TABLE 4-2

POWER CEPSTRUM AT/FOR	NW,NS	NW,S	W,NS	W,S
τ_1	264-2950	9.6876	1.3447	.1123
τ_2	158-4480	18.6844	3.4655	.1072
$\tau_2 - \tau_1$	76.9708	27.1098	4.1172	.2226
$\tau_1 + \tau_2$	95.4120	41.1492	7.4753	.1962

This table is similar to Table 4-1b except $\tau_2 = .21$ seconds is a multiple integer of $\tau_1 = .07$ seconds. See Figures G-4a and G-4b for the waveform and its cepstral plot.

TABLE 4-3a

CEPSTRUM AT	$\alpha = .2$	$\alpha = .4$	$\alpha = .6$	$\alpha = .8$	$\alpha = 1.0$	$\alpha = 1.2$	$\alpha = 1.4$	$\alpha = 1.6$
$\tau_2 = .01$	379.91	380.86	381.34	381.64	381.84	381.99	382.11	382.21
$\tau_2 = .03$	411.34	412.28	412.76	413.06	413.26	413.42	413.54	413.63
$\tau_2 = .05$	414.34	415.30	415.79	416.10	416.31	416.47	416.60	416.69
$\tau_2 = .07$	420.37	421.34	421.83	422.15	422.37	422.53	422.65	422.76
$\tau_2 = .1$	411.04	411.98	412.47	412.78	412.99	413.16	413.28	413.38

Variation of magnitude of the power cepstrum of
a cosine type waveform when τ_2 and α are changing.

TABLE 4-3b

CEPSTRUM FOR/AT	$\alpha = .2$	$\alpha = .4$	$\alpha = .6$	$\alpha = 0.8$	$\alpha = 1.0$	$\alpha = 1.2$	$\alpha = 1.4$	$\alpha = 1.6$
$\tau_2 = .01$.90	.90	.90	.90	.90	.90	.90	.90
$\tau_2 = .03$.97	.98	.98	.98	.98	.98	.98	.98
$\tau_2 = .05$.98	.98	.98	.98	.98	.99	.99	.99
$\tau_2 = .07$.99	1.00	1.00	1.00	1.00	1.00	1.00	1.00
$\tau_2 = .1$.97	.97	.98	.98	.98	.98	.98	.98

Normalized form of Table 4-3a

TABLE 4-4a

CEPSTRUM AT/FOR	$\alpha = .2$	$\alpha = .4$	$\alpha = .6$	$\alpha = .8$	$\alpha = 1.0$	$\alpha = 1.2$	$\alpha = 1.4$	$\alpha = 1.6$
$\tau_1 - \tau_2$	15.53	16.39	14.48	13.46	12.32	13.94	15.07	15.48
τ_1	357.20	303.25	256.83	236.01	212.35	190.40	172.35	157.63
τ_2	63.45	113.60	154.06	185.00	210.01	227.90	243.05	256.44
$\tau_1 + \tau_2$	53.01	79.52	94.42	100.67	102.91	100.20	96.82	93.57

Cepstrum values at $\tau_2 - \tau_1$, τ_1 , τ_1 and $\tau_1 + \tau_2$ for a cosine type waveform when α changes and $\tau_1 = .07$, $\tau_2 = .12$ seconds are fixed. See Figure G-17.

TABLE 4-4b

CEPSTRUM AT/FOR	$\alpha = .2$	$\alpha = .4$	$\alpha = .6$	$\alpha = .8$	$\alpha = 1.0$	$\alpha = 1.2$	$\alpha = 1.4$	$\alpha = 1.6$
$\tau_1 - \tau_2$.04	.05	.04	.04	.03	.04	.04	.04
τ_1	1.00	.85	.72	.66	.59	.53	.48	.44
τ_2	.18	.32	.43	.52	.59	.64	.68	.72
$\tau_1 + \tau_2$.15	.22	.26	.28	.29	.28	.27	.26

Normalized form of Table 4-4a

The damped exponential signal with a single echo is

$$(t - \tau_1) e^{-30(t-\tau_1)} u(t-\tau_1) + .6 (t - \tau_2) e^{-30(t-\tau_2)} u(t-\tau_2) \quad (4-2)$$

with equation (4-2) being comprised of two parts, the first part the original signal and the second part the echo. The damping coefficient has been chosen so as to drive the signal down in a way which approximates some physical phenomenon which we are modeling. As in the previous case, the study is done for four different conditions depending on the use of windowing and/or smoothing.

Table 4-5a shows variation of the power cepstrum and effect of windowing and/or smoothing on the power cepstra when $\tau_1 = 0$ and τ_2 assumes two different values. Table 4-5b shows the power cepstrum at four important points when $\tau_1 = .07$ and $\tau_2 = .12$ seconds with $\alpha = .6$. Table 4-5c shows the peak value at the same four locations as for Table 4-5b but for this table τ_2 is an integer multiple of the τ_1 . As mentioned in the case of cosine signals windowing or smoothing would not do any good, but rather it actually degrades the results.

Looking closely in Table 4-5b one finds it interesting to see that the highest peak value of the power cepstrum is located at $\tau_2 - \tau_1$, the same place as was mentioned in Chapter III. For this Table C, the damping coefficient, is equal to 30.0. As was previously noted the location of the highest peak value is very much related to the damping coefficient. In Appendix G it may be seen how changing C, the damping coefficient, changes the location of the highest peak or its value in the cepstrum plot.

TABLE 4-5a

POWER CEPSTRUM AT/FOR	NW,NS	NW,S	W,NS	W,S
$\tau_2 = .01$	173.026	41.6319	5.3620	.6055
$\tau_2 = .05$	63.347	20.6159	2.3575	.2350

Effect of using windowing and/or smoothing on the power cepstrum of damped exponential waveform. τ_2 shows the location of the highest peak value as well as being the epoch or delay time for echo signal. $\tau_1 = 0$ for both cases. For the waveforms and their cepstral plots see Figure G-11 and G-12.

TABLE 4-5b

POWER CEPSTRUM AT/FOR	NW,NS	NW,S	W,NS	W,S
τ_1	.5413	3.7263	.5501	.0491
τ_2	2.3317	.7425	.1281	.0098
$\tau_2 - \tau_1$	257.817	28.2807	3.2023	.3175
$\tau_2 + \tau_1$.2384	.4015	.0756	.0036

Value of the power cepstrum at the epoch times as well as at the difference and sum of the epoch times for $\tau_1 = .07$ and $\tau_2 = 0.12$ seconds for a damped exponential waveform, also of notice is the effect of windowing and/or smoothing. See Figures G-13a, 13b,c,d,e, for the waveform and its cepstral plot.

TABLE 4-5c

POWER CEPSTRUM AT/FOR	NW,NS	NW,S	W,NS	W,S
τ_1	10.2740	3.6232	.6234	.0565
τ_2	42.4780	1.5976	.2140	.0086
$\tau_2 - \tau_1$	294.2910	19.5166	2.3079	.1241
$\tau_2 + \tau_1$	83.9251	2.5583	.3056	.0106

This table is similar to Table 4-5b except $\tau_2 = .21$ seconds is a multiple integer of $\tau_1 = .07$ seconds for the waveforms. See Figures G-14a, 14b.

The following waveform is chosen for the study of damped cosine signals (4-3) being comprised of two parts, the original

$$e^{-2(t-\tau_1)} \cos(200\pi(t-\tau_1)) + .6 e^{-2(t-\tau_2)} \cos(200\pi(t-\tau_2)) u(t-\tau_2) \quad (4-3)$$

signal and the echo signal. Looking closely at (4-3) we will find it to be a combined form of (4-1) and (4-2), with a different damping coefficient. As was mentioned in Chapter III, the damping coefficient plays an important role in shaping the cepstrum and the damping coefficient has been chosen after careful study of the cepstrum plots. The study is done for four different cases depending on whether we have used windowing and/or smoothing.

Table 4-6a shows variation of the power cepstrum and effect of windowing and/or smoothing on the power cepstra when

$\tau_1 = 0$ and τ_2 assumes two different values. Table 4-6b shows the power cepstrum at four important points when $\tau_1 = .07$ and $\tau_2 = .12$ seconds with $\alpha = .6$. Table 4-6c shows the peak value at the same four locations as for Table 4-6b but for this table τ_2 is an integer multiple of τ_1 . As was mentioned for the two previous cases, windowing or smoothing would not do any good, but rather it actually degrades the results.

Looking closely at table 4-6b we notice that the behavior of this case is like the behavior of two previous cases combined together meaning that we have noticeable peaks at τ_1 , τ_2 and $\tau_2 - \tau_1$. For this Table c, the damping coefficient is equal to 2 and the frequency of cosine signal is 100 Hz same as for cosine type case. As we said earlier location and the height (strength) of the highest peak very much is dependent on the damping coefficient. In Appendix G we will see how changing c , the damping coefficient, has changed the shape of the cepstrum plot.

TABLE 4-6a

POWER CEPSTRUM AT/FOR	NW,NS	NW,S	W,NS	W,S
$\tau_2 = .01$	326.876	177.362	28.9625	3.3593
$\tau_2 = .05$	292.795	196.807	33.6112	3.4963

Effect of using windowing and/or smoothing on the power cepstrum of damped cosine waveform. τ_2 shows the location of the highest peak value as well as being the epoch or delay time for echo signal. $\tau_1 = 0$ for all two cases. For the waveforms and their cepstral plots, see Figures G-6 and G-7.

TABLE 4-6b

POWER CEPSTRUM AT/FOR	NW,NS	NW, S	W,NS	W,S
τ_1	236.7580	120.3460	20.7965	1.9372
τ_2	50.9903	4.4276	1.4184	0.1101
$\tau_2 - \tau_1$	207.6670	108.0450	18.2647	1.8819
$\tau_2 + \tau_1$	41.0980	17.9547	1.9821	.0645

Value of the power cepstrum at the epoch times as well as at the difference and sum of the epoch times for $\tau_1 = .07$ and $\tau_2 = 0.12$ seconds for a damped cosine waveform, also of notice is the effect of windowing and/or smoothing. See Figure G-8 for the waveform and its cepstral plot.

TABLE 4-6c

POWER CEPSTRUM AT/FOR	NW,NS	NW,S	W,NS	W,S
τ_1	246.4780	181.1640	31.6476	2.9500
τ_2	71.8209	21.5712	6.5571	.2030
$\tau_2 - \tau_1$	181.6310	74.9125	12.1095	.6719
$\tau_2 + \tau_1$	54.0482	10.1252	.9468	.0229

This table is similar to Table 4-6b except $\tau_2 = .21$ seconds is a multiple integer of $\tau_1 = .07$ seconds. See Figure G-9 for the waveform and its cepstral plot.

Multiple Echoes

Because of complexity in the case of multiple echoes we restricted our study for two and three echo cases. As we can see from Figures 4-1 through 4-4, when the number of echoes increases, it becomes very difficult to detect the delay time of these echoes. In study of multiple echoes for the cosine waveforms we tried to change the time between two echoes and see the effect on the power cepstrum. As we see in Table 4-7a, if α is fixed there is no change in the magnitude of the power cepstrum, at the two epoch times, but the value of the cepstrum changes at the sum and the difference of the epoch times. This will further show the dependence of the power cepstrum on epoch times as well as other parameters. Table 4-7b shows the normalized values of Table 4-7a. For more plots of multiple echo case see Appendix G.

Table 4-8, 4-9 and 4-10 show the magnitude of the cepstrum at some important points for two echo cases also reflects the effect of windowing and smooting, notice we have peaks at the time difference as well as sum of delay times. This is exactly what we expect from a cepstrum plot.

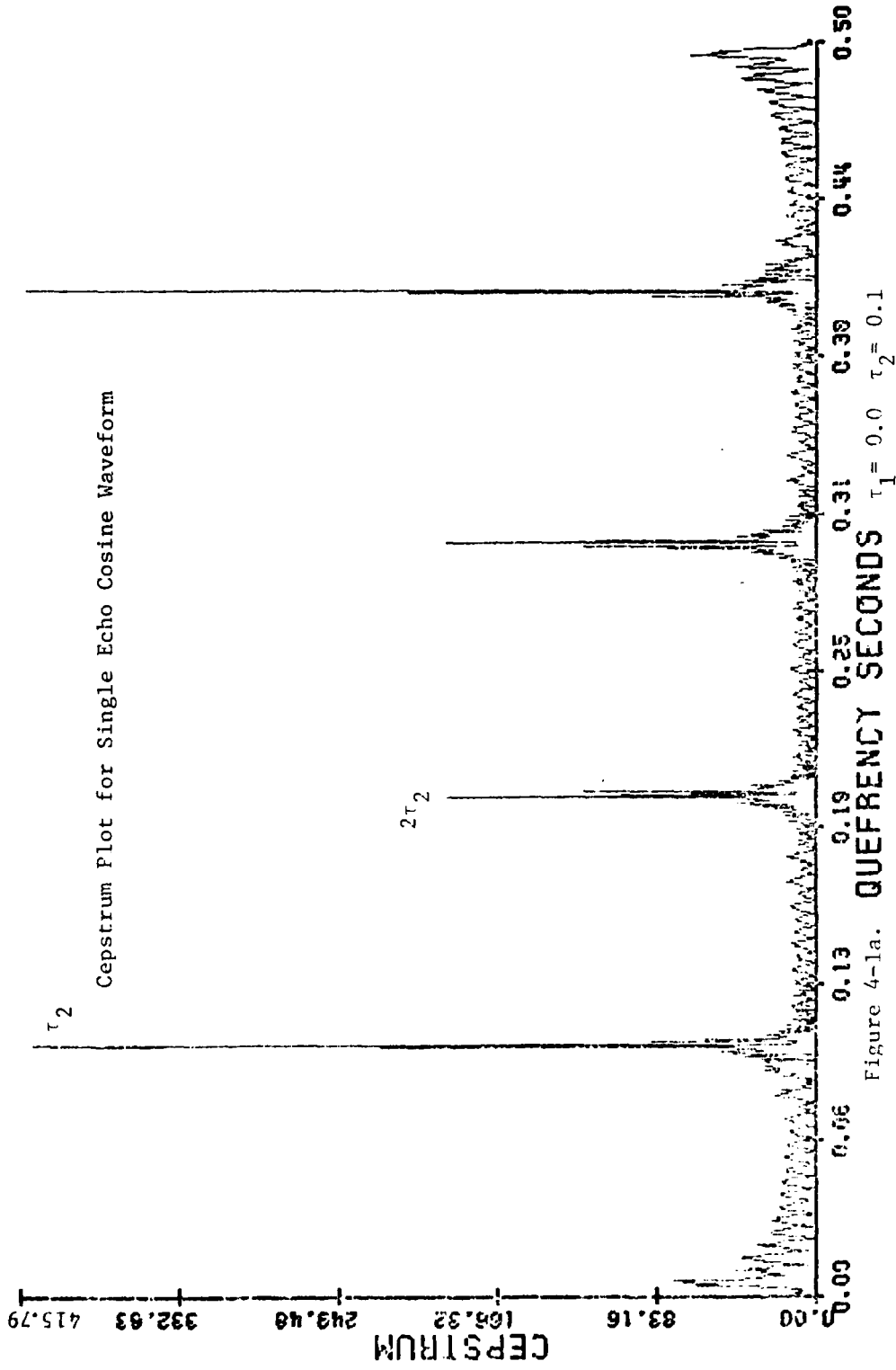


Figure 4-1a.

$$(T - T_0) \cdot \exp(-30 \cdot (T - T_0)) + (T - T_0) \cdot \exp(-1.6 \cdot (T - T_0)) + (T - T_0) \cdot \exp(-30 \cdot (T - T_0)) + (T - T_0) \cdot \exp(-1.6 \cdot (T - T_0))$$

Cepstrum Plot for Single Echo Damped
Exponential Waveform

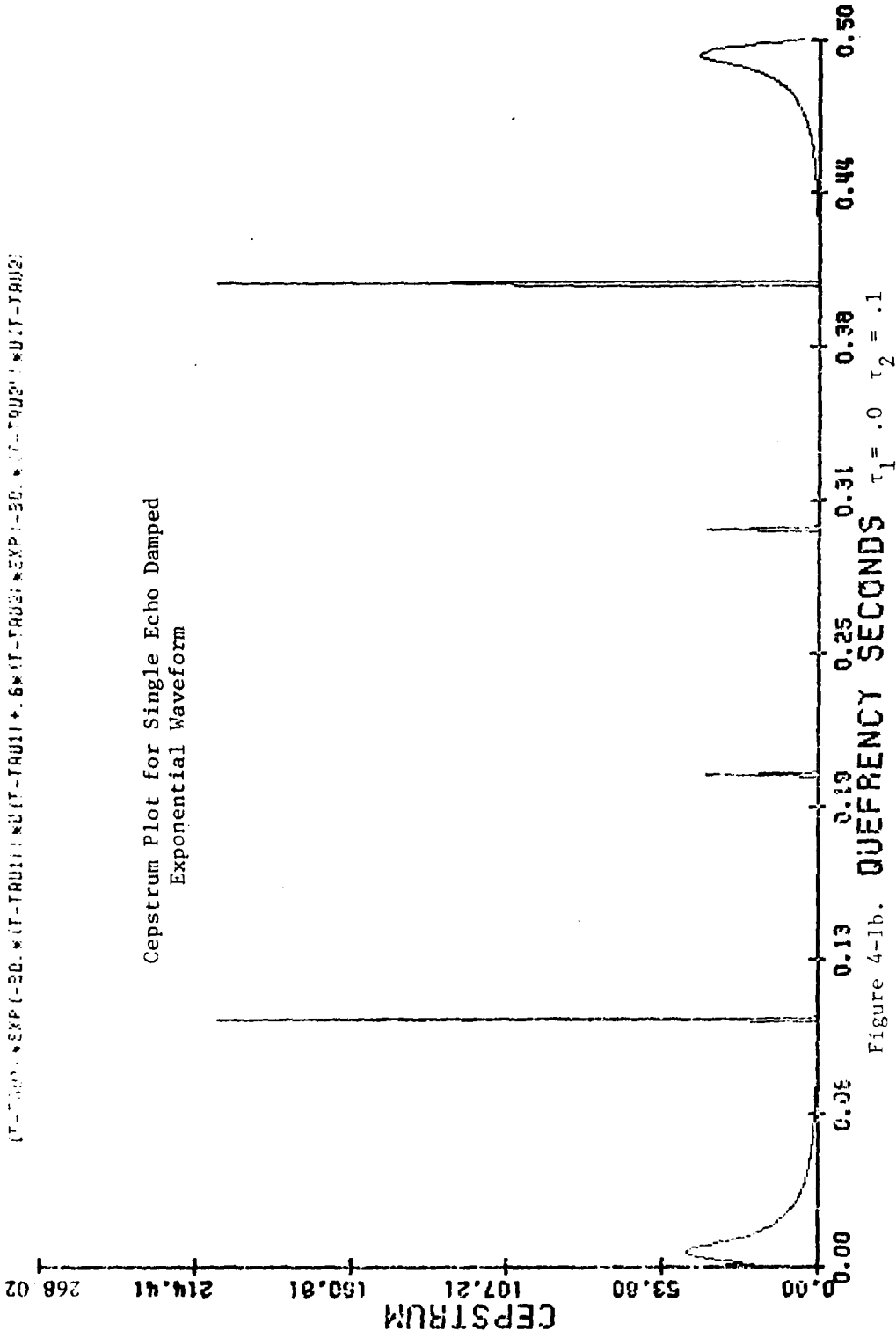
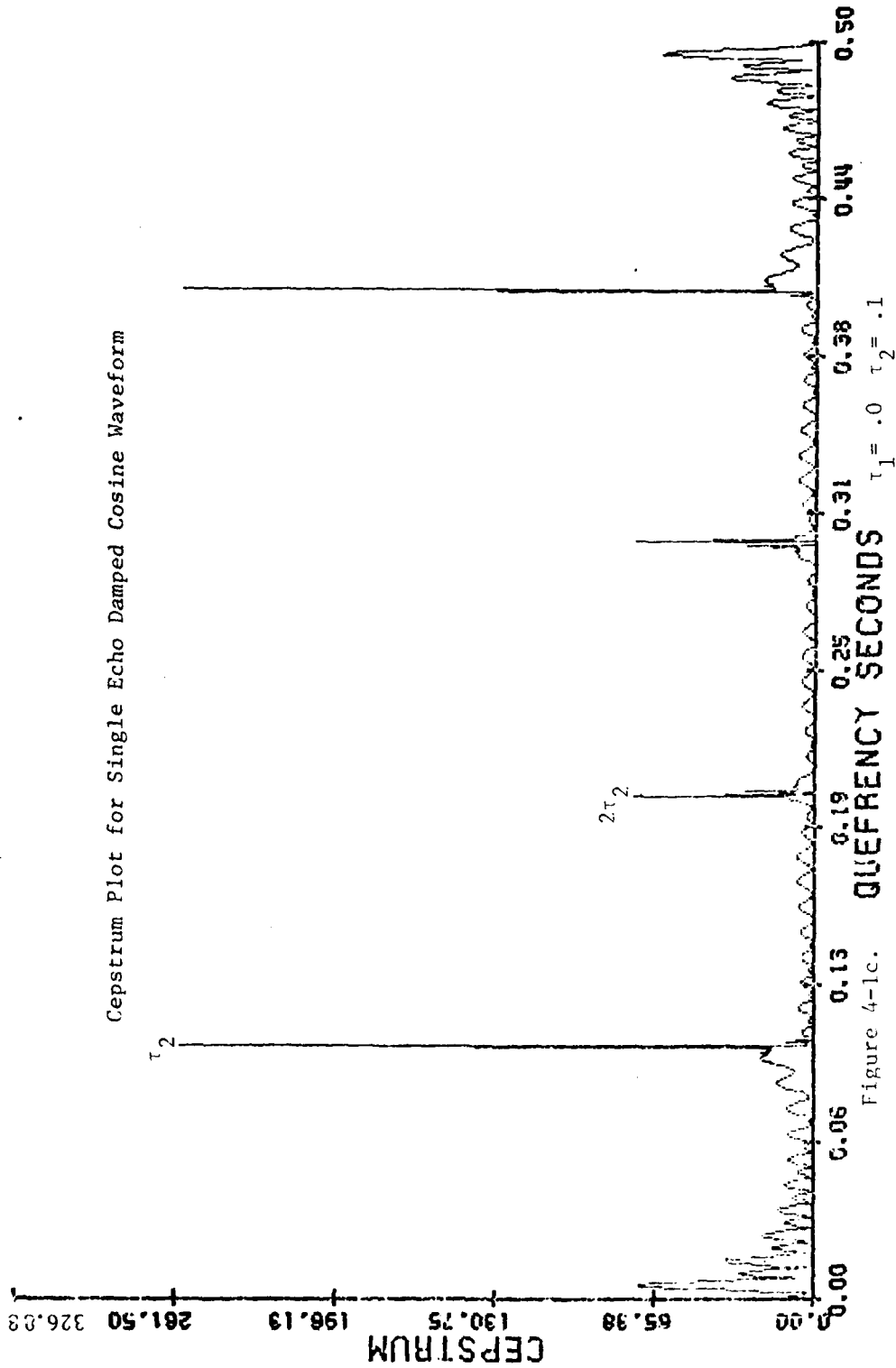


Figure 4-Ib. $\tau_1 = .0$ $\tau_2 = .1$

Cepstrum Plot for Single Echo Damped Cosine Waveform



0851200*PI*IT (PUSI) *OUT-TRUSI + B*005 1250*P2*IT-T200I *BIT-TRUSI

Cepstrum Plot for Single Echo Cosine Waveform

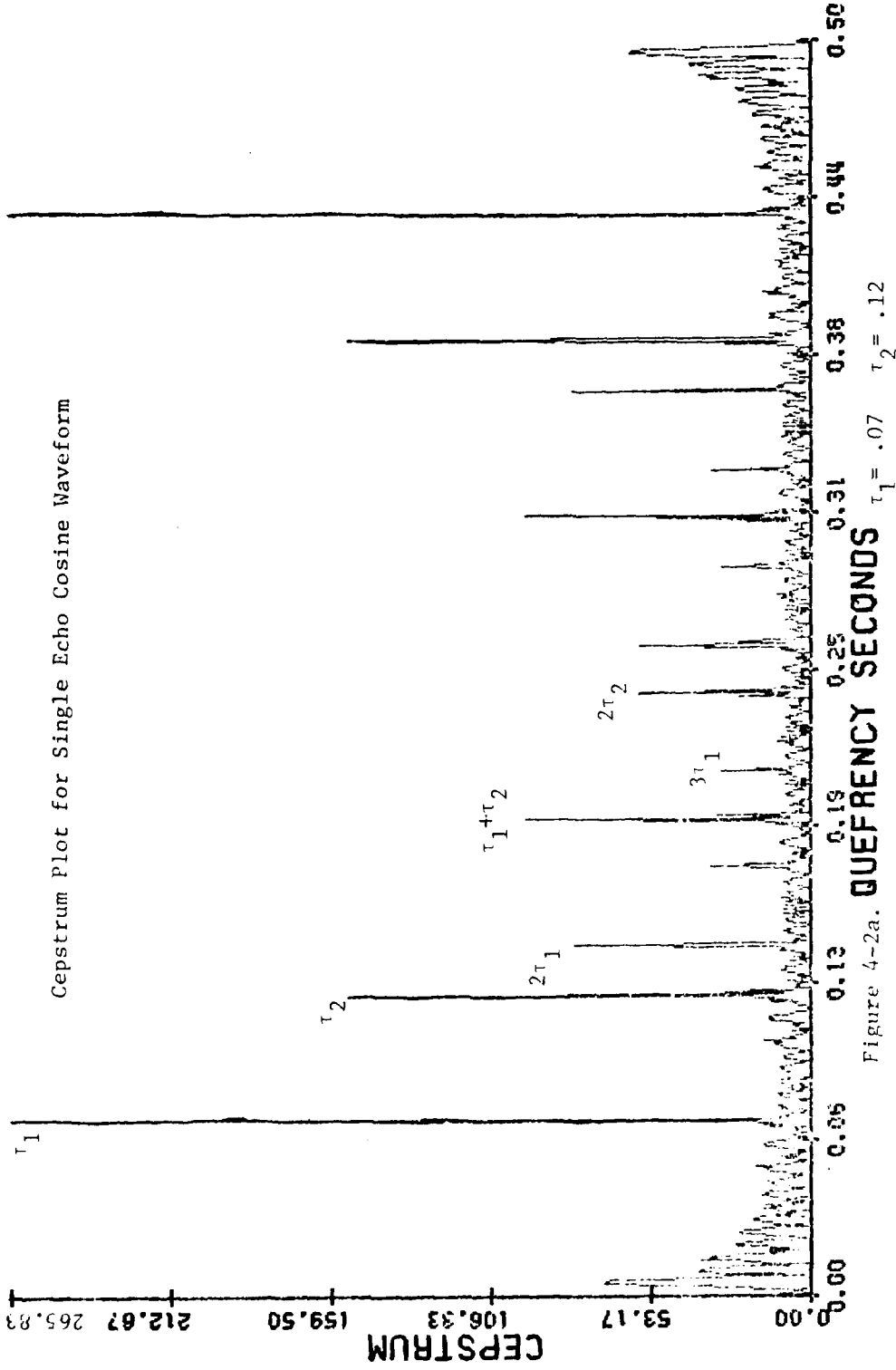


Figure 4-2a. $\tau_1 = .07$ $\tau_2 = .12$

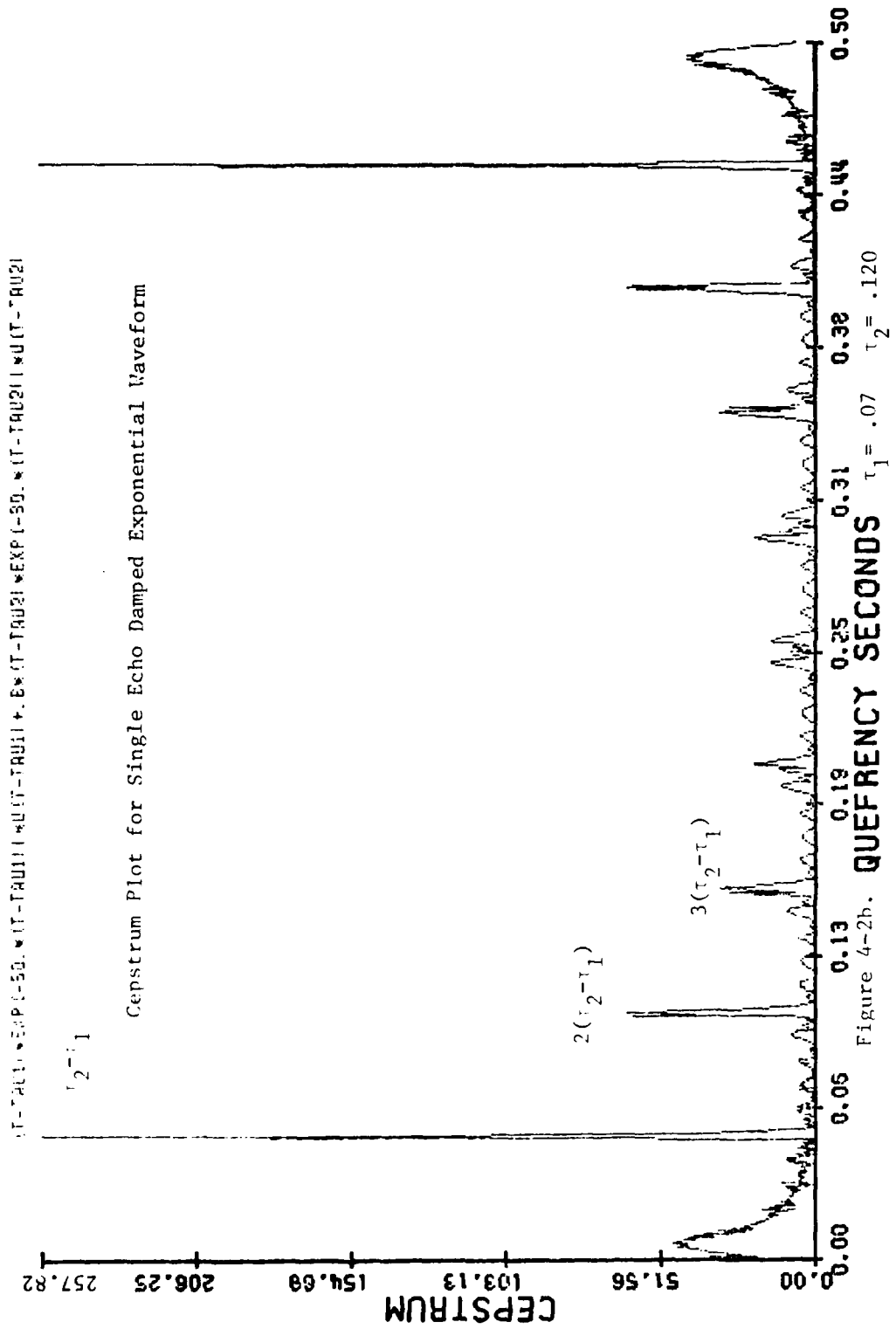


Figure 4-2b.

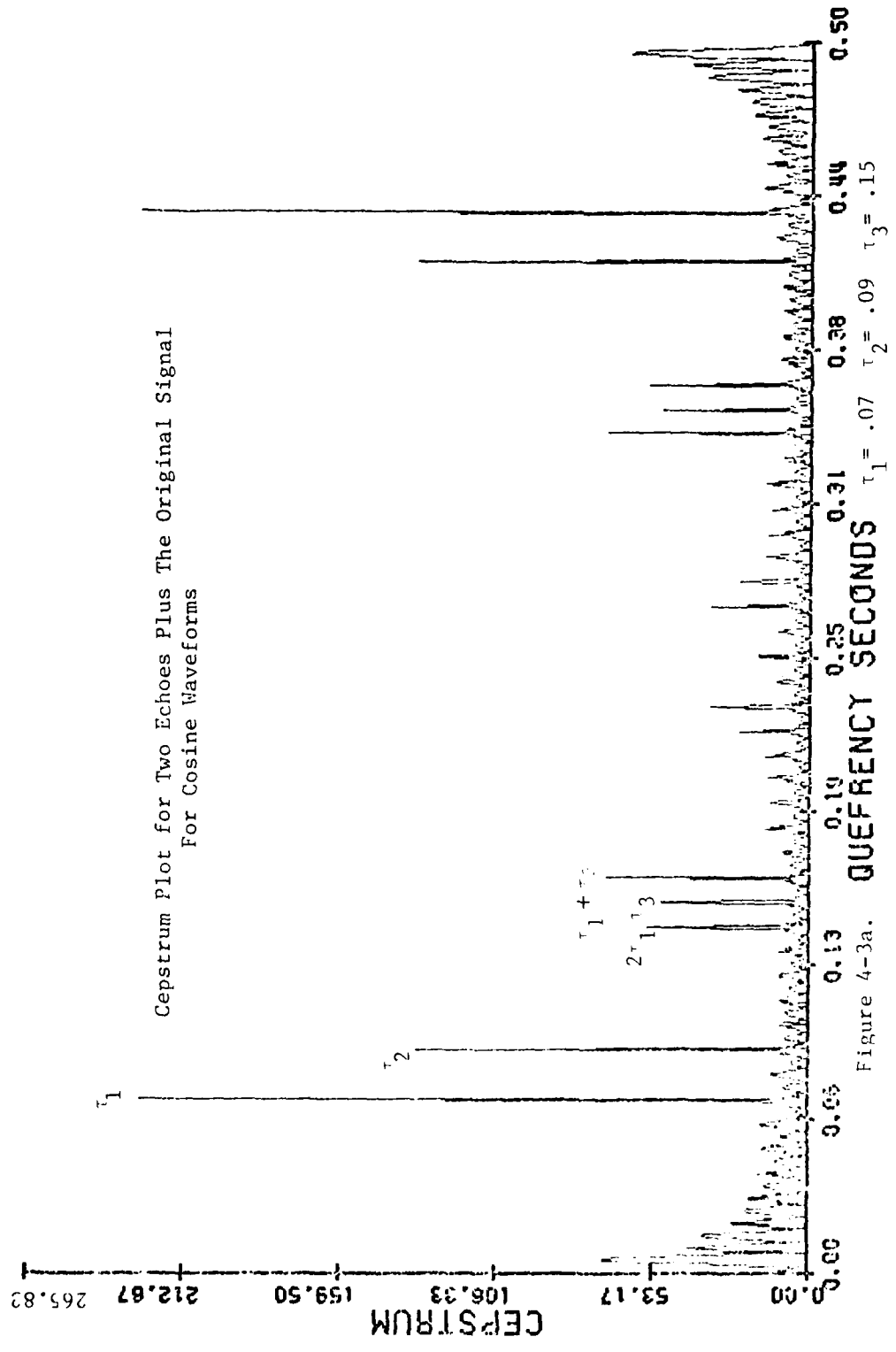


Figure 4-3a.

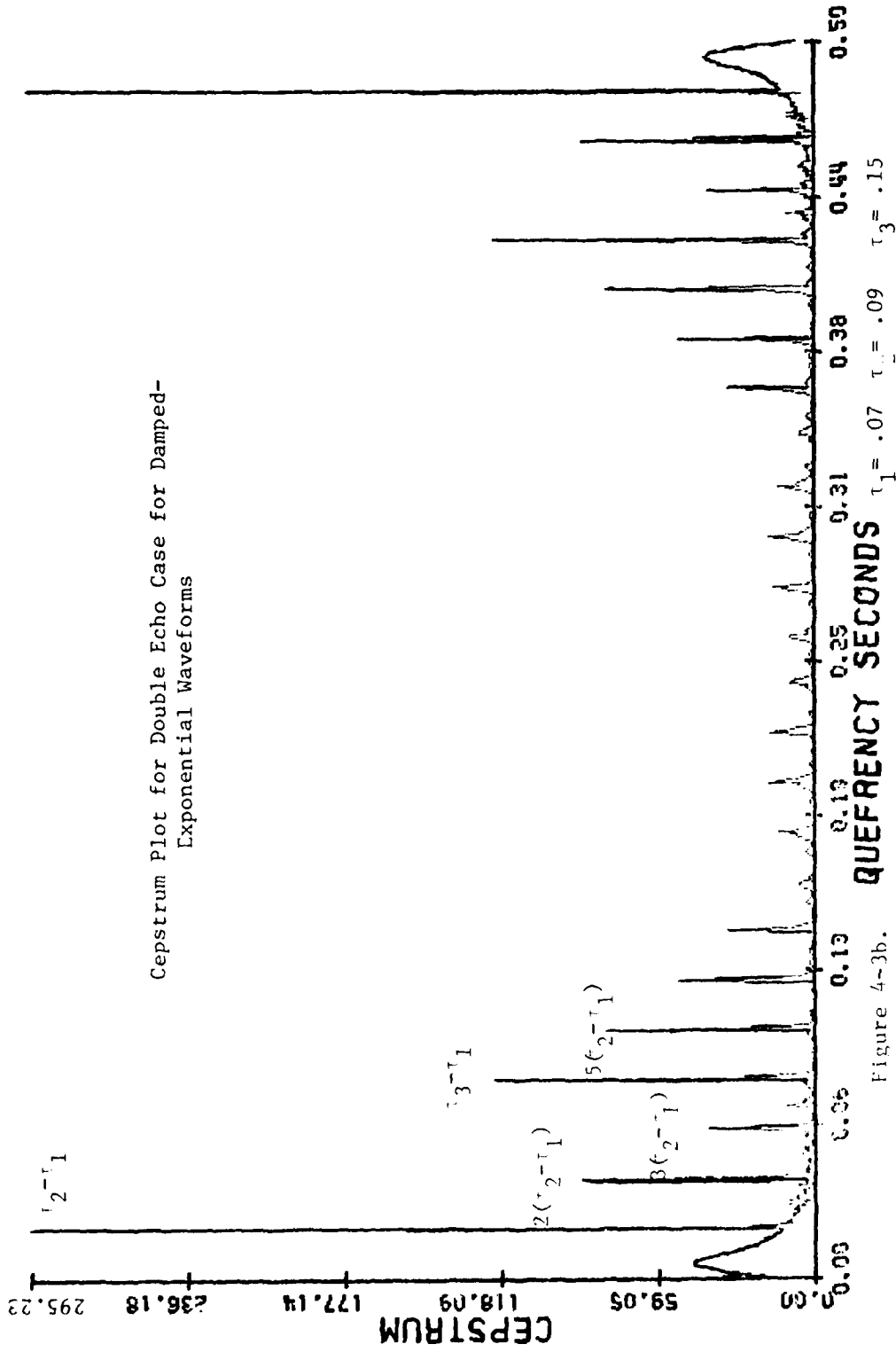


Figure 4-3b.

DAMPED COSINE

Double Echo Case

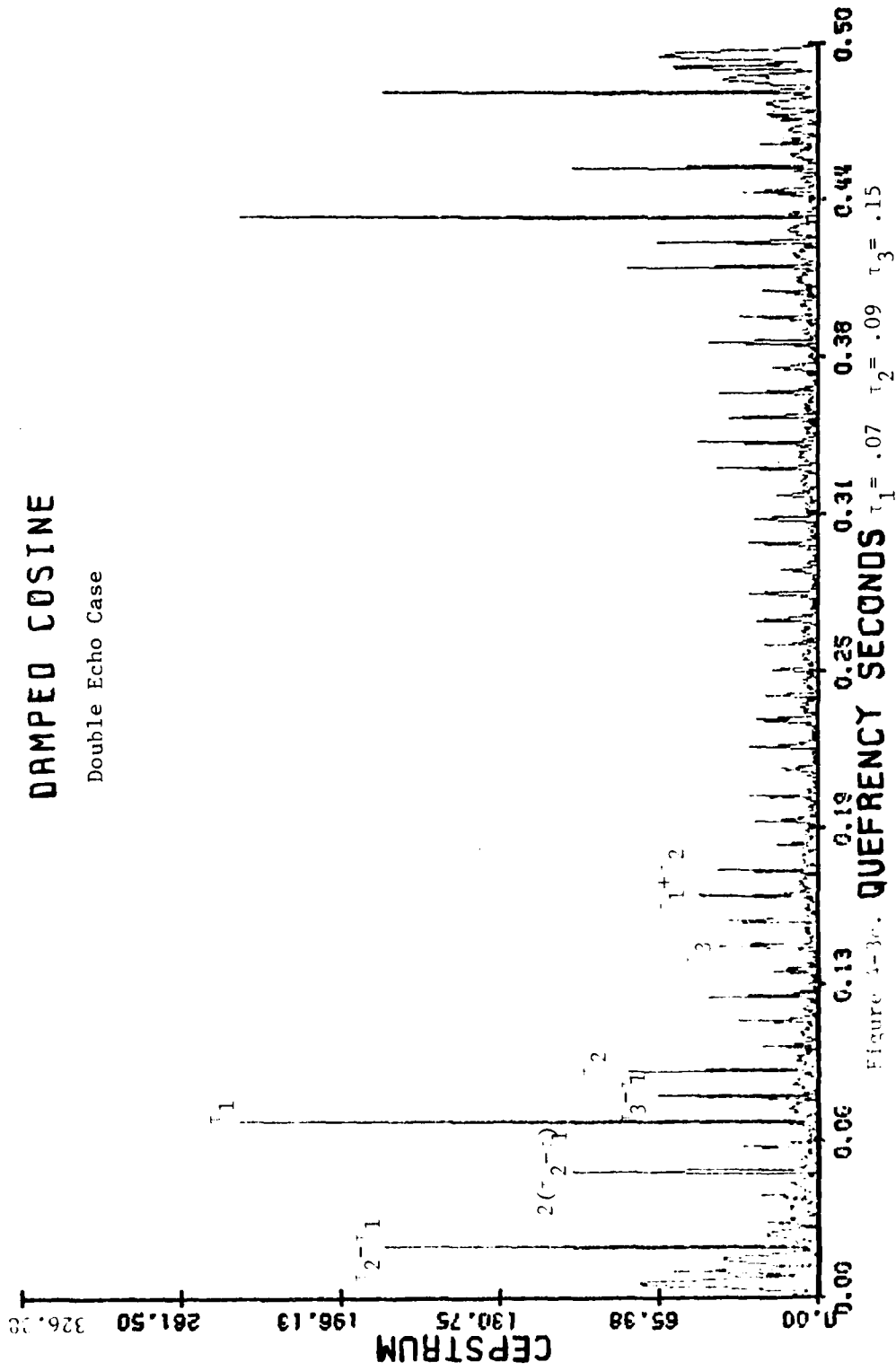


Figure 1-3a. $\tau_1 = .07$ $\tau_2 = .09$ $\tau_3 = .15$

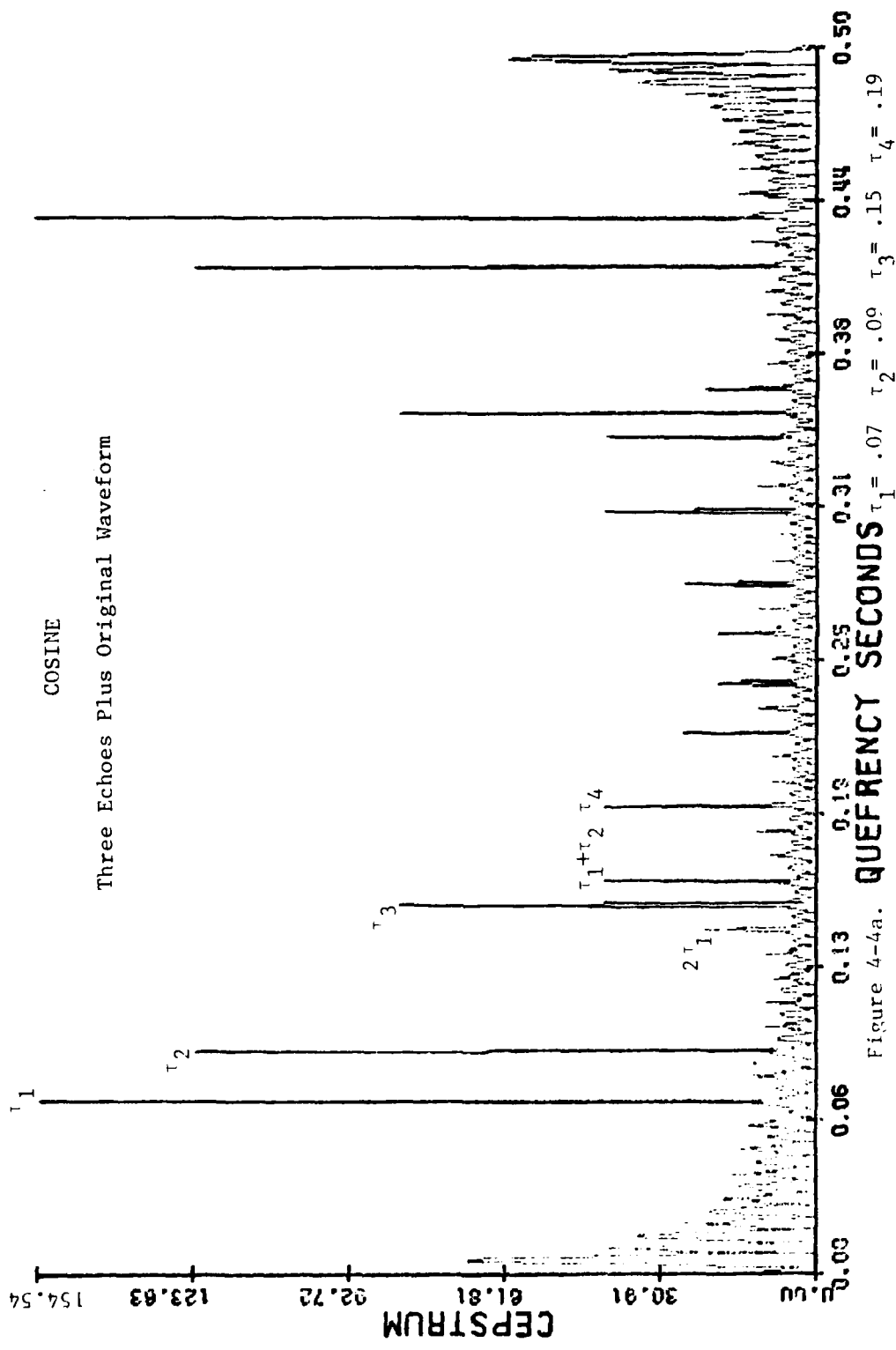
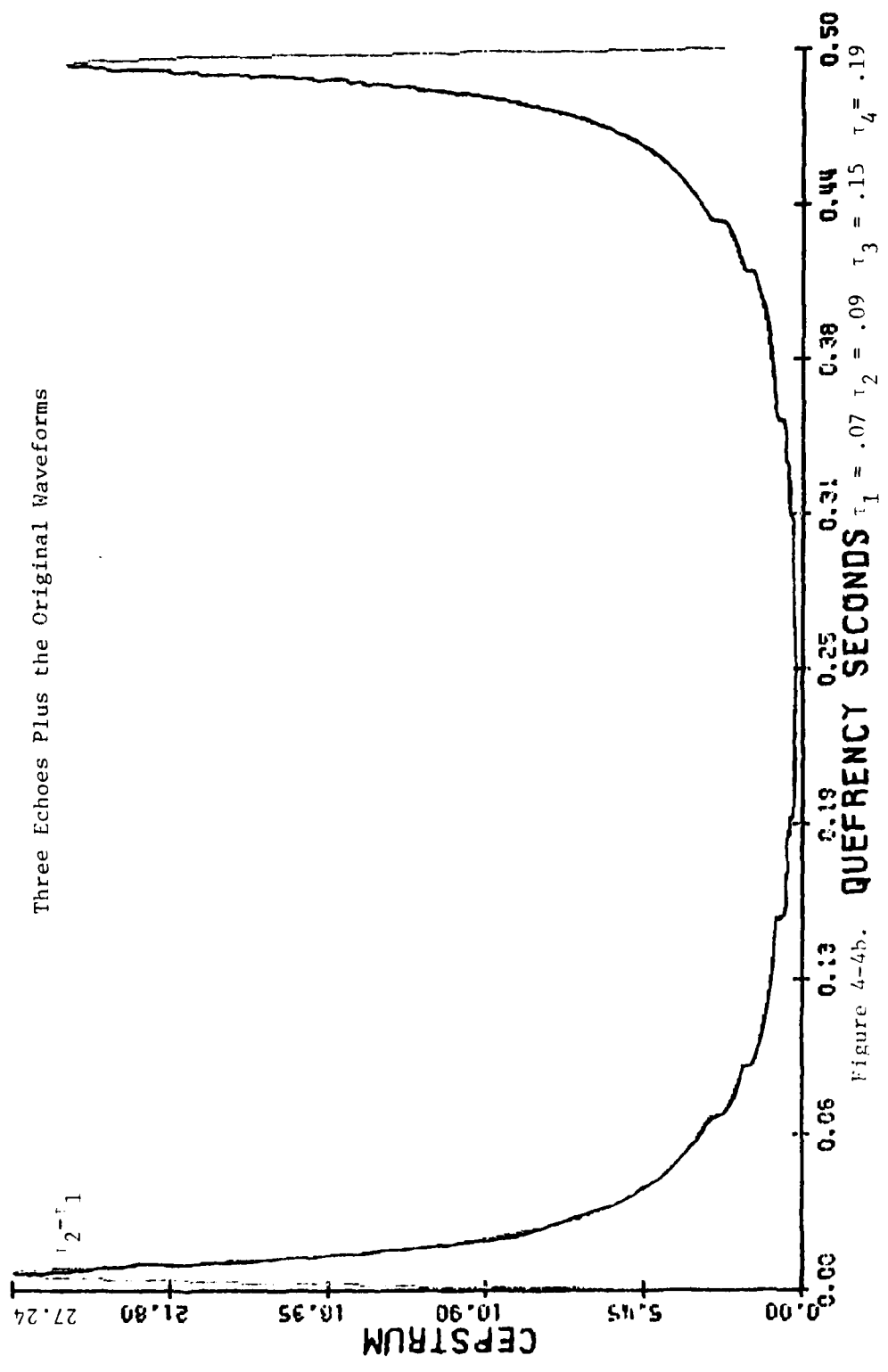


Figure 4-4a.

EXPONENTIAL

Three Echoes Plus the Original Waveforms



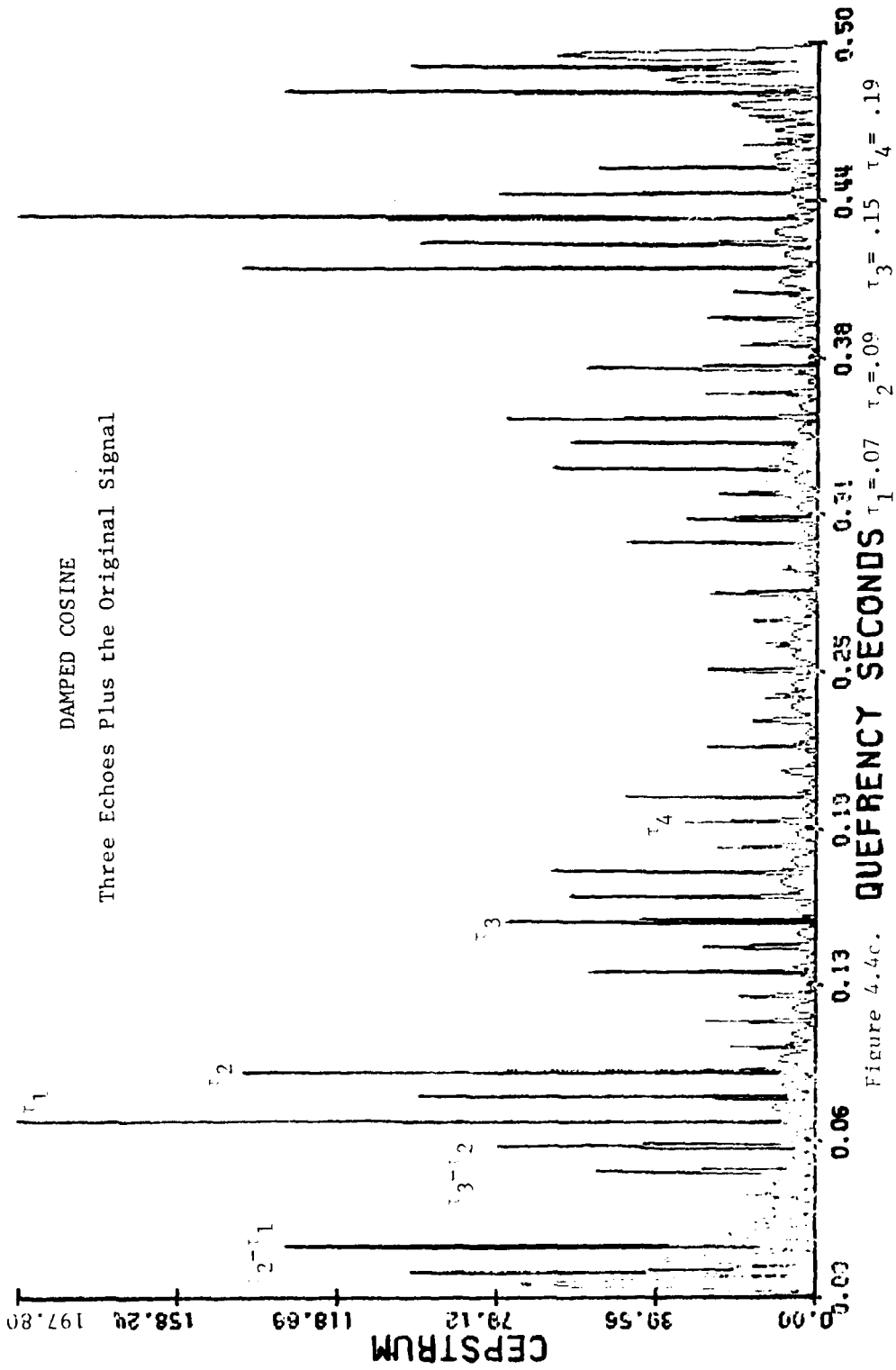


Figure 4.4c.

TABLE 4-7a

CEPSTRUM AT/TOR	$\tau_3 - \tau_2 = .05$	$\tau_3 - \tau_2 = .07$	$\tau_3 - \tau_2 = .09$	$\tau_3 - \tau_2 = .11$	$\tau_3 - \tau_2 = .13$
$\tau_3 - \tau_2$	15.98340	21.14880	12.18420	10.57410	6.18194
τ_2	290.63900	291.00700	291.16900	291.61300	293.76900
τ_3	120.89500	118.20600	120.03500	121.73000	123.10200
$\tau_2 + \tau_3$	79.22850	80.90570	80.00970	25.40220	20.23680

Power cepstrum variation when the time difference between two echoes is changing and the relative magnitude of the echoes with respect to the original signal is fixed. τ_1 the epoch time of the original signal is set equal to zero.

TABLE 4-7b

CEPSTRUM AT/FOR	$\tau_3 - \tau_2 = .05$	$\tau_3 - \tau_2 = .07$	$\tau_3 - \tau_2 = .09$	$\tau_3 - \tau_2 = .11$	$\tau_3 - \tau_2 = .13$
$\tau_3 - \tau_2$.05441	.07199	.04148	.03599	.02104
τ_2	.98935	.99060	.99115	.99266	1.00000
τ_3	.41153	.40238	.40860	.41437	.41904
$\tau_2 + \tau_3$.26970	.27541	.27236	.08647	.06889

Normalized form of Table 4-7a

TABLE 4-8a

CEPSTRUM AT/FOR	NW,NS	NW,S	W,NS	W,S
τ_1	228.4860	103.2690	17.2839	1.6130
τ_2	131.9120	44.8394	7.0003	.4590
τ_3	68.2902	15.5707	1.4308	.0430
$\tau_2 - \tau_1$	14.5433	113.188	20.6583	2.1491
$\tau_3 - \tau_1$	131.9120	44.8394	7.0003	.4590
$\tau_3 - \tau_2$	228.4860	103.2690	17.2839	1.6130
$\tau_1 + \tau_2$	68.2902	15.5707	1.4308	.0430
$\tau_1 + \tau_3$	25.2834	1.0093	.5299	.0480
$\tau_2 + \tau_3$	68.2902	15.5707	1.4308	.0430
$\tau_1 + \tau_2 + \tau_3$	131.9120	44.8394	7.0003	.4590

Cepstrum values at epoch times, sum and the difference of epoch times for a signal comprised of three cosine waveforms. The epoch times are $\tau_1 = .07$, $\tau_2 = .12$ and $\tau_3 = .19$ seconds. Notice the difference between two epoch times is another one. Also notice the effect of windowing and/or smoothing.

TABLE 4-8b

CEPSTRUM AT/FOR	NW,NS	NW,S	W,NS	W,S
τ_1	226,6940	103.8470	17.3460	1.6187
τ_2	133.3340	51.9006	9.3475	0.7776
τ_3	50.0748	.2271	0.5901	.0037
$\tau_2 - \tau_1$	25.6765	150.0360	27.1378	3.1250
$\tau_3 - \tau_1$	12.5899	80.4513	15.2132	1.3470
$\tau_3 - \tau_2$	16.1891	24.9517	4.1131	.4036
$\tau_1 + \tau_2$	68.9133	40.4236	6.5466	.3025
$\tau_1 + \tau_3$	23.5328	2.6927	.2699	.0112
$\tau_2 + \tau_3$	11.2428	7.2127	1.6272	.0396
$\tau_1 + \tau_2 + \tau_3$	12.8564	11.8401	2.4185	.0857

This table is the same as Table 4-8a except the epoch times are $\tau_1 = .07$, $\tau_2 = .09$ and $\tau_3 = .15$ seconds, difference of two of them is not equal to the other one. See Figure G-5.

TABLE 4-9a

CEPSTRUM AT/FOR	NW,NS	NW,S	W,NS	W,S
τ_1	25.9059	4.8733	.6452	.0566
τ_2	110.4580	7.4845	.8232	.0527
τ_3	13.4191	.4786	.0504	.0058
$\tau_2 - \tau_1$	223.8570	25.5724	2.9127	.2899
$\tau_3 - \tau_1$	110.4580	7.4845	.8232	.0527
$\tau_3 - \tau_2$	223.8570	25.5724	2.9127	.2899
$\tau_1 + \tau_2$	13.4191	.4786	.0504	.0058
$\tau_1 + \tau_3$	12.7848	.5522	.0707	.0057
$\tau_2 + \tau_3$	13.4191	.4786	.0504	.0058
$\tau_1 + \tau_2 + \tau_3$	2.2451	.3971	.0614	.0080

Cepstrum values at epoch times, sum and difference of epoch times for a signal comprised of three damped exponential waveforms. The epoch times are $\tau_1 = .07$, $\tau_2 = .12$ and $\tau_3 = .19$ seconds. Notice the difference between two epoch times is another one. Also notice the effect of windowing and/or smoothing.

TABLE 4-9b

CEPSTRUM AT/FOR	NW,NW	NW,S	W,NS	W,S
τ_1	5.4707	5.0114	.7707	.0698
τ_2	1.2989	2.5488	.4121	.0332
τ_3	.4639	.8940	.1636	.0083
$\tau_2 - \tau_1$	295.226	43.1720	5.1853	.5729
$\tau_3 - \tau_1$	35.2401	4.3895	.6427	.0546
$\tau_3 - \tau_2$	39.8588	.8640	.3122	.0307
$\tau_1 + \tau_3$	3.8335	.7185	.1402	.0069
$\tau_1 + \tau_2$	16.2440	.0853	.0133	.0030
$\tau_2 + \tau_3$	9.1920	.6145	.0996	.0049
$\tau_1 + \tau_2 + \tau_3$.3356	.2326	.0420	.0028

This table is the same as Table 4-9a except the epoch times are $\tau_1 = .07$, $\tau_2 = .09$ and $\tau_3 = .15$ seconds, difference of two of them is not equal to the other one. See Figure G-15b.

TABLE 4-10a

CEPSTRUM AT/FOR	NW,NS	NW,S	W,NS	W,S
τ_1	254.6810	110.0010	17.6356	1.6235
τ_2	74.0872	4.3336	.2014	.0122
τ_3	52.2991	35.3602	6.5878	.2367
$\tau_2 - \tau_1$	171.7540	54.6719	9.5635	.9905
$\tau_3 - \tau_1$	74.0872	4.3336	.2014	.0122
$\tau_3 - \tau_2$	171.7540	57.6719	9.5635	.9905
$\tau_1 + \tau_2$	52.2991	35.3602	16.5878	.2367
$\tau_1 + \tau_3$	52.2991	35.3602	6.5878	.2367
$\tau_2 + \tau_3$	52.2991	35.3602	6.5878	.2367
$\tau_1 + \tau_2 + \tau_3$	23.5596	1.3349	.0397	.0030

Cepstrum values at epoch times, sum and the difference of epoch times for a signal comprised of three damped cosine waveforms. The epoch times are $\tau_1 = .07$, $\tau_2 = .12$ and $\tau_3 = .19$ seconds. Notice the difference between two epoch times is another one. Also notice the effect of windowing and/or smoothing.

TABLE 4-10b

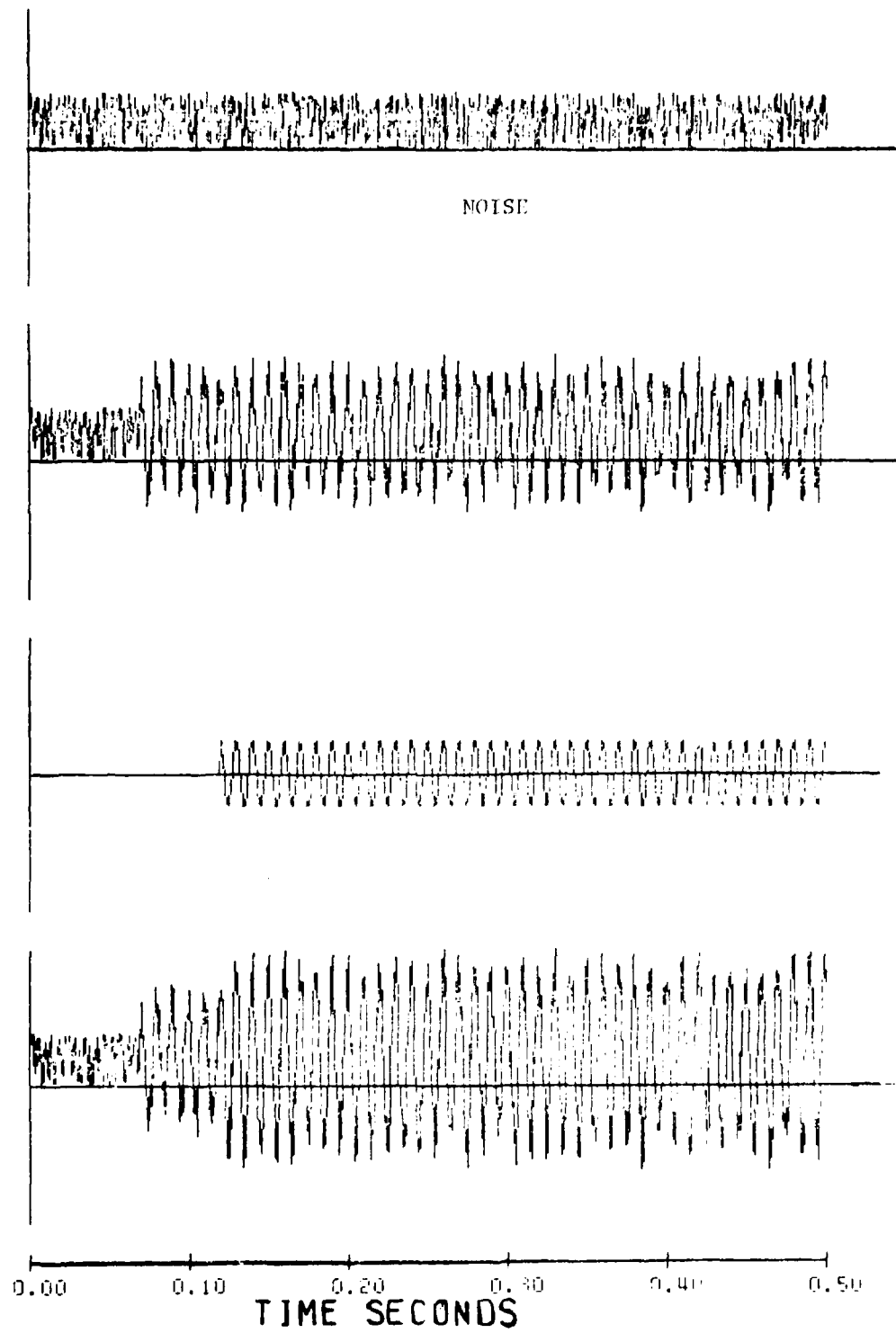
CEPSTRUM AT/FOR	NW,NS	NW,S	W,NS	W,S
τ_1	237.3590	125.9470	24.3554	2.3035
τ_2	77.9314	10.2232	2.9567	.2470
τ_3	36.1534	2.9230	.2263	.0184
$\tau_2 - \tau_1$	178.248	42.2664	5.5692	.6033
$\tau_3 - \tau_1$	65.9162	1.4719	.1869	.0262
$\tau_3 - \tau_2$	30.5698	30.1385	6.9430	.7109
$\tau_1 + \tau_2$	49.8258	26.8940	4.0052	.1856
$\tau_1 + \tau_3$	28.4976	14.2389	14.2389	2.9279
$\tau_2 + \tau_3$	21.7595	1.9567	.8000	.0258
$\tau_1 + \tau_2 + \tau_3$	25.7880	5.8081	1.2962	.0509

This table is the same as Table 4-10a except the epoch times are $\tau_1 = .07$, $\tau_2 = .09$ and $\tau_3 = .15$ seconds, difference of two of them is not equal to the other one. See Figure G-10b.

Noisy Case

The study included the cosine type signals for the noisy case. The reason for using the cosine waves was that in the cepstrum plot of a cosine waveform there are many ripples besides the original ones, and this makes a good choice for a noisy case. Different signals to noise ratios were chosen from 2.43 up to 15.43 db and it was found that the cepstrum plot is not of any help up to 15 db. It is for signal to noise ratios above this level that the epoch or delay times in the cepstrum plots are distinguishable.

Figures 4-5 and 4-6 show the cepstrum plot for signal to noise ratios of 2.43 and 15.44 db. As in all of the previous cases there is no discernable improvement in the cepstrum plots by using windowing and/or smoothing.



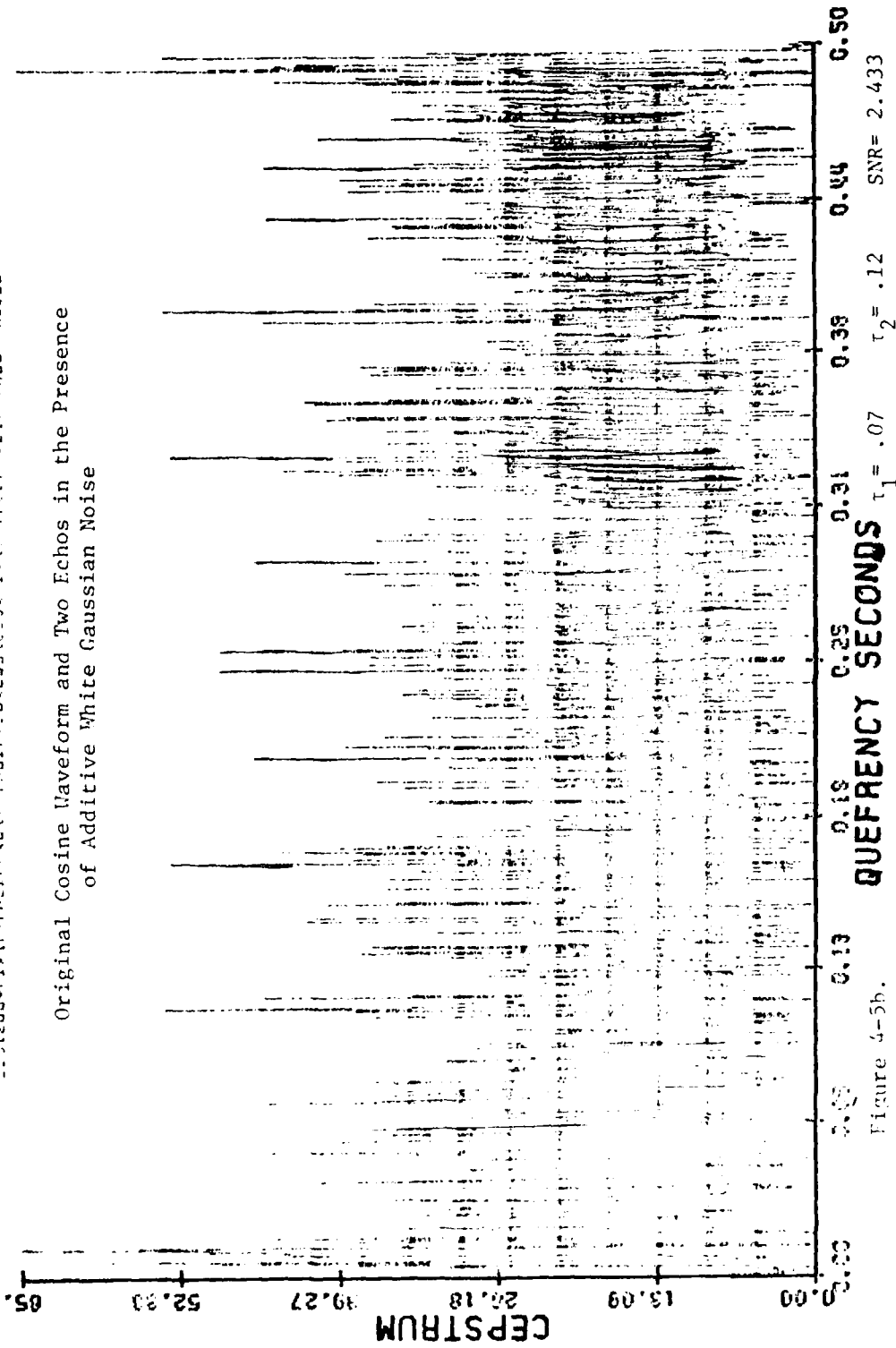
$$\cos(200\pi t - \tau_1) + 0.6 \cos(200\pi t - \tau_2) + 0.4 \cos(200\pi t - \tau_3) + \text{NOISE}$$

5MB 2.4.1

Figure 4-5a.

200000*PI*(T-TR001)*COS(2*PI*(F0*(T-TR001)+2*PI*(F1*(T-TR001)+F2*(T-TR001)+NOISE

Original Cosine Waveform and Two Echos in the Presence
of Additive White Gaussian Noise

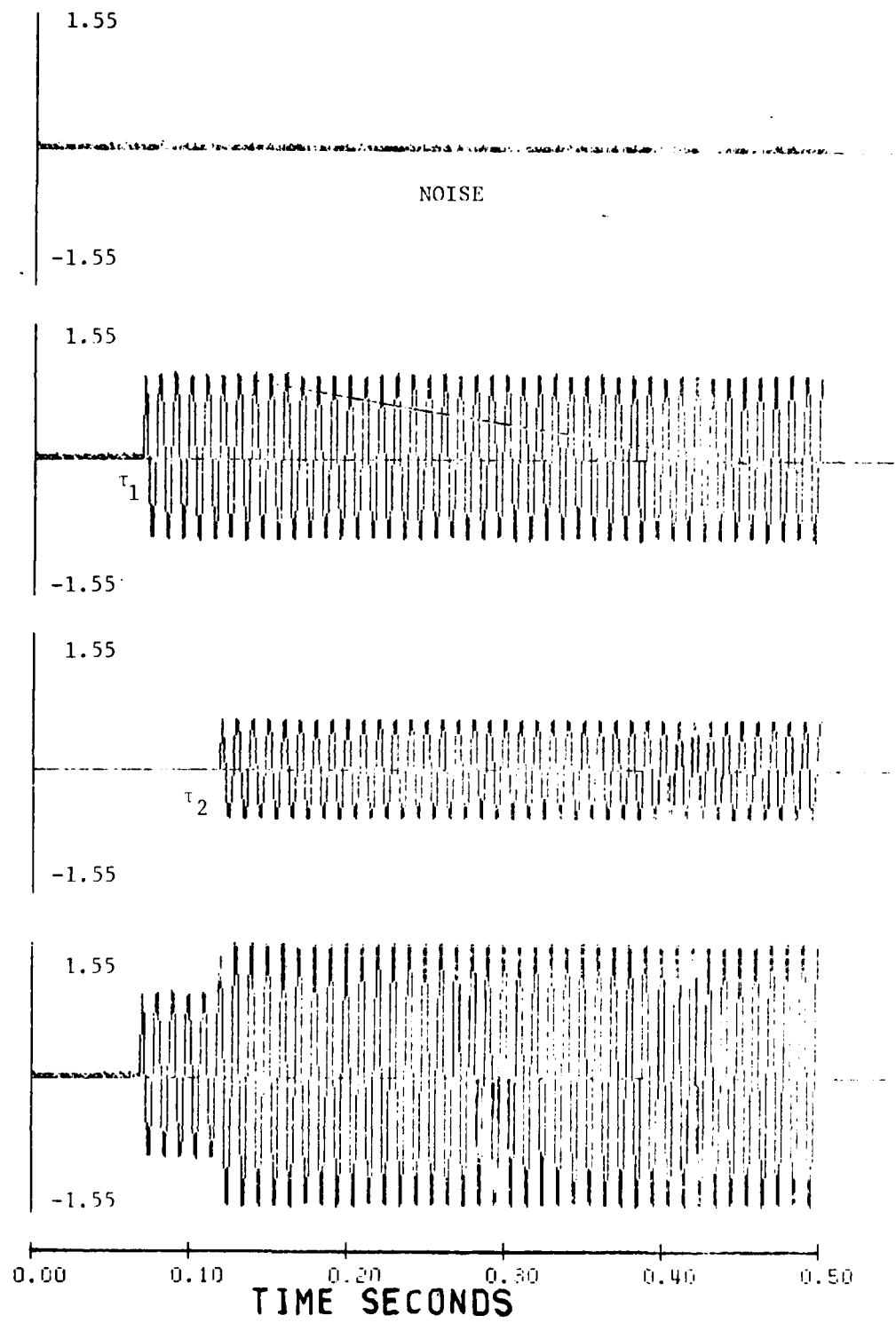


SNR= 2.433

$\tau_2 = .12$

$\tau_1 = .07$

Figure 4-5b.



$$\cos(200\pi \cdot (t - \tau_{11})) + 0.5 \cos(200\pi \cdot (t - \tau_{11})) + 0.5 \cos(200\pi \cdot (t - \tau_{21})) + 0.5 \cos(200\pi \cdot (t - \tau_{21})) + \text{NOISE}$$

Figure 4-6a.

SNR = 15.43

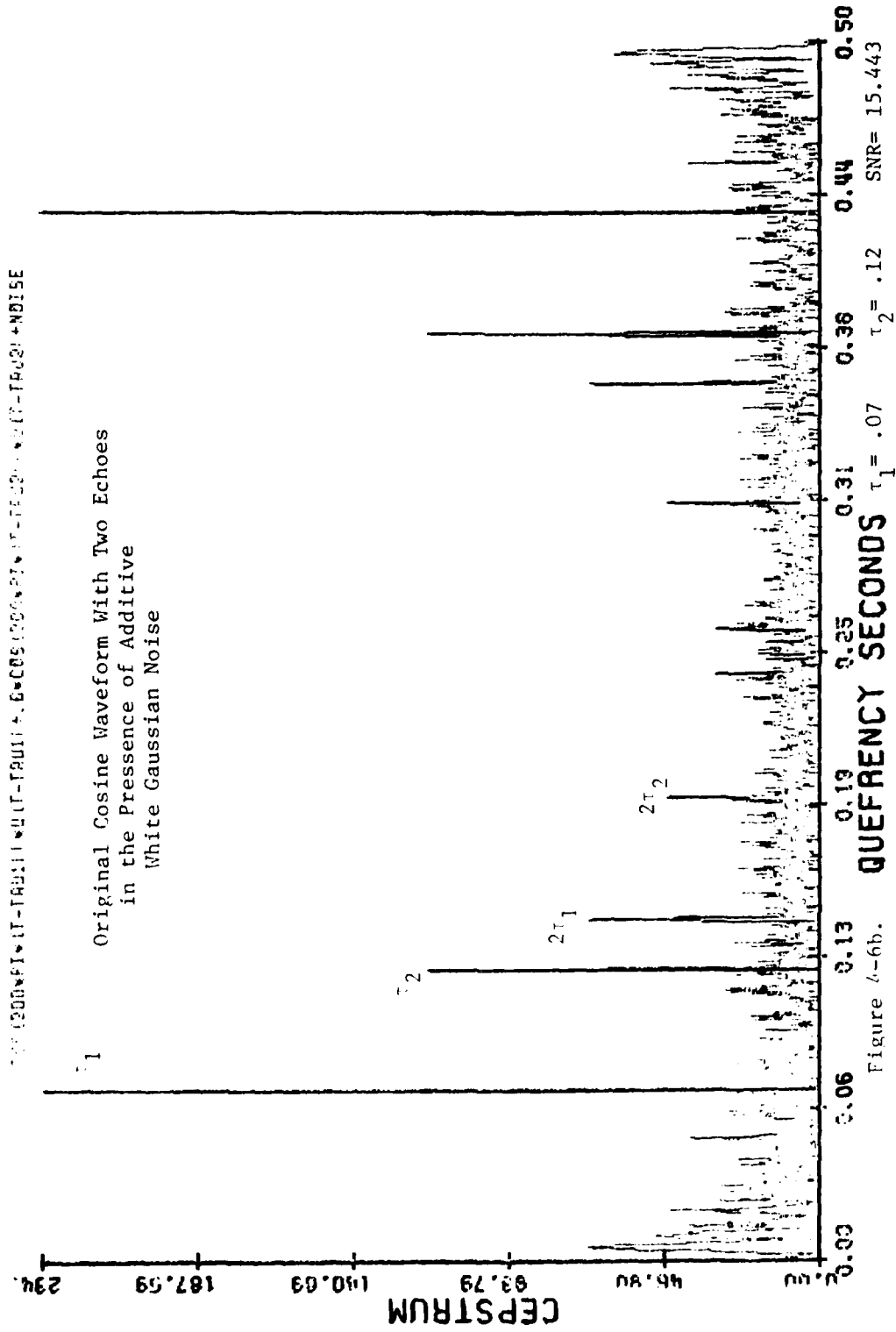


Figure 4-6b.

CHAPTER V

CONCLUSIONS AND RECOMMENDATIONS

The power cepstrum technique demonstrated the ability to determine the epoch times of the echoes for the single and multiple echo cases with echo amplitude being less or greater than that of the reference wavelet. It was noticed that changing the relative magnitude of the echo with respect to the original signal would not change significantly the peak magnitude of the power cepstrum. The experimental results proved to be in compliance with the theory. It proved once more as reported in the literature, that the cepstrum is very much data related as seen in the cases of damped exponential and damped cosine waveforms. In the damped exponential type signals it was apparent that if the relative magnitude of the signal is small compared to the original one and also if the damping coefficient is high enough, the only place that a strong peak occurs in the cepstrum plot is at the time difference of the echoes, while in the case of the cosine type waveforms, only at the epoch times is the cepstrum peak strong enough to be detected and the time difference is not discernable. In the case of damped cosine a shift was noticed in the form of the power cepstrum. If the damping coefficient is high it will react like a damped exponential waveform, and when damping coefficient is not high, it will behave as a cosine waveform.

When both signal and its echo start at any point in time except at the time zero, and α is changing, the value of the cepstrum at

two different epoch times would change, but sum of these peaks together will remain almost constant (see Table 4-4b for cosine type signal).

Adding some noise to the signals, the cepstrum was found to be detectable, although the signal to noise ratio (SNR) should be greater than 15.0 db (only the case of cosine waveform was tested).

Complexity and enormous number of peaks at the epoch times and their harmonics makes it practically impossible to deal with more than two echoes, as seen in our plots for three echoes, even in the noiseless case it is very hard to exactly detect the correct epoch times of the echoes. In double echo case, no detectable change in the magnitude of the peaks in the power cepstrum were noticed when the time distance was kept between two echoes constant.

The study was conducted with computer simulation techniques, which might be different from real time problems, but comparison with the theoretical results showed that it is not very far from being correct. Most of the previous studies which have been made using cepstrum techniques have been in the field of seismic or oceanography and little has been done in medicine with the exception of a few theses and dissertation research from the University of Florida. Further study should be conducted in the neurological field, where reflection plays an important role. If the technique is improved enough and progress is made, then one day human beings might suffer less by early detection of any malfunction in their neurological system.

In the battlefield if the study is conducted for a majority of armored vehicles, perhaps by making a table look-up type device, the type of the vehicle can be recognized and so its capture or destruction would be possible. Today with the help of LSI technology, it is possible to make FFT processors and so it is relatively easy to build processing equipments in which cepstrum techniques can be of help.

Finally in Tables 5-1, 5-2, and 5-3, is a quick cross reference for the study.

TABLE 5-1 (SINGLE ECHO)

TYPE OF FUNCTION	TIME PLOT FIGURE	PEAK SHOULD OCCUR AT	CEPSTRUM EQUATION AT	CEPSTRUM PLOT	TABULATED SUMMARY
COSINE	3-1 AND APPENDIX G	τ_1 & τ_2 AND $\tau_1 + \tau_2$	APPENDIX C, D,	3-2, 4-1a 4-2a, and APPENDIX G	4-1a, b, 4-2, 4-3a, b, 4-4a, b
DAMPED EXPONENTIAL	3-5, APPENDIX G	$\tau_2 - \tau_1$	APPENDIX E	3-6, 4-1b 4-2b, and APPENDIX G	4-5a, b, c
DAMPED COSINE	3-7, APPENDIX G	$\tau_1, \tau_2,$ $\tau_1 + \tau_2$ AND $\tau_2 - \tau_1$		3-8, 4-1c 4-2c, and APPENDIX G	4-6a, b, c

TABLE 5-2 (MULTIPLE ECHOES)

TYPE OF FUNCTION	TIME PLOT FIGURE	PEAK SHOULD AT	CEPSTRUM PLOT	TABULATED SUMMARY
COSINE	APPENDIX G	$\tau_1, \tau_2, \tau_3, \tau_4$ AND $\tau_1 + \tau_2, \tau_1 + \tau_3$ $\tau_2 + \tau_3, \tau_1 + \tau_2$ $+ \tau_3 + \tau_4$	4-3a, 4-4a AND APPENDIX G	4-7a, b AND 4-8a, b
DAMPED EXPONENTIAL	APPENDIX G	$\tau_2 - \tau_1$, $\tau_3 - \tau_1$	4-3b, 4-4b AND APPENDIX G	4-9a, b
DAMPED COSINE	APPENDIX G	$\tau_1, \tau_2, \tau_3, \tau_4$ $\tau_1 + \tau_2$ AND $\tau_2 - \tau_1, \tau_3 - \tau_1$ $\tau_3 - \tau_2$	4-4c, 4-4c AND APPENDIX G	4-10a, b

TABLE 5-3 (NOISY CASE)

TYPE OF FUNCTION	TIME PLOT FIGURE	PEAKS SHOULD BE AT	CEPSTRUM PLOT
COSINE	4-5a, 4-6a AND APPENDIX C	τ_1, τ_2 AND $\tau_1 + \tau_2$	4-5b, 4-6b AND APPENDIX C

APPENDIX A

DEFINITION OF TERMS USED IN THE REPORT

DEFINITION OF TERMS USED IN THIS PAPER

In order to get a meaningful terminology for the cepstrum technique, Bogert et al suggested the use of certain paraphrased words for the various quantities encountered. Table I shows these paraphrased words also its equivalent in frequency domain.

TABLE I

Power Cepstrum Domain	Frequency Domain	Definition
Time	Frequency	
Frequency	Time	
Quefrequency	Frequency	
Cepstrum	Spectrum	
Analysis	Analysis	Procedure of summarizing, looking at, or dissecting data
Cepstrum	Spectrum	A dissection of the variance of time series into portions associated with various quefrequencies (frequencies)
Complex Demodulation	Complex Demodulation	A shifting of frequency (frequency) in a time series by multiplication by sines, and by cosines, of a center quefrequency (frequency), followed by smoothing (and sometimes decimation) of the two resulting time series, which can be regarded as the real and imaginary parts of a complex series (analogous to single-side-band modulation)

TABLE 1 (Continued)

Power Cepstrum Domain	Frequency Domain	Definition
Cross Cepstrum	Cross Spectrum	A dissection of the common variation of two time series, into portions associated with various quefrequencies (frequencies) which takes into account, and separates both synchronized common variance (covariance) and anti-synchronized common variance (covariance) and antisynchronized common variation (quadrature)
Darius	Radius	Modulus of complex number
Gamnitude	Magnitude	Modulus of complex number
Liftering	Filtering	A transformation of one time series into another which a) obeys the superposition rule (is additive) and b) is invariant under changes of time origin.
Lifter	Filter	A device, formula or process for making such a transformation
Long Pass Lifter	High-Pass Filter	One which passes more rapidly time varving components more readily
Lopar	Polar	Plot or coordinates in terms of modulus and angle
Quefrequency	Frequency	The number of a time series per unit time.

TABLE 1 (Continued)

Power Cepstrum Domain	Frequency Domain	Definition
Rahmonic	Harmonic	One of the higher que- frequency (frequency) com- ponents generated from a sinusoidal component of time series by a non- linear process applied to the time series or any equivalent time function
Repiod	Period	The amount of time required for one cycle of a time series
Saphe	Phase	Angular displacement between a sinusoidal oscillation and a ref- erence cosinusoid of the same quefrequency (frequency)
Short-Pass Lifter	Los-Pass Filter	One which passes rapidly varying time components more readily

APPENDIX B

CEPSTRUM DERIVATION FOR MULTIPLE ECHOES

Extending the cepstrum discussion to more than one echo or multi-path signal is not difficult. We limit our study to the case of an original signal plus two echoes. Suppose $z(t)$ is the signal comprised of the original signal $y(t)$ and two echoes, then $z(t)$ can be written as

$$z(t) = y(t) + \alpha_1 y(t - \tau_1) + \alpha_2 y(t - \tau_2) \quad (\text{B-1})$$

taking the Fourier transform of both sides in (B-1)

$$\begin{aligned} F(z(t)) &= F(y(t) + \alpha_1 y(t - \tau_1) + \alpha_2 y(t - \tau_2)) \\ &= F(y(t)) + \alpha_1 F(y(t - \tau_1)) + \alpha_2 F(y(t - \tau_2)) \end{aligned} \quad (\text{B-2})$$

where $F(\cdot)$ is the Fourier transform.

Calling Fourier transform of $z(t)$ and $y(t)$, $Z(\omega)$ and $Y(\omega)$ respectively and considering time shifting property of the Fourier transform (B-2) can be written as

$$Z(\omega) = Y(\omega) + \alpha_1 y(\omega) e^{-j\omega\tau_1} + \alpha_2 y(\omega) e^{-j\omega\tau_2} \quad (\text{B-3})$$

or

$$Z(\omega) = Y(\omega) (1 + \alpha_1 e^{-j\omega\tau_1} + \alpha_2 e^{-j\omega\tau_2}) \quad (\text{B-4})$$

taking absolute value of both sides

$$|Z(\omega)|^2 = |Y(\omega)|^2 |1 + \alpha_1 e^{-j\omega\tau_1} + \alpha_2 e^{-j\omega\tau_2}|^2 \quad (\text{B-5})$$

(B-5) is comprised of two parts

$$|Y(\omega)|^2 \quad (\text{B-6})$$

and

$$|1 + \alpha_1 e^{-j\omega\tau_1} + \alpha_2 e^{-j\omega\tau_2}|^2 \quad (\text{B-7})$$

expanding (B-7) one gets

$$\begin{aligned}
 & |(1 + \alpha_1 \cos \omega \tau_1 - j \alpha_1 \sin \omega \tau_1 + \alpha_2 \cos \omega \tau_2 - j \alpha_2 \sin \omega \tau_2)|^2 \\
 &= |(1 + \alpha_1 \cos \omega \tau_1 + \alpha_2 \cos \omega \tau_2) - j(\alpha_1 \sin \omega \tau_1 + \alpha_2 \sin \omega \tau_2)|^2 \\
 &= 1 + \alpha_1^2 + \alpha_2^2 + 2 \alpha_1 \cos \omega \tau_1 + 2 \alpha_2 \cos \omega \tau_2 + \alpha_1 \alpha_2 \cos \omega(\tau_2 - \tau_1) \\
 &\quad + \alpha_1 \alpha_2 \cos \omega(\tau_2 + \tau_1) \tag{B-8}
 \end{aligned}$$

Lets call

$$\lambda = 1 + \alpha_1^2 + \alpha_2^2 \tag{B-9}$$

then (B-7) can be written as

$$\begin{aligned}
 \lambda \left(1 + \frac{2\alpha_1}{\lambda} \cos \omega \tau_1 + 2 \frac{\alpha_2}{\lambda} \cos \omega \tau_2 + \frac{\alpha_1 \alpha_2}{\lambda} \cos \omega(\tau_2 - \tau_1) \right. \\
 \left. + \frac{\alpha_1 \alpha_2}{\lambda} \cos \omega(\tau_2 + \tau_1) \right) \tag{B-10}
 \end{aligned}$$

now taking logarithm of both sides of (B-5)

$$\begin{aligned}
 2 \ln |Z(\omega)| = 2 \ln |Y(\omega)| + \frac{1}{2} \ln \lambda + \ln \left(1 + \frac{2\alpha_1}{\lambda} \cos \omega \tau_1 + \frac{2\alpha_2}{\lambda} \cos \omega \tau_2 \right. \\
 \left. + \frac{\alpha_1 \alpha_2}{\lambda} \cos \omega(\tau_2 - \tau_1) + \frac{\alpha_1 \alpha_2}{\lambda} \cos \omega(\tau_2 + \tau_1) \right) \tag{B-11}
 \end{aligned}$$

Note that α_1 and α_2 are both less than one and for some ω, τ_1 and τ_2 we can have

$$\begin{aligned}
 -1 < \frac{2\alpha_1}{\lambda} \cos \omega \tau_1 + \frac{2\alpha_2}{\lambda} \cos \omega \tau_2 + \frac{\alpha_1 \alpha_2}{\lambda} \cos \omega(\tau_2 - \tau_1) + \frac{\alpha_1 \alpha_2}{\lambda} \cos \omega(\tau_2 + \tau_1) < 1 \tag{B-12}
 \end{aligned}$$

also $\ln(1 + X)$ can be expanded as

$$\ln(1 + X) = X - \frac{1}{2}X^2 + \frac{1}{3}X^3 - \frac{1}{4}X^4 \quad |X| \leq 1 \quad (\text{B-13})$$

Thus up to the first approximation (B-11) can be written as

$$2 \ln|Z(\omega)| = 2 \ln|Y(\omega)| + \frac{1}{2} \ln \lambda + \frac{2\alpha_1}{\lambda} \cos \omega \tau_1 + \frac{2\alpha_2}{\lambda} \cos \omega \tau_2 + \frac{\alpha_1 \alpha_2}{\lambda} \cos \omega (\tau_2 - \tau_1) + \frac{\alpha_1 \alpha_2}{\lambda} \cos \omega (\tau_2 + \tau_1) \quad (\text{B-14})$$

Taking the Fourier transform of both sides of (B-14) will result

$$\begin{aligned} C_p(z(t)) = \text{CEPSTRUM} &= F[2 \ln|Z(\omega)|] = F[2 \ln|Y(\omega)|] + F\left[\frac{1}{2} \ln \lambda\right] \\ &+ F\left[\frac{2\alpha_1}{\lambda} \cos \omega \tau_1 + \frac{2\alpha_2}{\lambda} \cos \omega \tau_2 + \frac{\alpha_1 \alpha_2}{\lambda} \cos \omega (\tau_2 - \tau_1)\right] \\ &+ \frac{\alpha_1 \alpha_2}{\lambda} \cos \omega (\tau_2 + \tau_1) \end{aligned} \quad (\text{B-15})$$

or

$$\begin{aligned} C_p(z(t)) = \text{CEPSTRUM} &= F[2 \ln|Y(\omega)|] + F\left[\frac{1}{2} \ln \lambda\right] + \frac{2\alpha_1}{\lambda} F[\cos \omega \tau_1] \\ &+ \frac{2\alpha_2}{\lambda} F[\cos \omega \tau_2] + \frac{\alpha_1 \alpha_2}{\lambda} F[\cos \omega (\tau_2 - \tau_1)] \\ &+ \frac{\alpha_1 \alpha_2}{\lambda} F[\cos \omega (\tau_2 + \tau_1)] \end{aligned} \quad (\text{B-16})$$

(B-16) has several terms, the first part will give a regular function not necessarily an impulse, the second term gives an impulse at the origin and the remaining parts would give impulses at the points τ_1 , τ_2 , $\tau_2 - \tau_1$ and $\tau_2 + \tau_1$ on the cepstral plot (Figure G-5b).

In the case of more than two echoes, the procedure is the same but a little more involved. In Appendix G we show cepstrum plots for the cases when there are more than two echoes.

APPENDIX C

CEPSTRUM DERIVATION FOR COSINE TYPE SIGNALS

It is desired to calculate the cepstrum for a signal which is a combination of two cosine signals. The signals have started at two different times with different strength and although both have the same frequency, they differ in phase. Figure C-1 shows these signals and their combination. The observation period is from time $t = 0$ to time $t = \tau$ seconds.

To proceed lets follow every step mentioned in the main text for calculating the cepstrum. Lets define the signals as

$$\begin{aligned} f_1(t) &= \cos \omega_o (t - \tau_1) u(t - \tau_2) & (C-1) \\ f_2(t) &= \alpha \cos \omega_o (t - \tau_3) u(t - \tau_4) \\ f(t) &= \cos \omega_o (t - \tau_1) u(t - \tau_2) + \alpha \cos \omega_o (t - \tau_3) u(t - \tau_4) \end{aligned}$$

The first step in the calculation of the cepstrum is finding the Fourier transform of the signal

$$\begin{aligned} F[f(t)] &= \int_{-\infty}^{\infty} f(t) e^{-j\omega t} dt \\ &= \int_{\tau_2}^{\tau} \cos \omega_o (t - \tau_1) e^{-j\omega t} dt + \int_{\tau_4}^{\tau} \alpha \cos \omega_o (t - \tau_3) e^{-j\omega t} dt & (C-2) \end{aligned}$$

using Euler's identity (C-2) becomes

$$\begin{aligned} F[f(t)] &= \frac{1}{2} \int_{\tau_2}^{\tau} [e^{j\omega_o (t - \tau_1)} + e^{-j\omega_o (t - \tau_1)}] e^{-j\omega t} dt \\ &+ \frac{1}{2} \alpha \int_{\tau_4}^{\tau} [e^{j\omega_o (t - \tau_3)} + e^{-j\omega_o (t - \tau_3)}] e^{-j\omega t} dt & (C-3) \end{aligned}$$

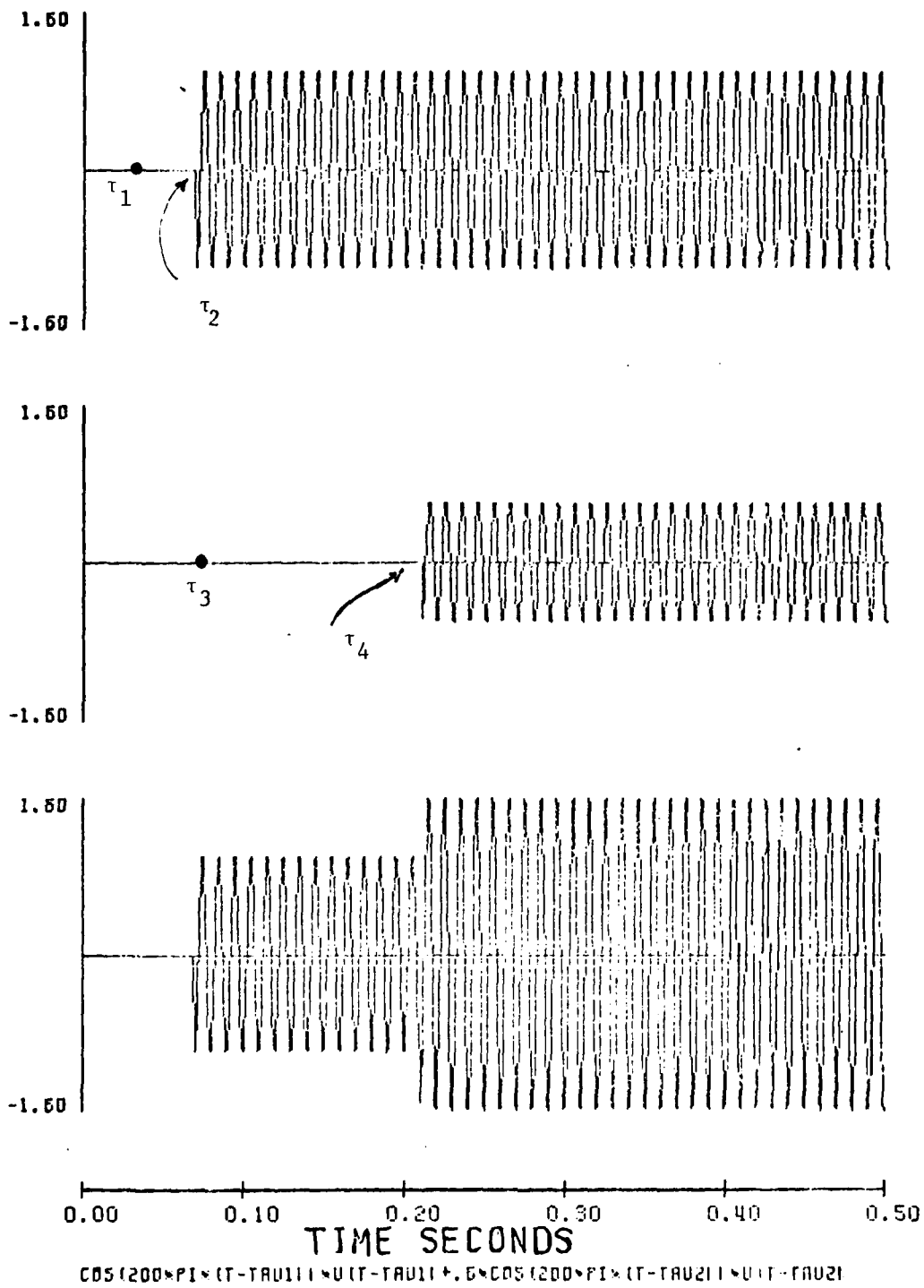


Figure C-1.

doing some mathematical manipulations (C-3) can be written as

$$\begin{aligned}
 F[f(t)] = & \frac{J}{(\omega^2 - \omega_0^2)} [\omega(\cos A - \cos B + \cos C - \cos D) \\
 & + \omega_0(\cos A - \cos B - \cos C + \cos D) \\
 & + J\omega(\sin A - \sin B + \sin C - \sin D) \\
 & + J\omega_0(\sin A - \sin B - \sin C + \sin D) \\
 & + \alpha\omega(\cos R - \cos S + \cos T - \cos U) \\
 & + \alpha\omega_0(\cos R - \cos S - \cos T + \cos U) \\
 & + j\alpha\omega(\sin R - \sin S + \sin T - \sin U) \\
 & + J\alpha\omega_0(\sin R - \sin S - \sin T + \sin U)]
 \end{aligned}
 \tag{C-4}$$

where

$$\begin{aligned}
 A &= \omega\tau - \omega_0\tau + \omega_0\tau_1 \\
 B &= \omega\tau_2 - \omega_0\tau_2 + \omega_0\tau_1 \\
 C &= \omega\tau + \omega_0\tau - \omega_0\tau_1 \\
 D &= \omega\tau_2 + \omega_0\tau_2 - \omega_0\tau_1 \\
 R &= \omega\tau - \omega_0\tau + \omega_0\tau_3 \\
 S &= \omega\tau_4 - \omega_0\tau_4 + \omega_0\tau_3 \\
 T &= \omega\tau - \omega_0\tau_4 - \omega_0\tau_3 \\
 U &= \omega\tau_4 + \omega_0\tau_4 - \omega_0\tau_3
 \end{aligned}
 \tag{C-5}$$

Equation (C-4) has real and imaginary parts, to find its magnitude both real and imaginary parts should be squared. Doing the previous operation involves lengthy and cumbersome calculations that finally would result the following:

$$\begin{aligned}
 |F(f(t))|^2 = & \omega^2 [4-2 \cos (A-B) + 2 \cos (A-C) - 2 \cos (A-D) \\
 & - 2 \cos (B-C) + 2 \cos (B-D) - 2 \cos (C-D)] \\
 + & \omega_0^2 [4-2 \cos (A-B) - 2 \cos (A-C) + 2 \cos (A-D) \\
 & + 2 \cos (B-C) - 2 \cos (B-D) - 2 \cos (C-D)] \\
 + & \omega^2 [4-2 \cos (R-S) - 2 \cos (R-T) + 2 \cos (R-U) \\
 & + 2 \cos (S-T) - 2 \cos (S-U) - 2 \cos (T-U)] \\
 + & \omega \omega_0 [-4 \cos (A-B) + 4 \cos (C-D) - 4 \cos (R-S) + 4 \cos (T-U)] \\
 + & \alpha \omega^2 [2 \cos (A-R) - 2 \cos (A-S) + 2 \cos (A-T) \\
 & - 2 \cos (A-U) - 2 \cos (B-R) + 2 \cos (B-S) \\
 & - 2 \cos (B-T) + 2 \cos (B-U) + 2 \cos (C-R) \\
 & - 2 \cos (C-S) + 2 \cos (C-T) - 2 \cos (C-U) \\
 & - 2 \cos (D-R) + 2 \cos (D-S) - 2 \cos (D-T) \\
 & + 2 \cos (D-U)]
 \end{aligned}$$

$$\begin{aligned}
& + \alpha \omega_o^2 [2 \cos (A-R) - 2 \cos(A-S) - 2 \cos (A-T) \\
& + 2 \cos(A-U) - 2 \cos (B-R) + 2 \cos(B-S) \\
& + 2 \cos(B-T) - 2 \cos (B-U) - 2 \cos(C-R) \\
& + 2 \cos (C-S) + 2 \cos (C-T) - 2 \cos (C-U) \\
& + 2 \cos (D-R) - 2 \cos (D-S) - 2 \cos (D-T) \\
& + 2 \cos(D-U)] \\
& + \alpha \omega_o [4 \cos (A-R) - 4 \cos(A-S) - 4 \cos (B-R) \\
& + 4 \cos(B-S) - 2 \cos (C-T) + 2 \cos (C-U) \\
& + 4 \cos (D-T) - 4 \cos(D-U)] \tag{C-6}
\end{aligned}$$

substituting values of A, B, C ... in each term of (C-6) will result terms that are completely independent of ω and also certain terms dependent on ω . To check on these, lets define

$$\begin{aligned}
\dot{\tau}_1 &= \omega_o (\tau_2 - \tau_1) \\
\dot{\tau}_2 &= \omega_o (2\tau_1 - 2\tau_1) \\
\dot{\tau}_3 &= \omega_o (2\tau_1 - \tau_2 - \tau_1) \\
\dot{\tau}_4 &= \omega_o (-2\tau_2 + 2\tau_1) \\
\dot{\tau}_5 &= \omega_o (\tau_1 - \tau_3) \\
\dot{\tau}_6 &= \omega_o (-\tau_1 + \tau_1 + \tau_4 - \tau_3) \\
\dot{\tau}_7 &= \omega_o (-2\tau_1 + \tau_1 + \tau_3) \\
\dot{\tau}_8 &= \omega_o (-\tau_1 + \tau_1 - \tau_4 + \tau_3)
\end{aligned}$$

$$\begin{aligned}
\phi_9 &= \omega_o (-\tau_2 + \tau_1 + \tau - \tau_3) \\
\phi_{10} &= \omega_o (-\tau_2 + \tau_1 + \tau_4 - \tau_3) \\
\phi_{11} &= \omega_o (-\tau_2 + \tau_1 - \tau + \tau_3) \\
\phi_{12} &= \omega_o (-\tau_2 + \tau_1 - \tau_4 + \tau_3) \\
\phi_{13} &= \omega_o (-\tau + \tau_4) \\
\phi_{14} &= \omega_o (-2\tau + 2\tau_3) \\
\phi_{15} &= \omega_o (-\tau + 2\tau_3 - \tau_4) \\
\phi_{16} &= \omega_o (-2\tau_4 + 2\tau_3)
\end{aligned}$$

and

$$\begin{aligned}
\gamma_1 &= \tau - \tau_2 \\
\gamma_2 &= \tau - \tau_4 \\
\gamma_3 &= \tau_2 - \tau_4
\end{aligned} \tag{C-7}$$

after substituting (C-7) into (C-6) then

$$\begin{aligned}
|F(f(t))|^2 &= \frac{1}{(\omega^2 - \omega_o^2)^2} \left[1 + \frac{\omega^2}{C} \left[C_1 - 2 \cos(-\omega\gamma_1 + \phi_1) \right. \right. \\
&\quad - 2 \cos(\omega\gamma_1 + \phi_3) - 2 \cos(-\omega\gamma_1 + \phi_3) \\
&\quad - 2 \cos(\omega(\gamma_1 - \phi_1)) - 2 \cos(\omega\gamma_2 + \phi_{13}) \\
&\quad - 2 \cos(\omega\gamma_2 + \phi_{15}) - 2 \cos(-\omega\gamma_2 + \phi_{15}) \\
&\quad \left. \left. - 2 \cos(\omega\gamma_2 - \phi_{13}) - 2 \cos(\omega\gamma_2 + \phi_6) \right] \right]
\end{aligned}$$

AD-A102 358

MISSISSIPPI STATE UNIV MISSISSIPPI STATE ENGINEERING--ETC F/6 17/1
INVESTIGATION OF CEPSTRUM ANALYSIS FOR SEISMIC/ACOUSTIC SIGNAL --ETC(U)
JAN 81 F M INGELS, G KOLEYNI AFOSR-80-0086

UNCLASSIFIED

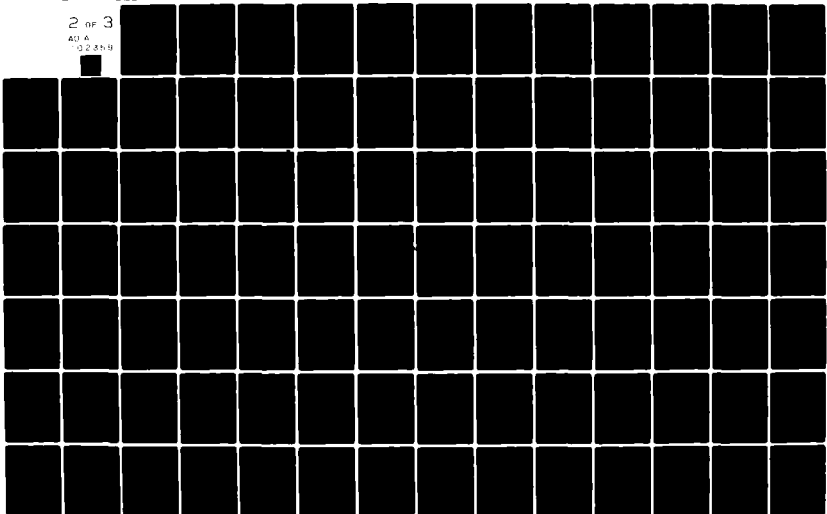
MSSU-EIRS-EE-81-2

AFOSR-TR-81-0603

NL

2 of 3

AD A
02 89 8



$$\begin{aligned}
& - 2 \cos (\omega \gamma_2 + \phi_8) - 2 \cos (-\omega \gamma_1 + \phi_9) \\
& + 2 \cos (\omega \gamma_3 + \phi_{10}) - 2 \cos (-\omega \gamma_1 + \phi_{11}) \\
& + 2 \cos (\omega \gamma_3 + \phi_{12}) - 2 \cos (\omega \gamma_2 - \phi_8) \\
& - 2 \cos (\omega \gamma_2 - \phi_3) - 2 \cos (-\omega \gamma_1 - \phi_{11}) \\
& + 2 \cos (\omega \gamma_3 - \phi_{12}) - 2 \cos (-\omega \gamma_1 - \phi_9) \\
& + 2 \cos (\omega \gamma_3 - \phi_{10})] \\
& + \frac{\omega}{C} [C_2 - 4 \omega_o \cos(\omega \gamma_1 + \phi_1) + 4 \omega_o \cos(\omega \gamma_1 - \phi_1) \\
& - 4 \alpha^2 \omega_o \cos(\omega \gamma_2 + \phi_{13}) + 4 \alpha^2 \omega_o \cos(\omega \gamma_2 - \phi_{13}) \\
& - 4 \alpha \omega_o \cos(\omega \gamma_2 + \phi_6) - 4 \alpha \omega_o \cos(-\omega \gamma_1 + \phi_9) \\
& + 4 \alpha \omega_o \cos(\omega \gamma_3 + \phi_{10}) + 2 \alpha \omega_o \cos(\omega \gamma_2 - \phi_3) \\
& + 4 \alpha \omega_o \cos(-\omega \gamma_1 - \phi_9) - 4 \alpha \omega_o \cos(\omega \gamma_3 - \phi_{10})] \\
& + \frac{\omega_o^2}{C} [-2 \cos (\omega \gamma_1 + \phi_1) + 2 \cos (\omega \gamma_1 + \phi_3) + 2 \cos (-\omega \gamma_1 + \phi_3) \\
& - 2 \cos (\omega \gamma_1 - \phi_1) - 2 \alpha^2 \cos(\omega \gamma_2 + \phi_{13}) \\
& + 2 \alpha^2 \cos(\omega \gamma_2 + \phi_{15}) + 2 \alpha^2 \cos (-\omega \gamma_2 + \phi_{15}) \\
& - 2 \alpha^2 \cos(\omega \gamma_2 - \phi_{13})] \tag{C-8}
\end{aligned}$$

with

$$C = \omega_0^2 [4 - 2 \cos \phi_2 - 2 \cos \phi_4] + (\alpha \omega_0)^2 [4 - 2 \cos \phi_{14} - 2 \cos \phi_{16}] \\ + \alpha \omega_0^2 [2 \cos \phi_5 - 2 \cos \phi_9] = \text{CONSTANT}$$

$$C_1 = [4 + 2 \cos \phi_2 + 2 \cos \phi_4] + \alpha^2 [4 + 2 \cos \phi_{14} + 2 \cos \phi_{16}] \\ + \alpha [2 \cos \phi_5 + 4 \cos \phi_7 + 2 \cos \phi_9] = \text{CONSTANT}$$

and

$$C_2 = \alpha \omega_0 [4 \cos \phi_5 - 2 \cos \phi_7] = \text{CONSTANT} \quad (\text{C-9})$$

then (C-8) can be written as

$$|F(f(t))|^2 = \frac{1}{(\omega^2 - \omega_0^2)^2} [1 + G(\omega)] \quad (\text{C-10})$$

taking logarithm of both sides of (C-10) one gets

$$\ln |F(f(t))|^2 = \ln \frac{1}{(\omega^2 - \omega_0^2)^2} + \ln (1 + G(\omega)) \quad (\text{C-11})$$

where $G(\omega)$ is a function of ω .

For some values of ω , there will be a $G(\omega)$ such that

$|G(\omega)| \leq 1$ and then $\ln(1 + G(\omega))$ can be expanded as

$$\ln(1 + G(\omega)) = G(\omega) - \frac{1}{2} (G(\omega))^2 + \frac{1}{3} (G(\omega))^3 + \dots \quad (\text{C-12})$$

taking the first term of this expansion (C-11) can be written

$$\ln |F(f(t))|^2 = -2 \ln(\omega^2 - \omega_0^2) + G(\omega) \quad (\text{C-13})$$

and finally cepstrum is found when the Fourier transform of both sides of (C-13) is calculated

$$C_p(f(t)) = \text{CEPSTRUM} = F[\ln|F(f(t))|^2] = F[-2 \ln(\omega^2 - \omega_0^2)] + F[G(\omega)] \quad (\text{C-14})$$

Right-handside of (C-14) is comprised of two parts, first part which is a function of ω with certain Fourier transform and the second part, Fourier transform of $G(\omega)$. $G(\omega)$ is a set of cosine waveforms such as $\cos(\omega\gamma_i + \phi_j)$, $i=1,2,3$, $J=1,2,\dots,16$ and their Fourier transforms have exponentially weighted impulses at points γ_1, γ_2 , and γ_3 . Consequently in the cepstrum plot peaks will be at points $\gamma_1 = \tau_1 - \tau_2$, $\gamma_2 = \tau_1 - \tau_4$, and $\gamma_3 = \tau_2 - \tau_4$ (Figure G-3b) or in the other word there is a peak at the time of beginning of each signal plus a peak at the time difference of two starting points for the signals. Examining the terms in (C-8) will reveal that the relative magnitude of the peak at the point $\gamma_3 = \tau_2 - \tau_4$ is small compared to those for starting times. Using more terms of the expansion in (C-12) would result in a term which causes a peak at point $\tau_2 + \tau_4$, sum of two starting points, in the cepstrum plots. The computer simulated plots for this case of our study can be found in Figures G-1 through G-4.

APPENDIX D

CEPSTRUM DERIVATION FOR COSINE TYPE WAVEFORMS WHEN
THERE IS A WINDOW WITHIN A WINDOW

Figures D-1 through D-4 are four cosine waveforms which have different phases and strengths. The equations for these four signals are

$$\begin{aligned} f_1(t) &= \cos \omega_0 t & f_2(t) &= \cos \omega_0 (t-\tau) \\ f_3(t) &= \alpha \cos \omega_0 (t-\nu) & f(t) &= \cos \omega_0 (t-\tau) + \alpha \cos \omega_0 (t-\nu) \end{aligned} \quad (D-1)$$

It is obvious from (D-1) that $f(t)$ is the combination of $f_2(t)$ and $f_3(t)$. These four signals have all started at times $t_i, i=1,2,3,4$ seconds with t_4 equal to t_2 or t_3 depending which is the smaller one.

Now suppose we want to study the cepstrum for $f(t)$ while it is observed through a time window having length $\lambda-\gamma$ seconds which is defined by

$$u(t-\gamma) - u(t-\lambda) \quad (D-2)$$

as is shown in Figure D-4 with dotted lines. The procedure to find the cepstrum is finding the Fourier transform of the signal, the squared spectrum, the log-squared spectrum, the Fourier transform, and finally the spectrum again. Now with regard to all above operations we proceed to do the calculations.

$$\begin{aligned} F[f(t)] &= \int_{-\infty}^{\infty} [\cos \omega_0 (t-\tau) + \alpha \cos \omega_0 (t-\nu)] \\ &\quad [u(t-\gamma) - u(t-\lambda)] e^{-j\omega t} dt \end{aligned} \quad (D-3)$$

Term $[u(t-\gamma) - u(t-\lambda)]$ is a combination of two unit step functions which cause the limits of the integration to be γ and λ . Now with these new limits (D-3) becomes

$$\begin{aligned} F[f(t)] &= \int_{\gamma}^{\lambda} [\cos \omega_0 (t-\tau) \\ &\quad + \alpha \cos \omega_0 (t-\nu)] e^{-j\omega t} dt \end{aligned} \quad (D-4)$$

using the Euler's identity for cosine (D-4) can be written as

$$F[f(t)] = \int_{\gamma}^{\lambda} \left[\frac{1}{2} [e^{j\omega_0(t-\tau)} + e^{-j\omega_0(t-\tau)}] + \frac{1}{2} [e^{j\omega_0(t-\nu)} + e^{-j\omega_0(t-\nu)}] \right] e^{-j\omega t} dt \quad (D-5)$$

multiplying $e^{-j\omega t}$ into the bracket and taking all variables not dependent on t out of integral one gets

$$\begin{aligned} F[f(t)] &= \frac{1}{2} e^{-j\omega_0 \tau} \int_{\gamma}^{\lambda} e^{-j(\omega - \omega_0)t} dt \\ &+ \frac{1}{2} e^{j\omega_0 \tau} \int_{\gamma}^{\lambda} e^{-j(\omega + \omega_0)t} dt \\ &+ \frac{1}{2} \alpha e^{-j\omega_0 \nu} \int_{\gamma}^{\lambda} e^{-j(\omega - \omega_0)t} dt \\ &+ \frac{1}{2} \alpha e^{j\omega_0 \nu} \int_{\gamma}^{\lambda} e^{-j(\omega + \omega_0)t} dt \end{aligned} \quad (D-6)$$

(D-6) is comprised of four parts each having a term such as

$$\int_{\gamma}^{\lambda} e^{\beta t} dt = \frac{1}{\beta} (e^{\beta \lambda} - e^{\beta \gamma}) \quad (D-7)$$

When these four terms are integrated and combined the result is

$$\begin{aligned} F[f(t)] &= -\frac{1}{j2(\omega - \omega_0)} [e^{-j(\omega_0 \tau + \omega \lambda - \omega_0 \lambda)} - e^{-j(\omega_0 \tau + \omega \gamma - \omega_0 \gamma)} \\ &+ \alpha e^{-j(\omega_0 \nu + \omega \lambda - \omega_0 \lambda)} - \alpha e^{-j(\omega_0 \nu + \omega \gamma - \omega_0 \gamma)}] \\ &- \frac{1}{j2(\omega + \omega_0)} [e^{-j(-\omega_0 \tau + \omega \lambda + \omega_0 \lambda)} - e^{-j(-\omega_0 \tau + \omega \gamma + \omega_0 \gamma)} \\ &+ \alpha e^{-j(-\omega_0 \nu + \omega \lambda + \omega_0 \lambda)} - \alpha e^{-j(-\omega_0 \nu + \omega \gamma + \omega_0 \gamma)}] \end{aligned} \quad (D-8)$$

$$f_1(t) = \cos \omega_0 t$$

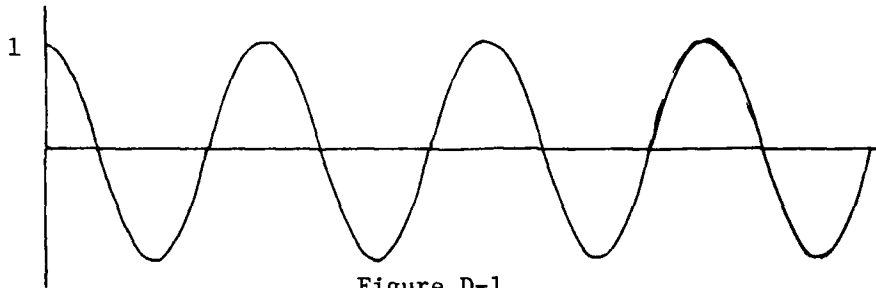


Figure D-1

$$f_2(t) = \cos \omega_0 (t - \tau)$$

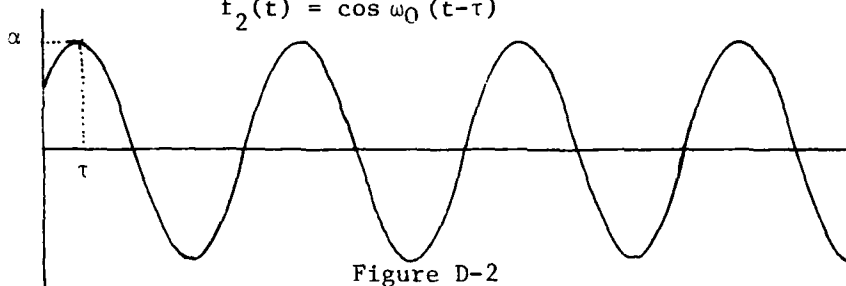


Figure D-2

$$f_3(t) = \alpha \cos \omega_0 (t - \nu)$$

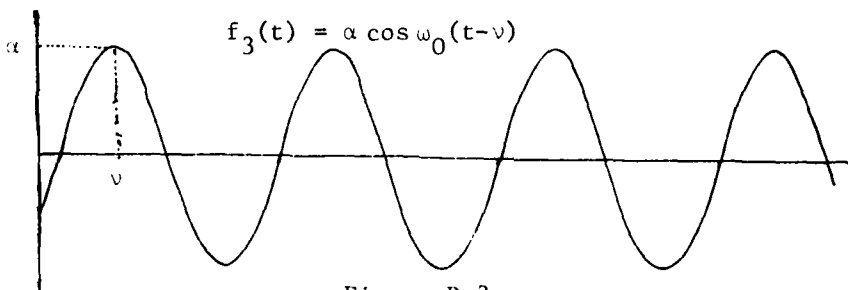


Figure D-3

$$f(t) = f_2(t) + f_3(t)$$

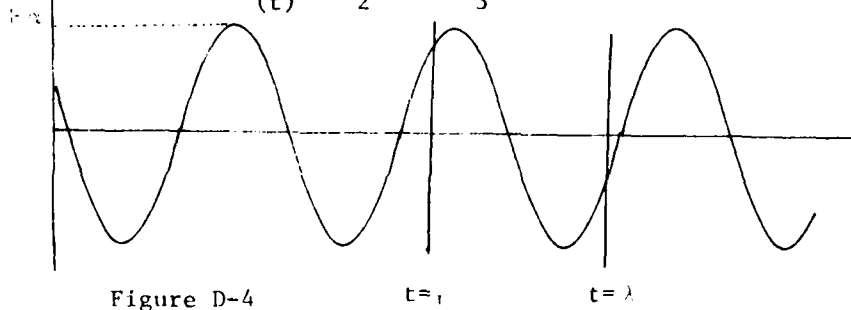


Figure D-4

 $t = \tau$
 $t = \lambda$

with (D-8) having real and imaginary parts.

The spectrum of a signal is found by squaring the real and imaginary parts and then taking its square root. In doing this after some mathematical manipulations one gets

$$\begin{aligned}
 |F(f(t))|^2 &= \left[\frac{1}{\omega^2 - \omega_0^2} \right] \left[1 + \frac{1}{8} (\cos \omega_0 (\tau - \gamma) + 3\alpha \cos \omega_0 (\tau - \gamma) \right. \\
 &- (1 + \alpha)^2 \cos (\omega - \omega_0) \phi - (1 + \alpha^2) \cos (\omega + \omega_0) \phi - \alpha \cos (\omega_0 (\tau - \gamma) + (\omega - \omega_0) \phi) \\
 &- \alpha \cos (\omega_0 (\tau - \gamma) - (\omega - \omega_0) \phi) - \alpha \cos (-\omega_0 (\tau - \gamma) + (\omega + \omega_0) \phi) \\
 &\left. - \alpha \cos (\omega_0 (\tau - \gamma) + (\omega + \omega_0) \phi) \right] \quad (D-9)
 \end{aligned}$$

where

$$\phi = \lambda - \gamma$$

To find the cepstrum logarithm of (D-9) should be taken.

As is shown previously $\ln(1 + X)$ when $|X| \leq 1$ can be expanded to

$$\ln(1 + X) = X - \frac{1}{2} X^2 + \frac{1}{3} X^3 - \frac{1}{4} X^4 + \dots \quad (D-10)$$

also

$$\ln AB = \ln A + \ln B \quad (D-11)$$

Knowing $\alpha \leq 1$ and also $|\cos X| \leq 1$, it will be justified to have assumed that the term in the parenthesis in (D-9) is less than one and with this (D-9) can be written as

$$\begin{aligned}
\ln |F(f(t))|^2 &= \ln \left[\frac{1}{\omega^2 - \omega_0^2} \right] + \frac{1}{8} (\cos \omega_0 (\tau - \gamma) + 3\alpha \cos \omega_0 (\tau - \gamma) \\
&- (1 + \alpha^2) \cos (\omega - \omega_0) \phi - (1 + \alpha^2) \cos (\omega + \omega_0) \phi - \alpha \cos (\omega_0 (\tau - \gamma) + (\omega - \omega_0) \phi) \\
&- \alpha \cos (\omega_0 (\tau - \gamma) - (\omega - \omega_0) \phi) - \alpha \cos (-\omega_0 (\tau - \gamma) + (\omega + \omega_0) \phi) \\
&- \alpha \cos (\omega_0 (\tau - \gamma) + (\omega + \omega_0) \phi)
\end{aligned} \tag{D-12}$$

The final step in finding cepstrum of $f(t)$ function is to find the Fourier transform of (D-12) again with this in mind that the variable of integration, representing time, here is ω instead of t . With a glance at (D-12) presence of several cosines such as $\cos \omega_0 (\tau - \gamma) = \text{CONSTANT}$ and $\cos(A + \omega \phi)$ with A as a constant phase is obvious. The Fourier transforms of these terms is

$$\begin{aligned}
B = A \text{ CONSTANT} &\longleftrightarrow B \delta(f) \\
\cos (\omega_c t + \theta) &\longleftrightarrow \frac{1}{2} [e^{j\theta} \delta(f - f_c) + e^{-j\theta} \delta(f + f_c)]
\end{aligned} \tag{D-13}$$

which shows impulses at $t = 0$ second and $t = f_c$ seconds. Translating terms such as these into the cepstrum plot would give peaks at $t = 0$ and $t = \lambda - \gamma$ seconds which proves the existence of peaks in the cepstrum plot only at points $K(\lambda - \gamma)$, $K=1, 2, \dots$ (length of time window) and its harmonics.

APPENDIX E

CEPSTRUM DERIVATION FOR DAMPED EXPONENTIAL TYPE SIGNALS

Figure (E-1) shows three signals which are exponentially damped. Figure (E-1c) is the combination of Figures (E-1a) and (E-1b). The equations for these signals are

$$f_1(t) = (t-\tau_1) e^{-C(t-\tau_1)} u(t-\tau_1)$$

$$f_2(t) = A(t-\tau_2) e^{-C(t-\tau_2)} u(t-\tau_2)$$

$$f(t) = f_1(t) + f_2(t)$$

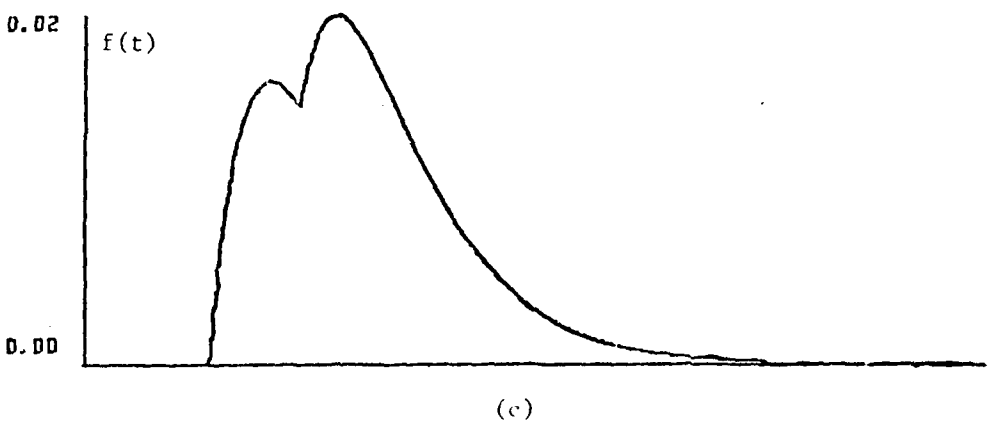
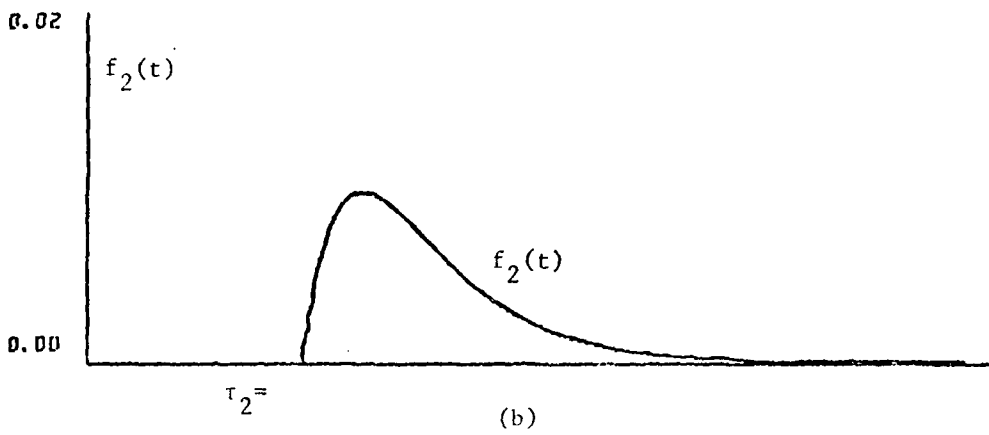
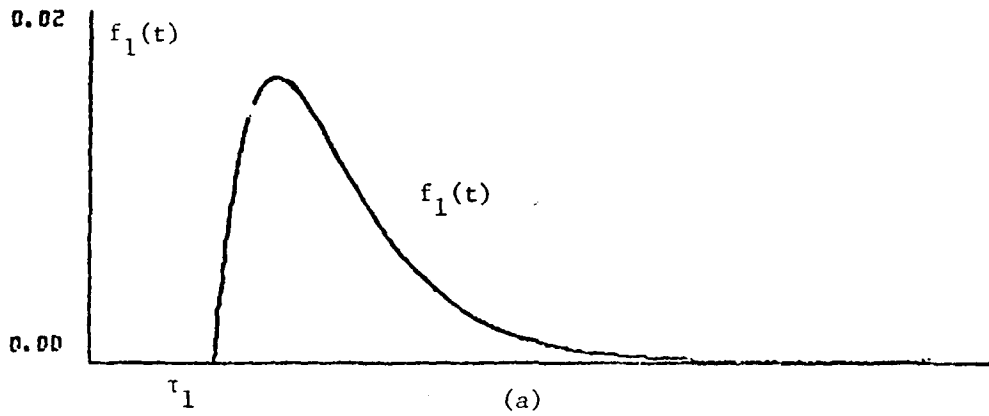
$$= (t-\tau_1) e^{-C(t-\tau_1)} u(t-\tau_1) + A(t-\tau_2) e^{-C(t-\tau_2)} u(t-\tau_2)$$

(E-1)

Fourier transforming $f(t)$ when it is observed from time $t=0$ to time $t=\tau$ seconds would result

$$\begin{aligned} F[f(t)] &= \int_{-\infty}^{\infty} f(t) e^{-j\omega t} dt \\ &= \int_{\tau_1}^{\tau} (t-\tau_1) e^{-C(t-\tau_1)} e^{-j\omega t} dt \\ &\quad + \int_{\tau_2}^{\tau} A(t-\tau_2) e^{-C(t-\tau_2)} e^{-j\omega t} dt \end{aligned} \tag{E-2}$$

(E-2) can be broken in four parts as follows



0.00 0.10 0.20 0.30 0.40 0.50
 TIME SECONDS

$$(f - \tau_{11}) \exp(-30(t - \tau_{11})) + 0.6(f - \tau_{21}) \exp(-30(t - \tau_{21})) + (f - \tau_{12})$$

Figure E-1.

$$\begin{aligned}
F[f(t)] &= \int_{\tau_1}^{\tau} t e^{-(C+j\omega)t} e^{C\tau_1} dt \\
&\quad - \tau_1 \int_{\tau_1}^{\tau} e^{-(C+j\omega)t} e^{C\tau_1} dt \\
&\quad + A \int_{\tau_2}^{\tau} t e^{-(C+j\omega)t} e^{C\tau_2} dt \\
&\quad - A \tau_2 \int_{\tau_2}^{\tau} e^{-(C+j\omega)t} e^{C\tau_2} dt
\end{aligned} \tag{E-3}$$

Lets have these new notations for the simplicity reason

$$\begin{aligned}
(1) &= \int_{\tau_1}^{\tau} t e^{-(C+j\omega)t} e^{C\tau_1} dt \\
(2) &= -\tau_1 \int_{\tau_1}^{\tau} e^{-(C+j\omega)t} e^{C\tau_1} dt \\
(3) &= A \int_{\tau_2}^{\tau} t e^{-(C+j\omega)t} e^{C\tau_2} dt \\
(4) &= -A\tau_2 \int_{\tau_2}^{\tau} e^{-(C+j\omega)t} e^{C\tau_2} dt
\end{aligned} \tag{E-4}$$

So (E-3) can be written as

$$F[f(t)] = (1) + (2) + (3) + (4) \tag{E-5}$$

To find the Fourier transform, each term is calculated separately and then the results will be added to give the Fourier transform of $f(t)$

$$(1) = \frac{e^{C\tau_1}(C^2 - \omega^2 - j2\omega C)}{(C^2 + \omega^2)^2} \left[(\alpha - j\beta\omega) \cos \omega\tau - (j\alpha + \beta\omega) \sin \omega\tau \right. \\ \left. + (j\lambda\omega - \gamma) \cos \omega\tau_1 + (j\gamma + \lambda\omega) \sin \omega\tau_1 \right] \quad (E-6)$$

with

$$\alpha = e^{-C\tau}(-C\tau - 1) \\ \beta = \tau e^{-C\tau} \\ \gamma = e^{-C\tau_1}(-C\tau_1 - 1) \\ \lambda = \tau_1 e^{-C\tau_1} \quad (E-7)$$

and

$$(2) = \left(\frac{HC - jH\omega}{C^2 + \omega^2} \right) \cos \omega\tau + \left(\frac{-H\omega - jHC}{C^2 + \omega^2} \right) \sin \omega\tau \\ + \left(\frac{-\tau_1 C + j\tau_1 \omega}{C^2 + \omega^2} \right) \cos \omega\tau_1 + \left(\frac{\tau_1 \omega + j\tau_1 C}{C^2 + \omega^2} \right) \sin \omega\tau_1 \quad (E-8)$$

with

$$H = \tau_1 e^{C(\tau_1 - \tau)} \quad (E-9)$$

$$(3) = A \frac{e^{C\tau_2}(C^2 - \omega^2 - j2\omega C)}{(C^2 + \omega^2)^2} \left[\alpha \cos \omega\tau - j\beta\omega \cos \omega\tau - j\alpha \sin \omega\tau - \beta\omega \sin \omega\tau \right. \\ \left. - v \cos \omega\tau_2 + j\omega \cos \omega\tau_2 + jv \sin \omega\tau_2 + \omega \sin \omega\tau_2 \right] \quad (E-10)$$

with

$$v = e^{-C\tau_2}(-C\tau_2 - 1) \\ \omega = \tau_2 e^{-C\tau_2} \quad (E-11)$$

and finally

$$(4) = \left(\frac{AKC - jAK\omega}{C^2 + \omega^2} \right) \cos \omega\tau + \left(\frac{-KA\omega - jAKC}{C^2 + \omega^2} \right) \sin \omega\tau$$

$$+ \left(\frac{-A\tau_2 C + jA\omega\tau_2}{C^2 + \omega^2} \right) \cos \omega\tau_2 + \left(\frac{A\tau_2 \omega + jA\tau_2 C}{C^2 + \omega^2} \right) \sin \omega\tau_2 \quad (E-12)$$

with

$$K = \tau_2 e^{C(\tau_2 - \tau)} \quad (E-13)$$

The Fourier transform of signal $f(t)$ is sum of (1), (2), (3), and (4). Doing summation operation one gets

$$F[f(t)] = (D_1 + jD_2) \cos \omega\tau + (D_2 - jD_1) \sin \omega\tau$$

$$+ (D_3 + jD_4) \cos \omega\tau_1 + (D_4 - jD_3) \sin \omega\tau_1$$

$$+ (D_5 + jD_6) \cos \omega\tau_2 + (D_6 - jD_5) \sin \omega\tau_2 \quad (E-14)$$

where

$$D_1 = M\alpha - N\beta\omega + P\alpha - Q\beta\omega + R_1 + R_2$$

$$D_2 = -B M\omega - N\alpha - P\beta\omega - Q\alpha - T_1 - T_2$$

$$D_3 = -\gamma M + N\lambda\omega - S_1$$

$$D_4 = M\lambda\omega + N\gamma + U_1$$

$$D_5 = -P\omega + O\omega\omega - S_2$$

$$D_6 = P\omega + vQ + U_2 \quad (E-15)$$

and

$$\begin{aligned}
 R_1 &= \frac{HC}{C^2 + \omega^2} & R_2 &= \frac{AKC}{C^2 + \omega^2} \\
 S_1 &= \frac{\tau_1 C}{C^2 + \omega^2} & S_2 &= \frac{A\tau_2 C}{C^2 + \omega^2} \\
 T_1 &= \frac{H\omega}{C^2 + \omega^2} & T_2 &= \frac{AK\omega}{C^2 + \omega^2} \\
 U_1 &= \frac{\tau_1 \omega}{C^2 + \omega^2} & U_2 &= \frac{A\tau_2 \omega}{C^2 + \omega^2} \\
 M &= e^{C\tau_1} \frac{C^2 - \omega^2}{(C^2 + \omega^2)^2} \\
 N &= e^{C\tau_1} \frac{2\omega C}{(C^2 + \omega^2)^2} \\
 P &= A e^{C\tau_2} \frac{C^2 - \omega^2}{C^2 + \omega^2} \\
 Q &= A e^{C\tau_2} \frac{2\omega C}{C^2 + \omega^2}
 \end{aligned} \tag{E-16}$$

Next step in calculating the cepstrum is of finding square of absolute value of (E-3). After some mathematical manipulations the final result is

$$\begin{aligned}
 |F(f(t))|^2 &= (D_1^2 + D_2^2 + D_3^2 + D_4^2 + D_5^2 + D_6^2) \\
 &+ (2D_1D_3 + 2D_2D_4) \cos \omega(\tau - \tau_1) \\
 &+ (2D_2D_3 - 2D_1D_4) \sin \omega(\tau - \tau_1) \\
 &+ (2D_4D_6 + 2D_3D_5) \cos \omega(\tau_2 - \tau_1) \\
 &+ (2D_1D_5 + 2D_2D_6) \cos \omega(\tau - \tau_2)
 \end{aligned}$$

$$\begin{aligned}
& + (2D_1D_6 - 2D_2D_5) \sin \omega(\tau_2 - \tau) \\
& + (2D_4D_5 - 2D_3D_6) \sin \omega(\tau_1 - \tau_2)
\end{aligned} \tag{E-17}$$

To find the cepstrum logarithm of (E-17) should be taken. As in the previous case (E-17) can be written as $1 + G(\omega)$ and for some ω , $\ln(1 + G(\omega)) = G(\omega)$. Then when the Fourier transform is taken, there should be weighted impulses at τ_1 , τ_2 , $\tau_2 - \tau_1$, but as we will show with an example the strength of these impulses depends strictly on the value of the damping coefficient C .

Example: Let

$$C = 30.0$$

$$\tau = .5 \text{ sec}$$

$$\tau_1 = .07 \text{ sec}$$

$$\tau_2 = .12 \text{ sec}$$

$$A = .6$$

Then

$$D_1 = -1.47 \times 10^{-4} \frac{C^2 - \omega^2}{C^2 + \omega^2} + 2.77 \times 10^{-4} \frac{\omega^2}{(C^2 + \omega^2)^2} + 9.81 \times 10^{-7} \frac{1}{C^2 + \omega^2}$$

$$D_2 = -4.61 \times 10^{-6} \frac{\omega(C^2 - \omega^2)}{C^2 + \omega^2} + 8.45 \times 10^{-3} \frac{\omega}{C^2 + \omega^2}$$

$$D_3 = 3.1 \frac{C^2 - \omega^2}{(C^2 + \omega^2)^2} + 2.1 \frac{2\omega^2 - 1}{C^2 + \omega^2}$$

$$D_4 = 0.07 \frac{\omega(C^2 - \omega^2)}{(C^2 + \omega^2)^2} - 186 \frac{\omega}{C^2 + \omega^2} + .07 \frac{\omega}{C^2 + \omega^2}$$

$$D_5 = \frac{1.56\omega^2 + 2.76 C^2 - 8.64}{C^2 + \omega^2}$$

$$D_6 = 7.2 \times 10^{-2} \frac{\omega(C^2 - \omega^2)}{C^2 + \omega^2} - 166 \frac{\omega}{C^2 + \omega^2}$$

Substituting values D_1 through D_6 into (E-17) will show that the only term with noticeable strength is the coefficient of $\cos \omega (\tau_2 - \tau_1)$ or the only visible peak in the cepstrum plot is the peak at the time difference $\tau_2 - \tau_1$. For computer simulated results see Figures G-11 through G-14.

APPENDIX F

A SYNOPSIS AND LISTING OF DIGITAL COMPUTER PROGRAMS

A SYNOPSIS OF DIGITAL COMPUTER PROGRAMS AND THEIR LISTING

The Univac 1108 computer at Mississippi State University Computing Center was used for the development of all runs and simulation plots in this study. The programs are all written in FORTRAN . IV.

The programs are all written in a machine independent form, such that they can be run in any type of computer with very little change. Effort has been done to write the programs as clear and as sufficient as possible so the computer run time and consequently the cost would be minimized. There are enough comments in each program to clarify any operation in the programs. At this point it is appropriate to give a brief summary of each program.

MAIN PROGRAM

The main program reads and writes the initial data input also calculates the power spectrum after taking the Fourier transform for the first time, then it finds the logarithm of the square of the power spectrum to send it to the subroutine FFT for Fourier transforming again, it then calculates the Cepstrum.

The number of sample points for the original signal is 2048 samples/second and the total period of sampling is 0.5 seconds. We tapered the first and last 20 points at each end of the cepstrum data. This tapering operation involves multiplication of the i^{th} value from each end by $1/2 [1 - \cos(i/20)]$, thus making a smooth transition from values multiplied by zero to those multiplied by unity. Finally we plot the cepstrum versus time to observe its peaks.

SUBROUTINE SIGNAL(Y) (Cosine)

This subroutine generates few cosine waveforms with different strength and phase but same frequency. The main signal is

$$y(t) = \cos(2\pi f(t-\tau_1)) u(t-\tau_1)$$

and the echoes are

$$y_i(t) = \alpha_i \cos(2\pi f(t-\tau_i)) u(t-\tau_i)$$

$$\alpha_i \leq 1.$$

where f is the frequency and τ_i is the epoch or echo delay time the composite signal is the one whose cepstrum is sought.

SUBROUTINE SIGNAL (Y) (Cosine plus Noise)

This subroutine is like the previous one except that it mixes the white Gaussian noise with the composite signal to make a noisy signal. The complex array Y is generated and sent to the main program. Statistical property of the noise is investigated, signal to noise ratio for the signal is also calculated.

SUBROUTINE SIGNAL (Y) (Damped Cosine)

Subroutine signal for damped cosine will generate a few damped cosine waveforms of the type

$$v_i(t) = \alpha_i \cos(2\pi f(t-\tau_i)) e^{-C(t-\tau_i)} u(t-\tau_i)$$

$$\alpha_i \leq 1.$$

each with different strength. Parameters f and τ_i are as in the previous case and C is the damping coefficient. All variables can get different values furnished through the main program.

SUBROUTINE SIGNAL (Y) (Damped Exponential)

In this subroutine few damping exponential signals are generated each starting at different times and having different strength. The signals are

$$Y_i(t) = \alpha_i(t-\tau_i) e^{-C(t-\tau_i)} u(t-\tau_i)$$

$$\alpha_i = \leq 1.$$

Again τ_i 's are the epoch or echo delay times. These signals will be added together to give the composite signal.

SUBROUTINE WINDOW (I,N,W)

This subroutine does the windowing process based on Kaiser-Bessel equations with $\beta = 8.0$. I is the sample point, N is the total number of samples and W is the weight which is calculated in this subroutine.

SUBROUTINE FFT(X,M)

This subroutine will calculate the Fourier transform of a complex array X with total number of data to be 2^M . The routine is a Fast Fourier Transformation based on Cooley-tukey algorithm.

The complex array X is returned as the Fourier transform of the input array X. The maximum value of M is 10 which can be increased if the respected dimensions in all routines of this report are changed.

SUBROUTINE SMOOTH (N,Y)

Smooth subroutine does smoothing process by Hanning method, N is the total number of points and Y is a complex array of data to be smoothed. After the process is done array Y, the smoothed one, would return.

SUBROUTINE RANSET (MAXINT, NSTRT)

Subroutine RANSET in cooperation with subroutine URAND constitute a machine independent random number generator having specially good statistical and correlation properties. MAXINT is a very big integer depending on size of the computer (for example 32000 for a PDP-11 computer) and NSTRT a small integer usually 0.

REAL FUNCTION URAND (FRAN)

This real function subprogram has been used in cooperation with subroutine RANSET to generate the white Gaussian noise. FRAN is a dummy variable which can be anything. The necessary parameters needed in this program are furnished through a common statement from RANSET subroutine.

SUBROUTINE SHEKL (B,A,NP,XNAME,YNAME,EMI,EXI,ICI)

Subroutine SHEKL is a plotting subroutine which plots array A versus array B. It is a machine independent plotting routine with NP being the total number of points to be plotted and not necessarily the total number of data in arrays A and B. XNAME and YNAME are two 16 character axis title for X and Y axis. EMI and EXI are the minimum and the maximum given to the Y-axis if desired to do so and finally ICI is set equal to zero if no desire for setting maximum and minimum for Y axis and is set equal to one otherwise.

SUBROUTINE RPRD

This is the only machine dependent routine used in the entire study. It is used to plot the Cepstrum and is fed for its variables through common statements by the main program and by the signal subroutine. SICCMP is a common statement bring variables from the signal subroutine and CMPLOO, CMPLO1 and CMPLO2 are three common statements responsible for transfer of variables from the main program to the subroutine.

A LISTING OF FORTRAN PROGRAMS

The following are programs and subroutines explained completely
in previous pages.

```

COMPLEX Y(1024)
DIMENSION AMAG(1024),XNAME(4),YNAME(4),P(1024)
COMMON/CMPL2/NP,T,F,ALF0,ALF1,COEF,TAU(3)
COMMON/DATA/HNAME(4),VNAME(4),Q(1024)
DATA XNAME/4HFREQ,4HUEN-,4HCY,4H /
DATA YNAME/4HMAGN,4HITU-,4HDE,4H /
DATA HNAME/4HTIME,4HSEC,4HOND,4H /
DATA VNAME/4HSIGN,4HAL,4H /
C**** IWNDW IS FOR WINDOWING IN TIME IWNDW 1 YES 0 NO
C**** IWNDF IS FOR WINDOWING IN FREQUENCY 1 YES 0 NO
1  FORMAT(1H1)
2  FORMAT(3(/))
C
C**** SET ALL CONSTANTS USED IN THE PROGRAM
C
      IC=2
      EM=1.
      EX=1.
      JJ=1
      PI=3.141592654
      PI20=PI/20.
C
C
C
C**** READ DATA FROM DATA CARD
C
      READ(5,5) M,ND,IWNDW,IWNDF,T,F,ALF0,ALF1,COEF
5      FORMAT(4I2,5F10.5)
      READ(5,10) (TAU(I),I=1,ND)
10     FORMAT(8F10.5)
C
C
C**** PRINT THE READ DATA
C
      WRITE(6,1)
12     WRITE(6,12) M,T,ND,IWNDW,IWNDF,F,ALF0,ALF1,COEF
      FORMAT(23X,2HM=,12/23X,2HT=,F10.5/21X,4H ND=,12/
      *19X,6HIWNDW=,11/19X,6HIWNDF=,11/23X,2HF=,F10.5/
      *20X,5HALF0=,F10.5/20X,5HALF1=,F10.5/20X,5HCOEF=,
      *F10.5)
      DO 20 I=1,ND
15     WRITE(6,15) I,TAU(I)
20     FORMAT(17X,4HTAU(,12,2H)=,F10.5)
      CONTINUE
C
      NP=2**M
      IF(JJ.NE.1) GO TO 26
C
C**** CALCULATE FREQUENCY FOR THE FOURIER TRANSFORM
C**** NOTE THAT WE ARE USING FFT AND THE FREQUENCY IS
C**** (NU)(FS)/NP WHERE FS=1/TS AND TS=SAMPLING FREQUENCY
      TS=T/NP
      FS=1/TS
      FSS=FS/NP
      TN=T/NP
      P(1)=0.
      NP1=NP-1
      DO 25 I=1,NP1
      Q(I)=TN*I
      NU=I+1
      P(NU)=I*FSS
25     CONTINUE

```

MAIN PROGRAM

```

C
C
C      Q(NP)=NP*TN
C
C
C
C**** GENERATION OF THE SIGNAL
CALL SIGNAL(Y)
C
C
26  CONTINUE
    IF(IWNDW.EQ.0) GO TO 40
C
C**** DO THE WINDOWING PROCESS
C
    DO 30 I=1,NP
    CALL WINDOW(I,NP,W)
    X=W*REAL(Y(I))
    Y(I)=CMPLX(X,AIMAG(Y(I)))
30  CONTINUE
40  CONTINUE
C
C**** FIND THE FIRST FOURIER TRANSFORM
C
    CALL FFT(Y,M)
C
C
C
C**** FIND THE LOG MAGNITUDE ALSO MAKE PREPARATION FOR
C**** TAKING THE SECOND FOURIER TRANSFORM
C
    DO 60 I=1,NP
    AMAG(I)=REAL(Y(I))**2+AIMAG(Y(I))**2
    IF(AMAG(I).EQ.0.0) GO TO 50
    X=ALOG10(AMAG(I))
    Y(I)=CMPLX(X,0.0)
50  GO TO 60
    CONTINUE
    X=-1.0E10
    Y(I)=CMPLX(X,0.0)
60  CONTINUE
C
C
C
C**** PLOT THE POWER SPECTRUM
C
    WRITE(6,2)
    WRITE(6,65)
65  FORMAT(10X,34HTHIS IS GRAPH OF THE FIRST FOURIER,
*33H TRANSFORM OF THE COMPOSIT SIGNAL)
    WRITE(6,2)
C
    NP=NP/2
    CALL SHEKL(Q,AMAG,NP,XNAME,YNAME,EM,EX,IC)
    NP=2*NP
C
    IF(IWPDF.EQ.0) GO TO 70
C
C**** DO THE SMOOTHING
C
    CALL SMOOTH(NP,Y)
C
C
70  CONTINUE

```

MAIN PROGRAM (Continued)

```

C
C**** FIND THE FOURIER TRANSFORM OF THE LOG SPECTRUM
C      CALL FFT(Y,M)
C
C**** CALCULATE THE POWER CEPSTRUM
C      WRITE(6,1)
C      NP=NP/2
C      DO 90 I=1, NP
C      AMAG(I)=SQRT(REAL(Y(I))**2+AIMAG(Y(I))**2)
C      IF(I.GT.20) GO TO 90
C      WRITE(6,80) Q(I),AMAG(I)
80      FORMAT(2(10X,G20.6))
90      CONTINUE
C
C**** DO SMOOTHING OF THE END POINTS BY MULTIPLYING
C**** THE FIRST 20 POINTS BY .5*(1.-COS(2.*PI*I/20.))
C**** I=1,2,.....,20
C      DO 100 I=1,20
C      Z1=PI/20*I
C      Z2=COS(Z1)
C      Z3=1.-Z2
C      Z4=.5*Z3
C      Z5=Z4+AMAG(I)
100     AMAG(I)=Z5
C      CONTINUE
C
C**** PLOT THE POWER CEPSTRUM
C      WRITE(6,1)
C      WRITE(6,120)
120     FORMAT(10X,25HTHIS IS THE CEPSTRUM PLOT)
C      WRITE(6,2)
C      CALL SHEKL(Q,AMAG,NP,XNAME,YNAME,EM,EX,IC)
C      STOP
C      END

```



```
30  WRITE(6,30)
    FORMAT(10X,33HTHIS IS GRAPH OF THE FIRST SIGNAL)
    WRITE(6,2)
    CALL SHEKL(Q,AMAG,MP,XNAME,YNAME,EM,EX,IC)
    WRITE(6,1)
40  WRITE(6,40)
    FORMAT(10X,34HTHIS IS GRAPH OF THE SECOND SIGNAL)
    WRITE(6,2)
    CALL SHEKL(Q,AMGA,MP,XNAME,YNAME,EM,EX,IC)
    IF(TAU(3).EQ.0.) GO TO 60
    WRITE(6,1)
50  WRITE(6,50)
    FORMAT(10X,33HTHIS IS GRAPH OF THE THIRD SIGNAL)
    WRITE(6,2)
    CALL SHEKL(Q,DMAG,MP,XNAME,YNAME,EM,EX,IC)
60  CONTINUE
    WRITE(6,1)
70  WRITE(6,70)
    FORMAT(10X,36HTHIS IS GRAPH OF THE COMPOSIT SIGNAL)
    WRITE(6,2)
    CALL SHEKL(Q,CMAG,MP,XNAME,YNAME,EM,EX,IC)
    WRITE(6,1)
    RETURN
    END
```

SUBROUTINE SIGNAL (Cosine) (Continued)

```

SUBROUTINE SIGNAL(Y)
COMPLEX Y(1024),AN(1024)
DIMENSION AMAG(1024),BMAG(1024),CMAG(1024),ANS(1024)
DIMENSION DMAG(1024)
COMMON/CM2/NP,T,F,ALF0,ALF1,COEF,TAU(3),FSNR,M
COMMON/DATAA/HNAME(4),VNAME(4),Q(1024)
C*****
C***** THIS SUBROUTINE WILL GENERATE FEW COSINE WAVEFORM
C***** WITH THE SAME FREQUENCY BUT DIFFERENT STRENGTH
C***** AND ARRIVING AT DIFFERENT TIMES,ALSO IT
C***** GENERATES AND MIXES NOISE WITH THE SIGNALS
C*****
1
2
C
C***** SET ALL CONSTANTS USED IN THE PROGRAM
C
PI=3.141592654
PI2=2.*PI
PI2F=PI2*F
TN=T/NP
SS=0.0
SSN=0.0
EM=1.
EX=1.
IC=2
SUM=0.0
SUM2=0.0
CS3=0.0
C
C
C
C***** INITIATE THE NOISE GENERATOR
C
CALL RANSET(1E+10,0)
C
C
C***** GENERATION OF THE SIGNAL
C
DO 20 I=1,NP
TM=TN*I
TM1=TM-TAU(1)
TM2=TM-TAU(2)
TM3=TM-TAU(3)
TM1P=PI2F*TM1
TM2P=PI2F*TM2
TM3P=PI2F*TM3
CS1=COS(TM1P)
CS2=ALF0*COS(TM2P)
CS3=ALF1*COS(TM3P)
IF(TM.LT.TAU(1))CS1=0.0
IF(TM.LT.TAU(2))CS2=0.0
IF(TM.LT.TAU(3))CS3=0.0
C
C***** NOISE GENERATION
C
CSN=URAND(X)
CSN=FSNR*CSN
SUM=SUM+CSN
SUM2=SUM2+CSN**2
AMAG(I)=CS1
BMAG(I)=CS2
CMAG(I)=CS3
CS=CS1+CS2+CS3

```

SUBROUTINE SIGNAL (Cosine Plus Noise)

```

Y(I)=CMPLX(CS,SS)
AN(I)=CMPLX(CSN,SSN)
ANS(I)=CSN
20 CONTINUE
C
C**** FIND MEAN, MEAN SQUARED, AND STANDARD DEVIATION
C
FNP=FLOAT(NP)
SUM=SUM/FNP
SUM2=SUM2/FNP
STDV=SQRT(SUM2-SUM**2)
C
C
C**** PRINT STATISTICAL PROPERTY OF THE NOISE
C
WRITE(6,2)
WRITE(6,30)
30 FORMAT(10X,35HSTATISTICAL PROPERTIES OF THE NOISE)
WRITE(6,2)
WRITE(6,40) SUM,SUM2,STDV
40 FORMAT(20X,5HMEAN=,G13.6/,17X,8HMEAN SQ=,G13.6/12X,
*13HSTANDARD DEV=,G13.6)
C
C
C**** FIND FFT OF THE NOISE AND THE SIGNAL
C
CALL FFT(Y,M)
CALL FFT(AN,M)
C
C
C**** FIND SIGNAL TO NOISE RATIO AND PRINT IT
C
TOTLS=0.0
TOTLN=0.0
DO 50 I=1,NP
TTS=REAL(Y(I))**2+AIMAG(Y(I))**2
TTN=REAL(AN(I))**2+AIMAG(AN(I))**2
TOTLS=TOTLS+TTS
TOTLN=TOTLN+TTN
50 CONTINUE
TOTLS=SQRT(TOTLS)
TOTLN=SQRT(TOTLN)
SNR=TOTLS/TOTLN
SNR=10.*ALOG10(SNR)
60 WRITE(6,60) SNR
FORMAT(21X,4HSNR=,F10.5,5H DB)
WRITE(6,2)
C
C
C**** MIX SIGNAL WITH THE NOISE
C
DO 65 I=1,NP
AMAG(I)=AMAG(I)+ANS(I)
DMAG(I)=AMAG(I)+BMAG(I)+CMAG(I)
CS=DMAG(I)
Y(I)=CMPLX(CS,SS)
65 CONTINUE

```

```
MP=300
WRITE(6,1)
WRITE(6,70)
70  FORMAT(10X,26HTHIS IS GRAPH OF THE NOISE)
    WRITE(6,2)
    CALL SHEKL(Q,ANS,MP,HNAME,VNAME,EM,EX,IC)
    WRITE(6,1)
    WRITE(6,80)
80  FORMAT(10X,33HTHIS IS GRAPH OF THE FIRST SIGNAL)
    WRITE(6,2)
    CALL SHEKL(Q,AMAG,MP,HNAME,VNAME,EM,EX,IC)
    WRITE(6,1)
    WRITE(6,90)
90  FORMAT(10X,34HTHIS IS GRAPH OF THE SECOND SIGNAL)
    WRITE(6,2)
    CALL SHEKL(Q,BMAG,MP,HNAME,VNAME,EM,EX,IC)
    IF(TAU(3).EQ.0.0) GO TO 105
    WRITE(6,1)
    WRITE(6,100)
100 FORMAT(10X,33HTHIS IS GRAPH OF THE THIRD SIGNAL)
    WRITE(6,2)
    CALL SHEKL(Q,CMAG,MP,HNAME,VNAME,EM,EX,IC)
105  CONTINUE
    WRITE(6,1)
    WRITE(6,110)
110 FORMAT(10X,37HTHIS IS GRAPH OF THE COMPOSIT SIGNAL)
    WRITE(6,2)
    CALL SHEKL(Q,DMAG,MP,HNAME,VNAME,EM,EX,IC)
    WRITE(6,1)
    RETURN
    END
```

SUBROUTINE SIGNAL (Cosine Plus Noise) (Continued)

```

SUBROUTINE SIGNAL (Y)
  COMPLEX Y(1024)
  COMMON/SIGLOO/F,ALFO,ALF1,COEF
  COMMON/SIGCMP/T,NP,TAU(3)
C****
C**** THIS SUBROUTINE WILL GENERATE FEW DAMPED COS SIGNALS
C**** WITH THE SAME FREQUENCY BUT DIFFERENT STRENGTH
C**** AND ARRIVING AT DIFFERENT TIMES
C**** TAU(I) I=1,2,.. IS THE DELAY IN SECONDS
C**** F IS THE FREQUENCY IN HERTZ
C
C
1  FORMAT (1H1)
2  FORMAT (3(/))
C
C**** SET THE CONSTANTS
C
  PI=3,141592654
  PI2=2.*PI
  PI2F=PI2*F
  TN=T/NP
  SS=0.0
  CS3=0.
C
C
C
C**** SIGNAL GENERATION
C  DO 20 I=1,NP
    TM=TN*I
    TMI=TM-TAU(1)
    TM2=TM-TAU(2)
    TM3=TM-TAU(3)
    TMM1=PI2F*TM1
    TMM2=PI2F*TM2
    TMM3=PI2F*TM3
    CSC1=COS(TMM1)
    CSC2=COS(TMM2)
    CSC3=COS(TMM3)
    CS1=CSC1*EXP(-COEF*TM1)
    CS2=ALFO*CSC2*EXP(-COEF*TM2)
    CS3=ALF1*CSC3*EXP(-COEF*TM3)
    IF(TM.LT.TAU(1))CS1=0.0
    IF(TM.LT.TAU(2))CS2=0.0
    IF(TM.LT.TAU(3))CS3=0.
    CS=CS1+CS2+CS3
    Y(I)=CMPLX(CS,SS)
20 CONTINUE
  RETURN
  END

```

SUBROUTINE SIGNAL (Damped Cosine)

```

SUBROUTINE SIGNAL(Y)
COMPLEX Y(1024)
DIMENSION AMAG(1024),BMAG(1024),CMAG(1024)
DIMENSION DMAG(1024)
COMMON/CMPL2/NP,T,F,ALF0,ALF1,COEF,TAU(3)
COMMON/DATAA/HNAME(4),VNAME(4),Q(1024)
C
C**** THIS SUBROUTINE WILL GENERATE FEW DAMPING
C**** EXPONENTIAL SIGNALS STARTING AT DIFFERENT TIMES
C**** AND HAVING DIFFERENT STRENGTHS
C
1   FORMAT(1H1)
2   FORMAT(3(/))
C
C**** SET THE CONSTANTS
C
   SS=0.
   TN=T/NP
   CS3=0.0
C
C
C**** SIGNAL GENERATION
C
   DO 10 I=1,NP
   TM=TN*I
   TM1=TM-TAU(1)
   TM2=TM-TAU(2)
   TM3=TM-TAU(3)
   TMM1=EXP(-COEF*TM1)
   TMM2=EXP(-COEF*TM2)
   TMM3=EXP(-COEF*TM3)
   CS1=TM1*TMM1
   CS2=ALF0*TM2*TMM2
   CS3=ALF1*TM3*TMM3
   IF(TM.LT.TAU(1)) CS1=0.0
   IF(TM.LT.TAU(2)) CS2=0.0
   IF(TM.LT.TAU(3)) CS3=0.0
   CS=CS1+CS2+CS3
   AMAG(I)=CS1
   BMAG(I)=CS2
   CMAG(I)=CS3
   DMAG(I)=CS
   Y(I)=CMPLX(CS,SS)
10  CONTINUE
C
C
C**** PLOT THE SIGNALS
C
   MP=300
   WRITE(6,1)
   WRITE(6,30)
30  FORMAT(10X,33HTHIS IS GRAPH OF THE FIRST SIGNAL)
   WRITE(6,2)
   CALL SHEKL(Q,AMAG,MP,HNAME,VNAME,1.,1.,2)
   WRITE(6,1)
   WRITE(6,40)
40  FORMAT(10X,34HTHIS IS GRAPH OF THE SECOND SIGNAL)
   WRITE(6,2)
   CALL SHEKL(Q,BMAG,MP,HNAME,VNAME,1.,1.,2)
   IF(TAU(3).EQ.0.0) GO TO 60
   WRITE(6,1)
   WRITE(6,50)
50  FORMAT(10X,33HTHIS IS GRAPH OF THE THIRD SIGNAL)

```

SUBROUTINE SIGNAL (Damped Exponential)

```
WRITE(6,2)
CALL SHEKL(Q,CMAG,MP,HNAME,VNAME,1.,1.,2)
60 CONTINUE
WRITE(6,1)
WRITE(6,70)
70 FORMAT(10X,36HTHIS IS GRAPH OF THE COMPOSIT SIGNAL)
WRITE(6,2)
CALL SHEKL(Q,DMAG,MP,HNAME,VNAME,1.,1.,2)
WRITE(6,1)
RETURN
END
```

SUBROUTINE SIGNAL (Damped Exponential) (Continued)

```
C**** SUBROUTINE WINDOW(I,N,W)
C**** THE WINDOWING PROCESS IS BASED ON KAISER-BESSEL
C**** (BETA=8.) EQUATIONS
S=1.0E-8
IB=N/2
A=(I-IB)/IB
X=8.*SQRT(1.-A**2)
E=1.
DE=1.0
Y=X/2.
DO 10 J=1,25
DE=DE*Y/FLOAT(J)
SDE=DE**2
E=E+SDE
IF(E*S-SDE) 10,10,20
CONTINUE
X=E
W=X/427.57
RETURN
END
```

10
20

SUBROUTINE WINDOW

```

SUBROUTINE FFT(X,M)
COMPLEX X(1024),U,W,T
C
C**** THIS SUBROUTINE WILL COMPUTE DFT BY FFT METHOD
C**** FOR REFERENCE SEE "THE FAST FOURIER TRANSFORM
C**** AND IT APPLICATIONS" BY JAMES W. COOLEY,P.A.W.LEWIS
C**** AND PETER D. WELCH IEEE TRANS ON ED,VOL.12,NO.1
C**** ,MARCH 1969 PP 27-34
C
C
N=2**M
N2=N/2
N1=N-1
J=1
DO 3 I=1,N1
IF(I.GE.J) GO TO 1
T=X(J)
X(J)=X(I)
X(I)=T
1
K=N2
IF(K.GE.J) GO TO 3
J=J-K
K=K/2
GO TO 2
3
J=J+K
PI=3.141592653589793
DO 5 L=1,M
LE=2**L
LE1=LE/2
U=(1,0,0,0)
W=CMPLX(COS(PI/LE1),SIN(PI/LE1))
DO 5 J=1,LE1
DO 4 I=J,N,LE
ID=I+LE1
T=X(ID)*U
X(ID)=X(I)-T
4
X(I)=X(I)+T
5
U=U*W
RETURN
END

```

SUBROUTINE FFT

```
      SUBROUTINE SMOOTH(N,Y)
      COMPLEX Y(1024)
C**** THIS SUBROUTINE DOES SMOOTHING PROCESS BY HANNING
C**** METHOD
      N1=N-1
      X=(REAL(Y(1))+REAL(Y(2)))/2.
      Y(1)=CMPLX(X,AIMAG(Y(1)))
      X=(REAL(Y(N1))+REAL(Y(N)))/2.
      Y(N)=CMPLX(X,AIMAG(Y(N)))
      DO 10 I=2,N1
      A=REAL(Y(I-1))/4.
      C=REAL(Y(I+1))/4.
      B=REAL(Y(I))/2.
      X=A+B+C
      Y(I)=CMPLX(X,AIMAG(Y(I)))
10    CONTINUE
      RETURN
      END
```

SUBROUTINE SMOOTH

```

SUBROUTINE RANSET(MAXINT,NSTRT)
COMMON/MG/RAN(10),GEN(10),NWRD,BASE,MOD,FBASE,FMOD
INTEGER RAN,GEN,BASE,CARRY,REM
C**** RANSET AND URAND CONSTITUTE A MACHINE INDEPENDENT
C**** RANDOM NUMBER GENERATOR HAVING SPECIALLY GOOD
C**** STATISTICAL AND CORRELATION PROPERTIES, FOUND IN
C**** VOLUME II OF THE FOLLOWING BASIC REFERENCE.
C**** E.G.MCGRATH .ET AL,"TECHNIQUES FOR EFFICIENT MONTE
C**** CARLO SIMULATION
C**** VOL I. SELECTING PROBABILITY DISTRIBUTIONS
C**** (AD-762-721)
C**** VOL II. RANDOM NUMBER GENERATION FOR SELECTED
C**** PROBABILITY DISTRIBUTIONS(AD-762-722)
C**** VOL III. VARIANCE REDUCTION (AD-762-723)
MAXI=MAXINT/4
IB=0
BASE=1
99 IF(BASE.GT.MAXI) GO TO 100
BASE=BASE*4
IB=IB+1
GO TO 99
100 BASE=2**IB
FBASE=BASE
NWRD=47/IB+1
REM=47-IB*(NWRD-1)
MOD=2**REM
FMOD=MOD
DO 101 N=1,10
RAN(N)=0
GEN(N)=0
101 CONTINUE
GEN(1)=5
DO 200 I=1,14
CARRY=0
DO 190 N=1,NWRD
GEN(N)=GEN(N)*5+CARRY
CARRY=0
IF(GEN(N).LT.BASE) GO TO 190
CARRY=GEN(N)/BASE
GEN(N)=GEN(N)-BASE+CARRY
190 CONTINUE
200 CONTINUE
NSTART=NSTRT
IF(NSTART.LE.0) NSTART=2001
NSTART=2*(NSTART/2)+1
DO 300 N=1,NWRD
NTEMP=NSTART/BASE
RAN(N)=NSTART-NTEMP*BASE
NSTART=NTEMP
300 CONTINUE
RETURN
END

```

SUBROUTINE RANSET

```

REAL FUNCTION URAND(FRAN)
COMMON/MG/RAN(10),GEN(10),NWRD,BASE,MOD,FBASE,FMOD
DIMENSION SUM(10)
INTEGER RAN,GEN,BASE,CARRY,SUM,PROD,HPROD
DO 30 IS=1,NWRD
SUM(IS)=0
30 CONTINUE
DO 1 IG=1,NWRD
N2=NWRD-IG+1
DO 1 IR=1,N2
IS=IR+IG-1
PROD=RAN(IR)*GEN(IG)
HPROD=PROD/BASE
LPROD=PROD-HPROD*BASE
SUM(IS)=SUM(IS)+LPROD
1 IF(IS.LT.NWRD) SUM(IS+1)=SUM(IS+1)+HPROD
CONTINUE
N2=NWRD-1
DO 5 IS=1,N2
CARRY=SUM(IS)/BASE
SUM(IS)=SUM(IS)-CARRY*BASE
SUM(IS+1)=SUM(IS+1)+CARRY
5 CONTINUE
SUM(NWRD)=SUM(NWRD)-MOD*(SUM(NWRD)/MOD)
DO 20 IS=1,NWRD
RAN(IS)=SUM(IS)
20 CONTINUE
FRAN=SUM(1)
DO 10 IS=2,NWRD
FRAN=FRAN/FBASE+FLOAT(SUM(IS))
10 CONTINUE
FRAN=FRAN/FMOD
URAND=FRAN
RETURN
END

```

FUNCTION URAND

.4339	.7489	.9904	.8066	.9647	.4108	.5079	.2305	.8254	.6424
.3727	.8990	.5700	.6670	.8995	.0316	.6046	.2887	.7004	.0771
.7623	.8476	.5595	.2498	.2727	.1386	.1320	.8203	.2988	.9647
.1032	.2196	.0736	.0596	.6543	.6999	.5667	.6486	.8879	.4846
.6556	.2540	.4236	.1514	.6888	.9273	.4725	.6948	.4600	.4813
.7548	.6872	.9456	.1947	.2782	.7067	.2894	.6862	.9025	.3586
.6712	.1616	.0778	.5483	.7350	.0764	.0634	.0419	.6368	.6480
.8595	.7904	.6176	.8909	.3715	.1236	.0323	.4017	.7728	.0014
.3249	.5456	.0430	.4225	.5105	.6921	.2788	.3441	.9040	.5348
.2714	.6929	.3603	.2550	.2914	.0058	.9934	.4185	.9584	.8090

```

1
2
DIMENSION A(10)
FORMAT(1H1)
FORMAT(10(1))
CALL RANSET(32767,0)
WRITE(6,1)
DO 70 I=1,10
DO 50 J=1,10
A(I,J)=URAND(X)
CONTINUE
WRITE(6,60) (A(I,J),J=1,10)
FORMAT(1H0,10X,10(1X,F6.4))
CONTINUE
WRITE(6,1)
STOP
END
50
60
70

```

A SAMPLE PROGRAM FOR GENERATING RANDOM NUMBERS

```

SUBROUTINE SHEKL(B,A,NP,XNAME,YNAME,EM1,EX1,IC1)
DIMENSION B(NP),A(NP),LINE(61),XNAME(4),YNAME(4)
REAL LINE
LOGICAL MANUAL,SYME
DATA HI/1HS/,LO/1H#/,BLANK/1H /,DOT/1H./,STAR/1H*/
EMIN=EM1
EMAX=EX1
ISC=IC1
MANUAL=.TRUE.
SYME=.FALSE.
IF(EMAX.EQ.EMIN) MANUAL=.FALSE.
IF(EMIN.GT.EMAX) GO TO 160
IISC=ISC
IF(MANUAL) IISC=1
IF(MANUAL) GO TO 11
YMIN=1.E38
YMAX=-1.E38
DO 10 I=1,NP
IF(A(I).GT.YMAX) YMAX=A(I)
IF(A(I).LT.YMIN) YMIN=A(I)
10 CONTINUE
GO TO 19
11 YMAX=EMAX
YMIN=EMIN
19 XMIN=ABS(B(1))
MIN=1
DO 20 J=2,NP
IF(ABS(B(J)).GE.XMIN) GO TO 20
XMIN=ABS(B(J))
MIN=J
20 CONTINUE
IF(IISC.EQ.0) GO TO 21
RANGE=YMAX-YMIN
KAXIS=60.*(-YMIN/RANGE)+1.5
IF(YMIN.GT.0.0) KAXIS=1
IF(YMAX.LT.0.0) KAXIS=61
DIS=RANGE/60.
GO TO 30
21 IF(YMIN.GE.0.) GO TO 22
IF(YMAX.LE.0.) GO TO 23
KAXIS=31
SYME=.TRUE.
ABY=ABS(YMIN)
RANGE=AMAX1(YMAX,ABY)
DIS=RANGE/30.
GO TO 30
22 KAXIS=1
RANGE=YMAX
DIS=RANGE/60.
GO TO 30
23 KAXIS=61
RANGE=-YMIN
DIS=RANGE/60.
30 CONTINUE
DO 40 K4=1,3
WRITE(6,50)
40 CONTINUE
50 FORMAT(1H0)
WRITE(6,60) XNAME(1),XNAME(2),YNAME(1),YNAME(2),
*YMIN,YMAX
60 *G13.6,3X,4HMAX=,G13.6)

```

SUBROUTINE SHEKL

```

70 WRITE(6,70) XNAME(3),XNAME(4),YNAME(3),YNAME(4),DIS
   FORMAT(2X,A4,A4,7X,A4,A4,25X,10HINCREMENT=,G13.6/)
   DO 80 J=1,61
80  LINE(J)=BLANK
   CONTINUE
   DO 100 J2=1,NP
   IF(J2.EQ.MIN) GO TO 110
   X=60.0*((A(J2)-YMIN)/RANGE)
   IF(IISC.EQ.0.AND.YMIN.GT.0.) X=60.*(A(J2)/RANGE)
   IF(SYME) X=30.*(A(J2)/RANGE)+30.
   K=X+1.5
   LINE(KAXIS)=DOT
   IF(K.GT.61) LINE(61)=HI
   IF(K.GT.61) KMAX=61
   IF(K.GT.61) GO TO 89
   IF(K.LT.1) LINE(1)=LO
   IF(K.LT.1) KMAX=KAXIS
   IF(K.LT.1) GO TO 89
   LINE(K)=STAR
   KMAX=KAXIS
   IF(K.GT.KMAX) KMAX=K
89  WRITE(6,90) B(J2),A(J2),(LINE(N4),N4=1,KMAX)
90  FORMAT(1X,G13.6,2X,G13.6,2X,61A1)
   IF(K.GT.61) LINE(61)=BLANK
   IF(K.GT.61) GO TO 100
   IF(K.LT.1) LINE(1)=BLANK
   IF(K.LT.1) GO TO 100
   LINE(K)=BLANK
100 CONTINUE
   GO TO 145
110 CONTINUE
   DO 120 J=1,61
   LINE(J)=DOT
120 CONTINUE
   X=60.0*((A(MIN)-YMIN)/RANGE)
   IF(IISC.EQ.0.AND.YMIN.GT.0.) X=60.*(A(J2)/RANGE)
   IF(SYME) X=30.*(A(J2)/RANGE)+30.
   KP1=X+1.5
   IF(KP1.GT.61) LINE(61)=HI
   IF(KP1.LT.1) LINE(1)=LO
   IF(KP1.LT.1.OR.KP1.GT.61) GO TO 129
   LINE(KP1)=STAR
129 WRITE(6,130) B(J2),A(J2),LINE
130 FORMAT(1X,G13.6,2X,G13.6,2X,61A1)
   DO 140 J=1,61
   LINE(J)=BLANK
140 CONTINUE
   GO TO 100
145 DO 150 K5=1,3
   WRITE(6,50)
150 CONTINUE
   EMAX=YMAX
   EMIN=YMIN
   RETURN
160 CONTINUE
170 WRITE(6,170)
   FORMAT(10X,34HHAVE A MISTAKE INPUTTING EMIN&EMAX)
   RETURN
END

```

SUBROUTINE SHEKL (Continued)

```

SUBROUTINE RPRD
COMMON/SIGCMP/T, NP, TAU(3), M, SNR
COMMON/CMPL00/XSZ, YSZ, XORG, YORG, H
COMMON/CMPL01/Q(1026), AMAG(1026), YMAX
COMMON/CMPL02/IFORM, NCOPY, LNF, NOSYM, IWNDW, IWNDF
C
C**** GIVE THE SIZE OF X AND Y NEEDED FOR THIS PLOT
C
CALL PLOTS(XSZ, YSZ, IFORM, NCOPY)
C
C
N=NP
C**** SPECIFY THICKNESS OF THE FRAME
C
CALL LINEWT(-1)
C
C**** SET THE ORIGIN AT THE POINT 1.,1. THEN FROM NOW
C**** ON IT WOULD BE POINT 0.,0.
C
CALL PLOT(1., 1., -3)
C
C**** DRAW THE FRAME FOR THE SIZE OF THE PAPER
C
CALL PLOT(XSZ, 0.0, 2)
CALL PLOT(XSZ, YSZ, 3)
CALL PLOT(0.0, YSZ, 2)
CALL PLOT(0.0, 0.0, 2)
C
C**** SET NEW ORIGIN
C
CALL PLOT(XORG, YORG, -3)
C
C**** DRAW THE COORDINATES FOR THE PLOT
C
XCOR=8.
YCOR=5.
CALL SCALE(Q(1), XCOR, N, 1)
CALL SCALE(AMAG(1), YCOR, N, 1)
N1=N+1
N2=N+2
AMAG(N2)=YMAX/YCOR
Q(N2)=T/XCOR
CALL AXIS(0.0, 0.0, 12H CEPSTRUM ,12, YCOR, 90.,
*AMAG(N1), AMAG(N2))
CALL AXIS(0.0, 0.0, 17HQUEFRENCY SECONDS, -17, XCOR,
*00.0, Q(N1), Q(N2))
C
C**** SPECIFY THE THICKNESS OF THE PLOT
C
CALL LINEWT(0)
C
C**** PLOTTING PROCESS
CALL LINE(Q(1), AMAG(1), N, 1, LNF, NOSYM, H)

```

SUBROUTINE RPRD

```

C
C**** PROCEDURE TO WRITE RELATED PARAMETERS ON THE PLOT
C
CALL PLOT(0.0,0.0,-3)
W=.0875
XW=2.00
IF(TAU(3).NE.0.0) XW=1.5
YW=-.75
CALL SYMBOL(XW,YW,H,6HIWNDW=,00.00,6,0)
XW=XW+6.*W
FW=FLOAT(IWNDW)
FF=FLOAT(IWPDF)
FN=FLOAT(N)
CALL NUMBER(XW,YW,H,FW,0.0,-1,0)
XW=XW+W*4.
CALL SYMBOL(XW,YW,H,6HIWPDF=,00.00,6,0)
XW=XW+6.*W
CALL NUMBER(XW,YW,H,FF,0.0,-1,0)
XW=XW+W*4.
CALL SYMBOL(XW,YW,H,2HN=,00.00,2,0)
XW=XW+2.*W
CALL NUMBER(XW,YW,H,FN,0.0,-1,0)
XW=XW+5.*W
CALL SYMBOL(XW,YW,H,5HTAU1=,00.00,5,0)
XW=XW+6.*W
CALL NUMBER(XW,YW,H,TAU(1),0.0,+3,0)
XW=XW+6.*W
CALL SYMBOL(XW,YW,H,5HTAU2=,00.00,5,0)
XW=XW+6.*W
CALL NUMBER(XW,YW,H,TAU(2),0.0,+3,0)
CALL PLOT(0.0,0.0,-3)
YCOR=YCOR+1.5*H
IF(TAU(3).NE.0.0) GO TO 10
XW=XW+5.*W
CALL SYMBOL(XW,YW,H,5H SNR=,00.00,5,0)
XW=XW+5.*W
CALL NUMBER(XW,YW,H,SNR,0.0,+3,0)
CALL SYMBOL(1.0,YCOR,H,74H COS(200*PI*(T-TAU1))*
* S(200*PI*(T-TAU2))*U(T-TAU2)+NOISE,0.0,74,0)
10 GO TO 20
CONTINUE
XW=XW+6.*W
CALL SYMBOL(XW,YW,H,5HTAU3=,00.00,5,0)
XW=XW+6.*W
CALL NUMBER(XW,YW,H,TAU(3),0.0,+3,0)
XW=XW+5.*W
CALL SYMBOL(XW,YW,H,5H SNR=,00.00,5,0)
XW=XW+5.*W
CALL NUMBER(XW,YW,H,SNR,0.0,+3,0)
CALL SYMBOL(.5,YCOR,H,104H COS(200*PI*(T-TAU1))*U(T
* 0*PI*(T-TAU2))*U(T-TAU2)+.25*COS(200*PI*(T-TAU3))*U
* 0.0,104,0)
20 CONTINUE
CALL PLOT(0.0,0.0,999)
RETURN
END

```

SUBROUTINE RPRD (Continued)

APPENDIX G

FIGURES

KEY TO THE FIGURES

This appendix presents time variation of several signals which have been discussed in detail in the main text. Following each signal waveform is its cepstral plot. In most of the signal plots or their cepstral plots the equation of the composite signal is written. If this equation is broken in "+" points, each part will give the equation of the individual waveforms.

Several notations have been used for the plots which have following meanings.

IWNOW = 0 \equiv no windowing process is performed in time domain

IWNOW = 1 \equiv windowing process is performed in time domain

IWNOF = 0 \equiv no smoothing is performed in frequency domain

IWNOF = 1 \equiv smoothing process if performed in frequency domain

N = total number of sample points

TAU_i = t_i = beginning time for the i^{th} signal

In the following pages figures G-1 through G-5 are cosine waveforms and their cepstral plots. The signals have different starting times and also the number of echoes which makeup the composite signal is different in some cases. The equation for the signals is given on each plot. In all plots $N=1024$, $IRNDW=0$, and $IRNDF=0$ except if they are defined otherwise.

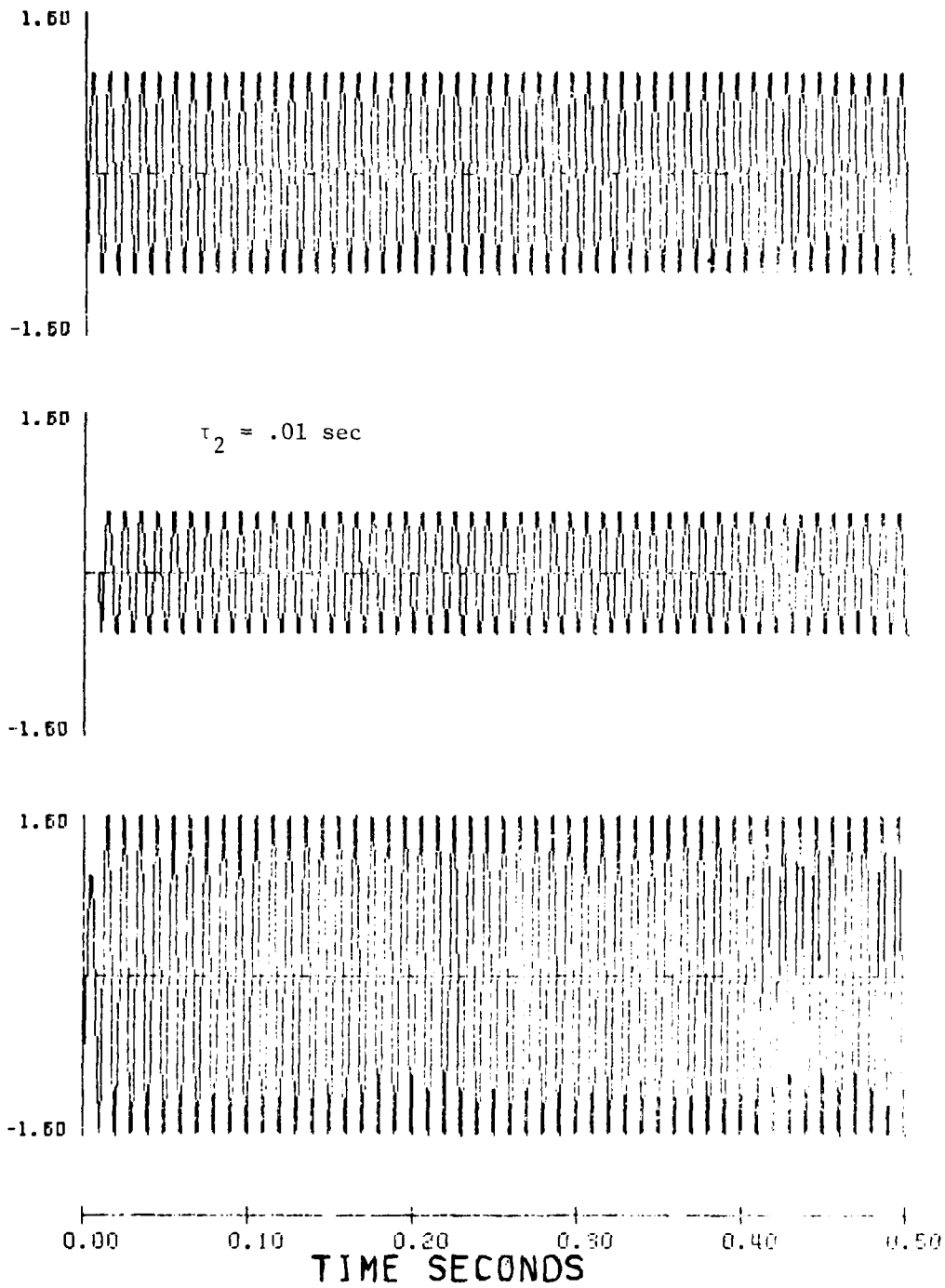


Figure G-1a

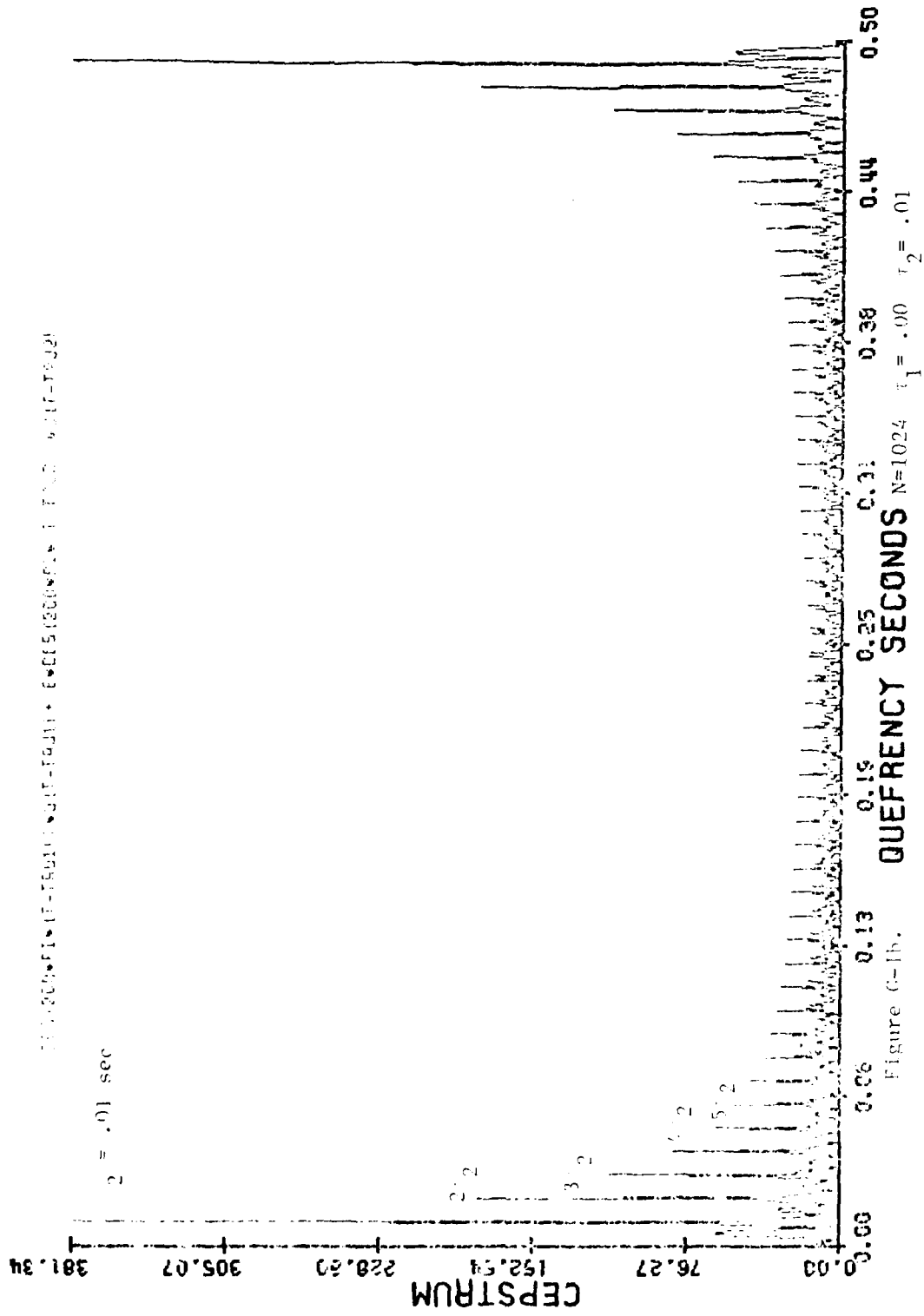


Figure C-1b.

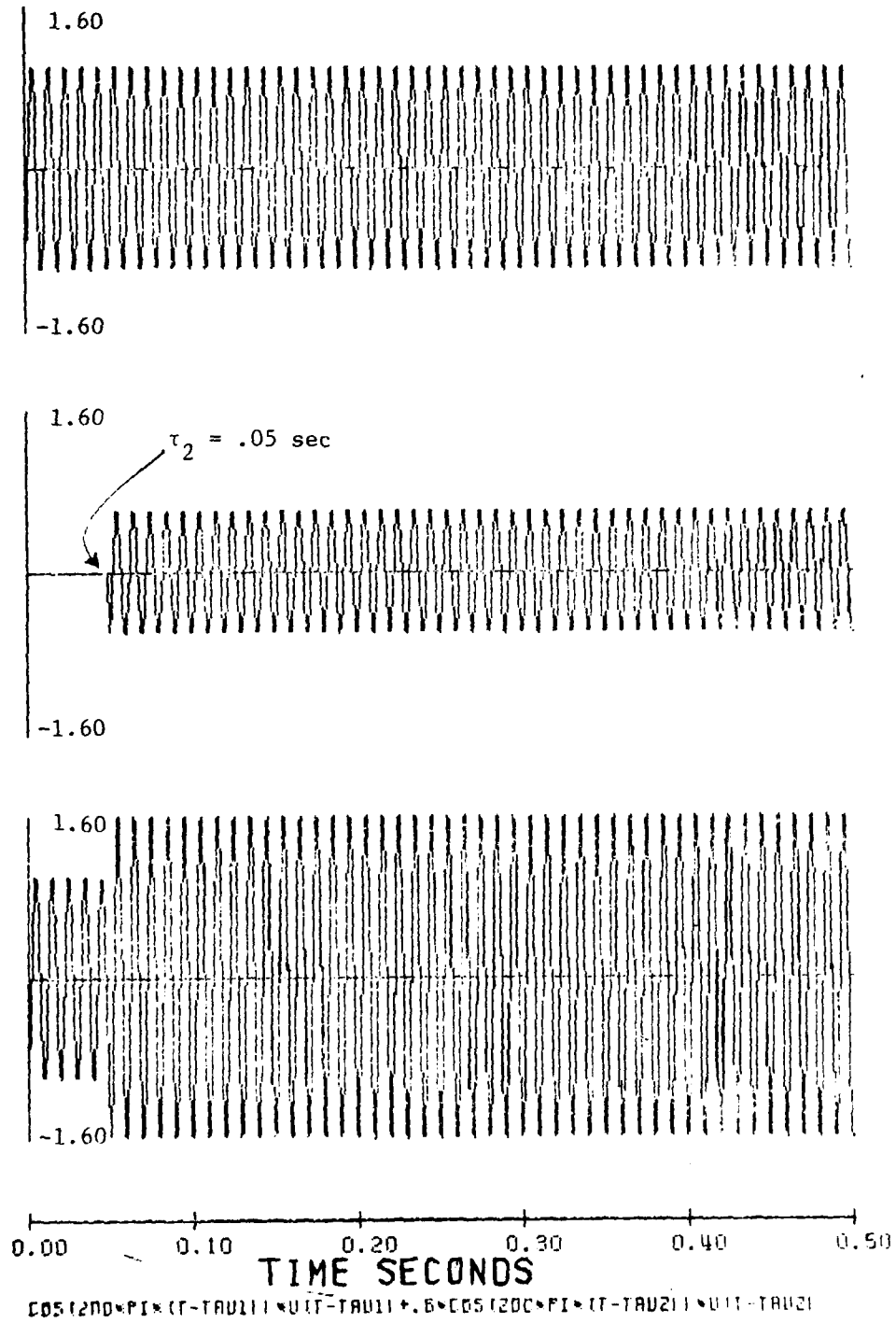


Figure G-2a

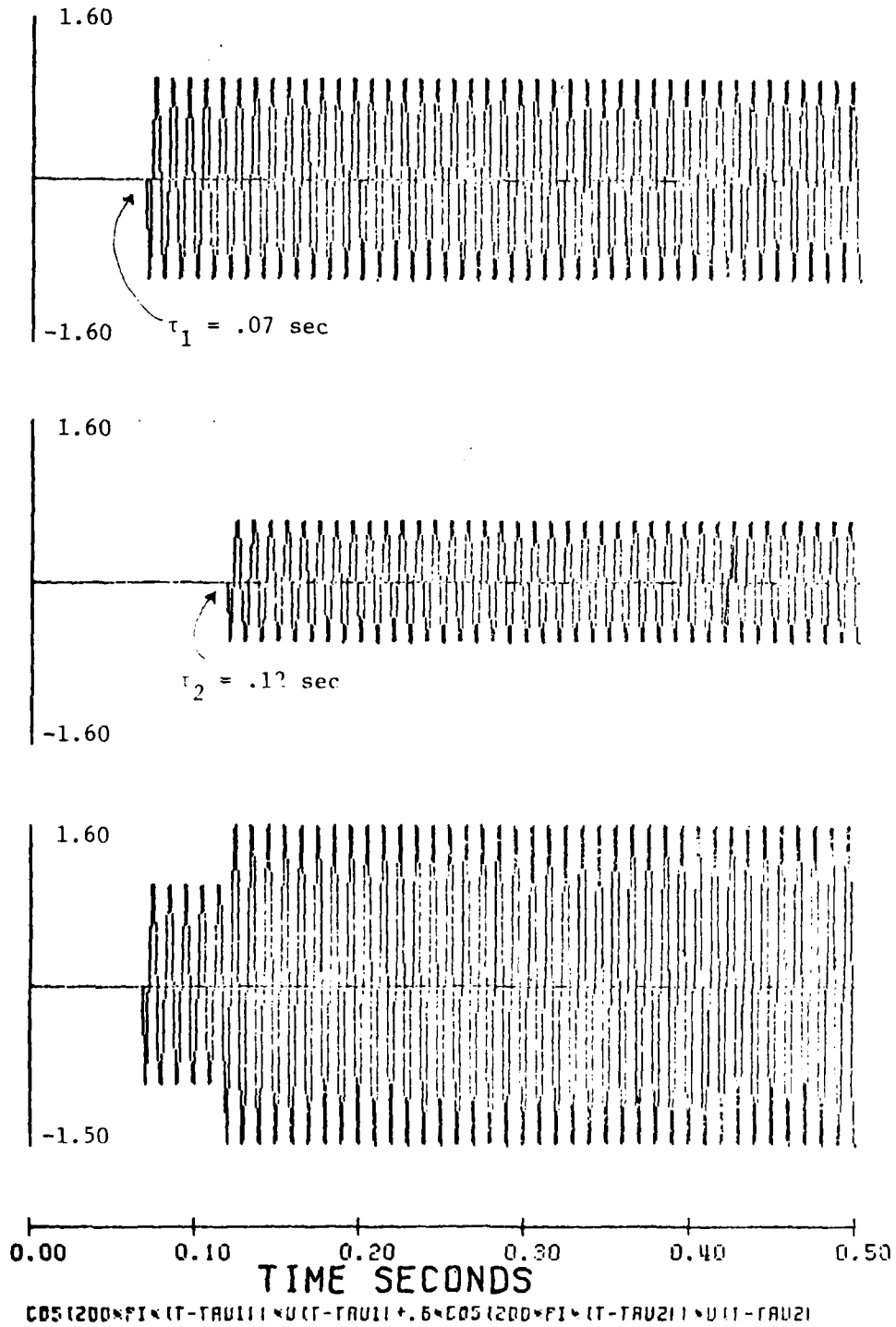


Figure G-3a.

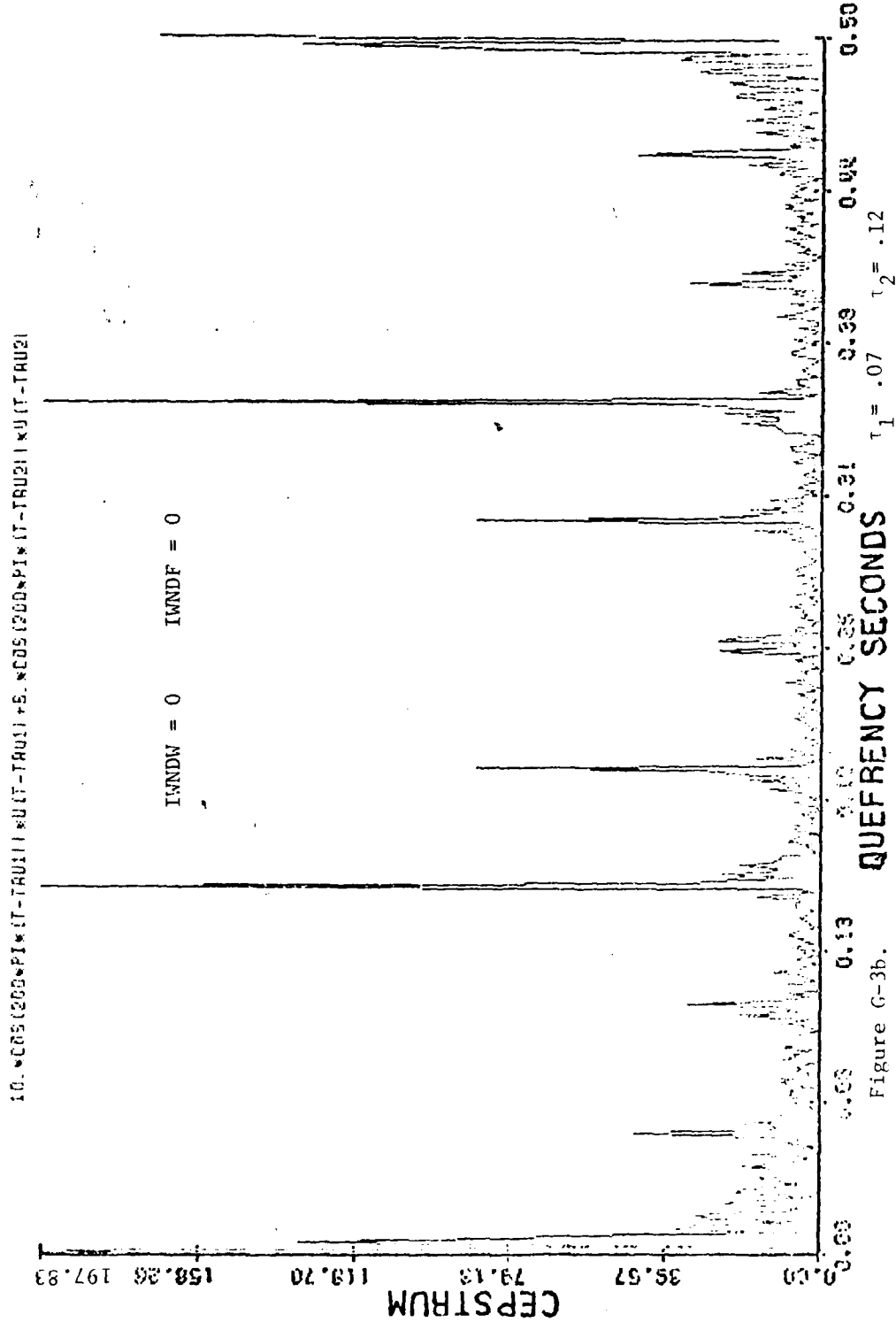
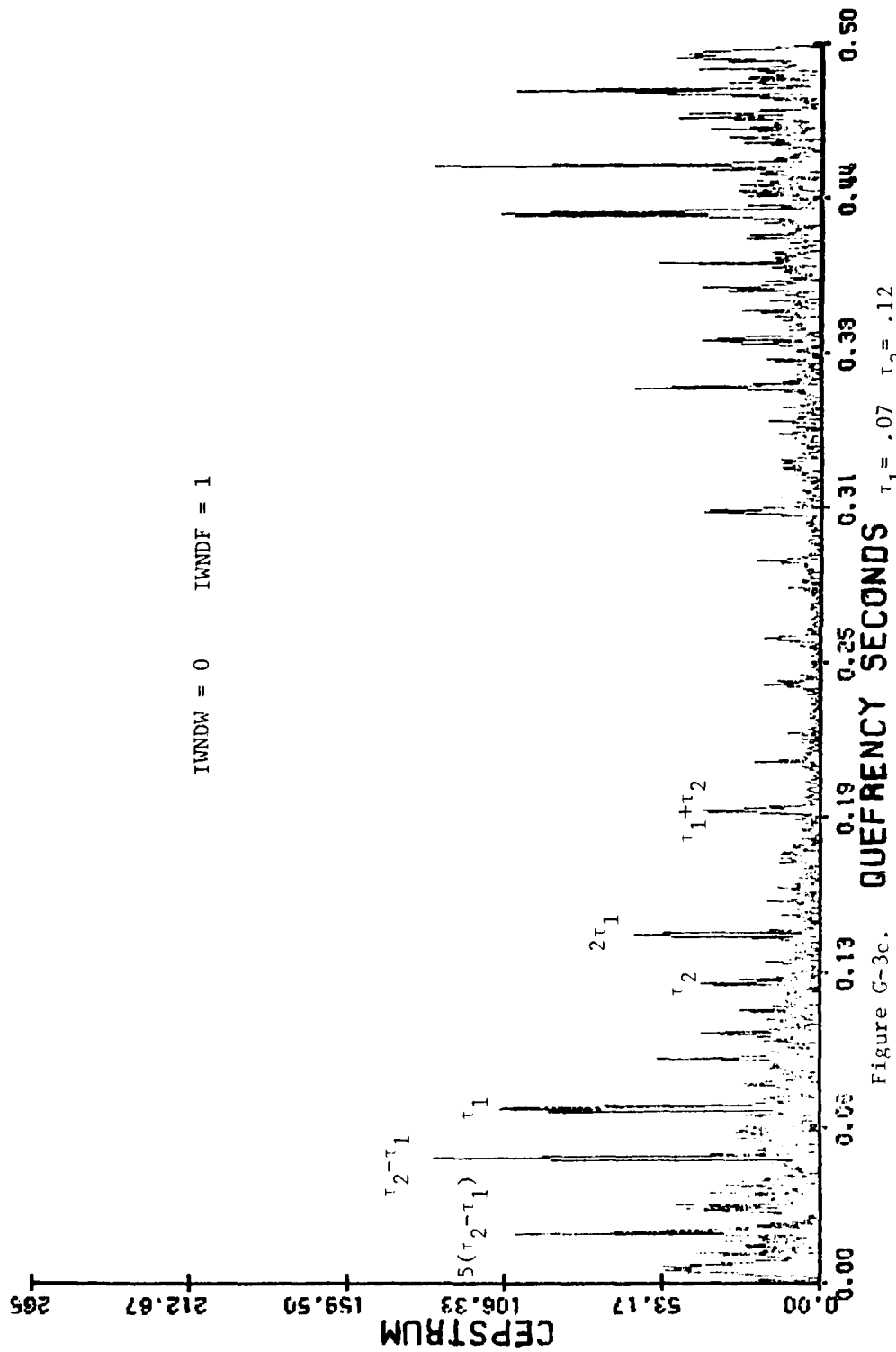


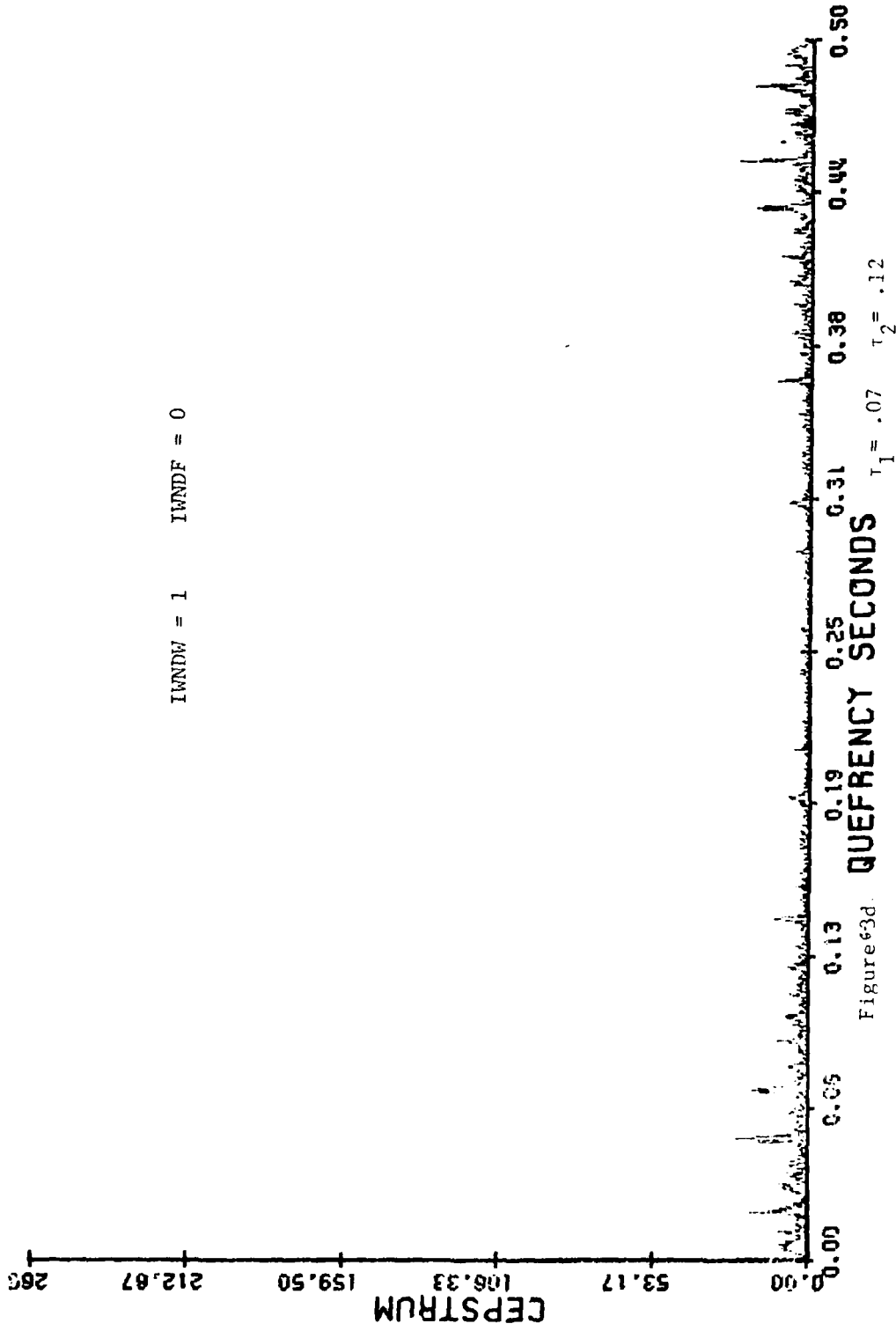
Figure G-3b.



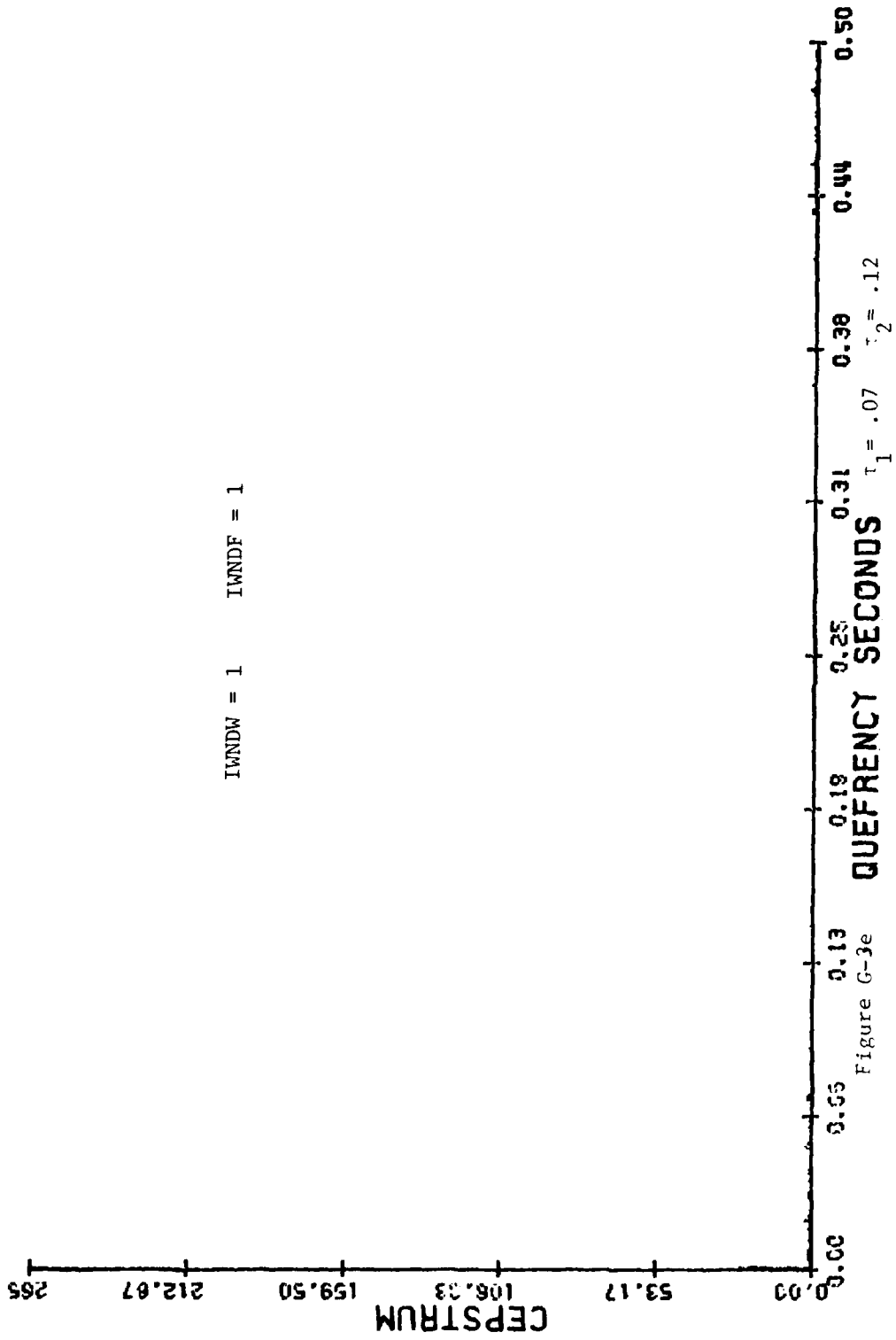
IWNDF = 0 IWNDF = 1

Figure G-3c.

IWNW = 1 IWNDF = 0



IWNDF = 1 IWNDF = 1



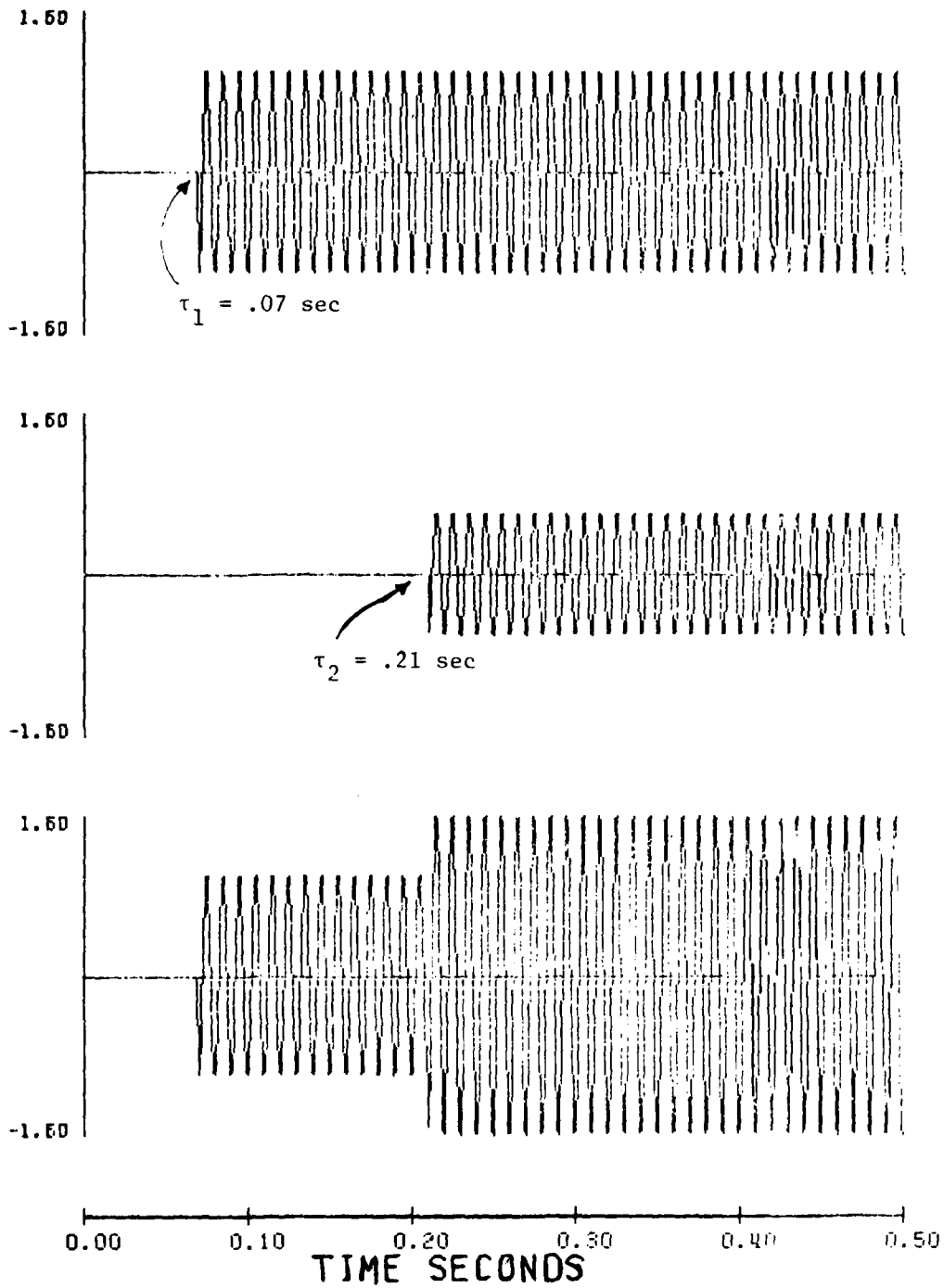


Figure G-4a.

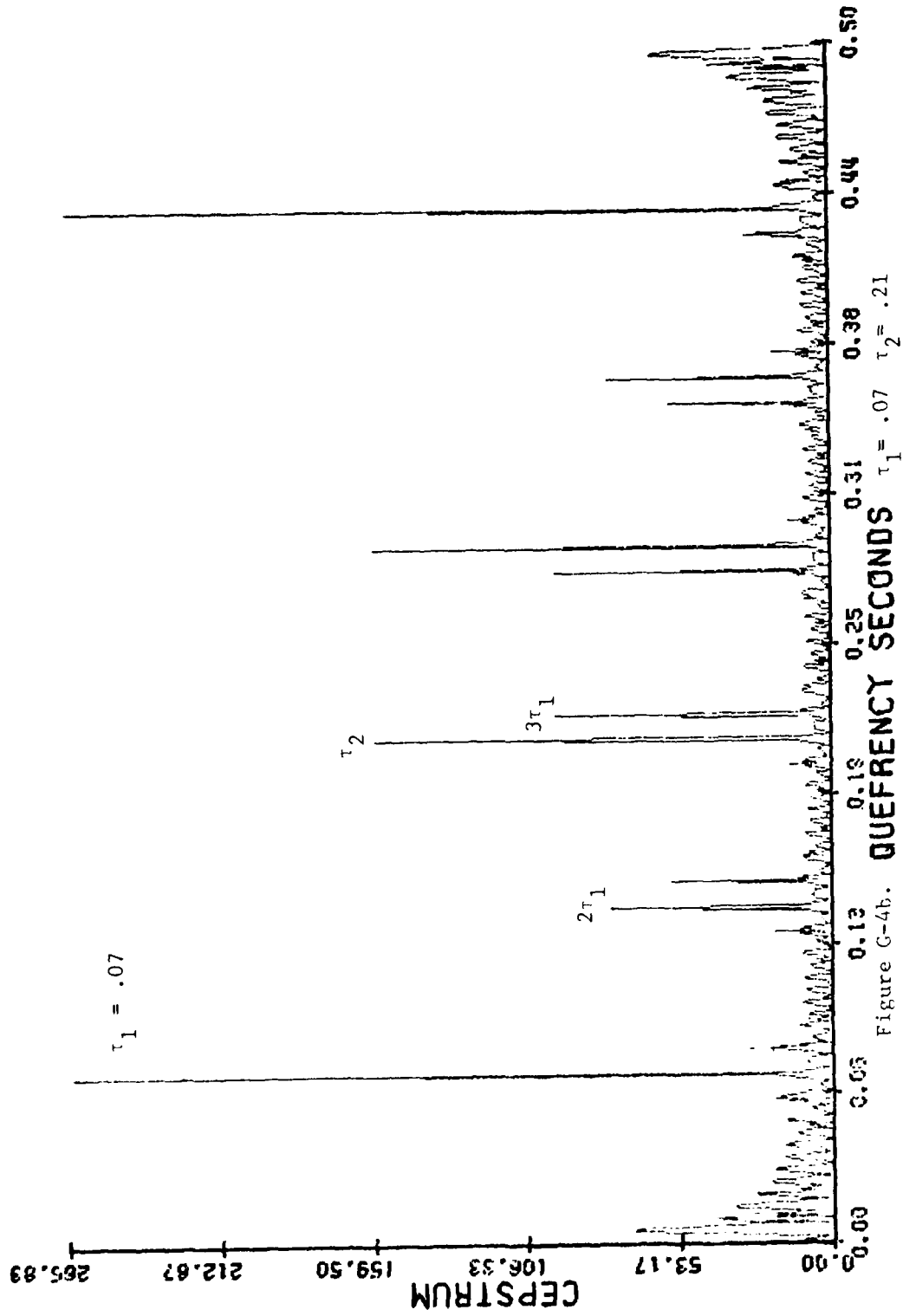
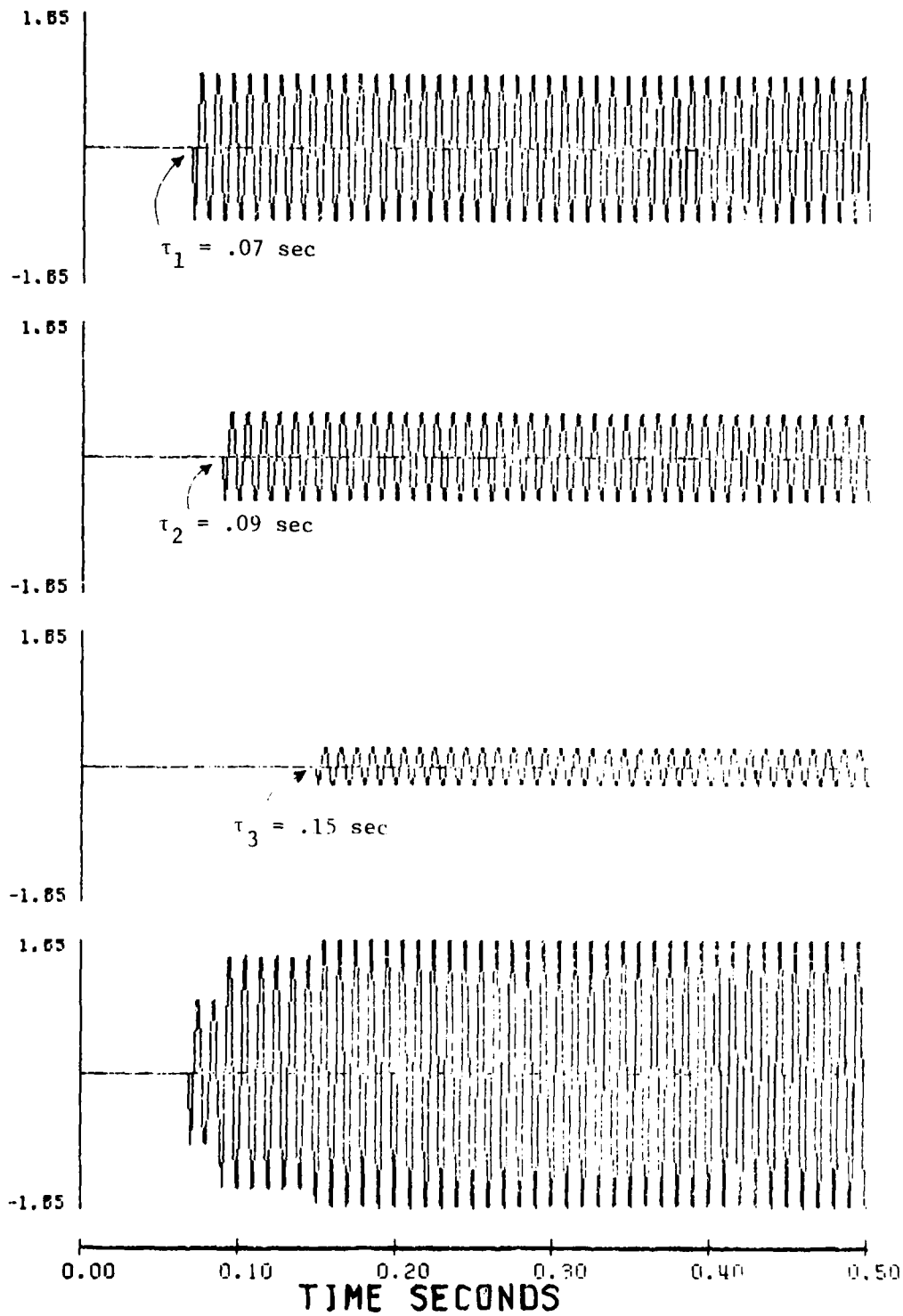


Figure G-4b.



$$\cos(200\pi \cdot (t - \tau_{A1})) \cdot U(t - \tau_{A1}) + .6 \cos(200\pi \cdot (t - \tau_{A2})) \cdot U(t - \tau_{A2}) \\ + .25 \cos(200\pi \cdot (t - \tau_{A3})) \cdot U(t - \tau_{A3})$$

Figure G-5a

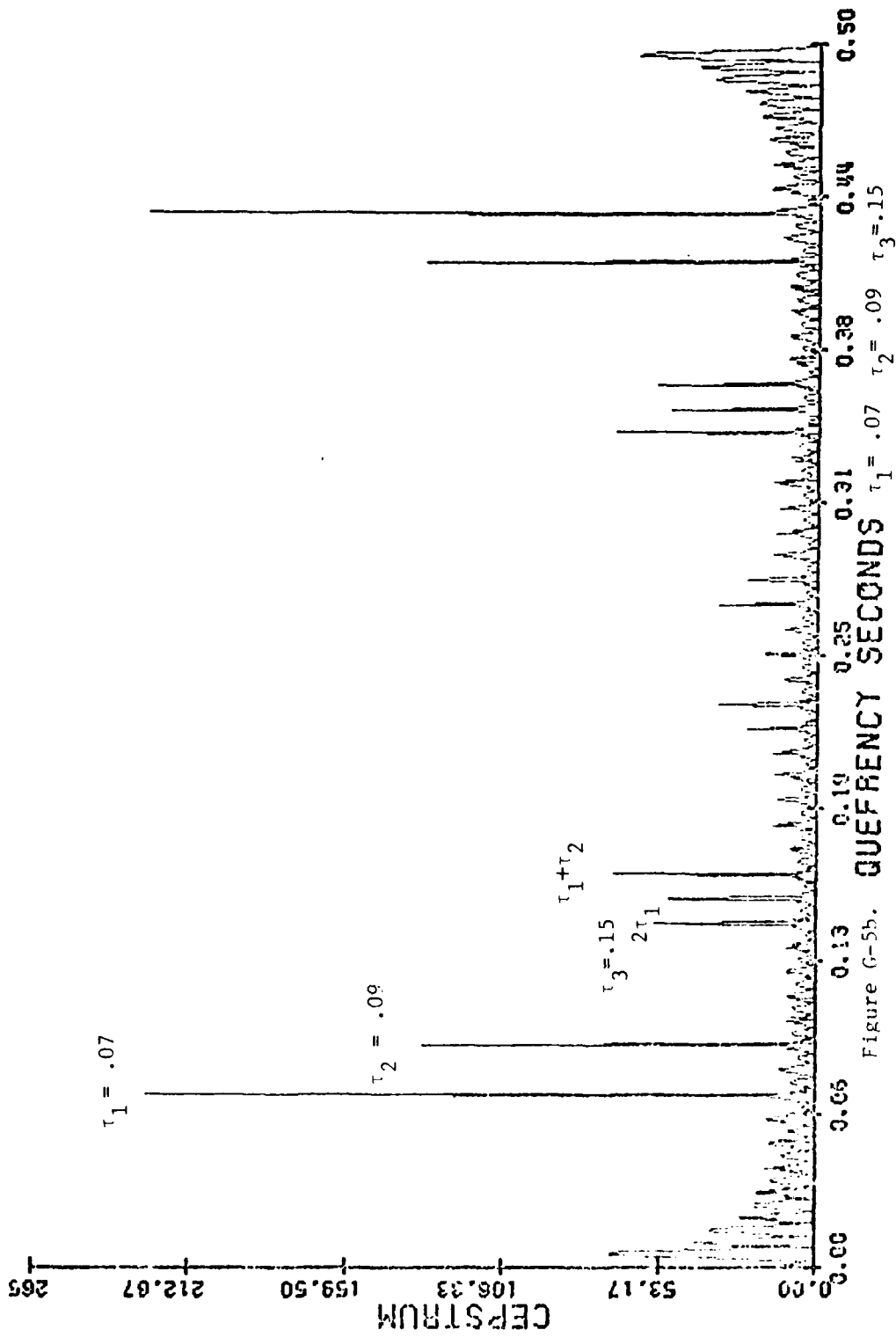


Figure G-5b.

Figures G-6 through G-10 pictorially show damped cosine waveforms and their cepstral plots. The starting time of the signals as well as the number of them might be different for each case. The equation for the composite signal is

$$\begin{aligned}
 & (t-\tau_1) e^{-2(t-\tau_1)} \cos (200 \pi (t-\tau_1)) u (t-\tau_1) \\
 & + (t-\tau_2) e^{-2(t-\tau_2)} \cos (200 \pi (t-\tau_2)) u (t-\tau_2) \\
 & + (t-\tau_3) e^{-2(t-\tau_3)} \cos (200 \pi (t-\tau_3)) u (t-\tau_3)
 \end{aligned}$$

with the third component being zero where only one echo signal has been studied. If the above equation is broken in "+" points each part will give the equation of the individual signals. In all figures, IWNDW=-, IWPDF=0, and N=1024 except if they are defined otherwise.

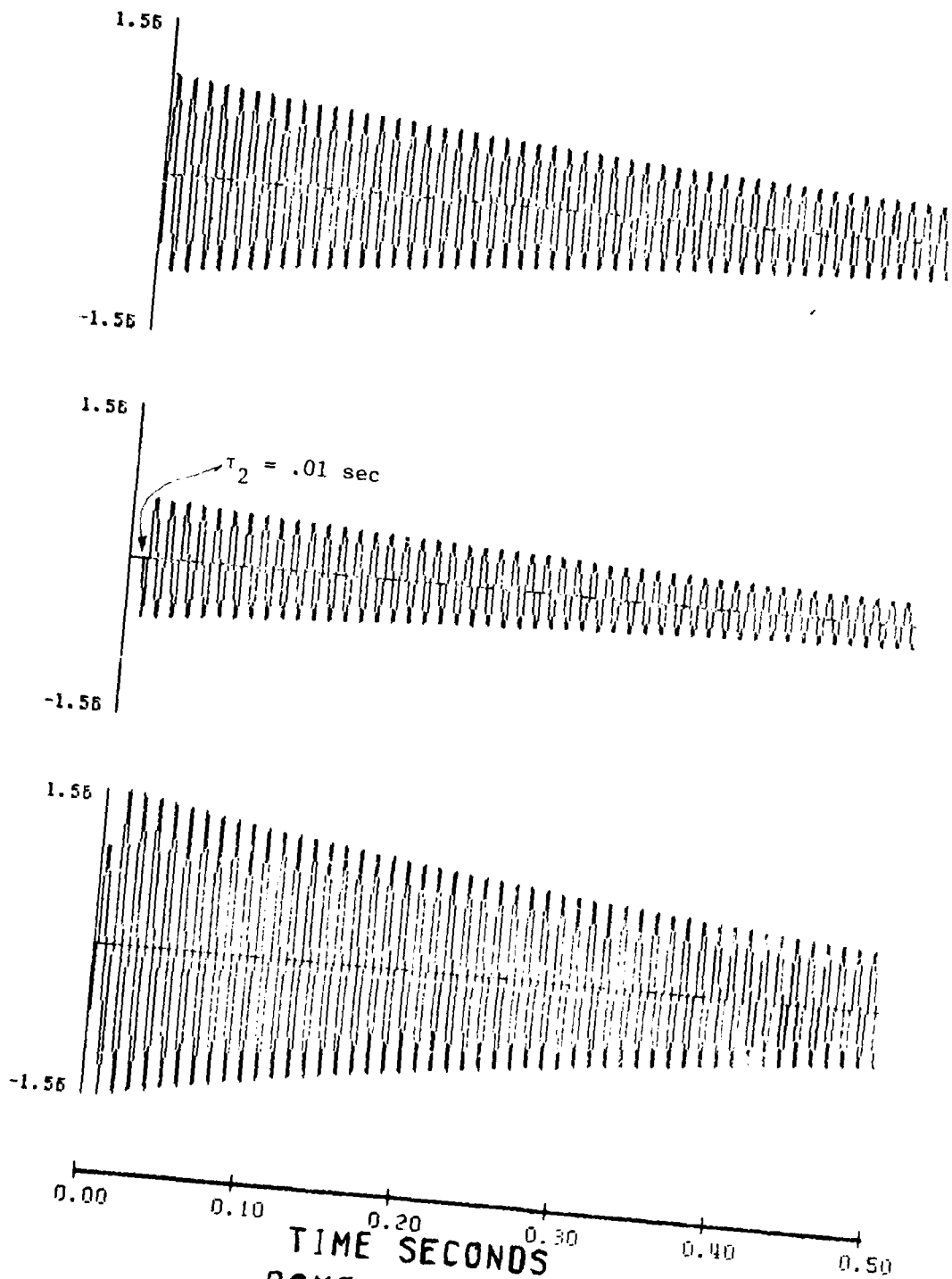


Figure G-6a

DAMPED COSINE

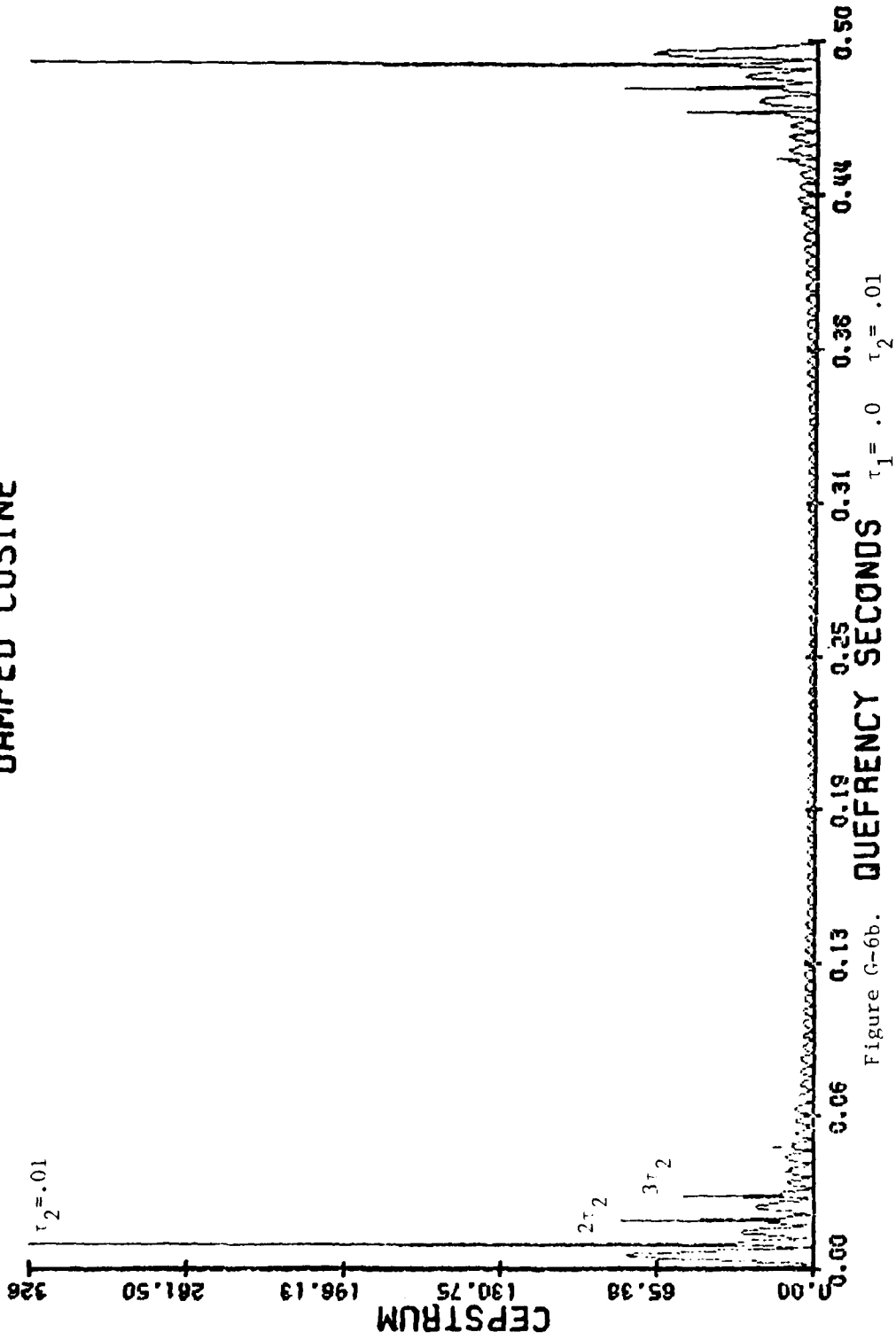
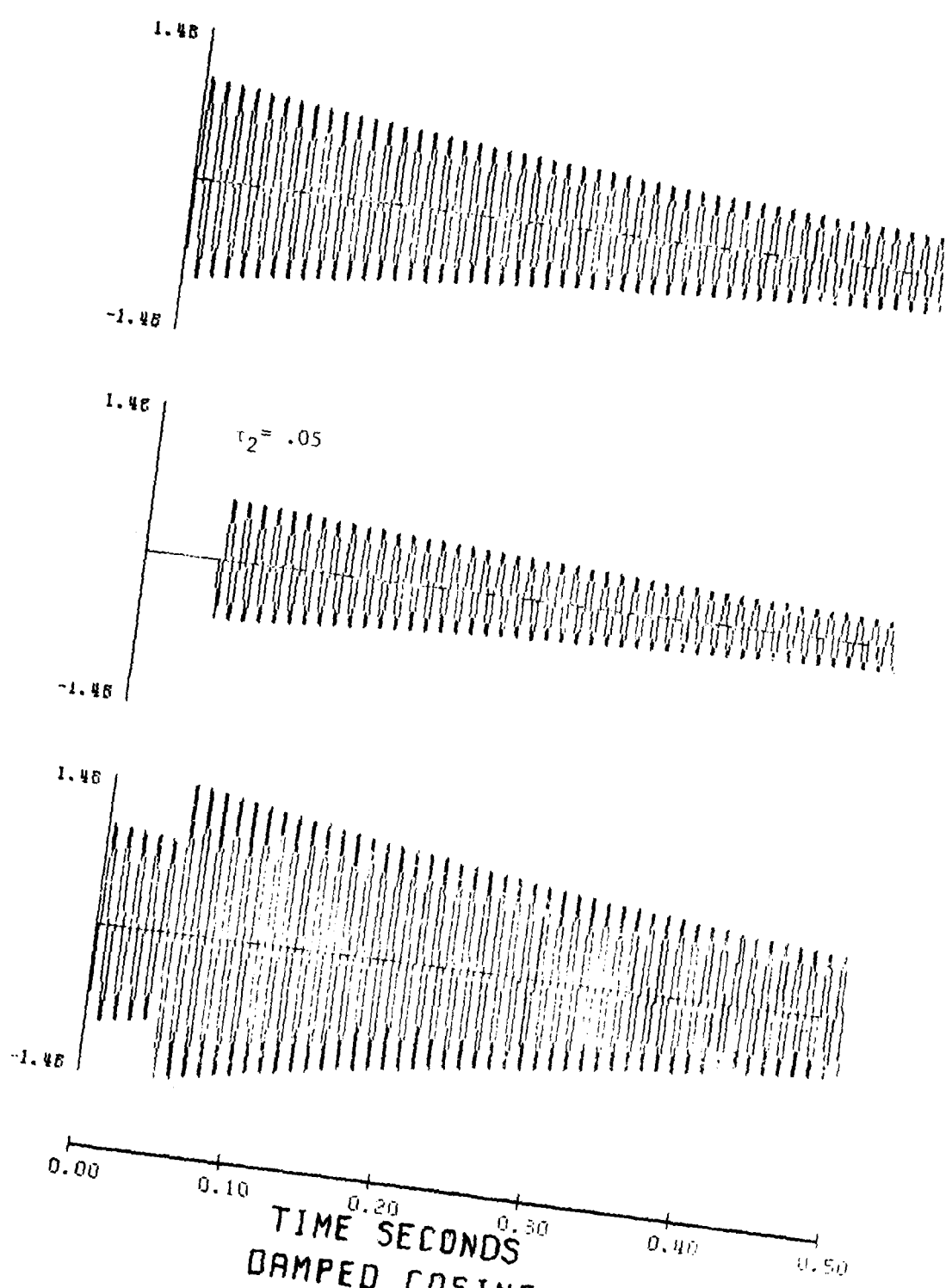


Figure G-6b.



TIME SECONDS
DAMPED COSINE

Figure G-7a.

DAMPED COSINE

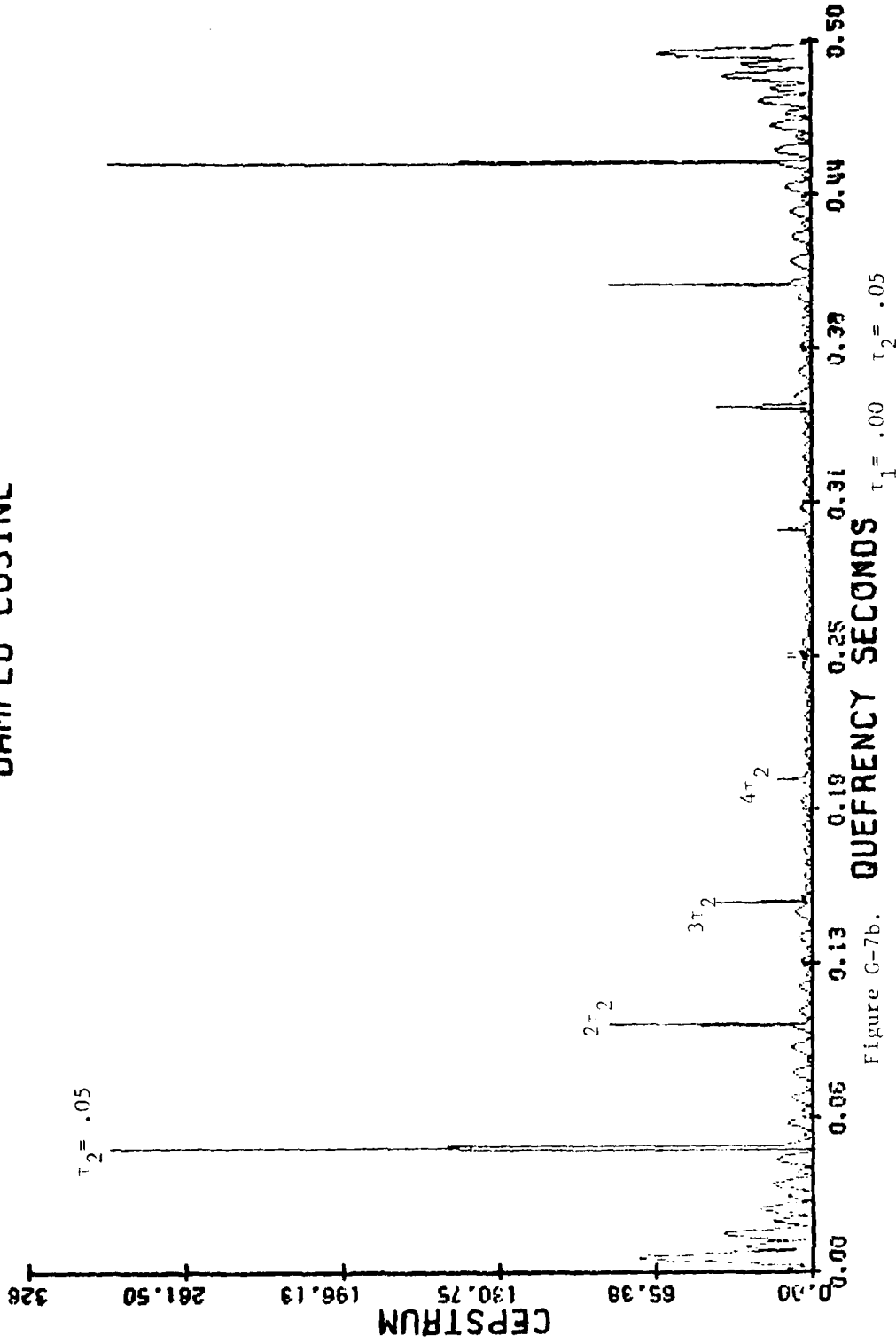
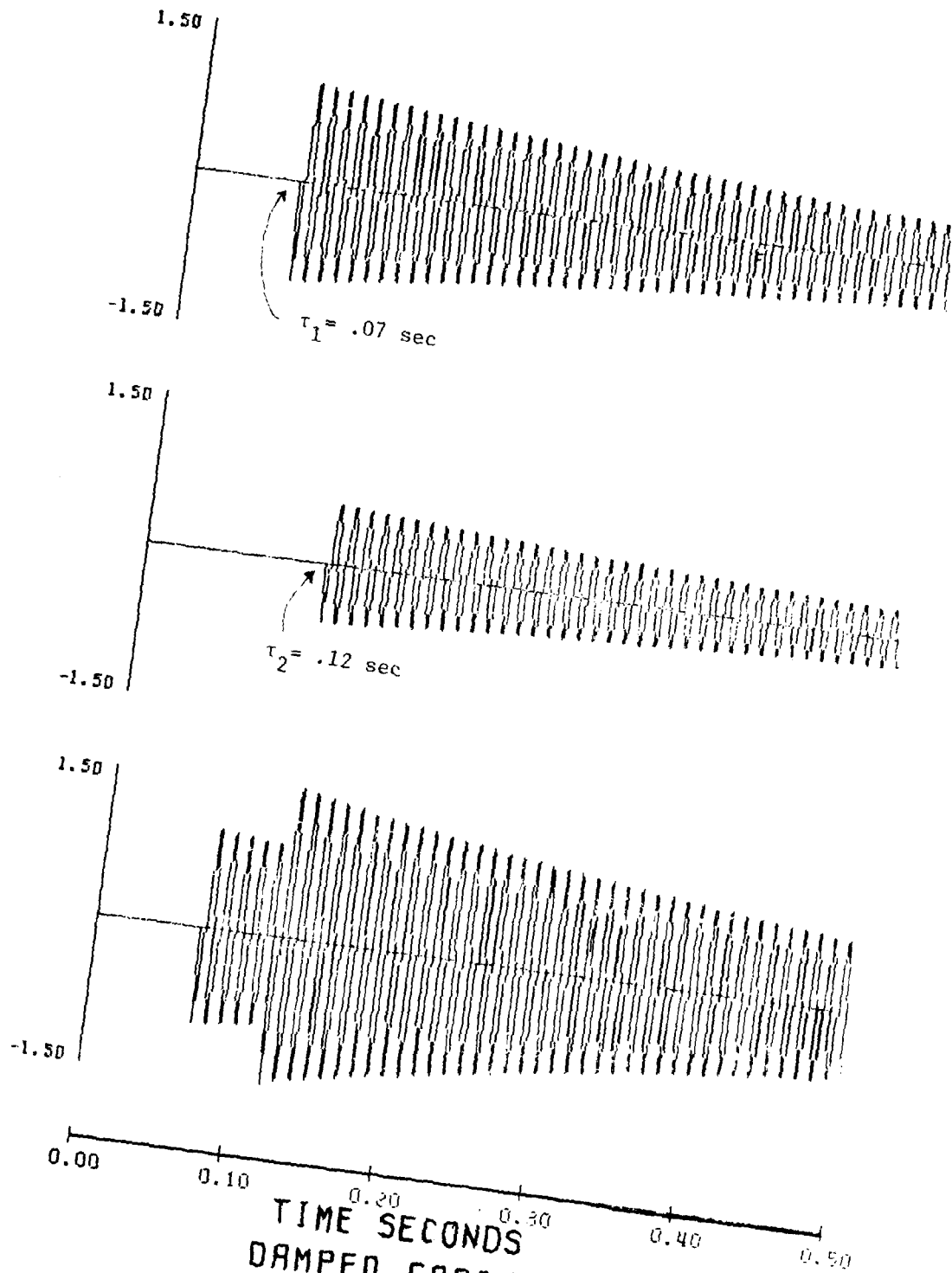


Figure G-7b.



0.00 0.10 0.20 0.30 0.40 0.50
TIME SECONDS

DAMPED COSINE

Figure G-3a

DAMPED COSINE

IWNDF = 0 IWNDF = 0

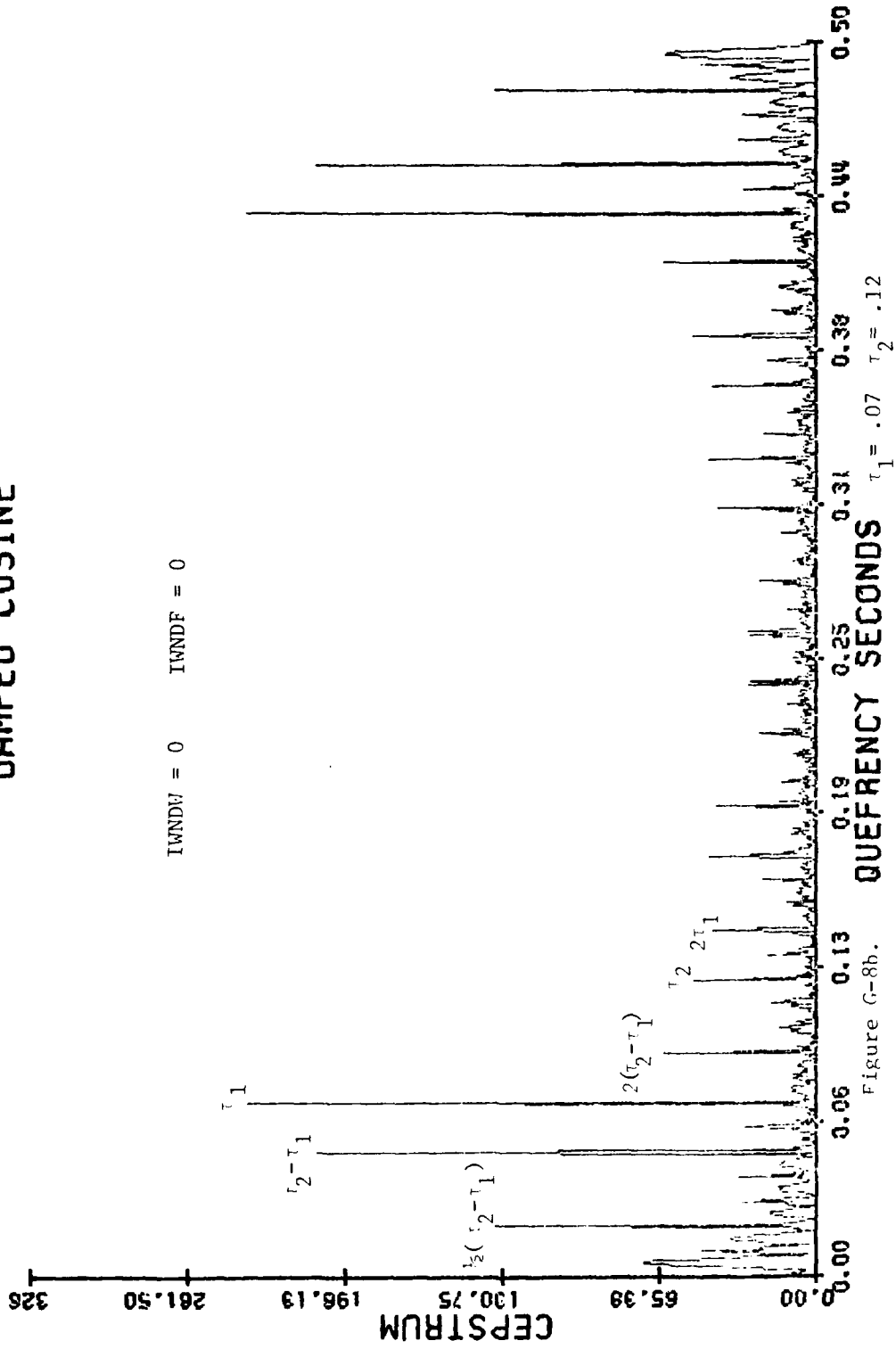


Figure G-8b. $\tau_1 = .07$ $\tau_2 = .12$

DAMPED COSINE

IWNDF = 0 IWNDF = 1

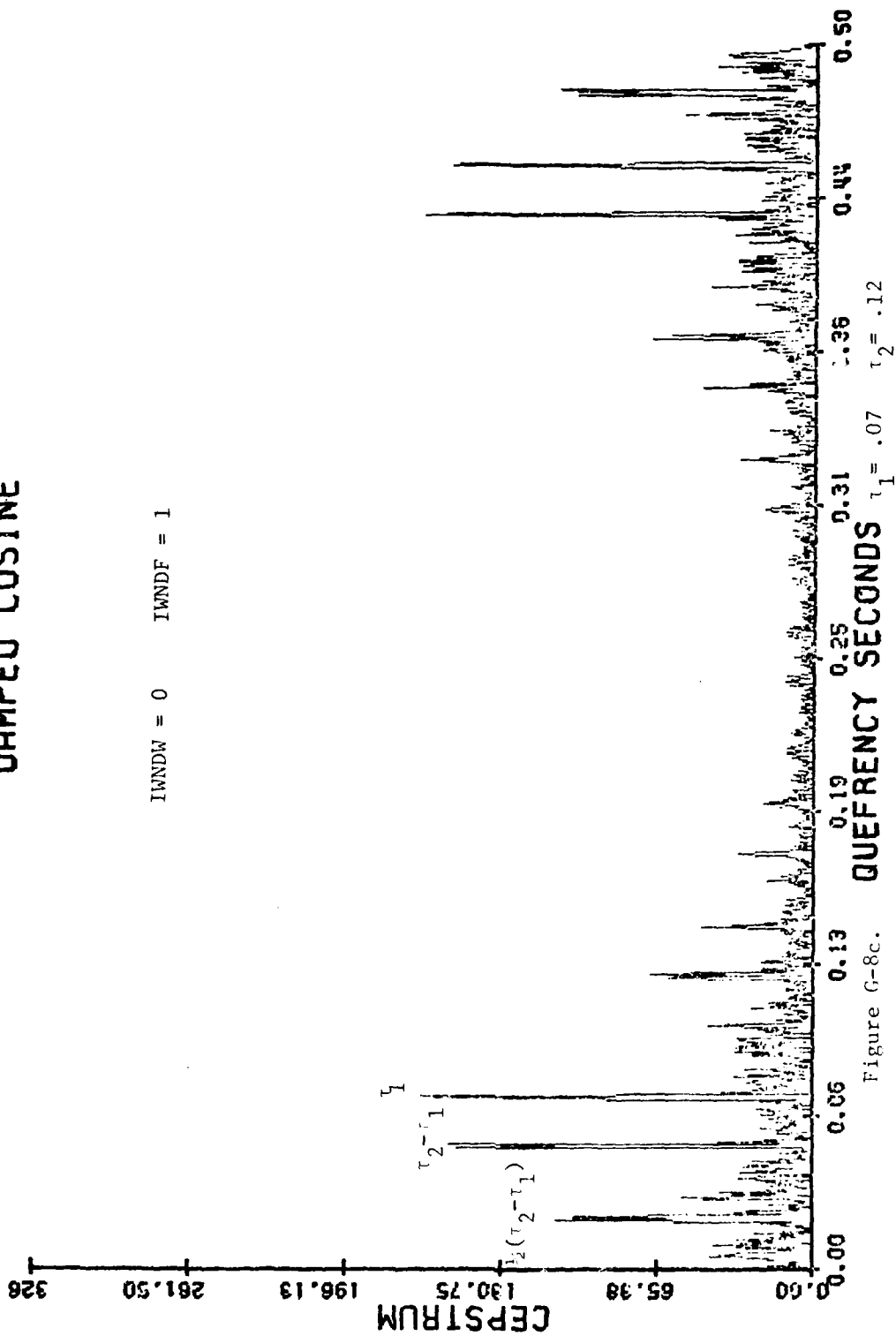
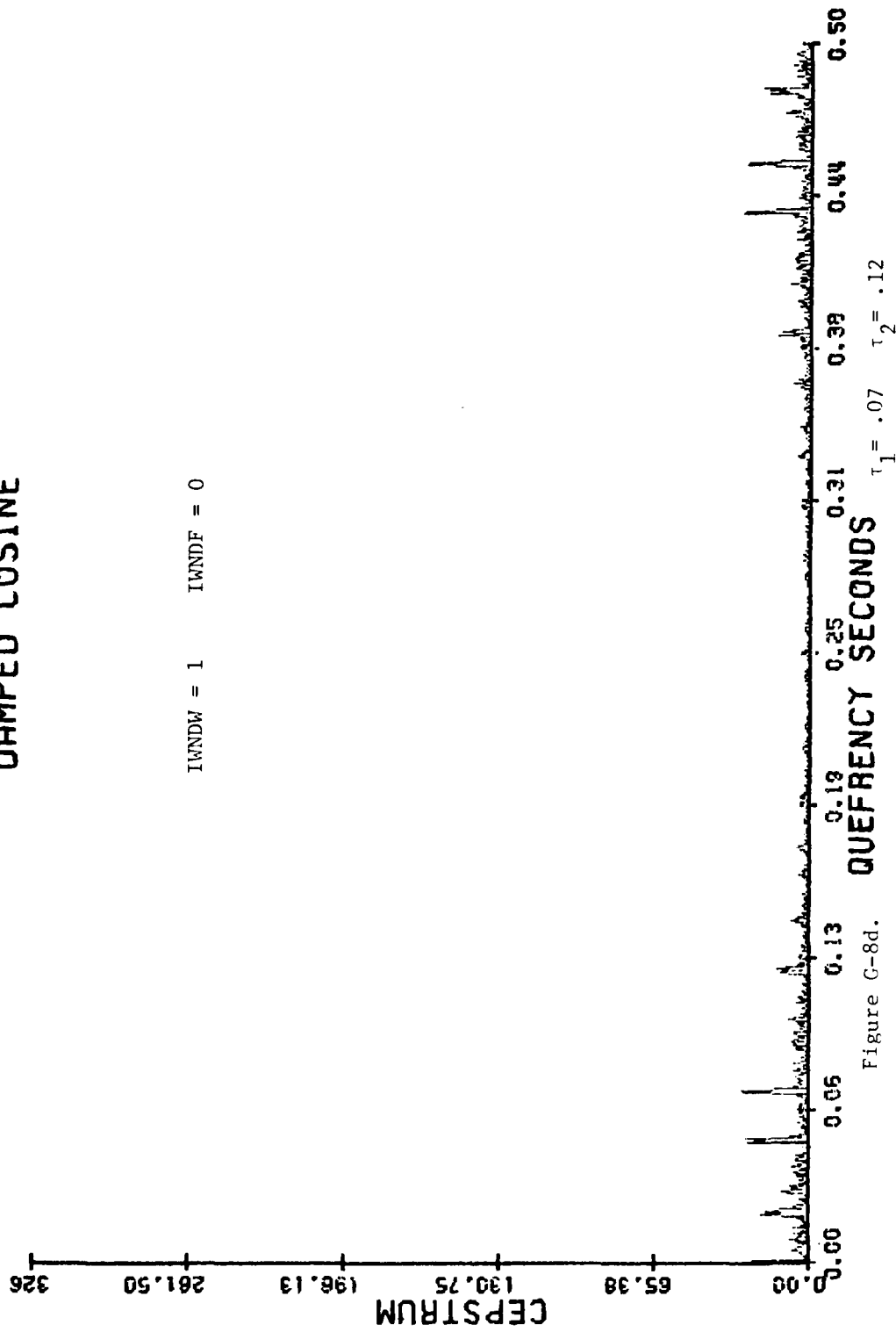


Figure G-8c.

DAMPED COSINE

IWNDF = 1 IWNDF = 0



DAMPED COSINE

INNDW = 1 INNDF = 1

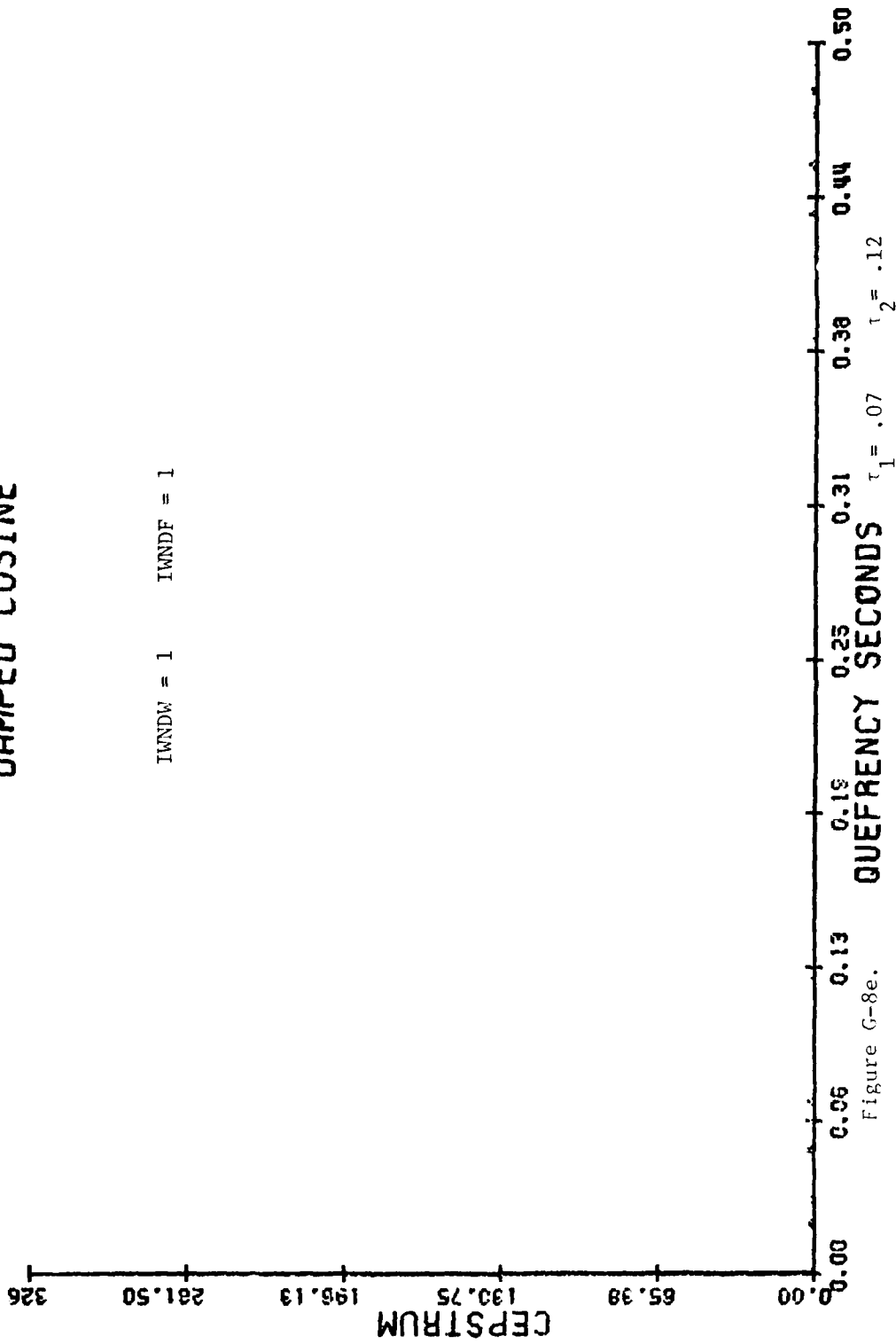
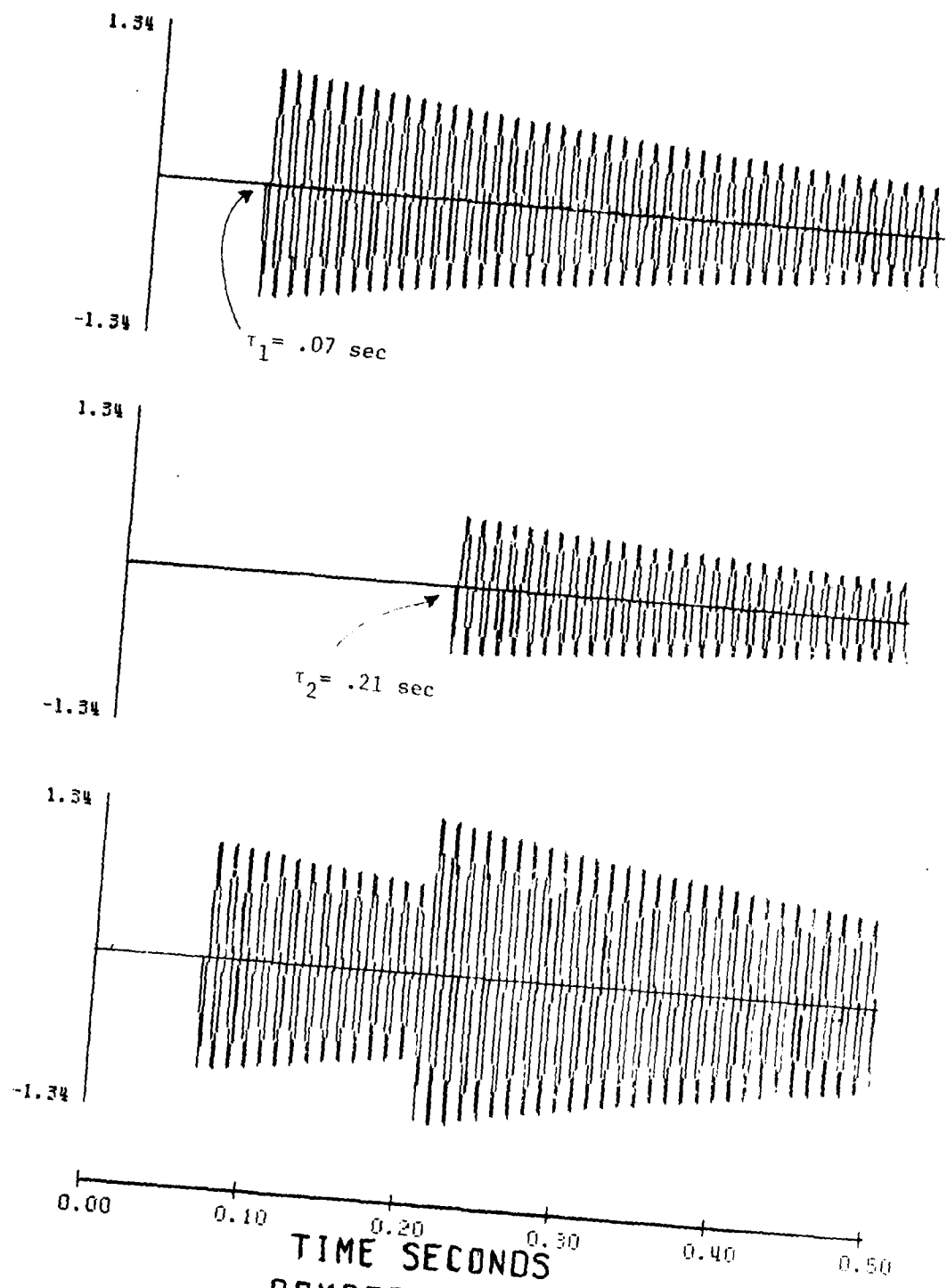


Figure G-8e.



TIME SECONDS
DAMPED COSINE

Figure G-9a.

DAMPED COSINE

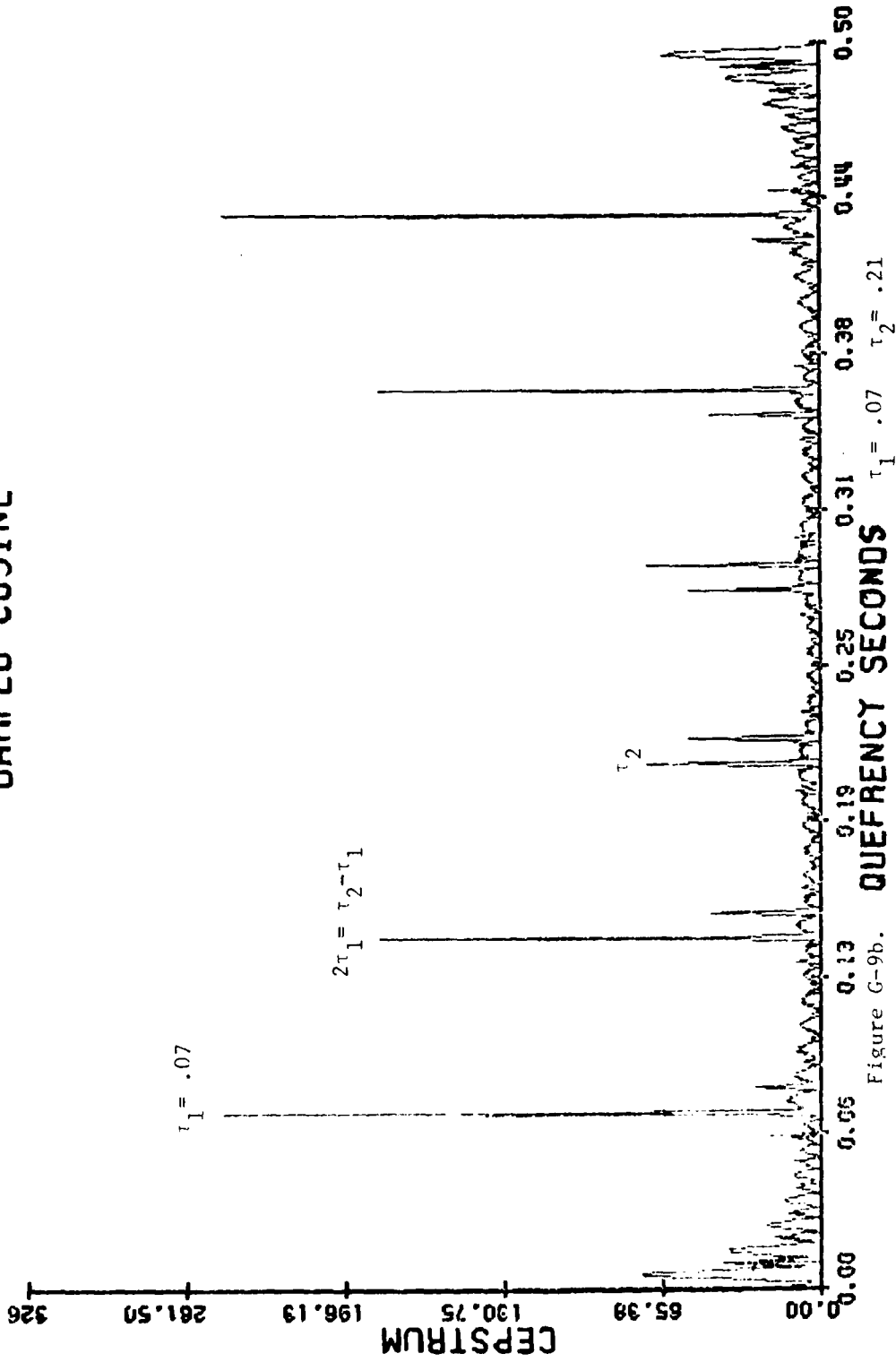


Figure G-9b. $\tau_1 = .07$ $\tau_2 = .21$

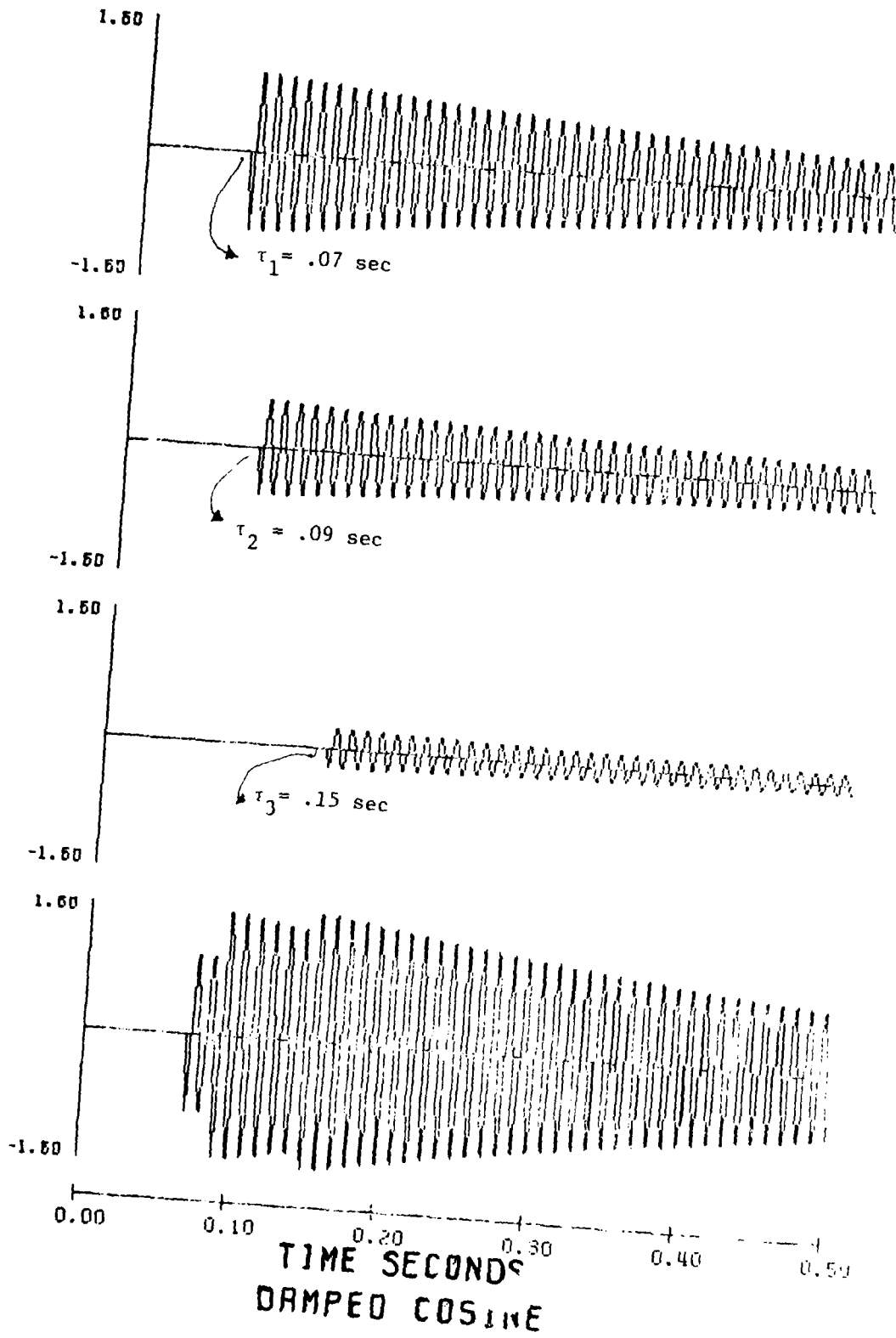


Figure G-10a

DAMPED COSINE

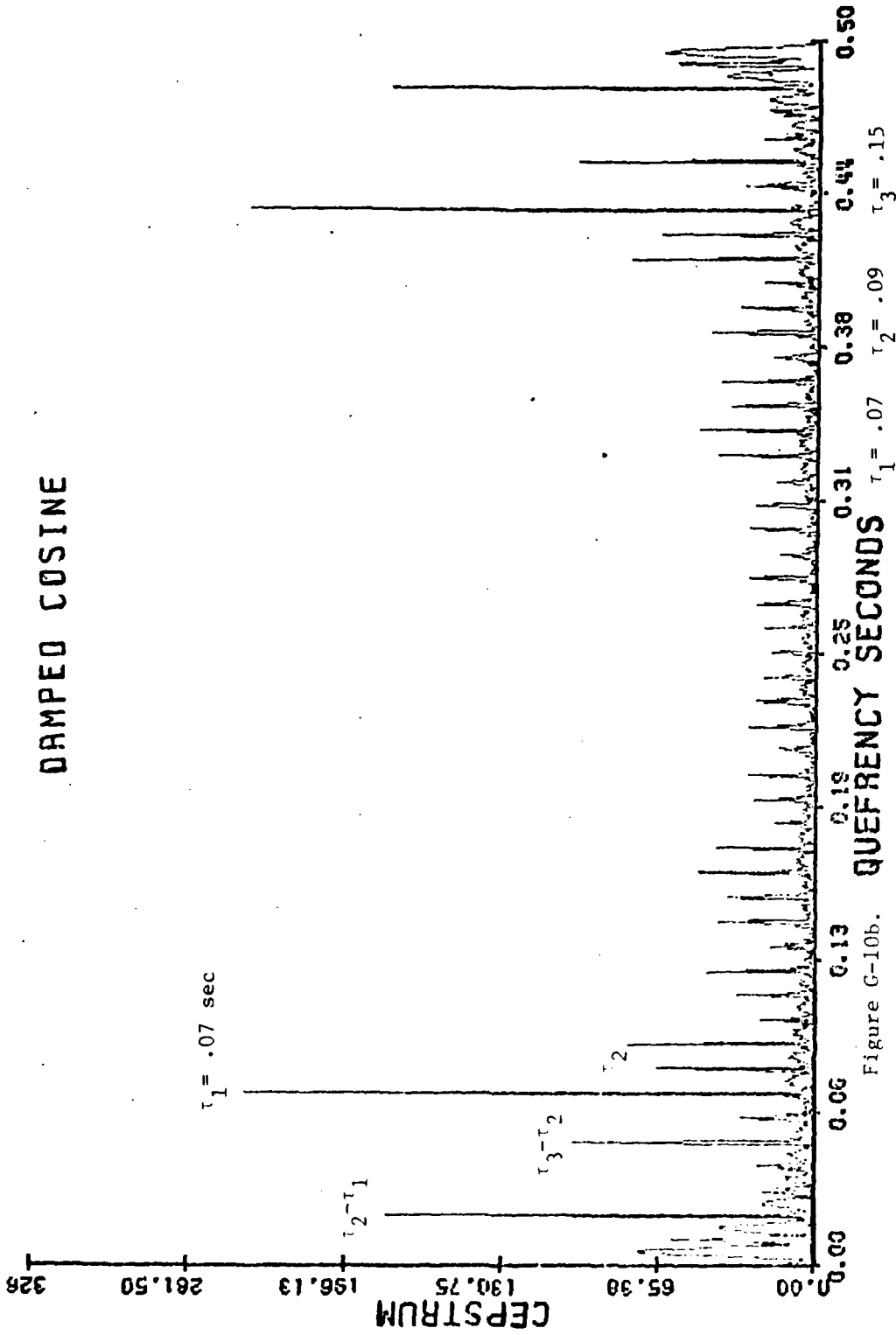


Figure C-10b.

Figures G-11 through G-15 present the damped exponential waveforms with their cepstral plots. The damping coefficient for all of these plots is 30 , and the whole period of study is .5 second. The equation of the composite signal is given in each plot, which if broken in "+" points will result in giving the equation of each individual signal. In all figures $N=1024$, $IWNDW=0$, and $IWNDF=0$ except if they are defined otherwise.

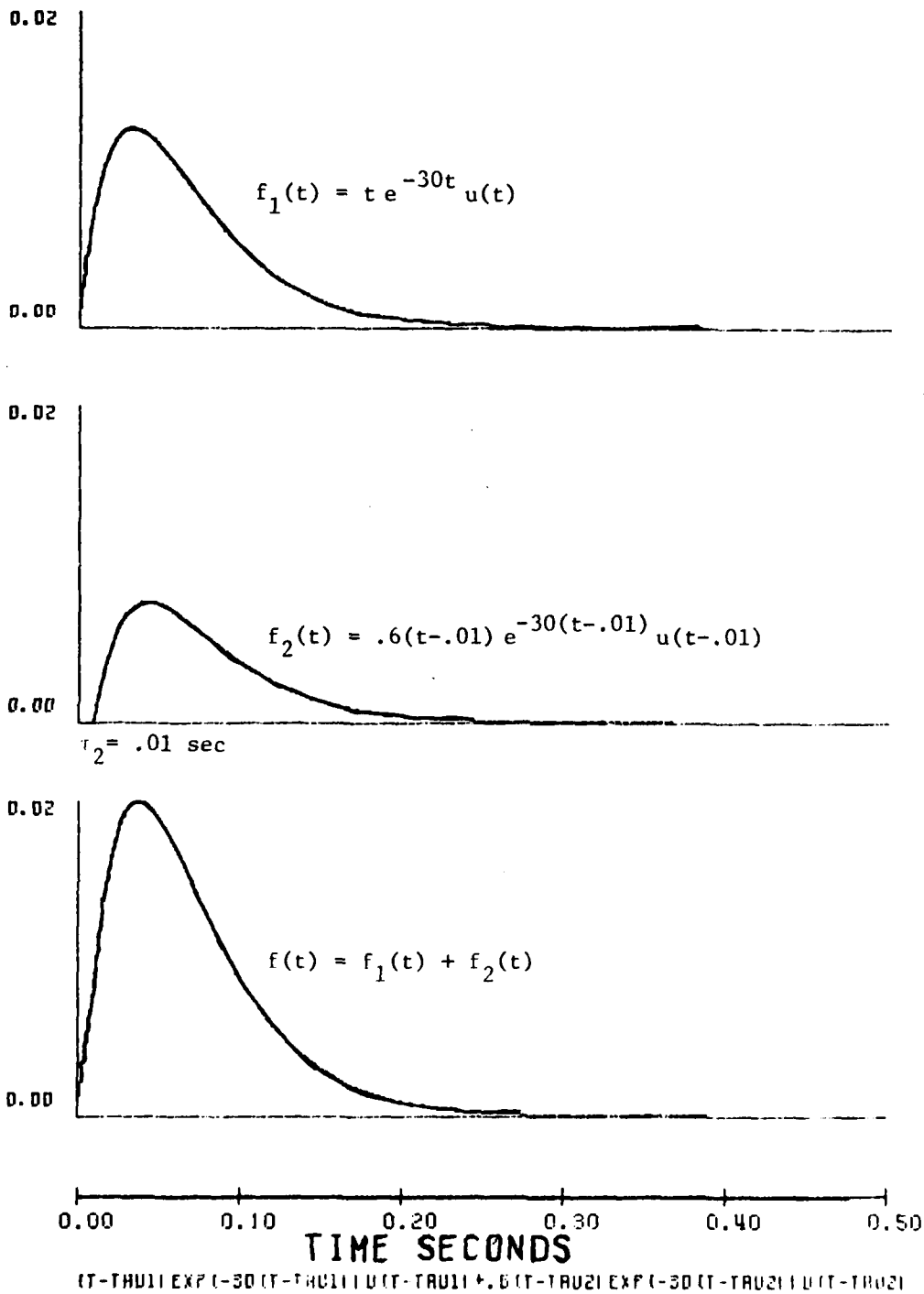


Figure G-11a

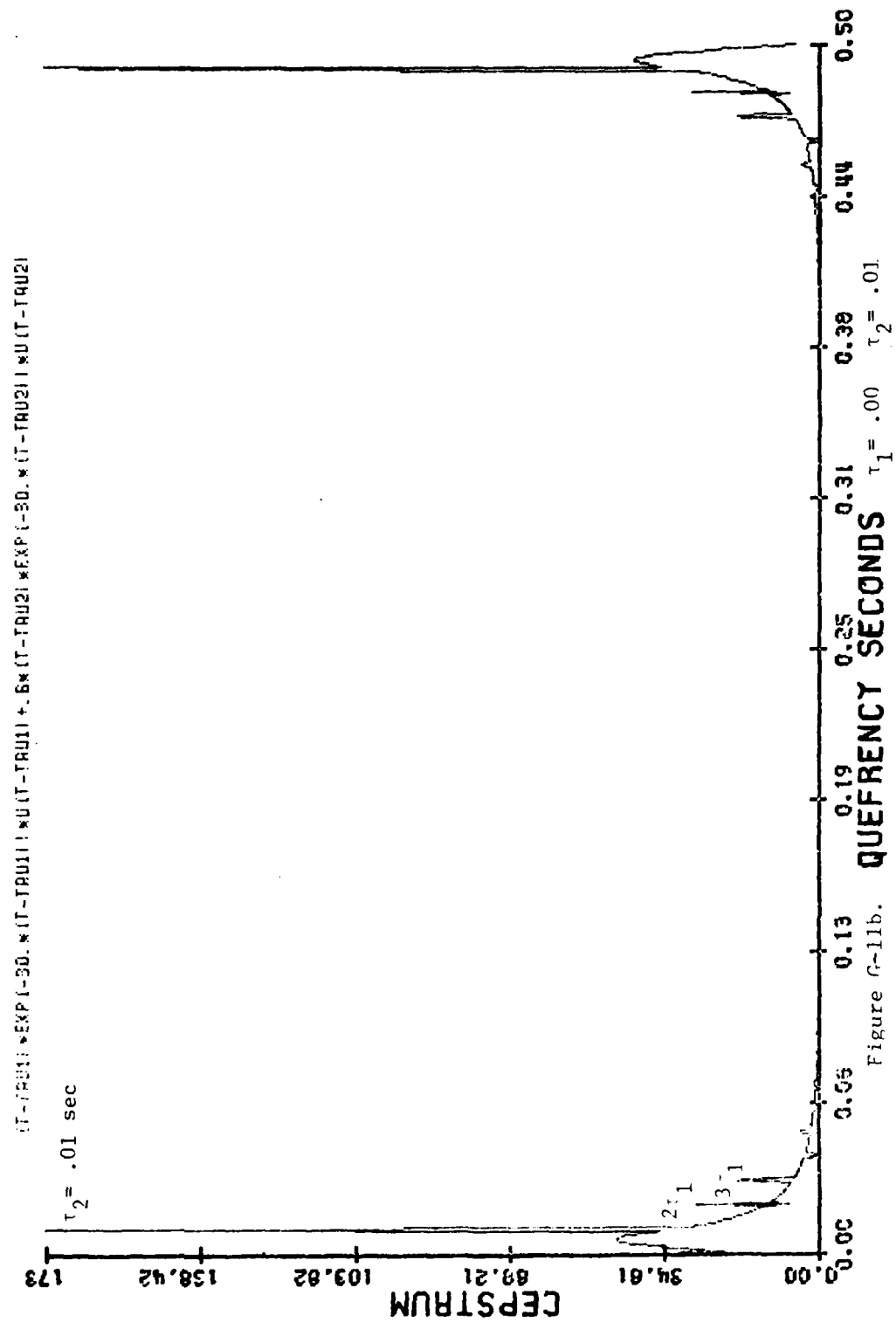
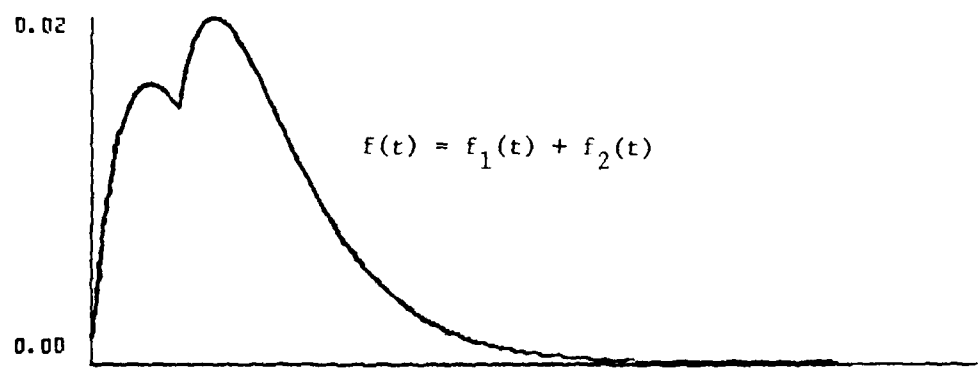
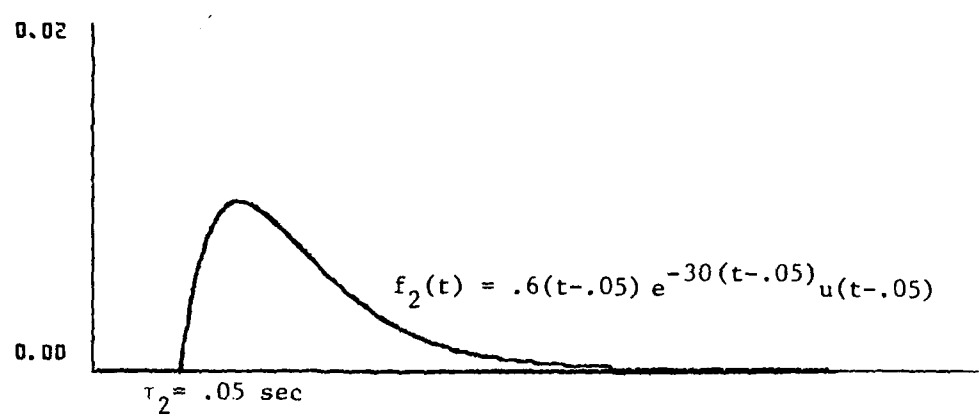
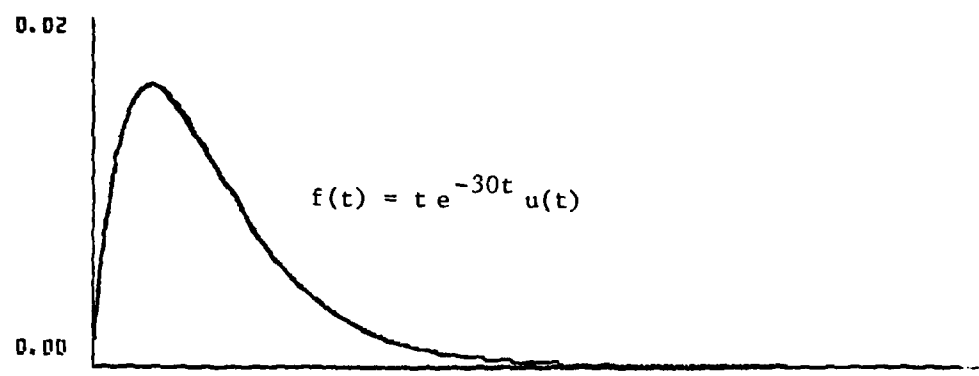


Figure G-11b. $\tau_1 = .00$ $\tau_2 = .01$



0.00 0.10 0.20 0.30 0.40 0.50
TIME SECONDS

$$(t-\tau_{A1}) \exp(-30(t-\tau_{A1})) u(t-\tau_{A1}) + .6(t-\tau_{A2}) \exp(-30(t-\tau_{A2})) u(t-\tau_{A2})$$

Figure G-12a

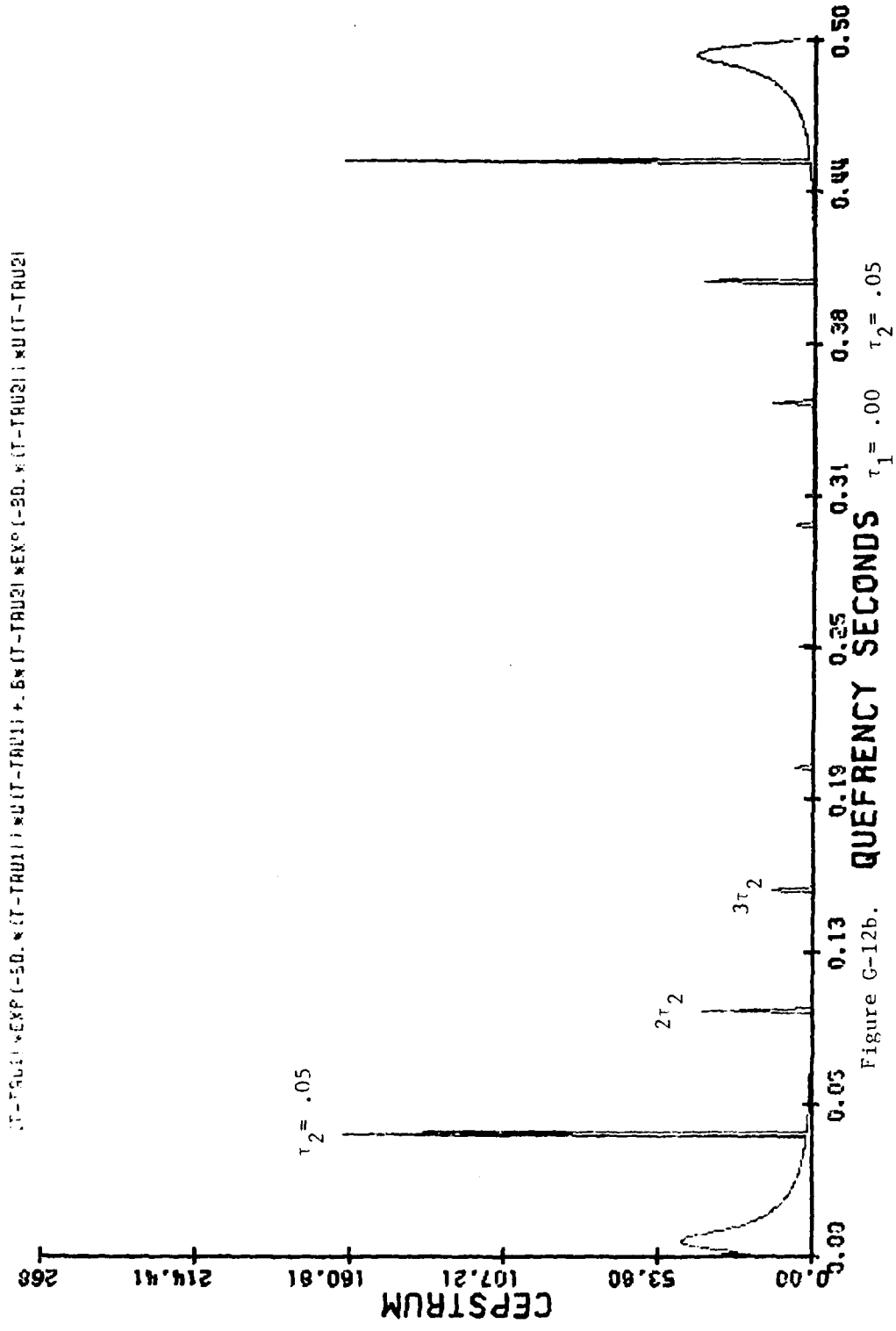


Figure G-12b.

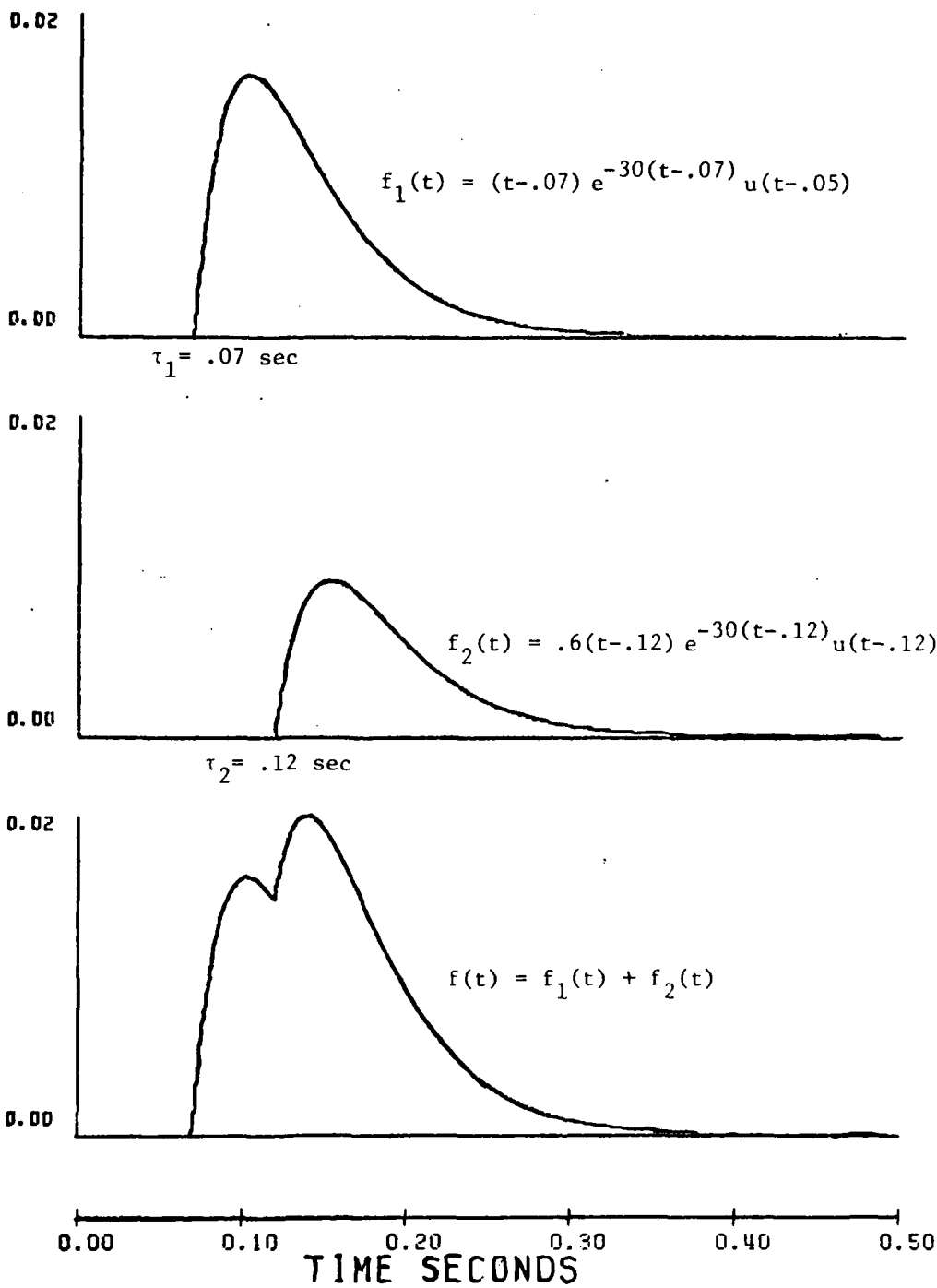


Figure G-13a

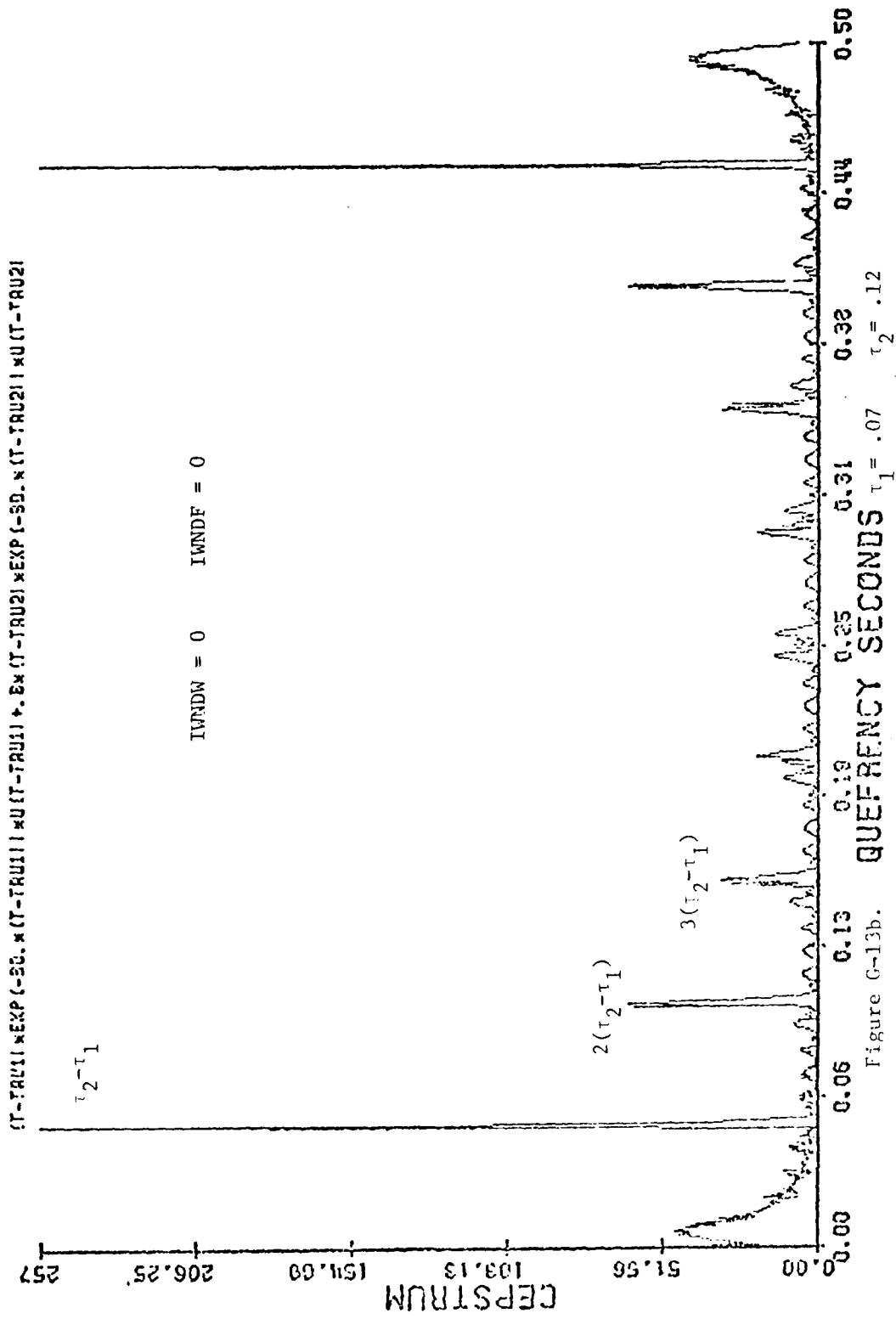


Figure G-13b.

EXP(-30.8*(T-TRU2)) * EXP(-30.8*(T-TRU2)) * EXP(-30.8*(T-TRU2)) * EXP(-30.8*(T-TRU2)) * EXP(-30.8*(T-TRU2))

IWNDF = 0 IWNDF = 1

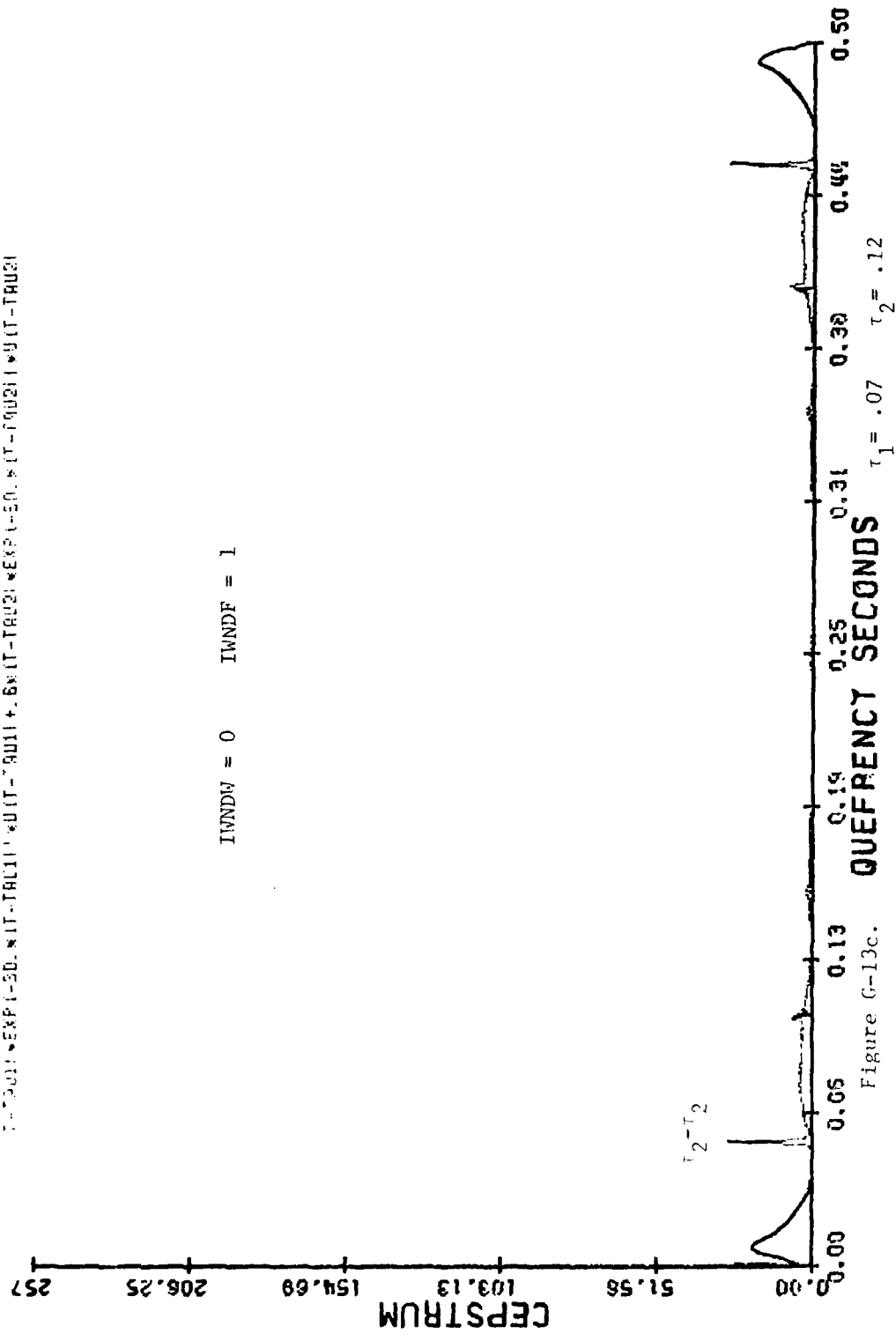
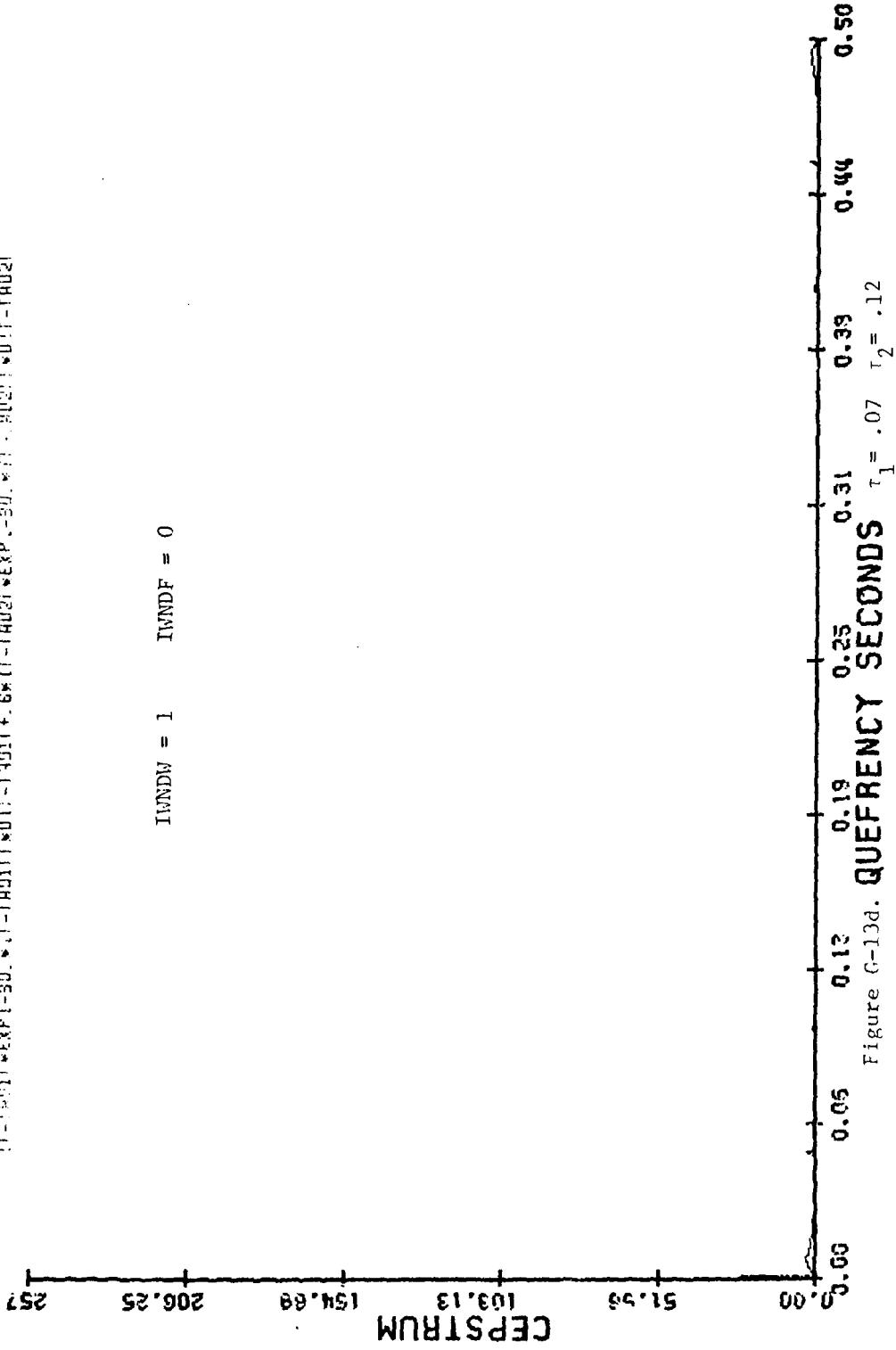


Figure G-13c.

(T-TAU2) * EXP(-30. * (T-TAU1)) * (T-TAU1) + 6 * (T-TAU2) * EXP(-30. * (T-TAU2)) * (T-TAU2)

IWNDF = 1 IWNDF = 0



$(f - \tau_{12}) \exp(-\beta_0) \cdot (T - \tau_{11}) \exp(-\beta_1) \cdot (T - \tau_{12}) \exp(-\beta_2) \cdot (T - \tau_{12}) \exp(-\beta_3) \cdot (T - \tau_{12}) \exp(-\beta_4) \cdot (T - \tau_{12}) \exp(-\beta_5)$

INNDW = 1 INNDF = 1

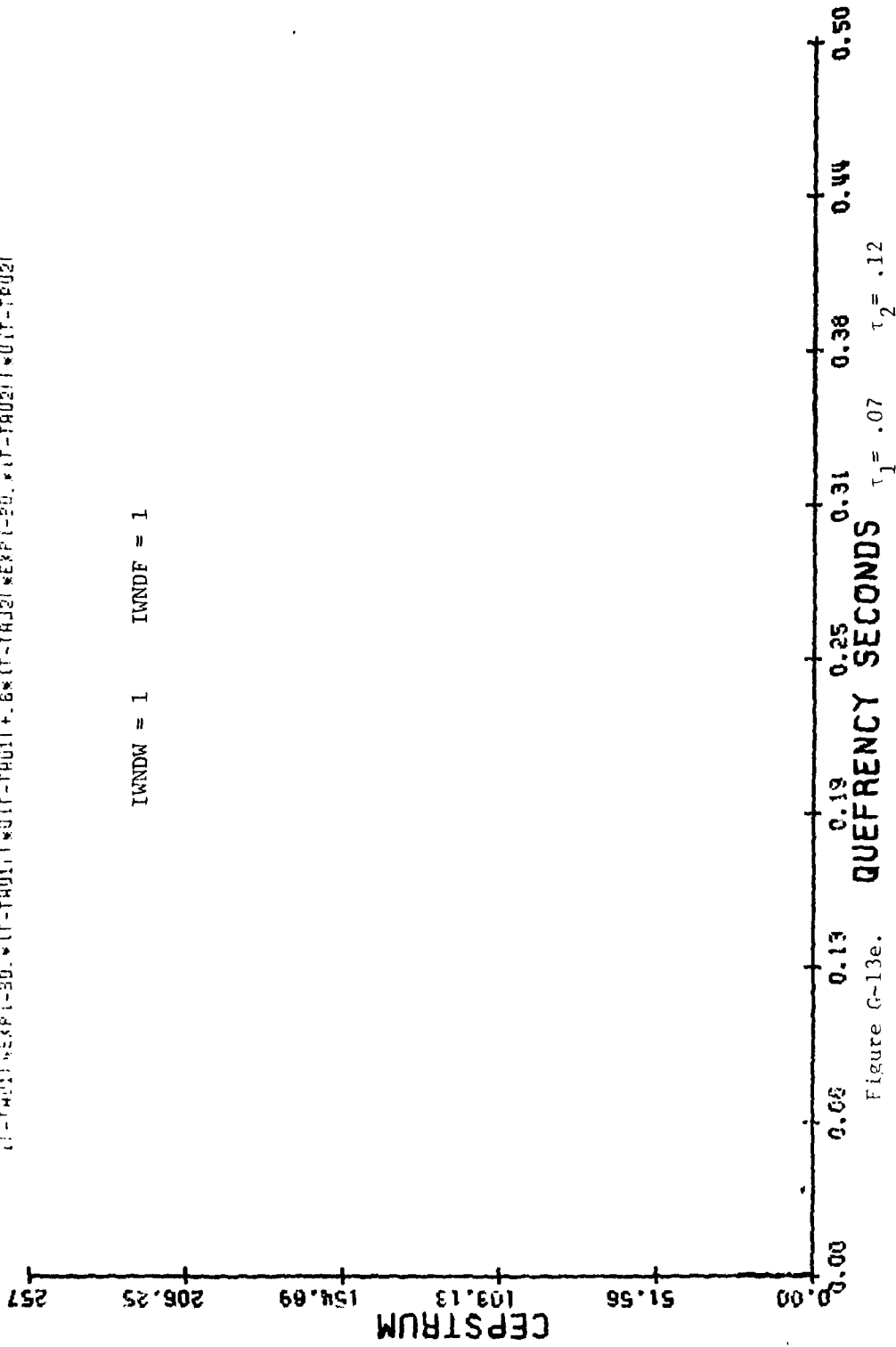
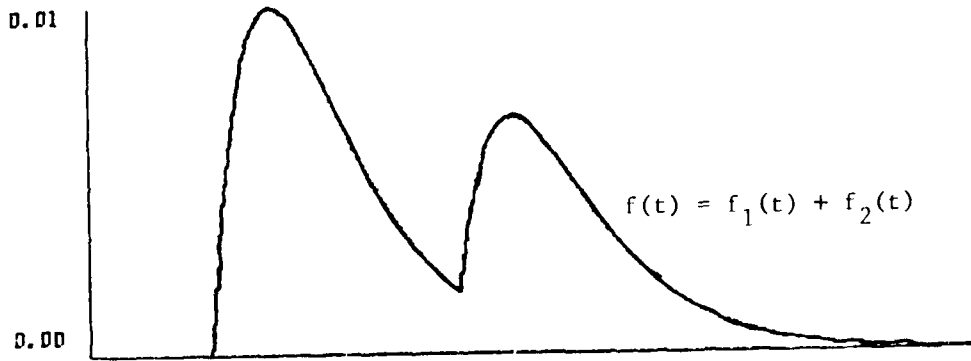
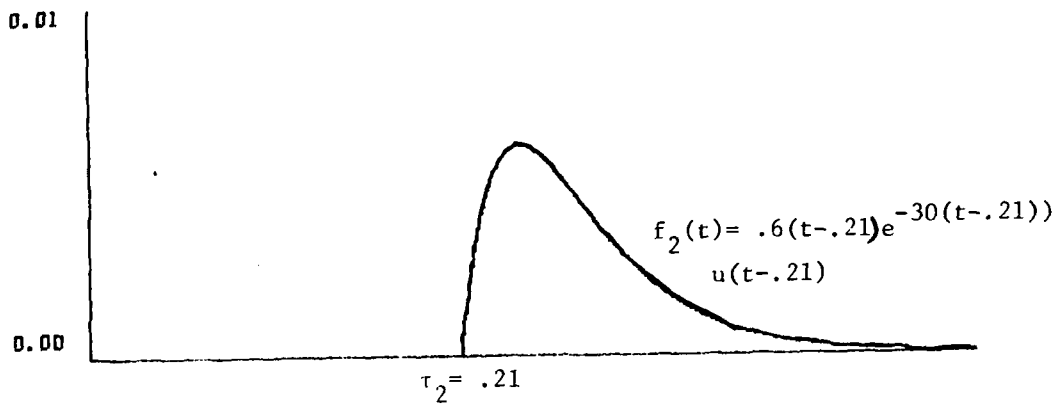
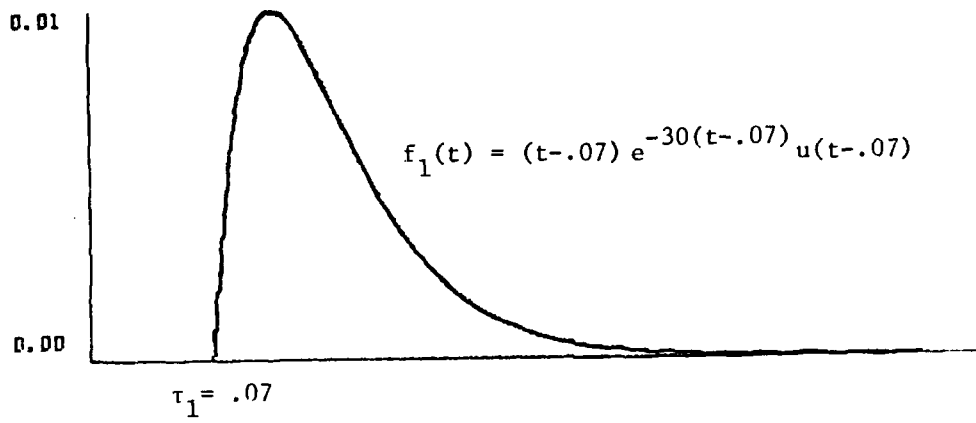


Figure G-13e.



0.00 0.10 0.20 0.30 0.40 0.50
TIME SECONDS

$$(t-.07) \exp(-30(t-.07)) u(t-.07) + .6(t-.21) \exp(-30(t-.21)) u(t-.21)$$

Figure G-14a

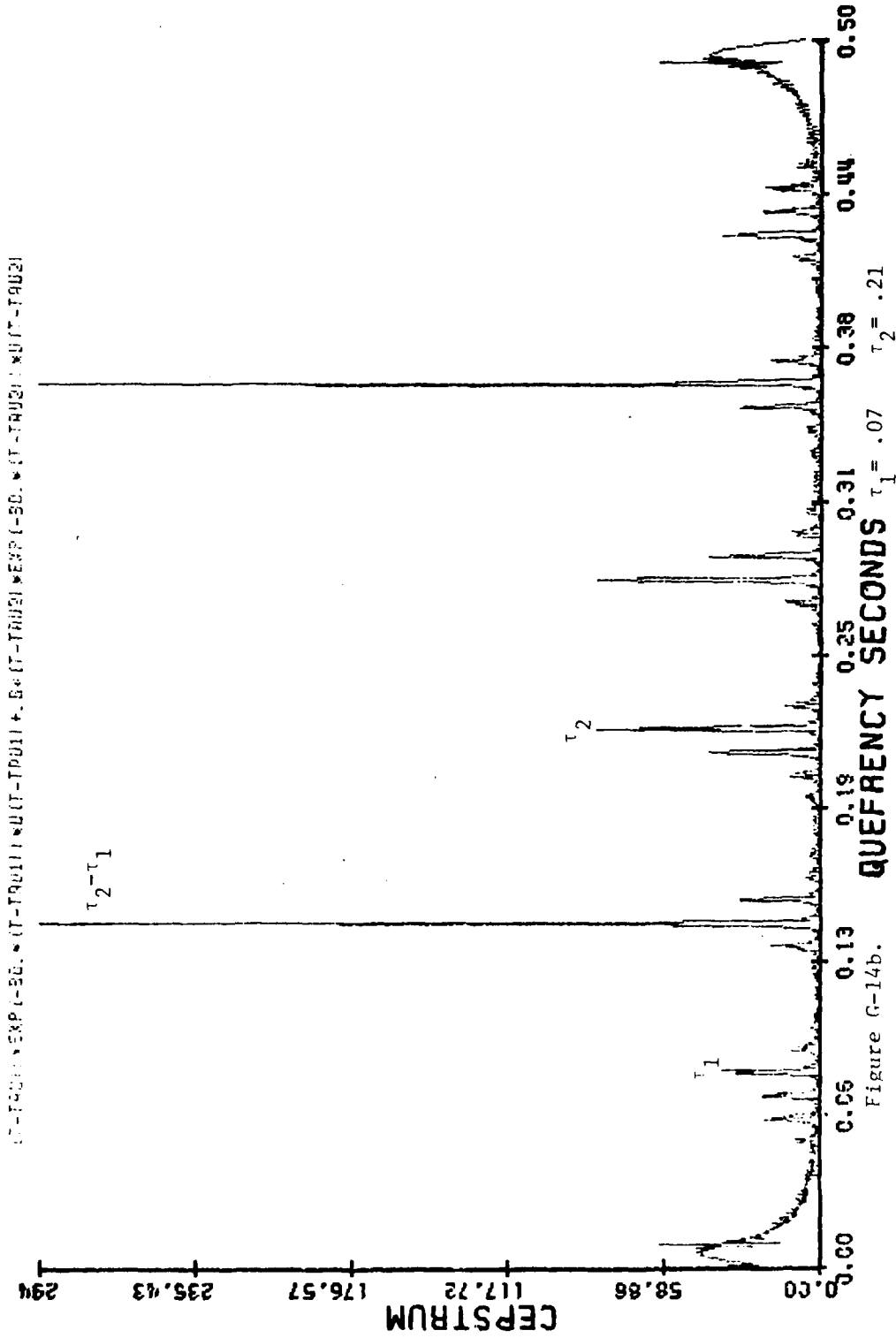


Figure G-14b.

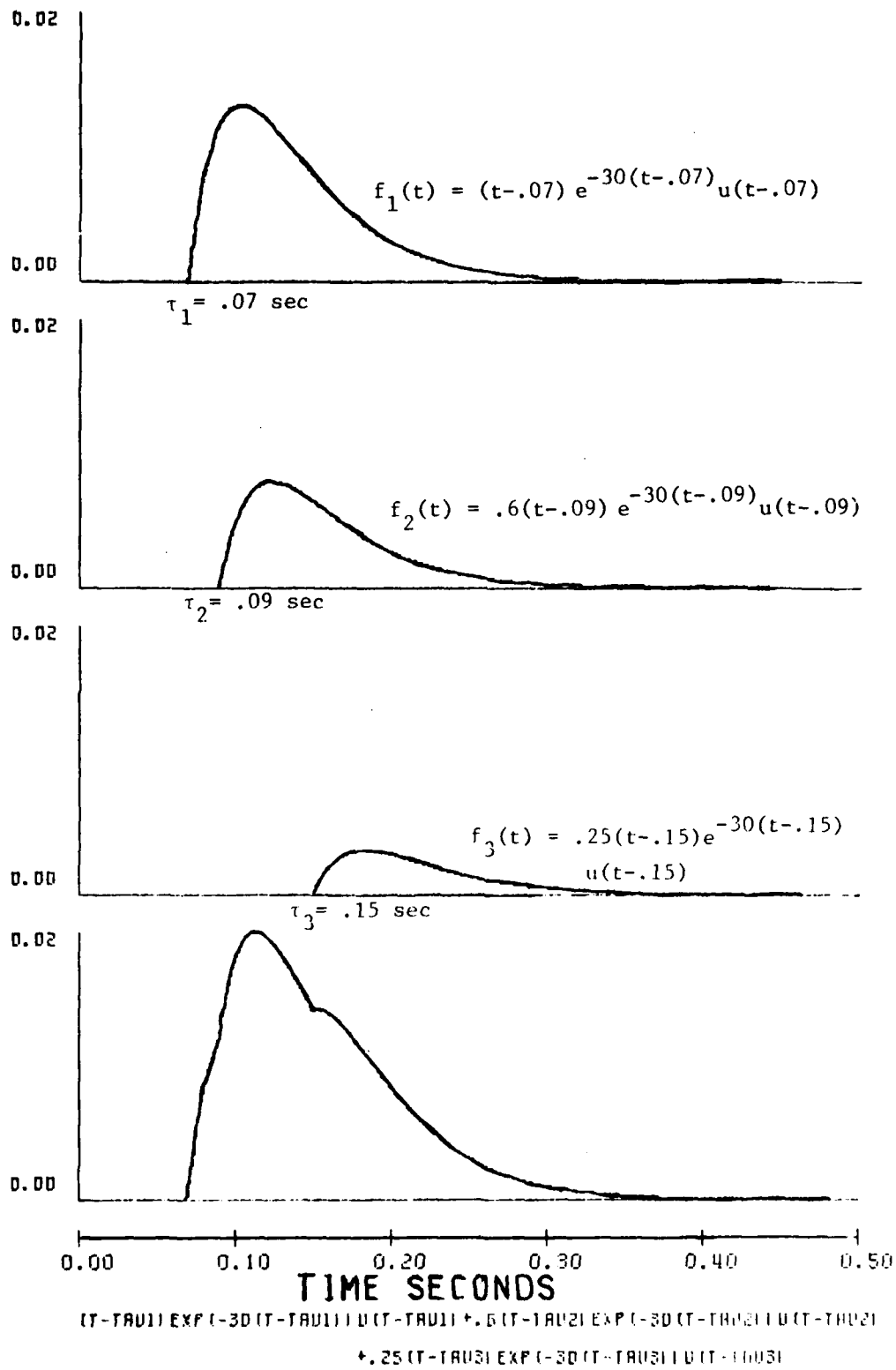
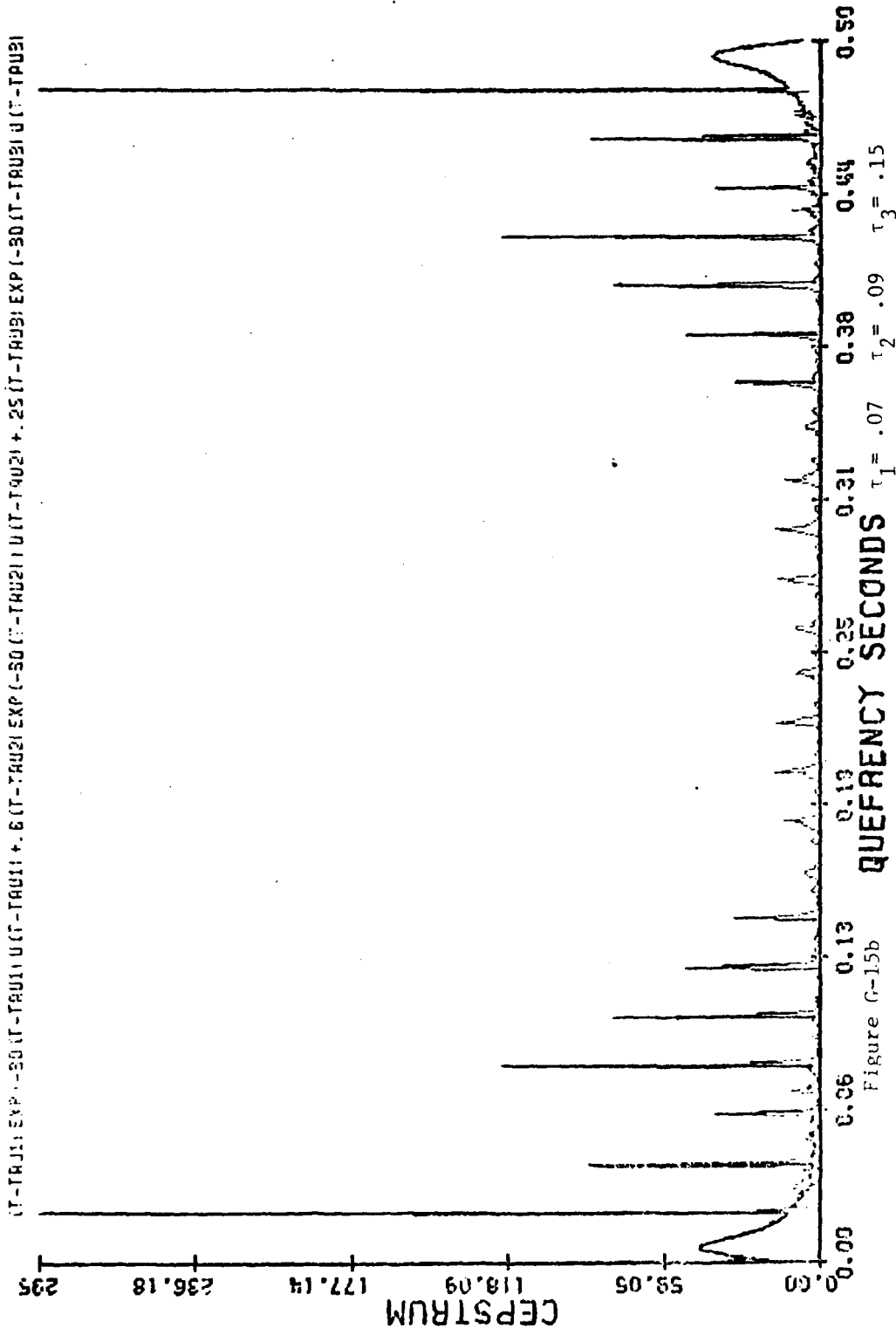


Figure G-15a



In the following pages the following figures have different significances. Figure G-16 shows the effect of under sampling, its sampling rate is 452 samples/sec. It does not represent the cosine waveform in its exact shape. Figure G-16 shows the cepstrum plot of Figure G-16a, which seems to be noisy. Figure G-16c is the enhanced version of Figure G-16b, meaning that after taking the Fourier transform of the cosine signal for the first time, the value of two impulses have been set equal to one. As we see from Figure G-16c there is some improvement.

Figures G-17a and G-17b show effect of having different strength for the echoes. As these Figures show there is no difference in the cepstral property of the plots except that the strength of the peaks has been changed accordingly.

Figures G-18a, G-18b, and G-18c are the cepstral plots when there are three echoes besides the original signal. As is obvious from these cepstral plots, it will be very hard to distinguish the exact locations of each epoch or echo delay time. In all figures $N=1024$, $IWNDW=0$, and $IWNDF=0$ except if they are defined otherwise.

10. $\pi \cos(200\pi t - \tau_{11}) + 6 \pi \cos(200\pi t - \tau_{12}) + 6 \pi \cos(200\pi t - \tau_{13}) + 6 \pi \cos(200\pi t - \tau_{14}) + 6 \pi \cos(200\pi t - \tau_{15}) + 6 \pi \cos(200\pi t - \tau_{16}) + 6 \pi \cos(200\pi t - \tau_{17}) + 6 \pi \cos(200\pi t - \tau_{18}) + 6 \pi \cos(200\pi t - \tau_{19}) + 6 \pi \cos(200\pi t - \tau_{20})$

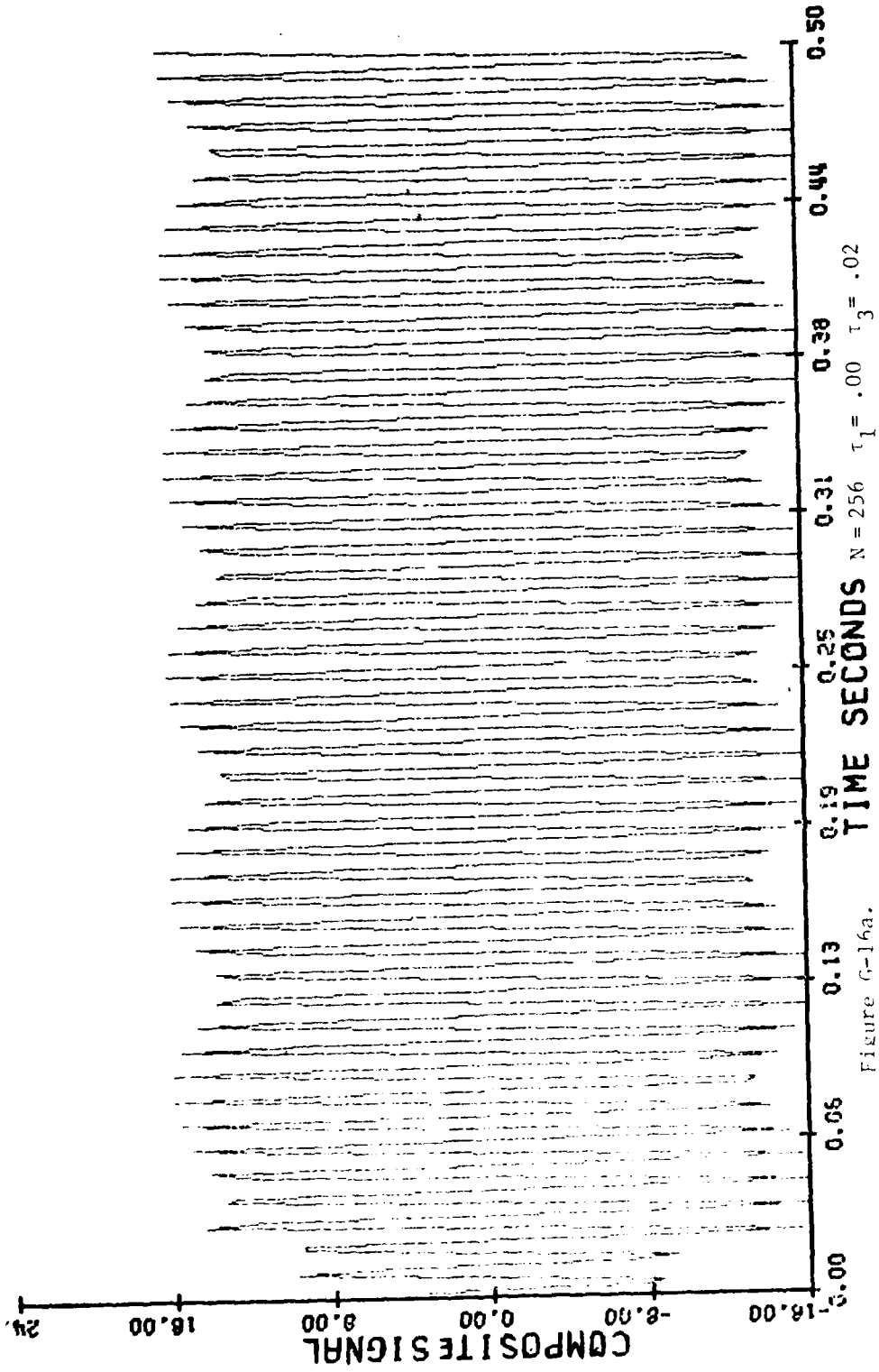


Figure G-16a. $N = 256$ $\tau_1 = .00$ $\tau_3 = .02$

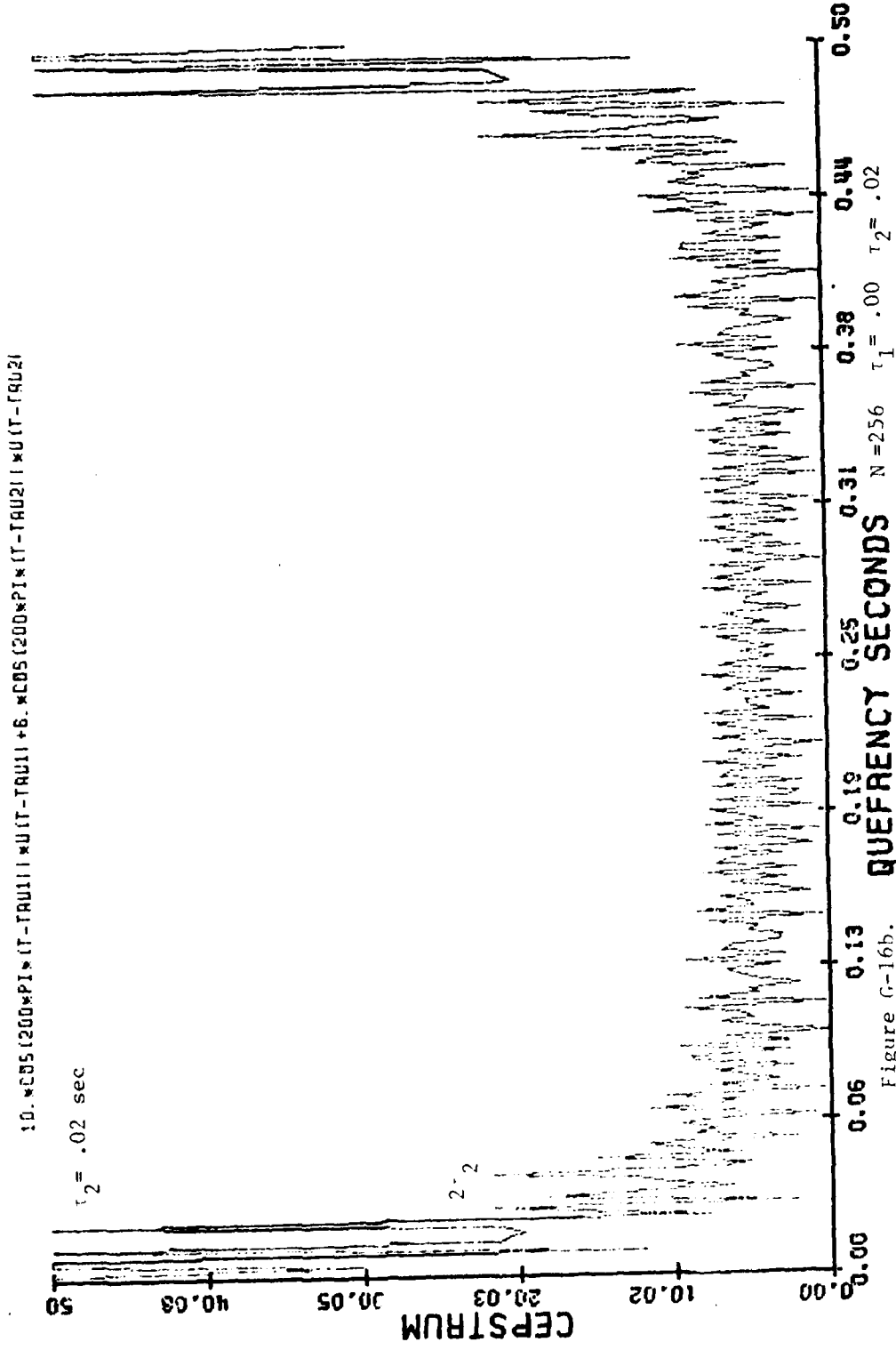


Figure G-16b.

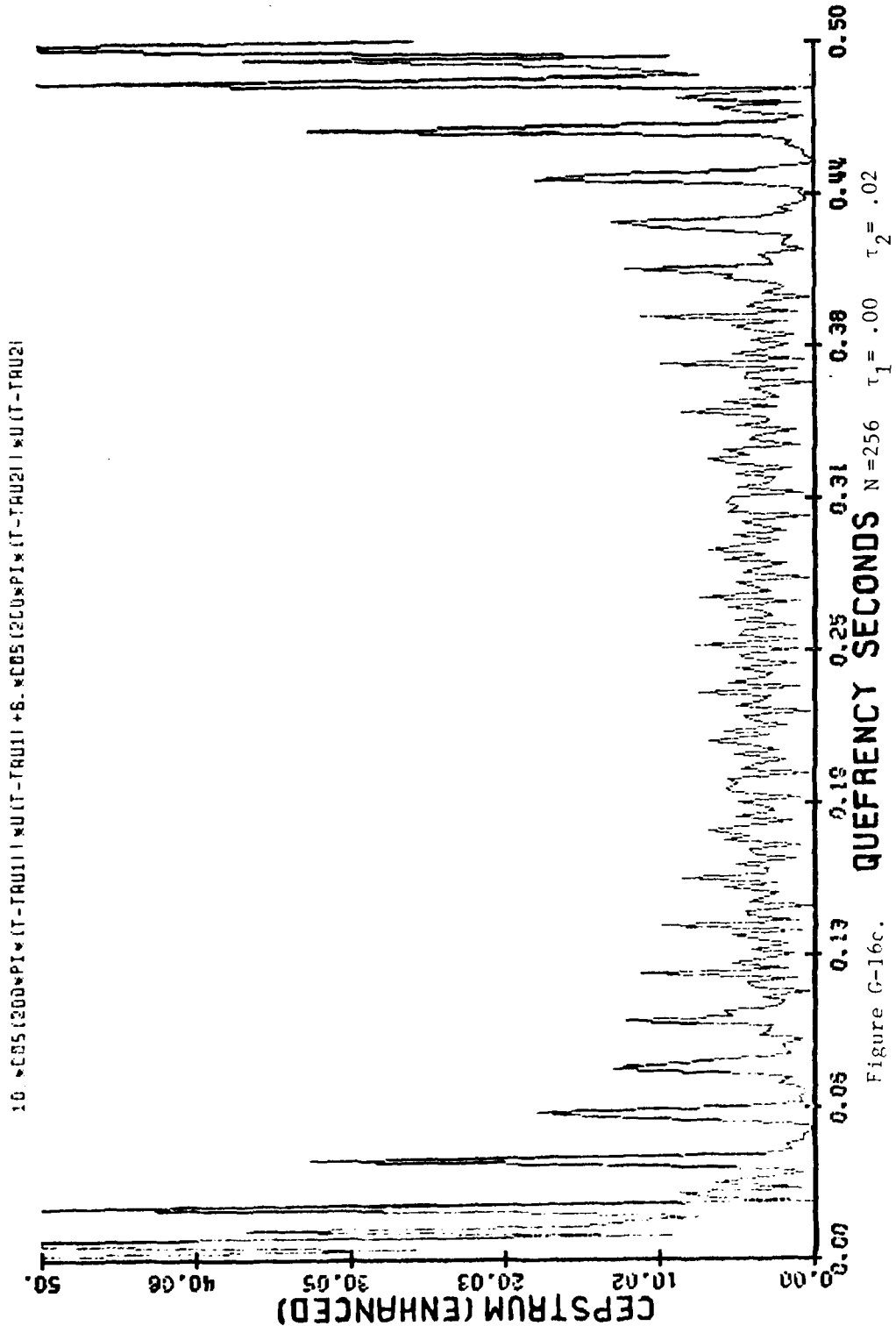


Figure G-16c.

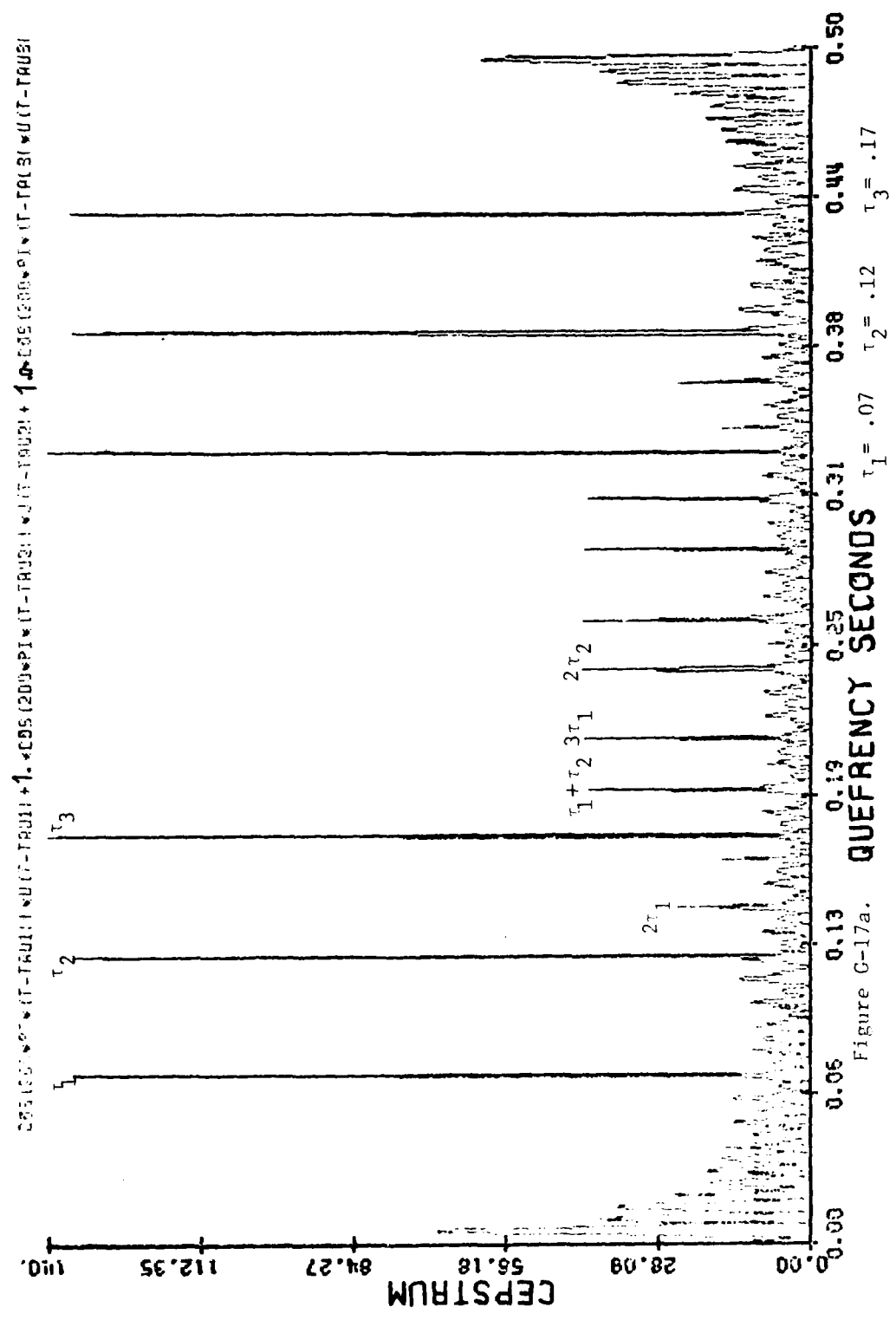


Figure G-17a.

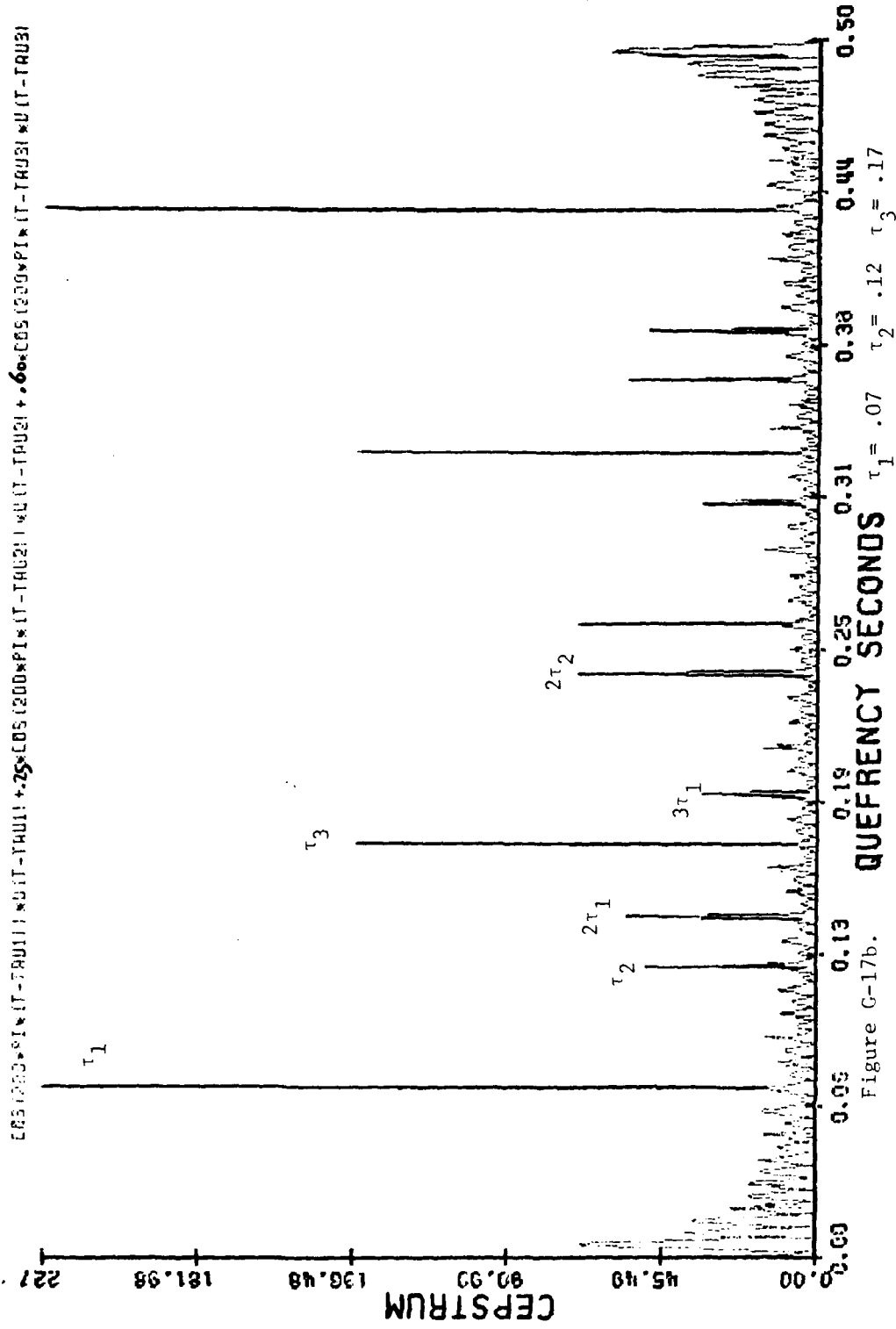


Figure G-17b.

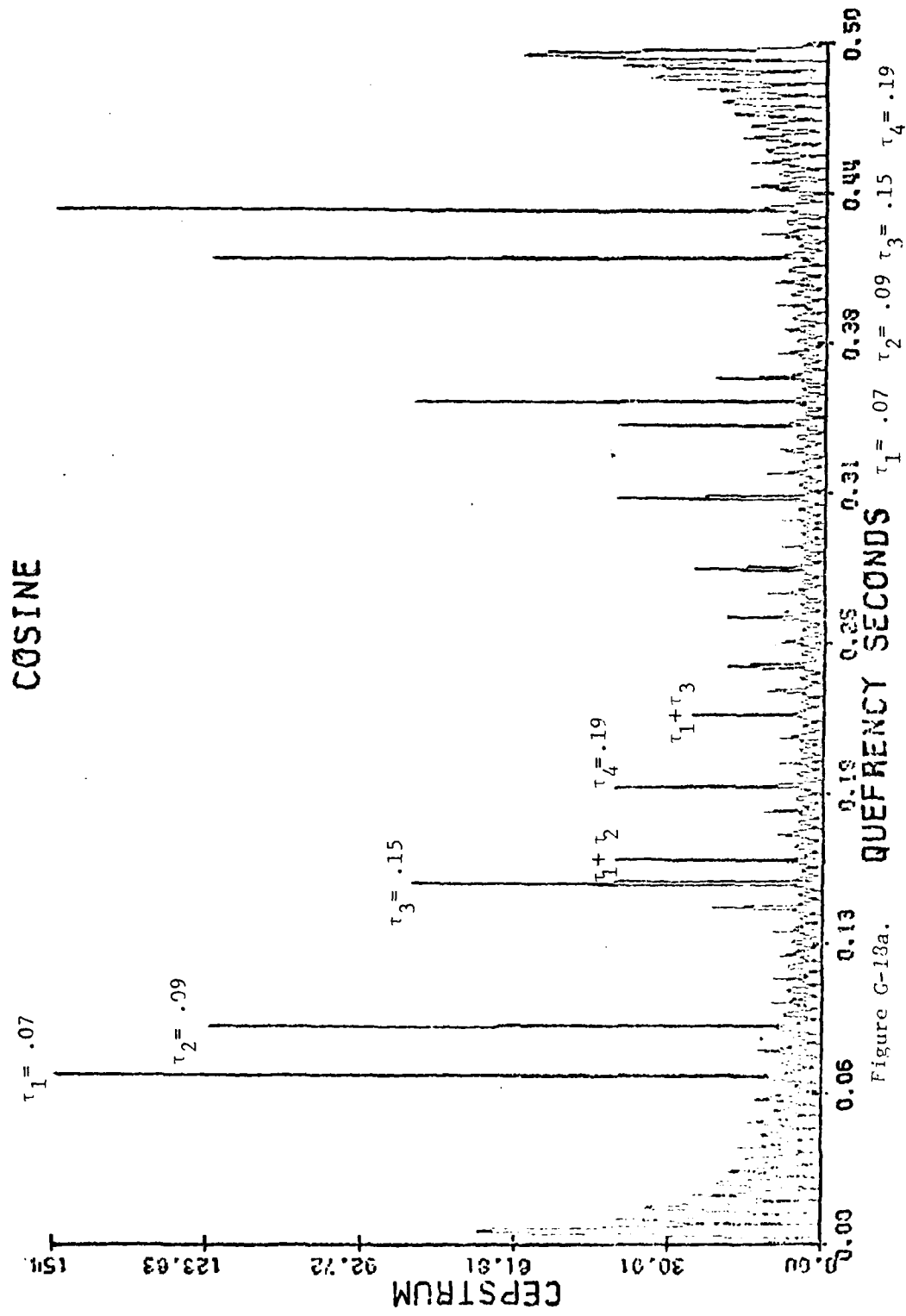


Figure G-13a.

AD-A102 358

MISSISSIPPI STATE UNIV MISSISSIPPI STATE ENGINEERING--ETC F/6 17/1
INVESTIGATION OF CEPSTRUM ANALYSIS FOR SEISMIC/ACOUSTIC SIGNAL --ETC(U)
JAN 81 F M INGELS, G KOLEYNI AFOSR-80-0086

UNCLASSIFIED

MSSU-EIRS-EE-81-2

AFOSR-TR-81-0603

NL

3 of 3

AD 4

102358



END
DATE
FILMED
8-81
DTIC

DAMPED COSINE

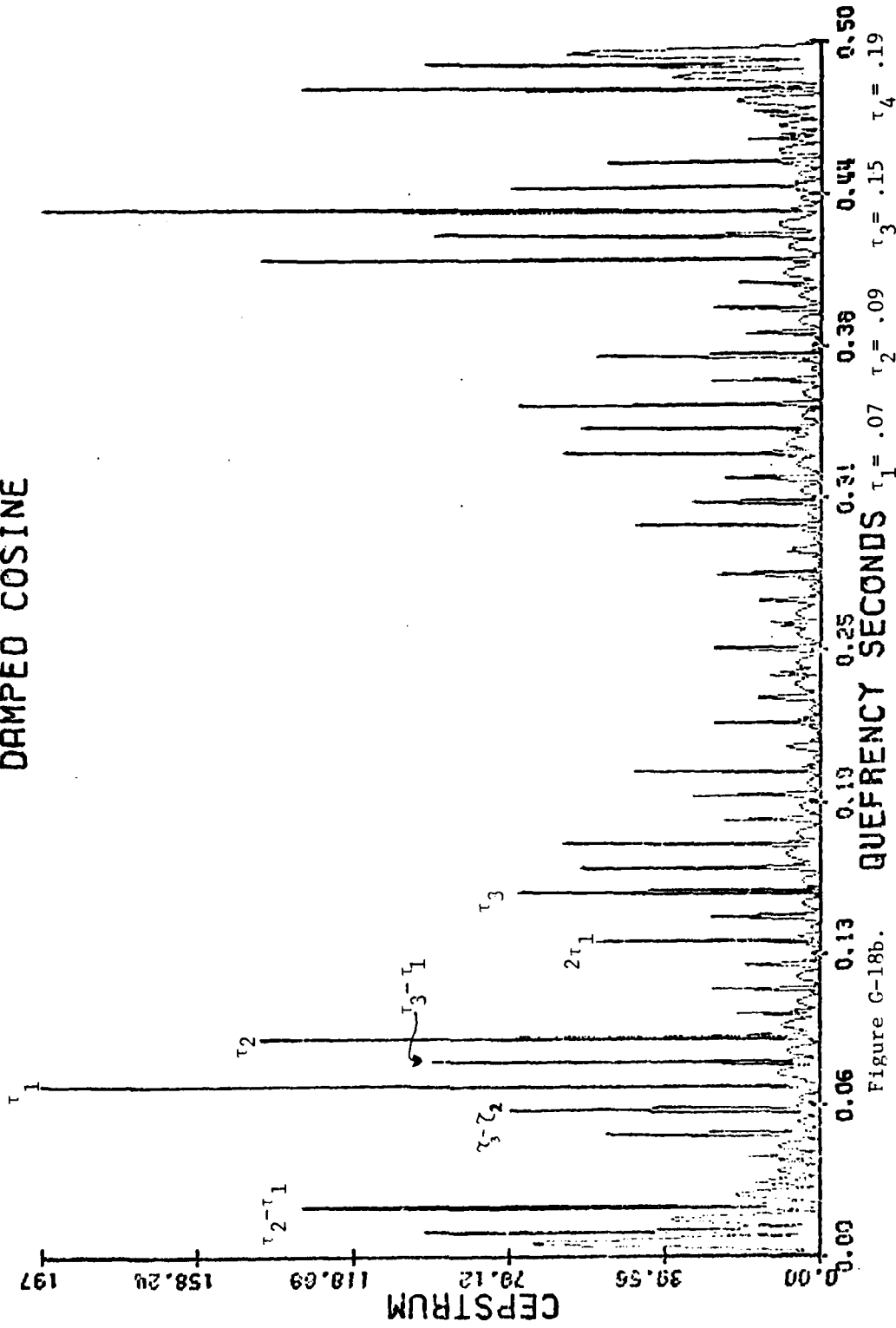


Figure G-18b.

EXPONENTIAL

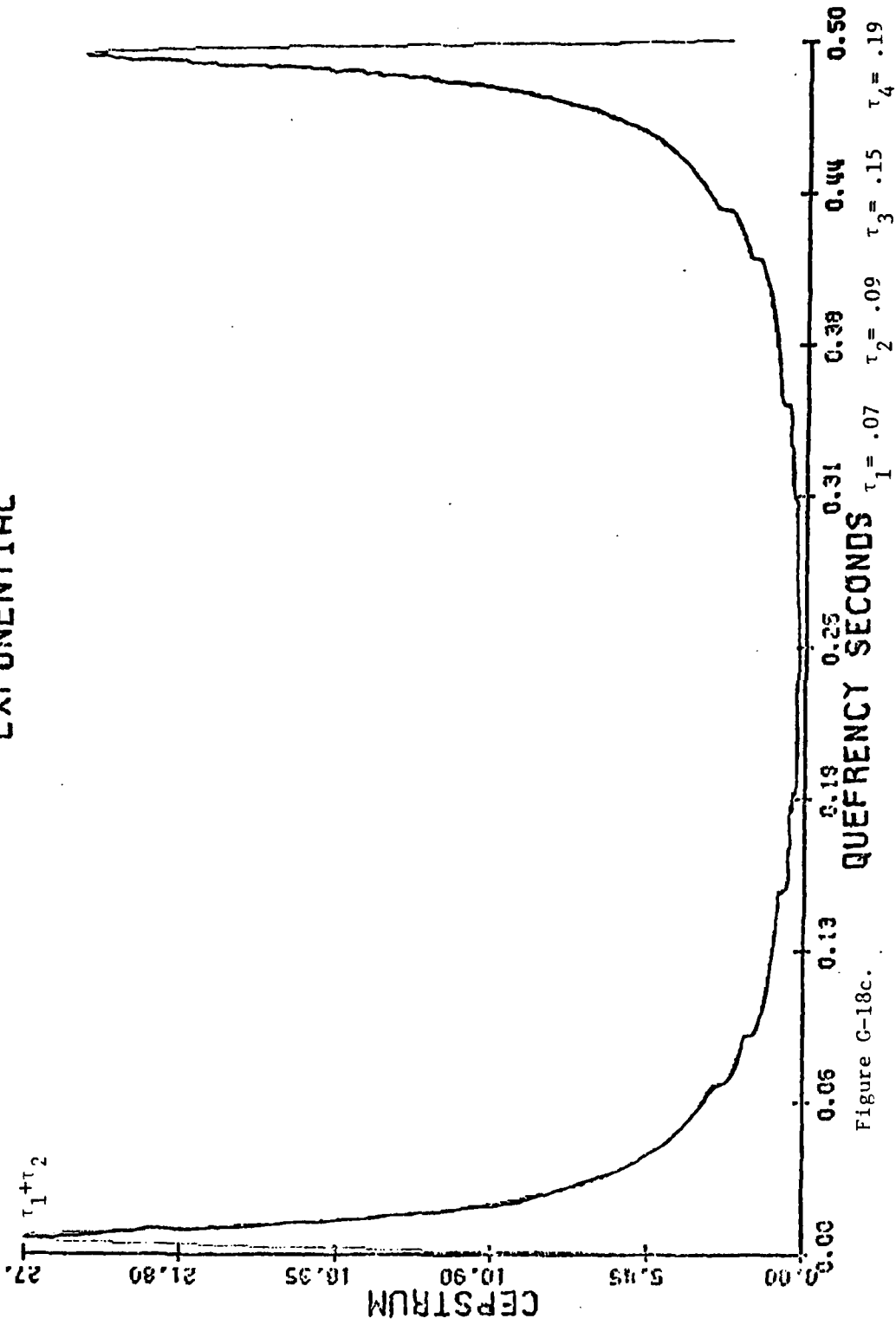


Figure G-18c.

Figures G-19 and G-20 show damped cosine waveforms with their respective cepstral plots for different damping coefficients. In all figures $N=1024$, $IWNDW=0$, and $IWNDF=0$, except if they are defined otherwise.

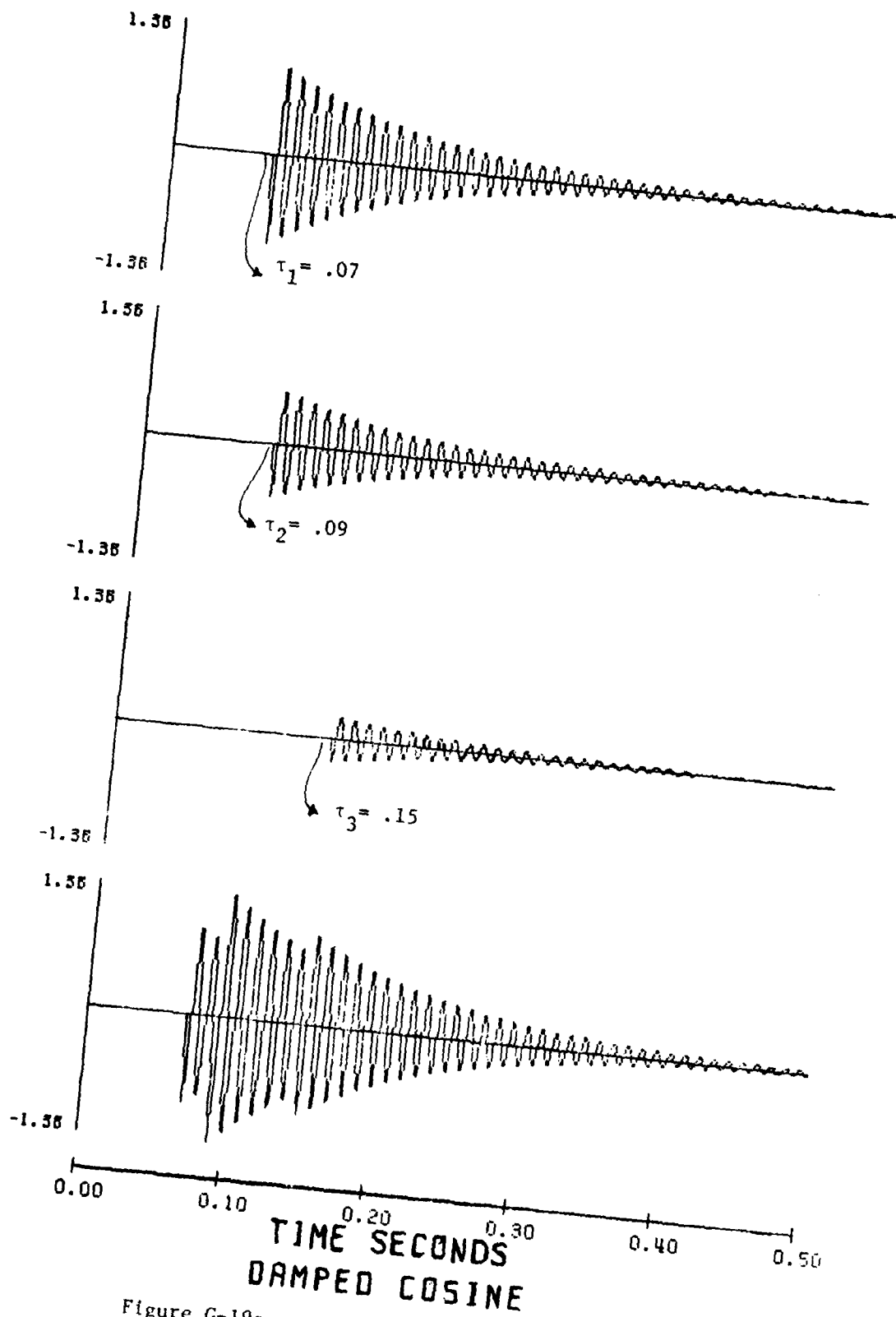


Figure G-19a. Damping Coefficient = 2

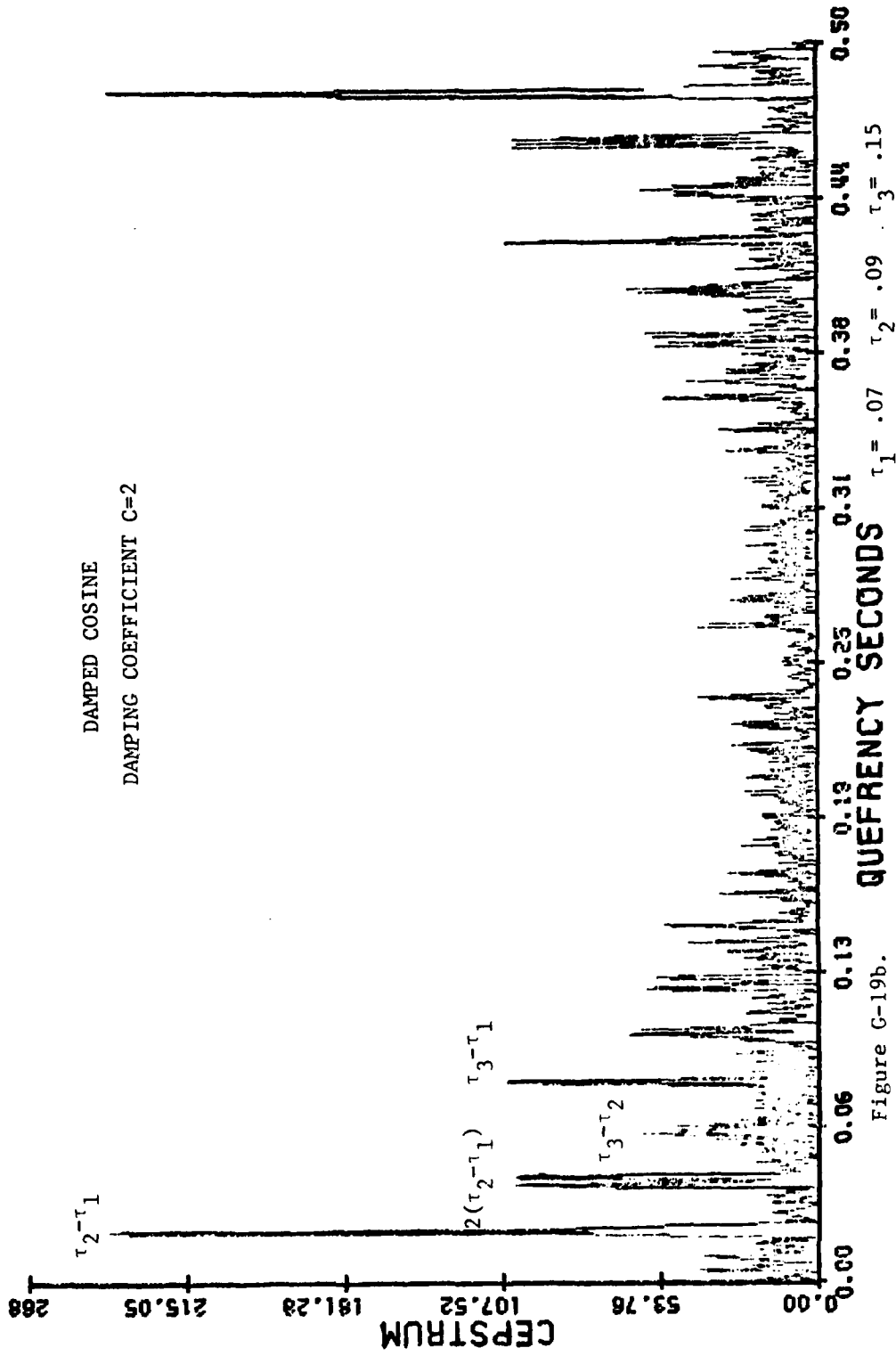


Figure G-19b.

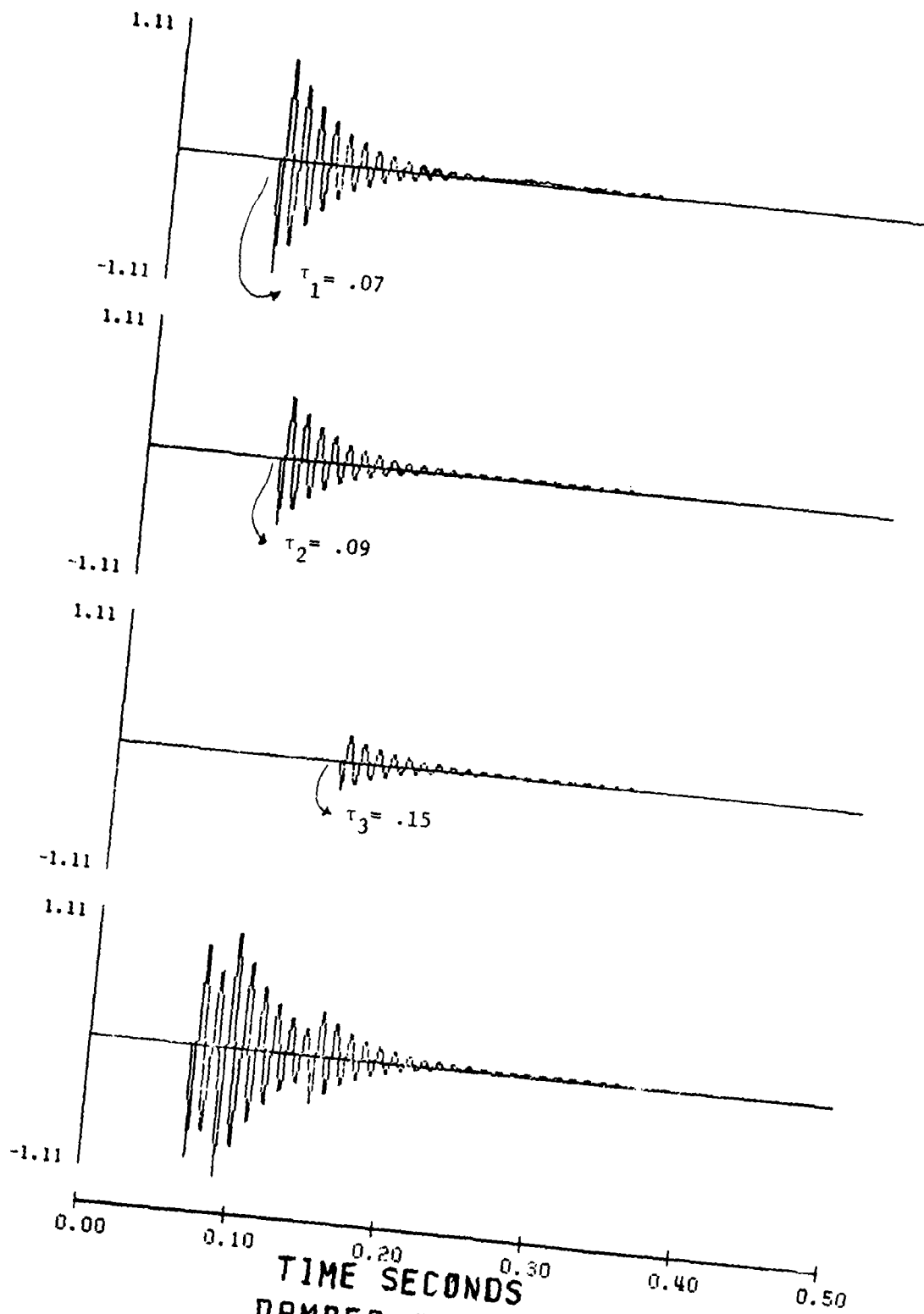


Figure G-20a. Damping Coefficient = 19

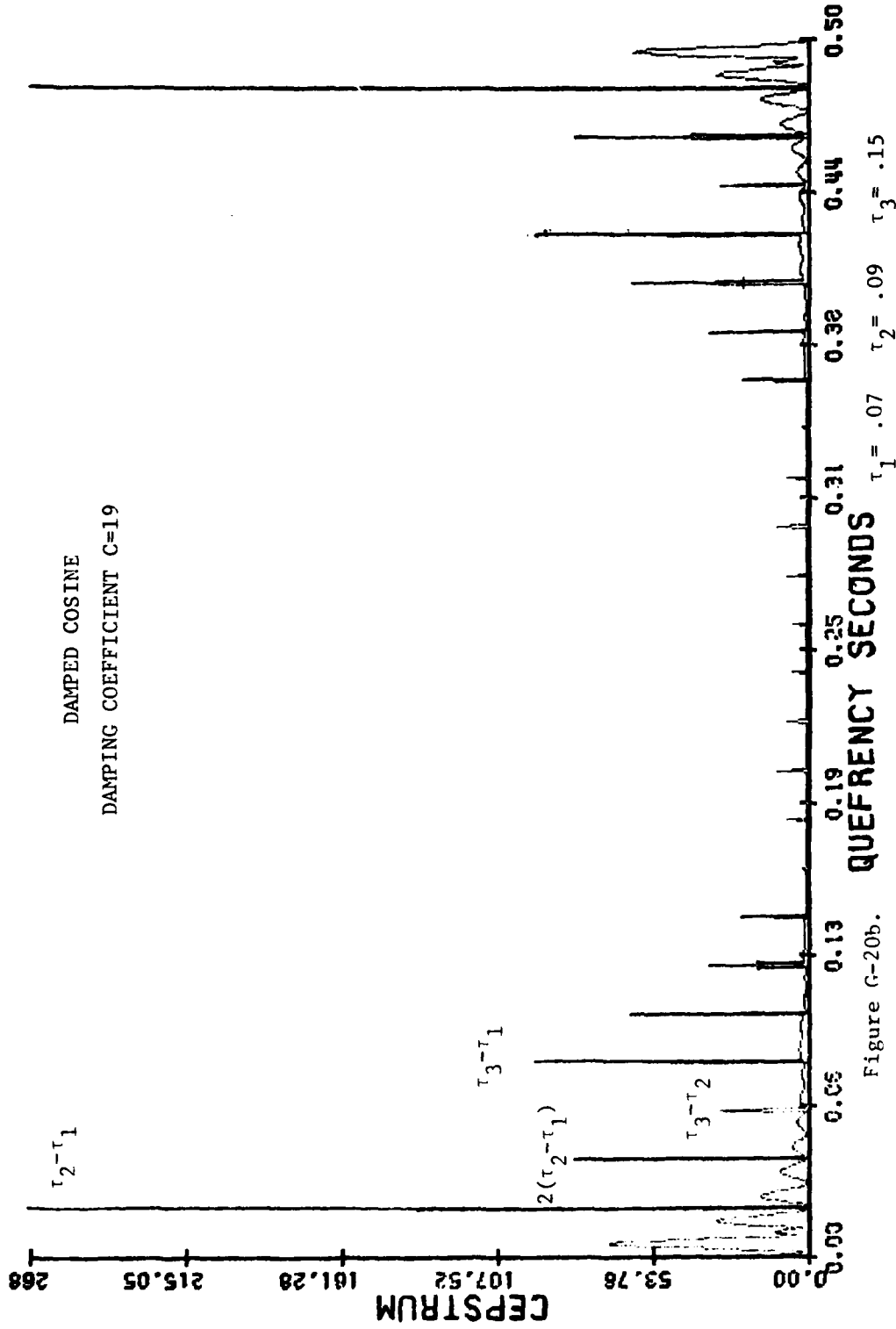


Figure G-20b.

APPENDIX H

BIBLIOGRAPHY AND LITERATURE SURVEY

LITERATURE SURVEY

In an effort to appraise the state of development of cepstrum technique, an extensive survey of cepstrum related literature was undertaken. The dates of the survey extends from the beginning of publication of a paper by Bogert, et al, in 1963 to the present time. The majority of this literature was available in the library of the Mississippi State University, or have been furnished to the author through the Inter Library Loan. The sources of the articles and the inclusive search dates are as follows:

1. Dissertation Abstract International, B, The Science and Engineering, January 1963 through August 1980.
2. Geophysics, January 1960 through August 1980.
3. Geophysics Journal of Royal Astronomical Society, 1970
4. Institute of Electrical and Electronics Engineers Proceedings, January 1963 through August 1980.
5. Institute of Electrical and Electronics Engineers Spectrum, January 1963 through August 1980.
6. Institute of Electrical and Electronics Engineers Transactions on Acoustic Speech and Signal Processing formerly Institute of Electrical and Electronics Engineers Transactions on Audio and Electroacoustics, January 1963 through August 1980.
7. Institute of Electrical and Electronics Engineers Transactions On Communications, January 1963 through August 1980.
8. Institute of Electrical and Electronics Engineers Transactions on Education, March 1969.
9. Institute of Electrical and Electronics Engineers Transactions on Information Theory, January 1963 through August 1980.
10. Institute of Electrical and Electronics Engineers Transactions on Systems Man and Cybernetics, January 1972.

11. Journal of Acoustical Society of America, January 1963 through August 1980.
12. Journal of Geophysical Research, October 1970.
13. Journal of Sound and Vibration, January 1974 through August 1980.
14. Report on 8th Annual Southeastern Symposium on System Theory, April 1976.
15. Simulation, March 1969.
16. The Bell System Technical Journal, January 1963 through August 1980.

For the purpose of making a meaningful summary, the aforementioned topics will be broken in two categories: (1) Fourier transform , specially the Fast Fourier Transform (FFT), (2) Cepstrum or the related topics. Included in the summary of each category will be a list of the most pertinent articles with a synopsis.

FOURIER TRANSFORM

The fourier transform of $f(x)$ is defined as

$$\int_{-\infty}^{\infty} f(x) e^{-j2\pi xs} dx$$

this integral, which is a function of s , may be written $F(s)$.

Transforming $F(s)$ by the same formula, we have

$$\int_{-\infty}^{\infty} F(s) e^{-j2\pi ws} ds$$

when $f(x)$ is an even function of x , that is, when $f(x) = f(-x)$, the repeated transformation yields $f(w)$, the same function with which we began. This is a cyclical property [82] of the Fourier transformation, and since the cycle is of two steps, the reciprocal property is implied: if $F(s)$ is the Fourier transform of $f(x)$, then $f(x)$ is the Fourier transform of $F(s)$.

The cyclical and reciprocal properties are imperfect, however, because when $f(x)$ is odd i.e., when $f(x) = -f(-x)$ the repeated transformation yields $f(-w)$. In general, whether $f(x)$ is even or odd or neither, repeated transformation yields $f(-w)$.

The customary formula exhibiting the reversibility of the Fourier transformation are [82]

$$F(s) = \int_{-\infty}^{\infty} f(x) e^{-j2\pi xs} dx$$

$$f(x) = \int_{-\infty}^{\infty} F(s) e^{j2\pi sx} ds .$$

In this form, two successive transformations are made to yield the original function.

It may happen that function values are given only at discrete values of the independent variable (pulses), as which physical measurements made at regular time intervals. Regardless of the form of the given function, if the transform is evaluated by numerical computing, the values of the transform will be available only at discrete intervals. We often think of this as though an underlying function of a continuous variable really exists and we are approximating it.

The rules for finding the frequency response samples from the pulse response and vice-versa were called the discrete Fourier Transform (DFT) and Inverse Discrete Fourier Transform (IDFT), respectively [81].

The Discrete Fourier Transform or DFT of the N-point sequence f_0, f_1, \dots, f_{N-1} is defined as the N-point sequence.

$$F_k = \sum_{n=0}^{N-1} f_n e^{-j2\pi n \frac{k}{N}}$$

The inverse discrete Fourier transform formula or IDFT is

$$f_n = \text{IDFT} [F_k] = \frac{1}{N} \sum_{k=0}^{N-1} F_k e^{j2\pi n \frac{k}{N}}$$

$$n = 0, 1, 2, \dots, N-1$$

In 1965 a method of computing discrete Fourier transforms suddenly became widely known (J.W. Cooley and J. W. Tukey, math. comput, vol. 19, April 1965, pp. 297-301) which revolutionized many fields where onerous computing was an impediment to progress.

Following is a chronological list of some of the most pertinent articles related to Fourier transform (FT) and Fast Fourier Transform (FFT). A brief synopsis is included with each article in this list.

1. Cochran, W. T., Cooley, J. W., Favon, D. L., Helms, H. D., Kaenel, R. A., Lang, W. W., Maling, Jr. G. C., Nelson, D. E., Rader, C. M. and P. W. Welch, "What is Fast Fourier Transform?", IEEE Transactions on Audio and Electroacoustics, Vol. Au-15, N8. 2, pp. 45-55, June 1967.

In this paper, the discrete Fourier transform of a time series is defined, some of its properties are discussed, the associated fast method (Fast Fourier Transform) for computing this transform is derived, and some of the computational aspects of the methods are presented.

2. Cooley, J. W., Lewis, P. A. W. and P. D. Welch, "Historical Notes on the Fast Fourier Transform", IEEE Transactions on Audio and Electroacoustics, Vol. Au-15, No.2, pp.76-84, June 1967.

In this paper, the contributions of many investigators are described and placed in historical perspective.

3. Rader, C. M., "Discrete Fourier Transforms When the Number of Data Samples is Prime", IEEE Proceedings, Vol. 56, No. 5, pp. 1107-1108, June 1968.

The discrete Fourier transform of a sequence of N points where N is a prime number, is shown to be essentially a circular correlation. This can be recognized by rearranging the members of the sequence and the transform according to a rule involving a primitive root of N . This observation permits this discrete Fourier transform to be computed by means of a

fast Fourier transform algorithm, with the associated increase in speed, even through N is prime.

4. Cooley, J. W., Lewis, P.A.W. and P. D. Welch, "The Fast Fourier Transform and its Applications", IEEE Transactions on Education, Vol. 12, No. 1, pp. 27-34, March 1969.

A description of the algorithm for FFT and its programming is given followed by a theorem relating its operands, the finite sample sequences, to the continuous functions they often are intuned to approximate. An analysis of the error due to discrete sampling over finite ranges is given in terms of aliasing. Procedures for computing Fourier integrals, convolution and lagged products are outlined.

5. Bergland, G. D., "A Radix-Eight Fast Fourier Transform Subroutine for Real-Valued Series", IEEE Transactions on Audio and Electroacoustics, Vol. AU-17, No. 2, pp. 138-144, June 1969.

Fast Fourier Analysis (FFA) and fast Fourier synthesis (FFS) algorithms are developed for computing the discrete Fourier transform of a real series, and for synthesizing a real series from its complex Fourier coefficients.

6. Singleton, R. C., "A Short Bibliography on the Fast Fourier Transform", IEEE Transactions on Audio and Electroacoustics, Vol. Au-17, No. 2, pp. 166-169, Jan. 1969.

A chronologically listed name of papers on Fast Fourier Transform", pp. 166-169, January 1969.

7. Singleton, R. C., "An Algorithm for Computing the Mixed Radix Fast Fourier Transform", IEEE Transactions on Audio and Electroacoustics, Vol. Au-17, No. 2, pp. 93-103, June 1969.

The paper presents an algorithm for computing the fast Fourier transform based on a method proposed by Cooley and Tukey. As in their algorithm, the dimension n of transform is factored (if possible), and n/p elementary transforms of dimension p are computed for each factor p of n . The algorithm is described mathematically and illustrated by a Fortran subroutine.

8. Uhrich, M. L., "Fast Fourier Transforms Without Sorting", IEEE Transactions on Audio and Electroacoustics, Vol. Au-17, No. 2, pp. 170-172, June 1969.
9. Markel, J. D., "FFT Pruning", IEEE Transactions on Audio and Electroacoustics, Vol. Au-19, No. 4, pp. 305-311, December 1971.

There are basically four modifications of the $N=2^m$ point FFT algorithm developed by Cooley and Tukey which give improved computational efficiency. It is shown that for situations in which the relative number of zero-valued samples is quite large, significant time saving can be obtained by pruning the FFT algorithm.

10. Harris, F. J., "On the Use of Windows for Harmonic Analysis With the Discrete Fourier Transform", IEEE Proceedings, Vol. 66, No. 1, pp. 51-83, January 1978.

This paper makes available a concise review of data windows and their effect on detection of harmonic signals in the presence of broad-band noise, and in the presence of nearby strong harmonic interference. Also calls attention

to a number of common errors in the application of windows when used with the Fast Fourier Transform.

In addition to the ten articles listed above, the following references to the bibliography in Appendix A are also related to Fourier transform or Fast Fourier Transform (FFT): 1,12,15,16,61, 66,69,70,77,78,79,80,81,and 82.

CEPSTRUM AND DECONVOLUTION

The first paper on the cepstrum has been published by Bogert, et al. [3] in 1963 and this has been the first paper in inventing and using this word a thorough investigation of the subject has been done through the text. The papers mainly deal with problems of power cepstrum. Also included are papers related to the complex cepstrum as defined by Schaffer [16]. The following list of articles applies to cepstrum analysis and related subjects.

1. Bogert, B. P., Healy, M. J. R. and J. W. Tukey, "The Quefreny Analysis of Time Series for Echoes: Cepstrum, Pseudo-Autocovariance, Cross-Cepstrum and Saphe Cracking", in Pro. Symp. on Time Series Analysis, M. Rosenblatt, Ed., New York, Wiley, Chap. 15, pp. 209-243, 1963.

The first published paper on cepstrum (power cepstrum) brings up the question of echoes and how to detect them, also compares the cepstrum method with autocorrelation. The authors define new terms paraphrased from known terminologies such as cepstrum which is a paraphrased word from spectrum.

2. Noll, A. M., "Short-Time Spectrum and Cepstrum, Techniques for Vocal-Pitch Detection", J. Acoust. Soc. Am., Vol. 36, No. 2, pp. 296-302, February 1964.

In this paper the author is trying to use the newly familiar subject of cepstrum for vocal-pitch detection in speech. The cepstrum of a speech signal has a peak corresponding to the fundamental period for voice speech but no peak for unvoiced speech. Thus a cepstrum analyzer can function both as a pitch and as voiced-unvoiced detector.

3. Noll, A. M., "Clipstrum Pitch Determination", J. Acoust. Soc. Am., Vol. 44, No. 6, pp. 1585-1591, December 1968.

In this paper the author presents a new method of pitch Determination similar to the cepstrum except that both the time signal and the log power spectrum are infinitely peak clipped before spectrum analysis has been simulated on a digital computer. It shows the clipping in the clipstrum might offer some advantages over cepstrum analysis in certain digital hardware implementations since multiplications could be replaced with addition or subtractions.

4. Childers, D. G., Varga, R. S. and N. W. Perry, Jr., "Composite Signal Decomposition", IEEE Transactions on Audio and Electroacoustics, Vol. Au-18, No. 4, pp. 461-477, December 1970.

This paper presents a technique for decomposing a composite signal, which consists of the superposition of known multiple signals overlapping in time, digital Data processing problems such as filter realizability,

signal resolution capability, the effect of additive noise, frequency (spectrum) compatibility between signal waveform and filter response pulse, and possible additional processing in certain cases are discussed.

5. Kemerait, R. C., and D. G. Childers, "Signal Detection and Extraction by Cepstrum Techniques", IEEE Transactions on Information Theory, Vol. IT-18, No. 6, pp. 745-759, November 1972.

Digital data-processing problems such as the detection of multiple echoes, various methods of linear filtering the complex cepstrum the picket-fence phenomenon, minimum-maximum phase situation, and amplitude-versus phase-smoothing for additive-noise cases are examined empirically and where possible theoretically, and are discussed.

6. Hassab, J. C., "Time Delay Processing Near the Ocean Surface", J. Sound and Vibration, Vol. 35, No. 4, pp. 489-501, 1974.

A study of a simple multi-path channel near the ocean surface where a direct path and a surface-reflected path link the source to the receiver. By using autocorrelation and cepstrum processing, extraction of the difference in arrival times between two paths, i.e. time delay, from a priori unknown signals is studied.

7. Hassab, J. C. and R. Boucher, "A Probabilistic Analysis of Time Delay Extraction by Cepstrum in Stationary Gaussian Noise", IEEE Transactions on Information Theory, Vol. IT-22, No. 4, July 1976.

A probabilistic analysis is conducted dealing with the effect of stationary Gaussian noise on the characteristics of such a nonlinear processor. The expected mean and standard deviation of reduction in the peak level at (time delay) due to noise are analytically described. The results point out the dependence of statistical measures upon the pointwise variation of input signal to noise spectra.

8. Childers, D. G., Skinner, D. P. and R. C. Kemerait, "The Cepstrum: A Guide to Processing", IEEE Proceedings, Vol. 65, No. 10, October 1977.

This paper is a pragmatic tutorial review of the cepstrum literature focusing on data processing. The effects of various forms of liftering the cepstrum are described. The results obtained by applying whitening and trend removal techniques to the spectrum prior to the calculation of the cepstrum are discussed. A good many numbers of references are given in this paper.

9. Dudgeon, D. E., "The Computation of Two-Dimensional Cepstra", IEEE Transactions on Acoustics, Speech, and Signal Processing, Vol. ASSP-25, No. 6, December 1977.

This paper explores two methods of computing the complex cepstrum of a two-dimensional signal. It considers the definitions of two-dimensional causality and two-dimensional minimum phase signals. It explores the relationship among the nonzero regions of a signal, its inverse, and its cepstrum.

10. Ingels, F. M., "Cepstrum Analysis Techniques for Possible Application to Seismic/Acoustic Ranging", Report No. FA9620-79-C-0038, Mississippi State University, August 1979.

This report is concerned with ranging problems. It studies use of one sensor to determine the range. It advocates cepstral analysis to determine the differences in time of arrival of two signals detected with the same sensor, also shows some results of applying the cepstrum technique.

Other papers, articles, letters, or books which are related to the cepstrum technique are listed in the bibliography of Appendix A. The following list of numbers indicate those entries in the bibliography: 1,5,6,8,9,10,11,12,16,25,26,27,29,31,32,34, 35,37,39,40,42,43,44,46,47,48,49,50,51,52,53,54,55,56,57,58,60, 67,71,73,74,77,79,80, and 81.

A COMPILED BIBLIOGRAPHY ON CEPSTRUM AND RELATED TOPICS

The following bibliography concerns the subjects of cepstrum homomorphic deconvolution, Fourier transform, Fast Fourier Transform (FFT), power spectrum and applications. The bibliography is divided into two sections as follows: (1) articles published in journals, (2) books. The entries are listed chronologically except when the month and the year of some publications are the same in which case the listing is alphabetical. An alphabetical author's index follows the publications listing with reference to numbered articles of the bibliography.

BIBLIOGRAPHY

ARTICLES

1. Fano, R. M., "Short-Time Autocorrelation Functions and Power Spectra", Journal of Acoustical Society of America, Vol. 22, No. 5, pp. 546-550, September 1950.
2. Schroeder, M. R. and B. S. Atala, "Generalized Short-Time Power Spectra and Autocorrelation Functions", Journal of Acoustical Society of America, Vol. 34, No. 11, pp. 1679-1683, November 1962.
3. Bogert, B. P., Healy, M. J. R. and J. W. Tukey, "The Quefrency Analysis of Time Series for Echoes: Cepstrum, Pseudo-Auto Covariance, Cross-Cepstrum and Saphe Cracking", in Pro. Symp. on Time Series Analysis, M. Rosenblatt, Ed., New York, Wiley, Chap. 15, pp. 209-243, 1963.
4. Noll, A. M., "Short-Time Spectrum and, , Cepstrum, , Techniques for Vocal-Pitch Detection", The Journal of the Acoustical Society of America, Vol. 36, No. 2, pp. 296-302, February 1964.
5. Noll, A. M. and M. R. Schroeder, "Short-Time, , Cepstrum, , Pitch Detection", The Journal of Acoustical Society of America, Vol. 36, No. 5, p. 1030, May 1964.
6. Young, T. Y., "Epoch Detection-A Method for Resolving Overlapping Signals", The Bell System Technical Journal, Vol. XLIV, No. 3, pp. 401-426, March 1965.
7. Kelly, J. M. and R. N. Kennedy, "Experimental Cepstrum Pitch Detector for Use in a 2400-Bit/Sec Channel Vocoder", The Journal of Acoustical Society of America, Vol. 40, No. 5, p. 1241, May 1966.
8. Noll, A. M., "Computer-Simulated Cepstrum Pitch Detector for Vocoder Excitation", The Journal of Acoustical Society of America, Vol. 40, No. 5, p. 1241, May 1966.
9. Bogert, B. P. and J. F. Ossanna, "Computer Experimentation of Echo Detection Using the Cepstrum and Pseudo Autocovariance", The Journal of Acoustical Society of America, Vol. 39, No. 6, p. 1258, June 1966.
10. Bogert, B. P. and J. F. Ossanna, "The Heuristics of Cepstrum Analysis of a Stationary Complex Echoed Gaussian Signal in Stationary Gaussian Noise", IEEE Transactions on Information Theory, Vol. IT-12, No. 3, pp. 373-380, July 1966.

11. Noll, A. M., "Cepstrum Pitch Determination", The Journal of the Acoustical Society of America, Vol. 41, No. 2, pp. 293-309, February 1967.
12. Bogert, B. P., and E. Parzen, "Informal Comments on the Uses of Power Spectrum Analysis", IEEE Transactions on Audio and Electroacoustics, Vol. Au-15, No. 2, pp. 74-76, June 1967.
13. Cochran, W. T., Cooley, J. W., Favin, D. L., Helms, H. D., Kaenel, R. A., Lang, W. W., Maling, G. C., Nelson, D. E., Rader, C. M., and P. D. Welch, "What is Fast Fourier Transform?", IEEE Transactions on Audio and Electroacoustics, Vol. Au-15, No. 2, pp. 45-55, June 1967.
14. Cooley, J. W., Lewis, P. A. W., and P. D. Welch, "Historical Notes on the Fast Fourier Transform", IEEE Transactions on Audio and Electroacoustics, Vol. Au-15, No. 2, pp. 76-79, June 1967.
15. Cooley, J. W., Lewis, P. A. W., and P. D. Welch, "Application of the Fast Fourier Transform to Computation of Fourier Integrals, Fourier series, and Convolution Integrals", IEEE Transactions on Audio and Electroacoustics, Vol. Au-15, No. 2, pp. 79-84, June 1967.
16. Schaffer, R. W., "Echo Removal by Generalized Linear Filtering", Ph.D. Dissertation, Massachusetts Institute of Technology, 1968.
17. Rader, C. M., "Discrete Fourier Transforms When the Number of Data Samples is Prime", IEEE Proceedings, Vol. 56, No. 5, pp. 1107-1108, June 1968.
18. Noll, A. M., "Cepstrum Pitch Detection", The Journal of Acoustical Society of America, Vol. 44, No. 6, pp. 1585-1591, December 1968.
19. Balas, L. F., "Digital Simulation of Low-Pass Gaussian Noise", Simulation, pp. 110-112, March 1969.
20. Cooley, J. W., Lewis, P. A. W., and P. D. Welch, "The Fast Fourier Transform and its Applications", IEEE Transactions on Education, Vol. 12, No. 1, pp. 27-34, March 1969.
21. Bergland, G. D., "A Radix-Eight Fast Fourier Transform Subroutine For Real-Valued Series", IEEE Transactions on Audio and Electroacoustics, Vol. Au-17, No. 2, pp. 138-144, June 1969.

22. Singleton, R. C., "A Short Bibliography on the Fast Fourier Transform", IEEE Transactions on Audio and Electroacoustics, Vol. Au-17, No. 2, pp. 166-169, June 1969.
23. Singleton, R. C., "An Algorithm for Computing the Mixed Radix Fast Fourier Transforms", IEEE Transactions on Audio and Electroacoustics, Vol. Au-17, No. 2, pp. 93-103, June 1969.
24. Uhrich, M. L., "Fast Fourier Transforms Without Sorting", IEEE Transactions on Audio and Electroacoustics, Vol. Au-17, No. 2, pp. 170-172, June 1969.
25. Cohen, T., "Source-Depth Determinations Using Sepstral, Pseudo-Autocorrelation and Cepstral Analysis", Geophys. J. Roy. Astro. Soc., Vol. 20, pp. 223-231, 1970.
26. Halpeney, O. S., "Epoch Detection by Digital Cepstrum", Master Thesis, University of Florida, 1970.
27. Schroeder, M. R., "Parameter Estimation in Speech: A Lesson in Unorthodoxy", IEEE Proceedings, Vol. 58, No. 5, pp. 707-712, May 1970.
28. Van Den Elzen, H. C., "Calculating Power Spectral Densities for Data Signals", IEEE Proceedings, Vol. 58, No. 6, pp. 942-943, June 1970.
29. Tast, Yi-Ben and K. Aki, "Precise Focal Depth Determination from Amplitude Spectra of Surface Waves", Journal of Geophysical Research, Vol. 75, No. 29, pp. 5729-5743, Oct. 1970.
30. Childers, D. G., Varga, R. S., and N. W. Perry, Jr., "Composite Signal Decomposition", IEEE Transactions on Audio and Electroacoustics, Vol. Au-18, No. 4, pp. 471-477, December 1970.
31. Kemerait, R. C., "Signal Detection and Extraction by Cepstrum Technique", Ph.D. Dissertation, University of Florida, Gainesville, Fla., August 1971.
32. Ulrych, T. J., "Application of Homomorphic Deconvolution to Seismology", Geophysics, Vol. 36, No. 4, pp. 650-660, August 1971.
33. Markel, J. D., "FFT Pruning", IEEE Transactions on Audio and Electroacoustics, Vol. Au-19, No. 4, pp. 305-311, December 1971.

34. Fujisaki, H. and Y. Tanabe, "Analysis and Evaluation of Time Domain Techniques for Pitch Extraction", The Journal of Acoustical Society of America, Vol. 52, No. 1, p. 146, January 1972.
35. Senmoto, S. and D. G. Childers, "Analysis of a Composite Signal by Complex Cepstrum and Adaptive Filter", Trans. Inst. Elec. Comm. Engrs., (Japan), pt. A, pp. 9-16, 1972.
36. Kemerait, R. C., and D. G. Childers, "Signal Detection and Extraction by Cepstrum Technique", IEEE Transactions on Information Theory, Vol. IT-18, No. 6, pp. 745-759, November 1972.
37. Noll, A. M., "The Cepstrum and Some Close Relatives", In Signal Processing, J. W. R. Griffiths, P. L. Stocklin, and C. Van Schooneveld, Eds. London: Academic Press, pp. 11-12, 1973.
38. Papoulis, A., "Minimum-Bias Window for High-Resolution Spectral Estimates", IEEE Transactions on Information Theory, Vol. IT-19, No. 1, pp. 9-12, January 1973.
39. Childers, D. G., "Composite Signal Decomposition Techniques", Int. Conf. on Comm. (ICC), Seattle, WA, Jun 11-13, pp.1-6, 1973.
40. Hassab, J. C., "On The Convergence Interval of the Power Spectrum", IEEE Transactions on Information Theory, Vol. IT-20, No. 1, pp. 111-112, January 1974.
41. Hassab, J. C., "Time Delay Processing Near the Ocean Surface", The Journal of Sound and Vibration, Vol. 35, No. 4, pp. 489-501, April 1974.
42. Buhl, P., Stoffa, P. L., and G. M. Bryan, "The Application of Homomorphic Deconvolution to Shallow-Water Marine Seismology-Part I: Models", Geophysics, Vol. 39, No. 4, pp. 401-416, August 1974.
43. Buhl, P. L. Stoffa and G. M. Bryan, "The Application of Homomorphic Deconvolution to Shallow-Water Marine Seismology - Part II: Real Data", Geophysics, Vol. 39, No. 4, pp. 417-426, August 1974.
44. Stoffa, P. L., Buhl, P., and G. M. Bryan, "Cepstrum Aliasing and the Calculation of the Hilbert Transform", Geophysics, Vol. 36, No. 4, pp. 543-544, August 1974.

45. Bohme, J. F., "The Cepstrum as a Generalized Function", IEEE Transactions on Information Theory, Vol. IT-20, No. 5, pp. 650-653, September 1974.
46. Tenold, J. L., Crowel, D. H., Jones, R. H., Daniel, T. H., McPherson, D. F., and A. N. Popper, "Cepstral and Stationarity Analysis of Full-Term and Premature Infant's Cries", The Journal of Acoustical Society of America, Vol. 56, No. 3, pp. 975-980, September 1974.
47. Lackoff, M. R., and L. R. Leblance, "Frequency-Domain Seismic Deconvolution Filgering", The Journal of Acoustical Society of America, Vol. 57, No. 1, pp. 151-159, January 1975.
48. Rom, R., "On the Cepstrum of Two-Dimensional Functions", IEEE Transactions on Information Theory, Vol. IT-21, No. 2, pp. 214-217, March 1975.
49. Dudgeon, D. E., "The existence of Cepstra for Two-Dimensional Rational Polynomials", IEEE Transactions on Acoustic, Speech and Signal Processing, Vol. Assp-23, No. 2, pp. 242-243, April 1975.
50. Wood, L. C. and S. Treitel, "Seismic Signal Processing", IEEE Proceedings, Vol. 63, No. 4, pp. 649-661, April 1975.
51. Smith, R. G., "Cepstrum Discrimination Function", IEEE Transactions Information Theory, Vol. IT-21, No. 3, pp. 332-334, May 1975.
52. Hassab, J. C., and R. Boucher, "Analysis of Signal Extraction, Echo Detection and Removal by Complex Cepstrum in Presence of Distortion and Noise", The Journal of Sound and Vibration, Vol. 40, No. 3, pp. 321-335, June 1975.
53. Miles, J. H., Stevens, G. H. and G. G. Leininger, "Analysis and Correction of Ground Reflection Effects in Measured Narrow Band Sound Spectra using Cepstral Techniques", Presented at 90th Meeting of Acous. Soc. Amer., November 4-7, 1975.
54. Skinner, D. P. and D. G. Childers, "The Power, Complex, and Phase Cepstra", Presented at 1975 Proc. Nat. Telecommun. Conf., December 1975.
55. Fjell, P. O., "Use of the Cepstrum Method for Arrival Times Extraction of Overlapping Signals Due to Multipath Conditions in Shallow Water", The Journal of Acoustical Society of America, Vol. 59, No. 1, pp. 209-211, January 1976.

56. Kemerait, R. C. and L. Balceda, "Signal Detection and Extraction by Weighted Cepstrum Techniques", In 1976 Southeastcon Clemson University, IEEE Catalog No. 76, Ch1059-5, Reg. 3, pp. 3b-1-3b-3, 1976.
57. Kemerait, R. C., "Pseudo-Heterodyning in the Cepstral Domain", in 8th Ann. Southeastern Symp. System Theory, pp. 37-41, April 26-27, 1976.
58. Skinner, D. P. and D. G. Childers, "Real-Time Composite Signal Decomposition", IEEE Transactions on Acoustics, Speech, and Signal Processing, Vol. Assp-24, No. 3, pp. 267-270, June 1976.
59. Hassab, J. C. and R. Boucher, "A Probabilistic Analysis of Time Delay Extraction by the Cepstrum in Stationary Gaussian Noise", IEEE Transactions on Information Theory, Vol. IT-22, No. 4, pp. 444-454, July 1976.
60. Hassab, J. C., "Further Derivations of Statistical Measures in the Cepstrum", IEEE Transactions on Information Theory, Vol. IT-23, No. 4, pp. 540-544, July 1977.
61. Kolba, D. P. and T. W. Parks, "A Prime Factor FFT Algorithm Using High Speed Convolution", IEEE Transactions on Acoustics, Speech, and Signal Processing, Vol. Assp-25, No. 4, pp. 281-294, August 1977.
62. Childers, D. G., Skinner, D. P. and R. C. Kemerait, "The Cepstrum: A Guide to Processing", IEEE Proceedings, Vol. 65, No. 10, pp. 1428-1443, October 1977.
63. Agarwal, R. C. and J. W. Cooley, "New Algorithm for Digital Convolution", IEEE Transactions on Acoustics, Speech, and Signal Processing, Vol. Assp-25, No. 5, pp. 392-410, October 1977.
64. Dudgeon, D. E., "The Computation of Two-Dimensional Cepstra", IEEE Transactions on Acoustics, Speech and Signal Processing, Vol. Assp-25, No. 6, pp. 476-484, December 1977.
65. Harris, F. J., "On the Use of Windows for Harmonic Analysis with Discrete Fourier Transform", IEEE Proceedings, Vol. 66, No. 1, pp. 51-83, January 1978.
66. Tadokoro, Y. and T. Higuchi, "Discrete Fourier Transform Computation Via the Walsh Transform", IEEE Transactions on Acoustics, Speech, and Signal Processing, Vol. Assp-26, No. 3, pp. 236-240, June 1978.

67. Childers, D. G., Skinner, D. P. and R. C. Kemerait, "Correction to "The Cepstrum: A guide to Processing"" IEEE Proceedings, Vol. 66, No. 10, p. 1290, October 1978.
68. Hassab, J. C. and R. E. Boucher, "Further Comments on Windowing in the Power Cepstrum", IEEE Proceedings, Vol. 66, No. 1, pp. 1290-1291, October 1978.
69. Blomqvist, Ake, "Figures of Merit of Windows for Power Density Spectrum Estimation with DFT", IEEE Proceedings, Vol. 67, No. 3, pp. 438-439, March 1979.
70. Kitai, R. and K. H. Siemens, "Discrete Fourier Transform Via Walsh Transform", IEEE Transactions on Acoustics, Speech, and Signal Processing, Vol. Assp-27, No. 3, p. 288, June 1979.
71. Lim, J. S., "Spectral Root Homomorphic Deconvolution System", IEEE Transactions On Acoustics, Speech and Signal Processing, Vol. ASSP-27, No. 3, pp. 223-233, June 1979.
72. Ingels, F. M., "Cepstrum Analysis Techniques for Possible Application to Seismic/Acoustic Ranging", Report # F49620-79-C-0038 Mississippi State University, August 1979.
73. Ingels, F. M., "Investigation of Cepstrum Analysis for Seismic/Acoustic Signal Sensor Range Determination", unpublished proposal, Mississippi State University, September 1979.
74. Ingels, F. M. and L. C. Stables, "The Analysis of Continuous Acoustic/Seismic Signals Using Cepstrum Techniques", a paper presented at Southeastern Conference on April 1980.
75. Mervyn, A. J., Grant, P. M. and J. H. Collins, "The Theory, Design and Applications of Surface Acoustic Wave Fourier-Transform Processors", IEEE Proceedings, Vol. 68, No. 4, pp. 450-468, April 1980.
76. Ingels, F. M., several unpublished notes plus personal conversations with the author.

BOOKS

77. Gold, B. and C. M. Rader, Digital Processing of Signals, McGraw-Hill, New York, N. Y. 1969.
78. Churchill, R. V., Operational Mathematics, McGraw-Hill, New York, N. Y., 1978.
79. Oppenheim, A. V. and R. W. Schaffer, Digital Signal Processing, Prentice Hall, Englewood Cliffs, N. J., 1975.
80. Rabiner, L. R. and B. Gold, Theory and Application of Digital Signal Processing, Prentice-Hall, Englewood Cliffs, N. J., 1975.
81. Tretter, S. A., Introduction to Discrete-Signal Processing, John Wiley & Son, New York, N.Y., 1976.
82. Bracewell, R. N., The Fourier Transform and Its Applications, McGraw-Hill, New York, N.Y., 1978.

AUTHOR INDEX

Author - Bibliography Entry Number

Agarwal, R. C.	: 63	Le Blanc, L. R.	: 47
Aki, K.	: 29	Leininger, D. G.	: 53
Atal, B. S.	: 2	Lewis, P. A. W.	: 14,15,20
Balas, L. F.	: 19	Lim, J. S.	: 71
Balceda, L.	: 56	Maling, G. C.	: 13
Bergland, G. D.	: 21	Markel, J. D.	: 33
Blomqvist, Ake.	: 69	McPherson, D. F.	: 46
Bogert, B.P.	: 3,9,10,12	Mervyn, A. J.	: 75
Böhme, J. F.	: 45	Miles, J. H.	: 53
Boucher, R.	: 52,59,68	Nelson, D. E.	: 13
Bracewell, R. N.	: 82	Noll, A. M.	: 4,5,8,11,18,37
Bryan, G. M.	: 42,43,44	Oppenheim, A. V.	: 79
Buhl, P.	: 42,43,44	Ossanna, J. F.	: 9,10
Childers, D. G.	: 30,35,39,54,58 62,67	Papoulis, A.	: 38
Churchil, R. V.	: 78	Parks, T. W.	: 61
Cocharan, W. T.	: 13	Parzen, E.	: 12
Cohen, T.	: 25	Perry, N. W.	: 30
Collins, J. H.	: 75	Popper, A. N.	: 46
Cooley, J. W.	: 13,14,15,20,63	Rabiner, L. R.	: 80
Crowel, D. H.	: 46	Rader, C. M.	: 13,17,77
Daniel, T. H.	: 46	Rom, R.	: 48
Dudgeon, D. E.	: 49,64	Schafer, R. W.	: 16,79
Fano, R. M.	: 1	Schroeder, M. R.	: 2,5,27
Favin, D. L.	: 13	Senmoto, S.	: 35
Fjell, P. O.	: 55	Siemens, K. H.	: 70
Fuji Sake, H.	: 34	Singleton, R. C.	: 22,23
Gold, B.	: 77,80	Skinner, D. P.	: 54,5,62,67
Grant, P. M.	: 75	Smith, R. G.	: 51
Halpeney, O. S.	: 26	Stevens, G. H.	: 53
Harris, F. J.	: 65	Stoffa, P. L.	: 42,43,44
Hassab, J. C.	: 40,41,52,59,60,68	Tadokoro, Y.	: 66
Healy, M.J.R.	: 3	Tanaba, Y.	: 34
Helms, H. D.	: 13	Tasi, Yi-Ben	: 29
Higuchi, T.	: 66	Tenold, J. L.	: 46
Ingels, F. M.	: 72,73,74,76	Treitel, S.	: 50
Jones, R. H.	: 46	Trotter, S. A.	: 81
Kaenel, R. A.	: 13	Tukey, J. W.	: 3
Kelly, J. M.	: 7	Uhrich, M. L.	: 24
Kemerait, R. C.	: 31,36,56,57,62,67	Ulrych, T. J.	: 32
Kennedy, R. N.	: 7	Van Den Elzen, H.C.	: 28
Kitai, R.	: 70	Varga, R. S.	: 30
Kolba, D. P.	: 61	Welch, P. D.	: 13,14,15,20
Lang, W. W.	: 13	Wood, L. C.	: 50
Lankoff, M. R.	: 47	Young, T. Y.	: 6

DATE
FILMED
-8